Supramolecular chemistry and reactivity of quinoline derivatives

A Dissertation submitted to the
Indian Institute of Technology Guwahati as
partial fulfillment for the Degree of
Doctor of Philosophy in Chemistry

Submitted by

Dipjyoti Kalita

Department of Chemistry

Indian Institute of Technology Guwahati

January 2012

Dedicated to My Family
&
Friends…

Statement

I hereby declare that this thesis entitled "**Supramolecular chemistry and reactivity of quinoline derivatives**" is the outcome of research work carried out by me under the supervision of Prof. Jubaraj B. Baruah, at the Department of Chemistry, Indian Institute of Technology Guwahati, India.

In keeping with the general practice of reporting scientific observations, due acknowledgement has been made whenever work described here has been based on the findings of other investigators.

Dipjyoti Kalita

IIT Guwahati
January, 2012

Dipjyoti Kalita

Certificate

This is to certify that Dipjyoti Kalita has been working under my supervision since July, 2008 as a regular registered Ph. D. student. I am forwarding his thesis entitled "**Supramolecular chemistry and reactivity of quinoline derivatives**" being submitted for the Ph. D. (Science) Degree of this Institute.

I certify that he has fulfilled all the requirements according to the rules of this institute regarding the investigations embodied in his thesis and this work has not been submitted elsewhere for a degree.

IIT Guwahati
January 20, 2012

Prof. Jubaraj B. Baruah

Acknowledgements

The enlightening experience of doing science under the guidance of Prof. Jubaraj B. Baruah can hardly be described in words. The numerous discussions and interactions I had with him expanded my horizons to hitherto unknown frontiers of science and knowledge. I am indebt to this wonderful person for all that he has given me and above all for motivating me towards scientific research.

I would like to acknowledge my sincere gratitude to all my doctoral committee members for their insightful advices and valuable suggestions. I would also like to thank Prof. Dietmar Stalke for his valuable suggestions and timely help. I am also grateful to the entire faculty and staff in the Department of Chemistry, Indian Institute of Technology Guwahati for providing a wonderful work atmosphere throughout this period.

I would like to thank my lab mates Dr. Anirban Karmakar, Dr. W. Marjit Singh, Dr. Rupam Sarma, Debendra Singh, Babulal Das, Bhaskar, Bigyan, Himangshu, Jayanta, Prithiraj, Nithi, Tapan, Subrata and Syam whom I had an opportunity to work with. No words can express my thankfulness for giving me their time and companionship, which made the time spent in the laboratory and outside pleasant and memorable. I would like to give my special thanks to my friends Sanjeev Mahanta, Ranjit Thakuria, Tridib, Rajeev, Kaushik, Priyanka, Pojul, Nilamoni and Moushumi for their timely help, support and for the wonderful time we shared during this period.

The financial support from Council of Scientific and Industrial Research (CSIR), New Delhi for the research fellowship is duly acknowledged.

I would also like to acknowledge all my teachers of JNV Nalbari, JNV Sonitpur, B. Borooah College and Gauhati University for their love and blessings.

Finally, my Ph. D. endeavor could not be completed without the endless love, unending support, tolerance and blessings from my family and my graduate teacher Dr. Diganta Choudhury. They are the main soul and inspiration for each and every step that I achieve in my life.

Preview

This thesis deals with the studies on synthesis, characterization, supramolecular chemistry, and reactivity of a few quinoline derivatives. The content of the thesis is divided into six chapters.

A general introduction to quinoline and quinoline derivative is brought forward in the first chapter. This includes a brief discussion on their synthesis, structural features and reactivity. The catalytic activity of metal complexes of quinoline derivatives and pharmaceutical application of quinoline derivatives are also discussed. This chapter also features discussions on several quinoline based supramolecular architectures and their inclusion compounds. Fluorescence sensing of pH by quinoline based receptors is included in this chapter. Further, various coordination polymers of quinoline ligands is included. Finally, a brief discussion on the scope of the thesis work is included.

The second chapter of the thesis deals with the synthesis, characterization and the anion recognition properties of few quinoline derivatives. The synthesis, characterisation of a number of amide and ester derivatives of quinoline (**2.1-2.8**) and their anion recognition properties in solution as well as in solid state are presented in this chapter.

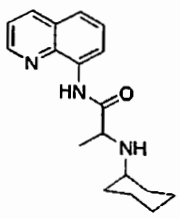

2.1

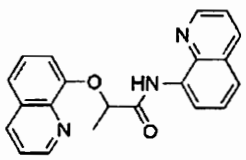

2.2

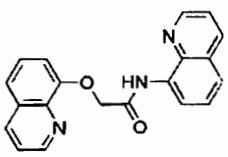

2.3

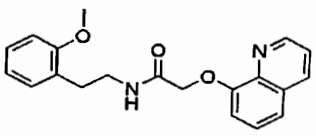

2.4

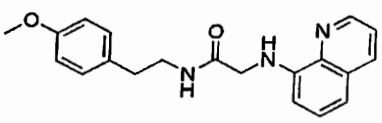

2.5

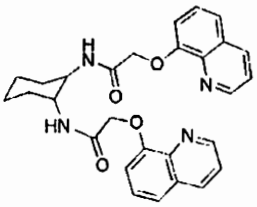

2.6

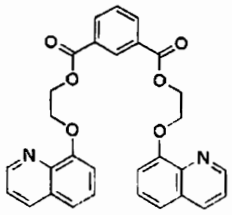

2.7

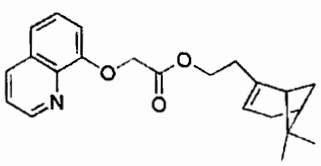

2.8

All these receptors are fluorescence active and they possess a binding site through the N atom of the quinoline ring and also can have supramolecular interactions through the amide linkages, they are suitable for interacting with an acid. The protonation process provides an extra H- bond environment to have complicated supramolecular interaction with an anion. Hence in anticipation of getting differences in fluorescence emission of the parent compound by anion recognition process we monitored the solution state fluorescence spectra of these compounds in presence of different acids. The trend in terms of intensity and the position of fluorescence are found to be highly selective, showing anion recognition by these receptors. From these fluorescence changes during titration, the binding constants were calculated.

The structural aspects of receptors **2.3**, **2.4**, **2.5** and their host-guest complexes with various anions are described. The crystal structures of all the host-guest complexes are studied and compared with the receptor molecules. The receptor **2.3** has a bent structure which is converted to a planar on binding to anions. The receptor **2.5** adopts a twizeer like geometry on binding with anions. The perchlorate salt of receptor **2.5** shows empty cylindrical voids.

Cyclisation reactions of some bromo-substituted 8-aminoquinoline derivatives leading to new hetorocycle are presented in the third chapter. Two quinoline derivatives namely 2-bromo-N-quinoline-8-yl-acetamide (**3.1**) and 2-bromo-N-(quinolin-8-yl)propanamide (**3.2**) are synthesized and their reactivity under different conditions are studied.

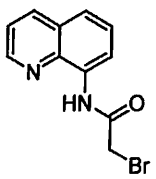

3.1

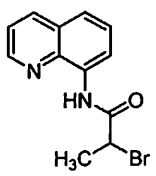

3.2

A three component reaction between 2-bromo-N-quinoline-8-yl-acetamide (**3.1**), 2-(4-methoxyphenyl) ethylamine and acetone gives a fused ring heterocyclic compound **3.3** as illustrated in scheme 1. On changing the amine to 2-(2-methoxyphenyl) ethylamine another product **3.5** is obtained. The compound **3.3** and **3.5** on treatment with perchloric acid further rearranges to give another heterocycle **3.4**.

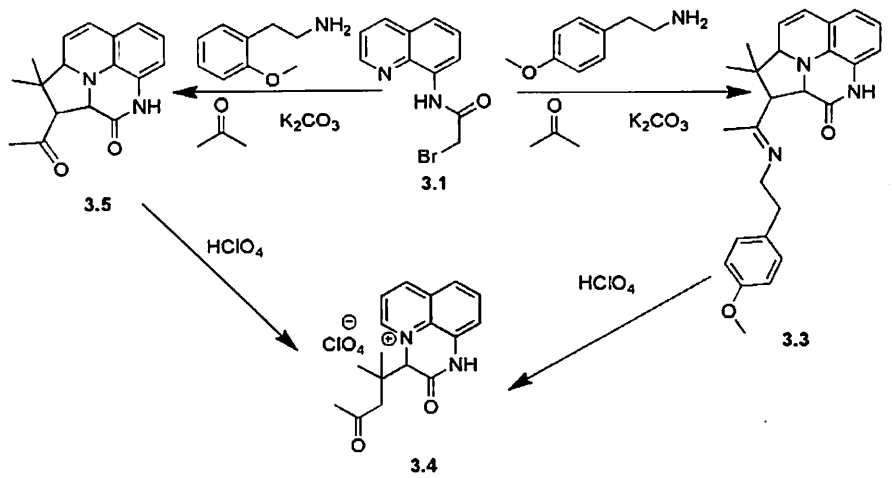

Scheme 1

The 2-bromo-N-(quinolin-8-yl)propanamide (**3.2**) underwent cyclisation reactions through C-N bond formation in methanol in the presence of different metal salts of copper(II) and nickel(II). The reactions are found to be highly solvent dependent and also metal dependent. When copper(II) salts were used in methanol exclusively cyclised product **3.9** in the form of salt of the corresponding ions were obtained via C-N bond formation. When the cyclisation reactions were attempted in ethanol with copper(II) salts, no cyclisation of **3.2** was observed, but nucleophilic substitution leading to C-O bond gave compound **3.10**. It is also observed that the intra-molecular cyclisation reaction of **3.2** is promoted by nickel(II) salts and the compound **3.11** is formed in both methanol and ethanol (scheme 2).

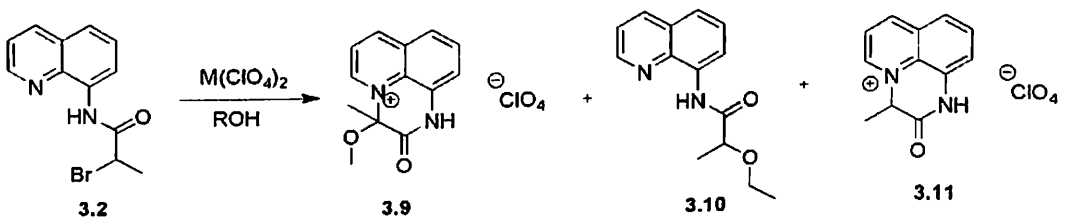

% ratio of product 3.9: 3.10: 3.11			
M = Cu, R=CH_3 ;	100	0	0
M = Cu, R=CH_3CH_2 ;	0	100	0
M = Ni, R=CH_3CH_2, CH_3 ;	0	0	100

Scheme 2

The synthesis, characterisation and the anion binding properties of urea and carbamide derivative **4.1**, **4.2**, and **4.3** of quinoline are presented in chapter 4. These compounds are synthesized by reacting phenylisocyanate with the corresponding amino or hydroxyquinoline. Urea and carbamide derivatives are classified with dicarboxylic acids.

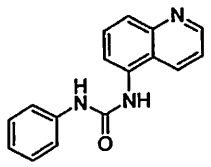

4.1

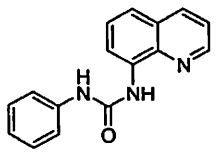

4.2

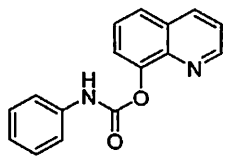

4.3

The urea derivative, 1-phenyl-3-(quinolin-5-yl)urea (**4.1**) is crystallized with different dicarboxylic acids such as fumaric acid (**4.4**), maleic acid (**4.5**), 1,4-phenylenediacetic acid (**4.6**), malonic acid (**4.7**), phthalic acid (**4.8**), terephthalic acid (**4.9**), adipic acid (**4.10**) and pyridine 2,3-dicarboxylic acid (**4.11**) to obtain either the salt or co-crystal of the corresponding acid as shown in scheme 3. These salts or co-crystals can be distinguished from their optical spectra. Generally the co-crystals are colourless whereas the salts are yellow in colour.

The mineral acid binding of the receptor **4.1**, **4.2**, and **4.3** lead to the formation of symmetry non-equivalent molecules i.e., the existence of more than one molecule in the crystallographic asymmetric unit. The number of molecules in the asymmetric unit is represented by the symbol Z′. For example, in case of the receptor **4.1** the number of molecules in the asymmetric unit (Z′) changes from 1 to 3 on coordination with perchlorate anions. The detailed analysis of the structures of all the receptors and the salts are discussed in this chapter.

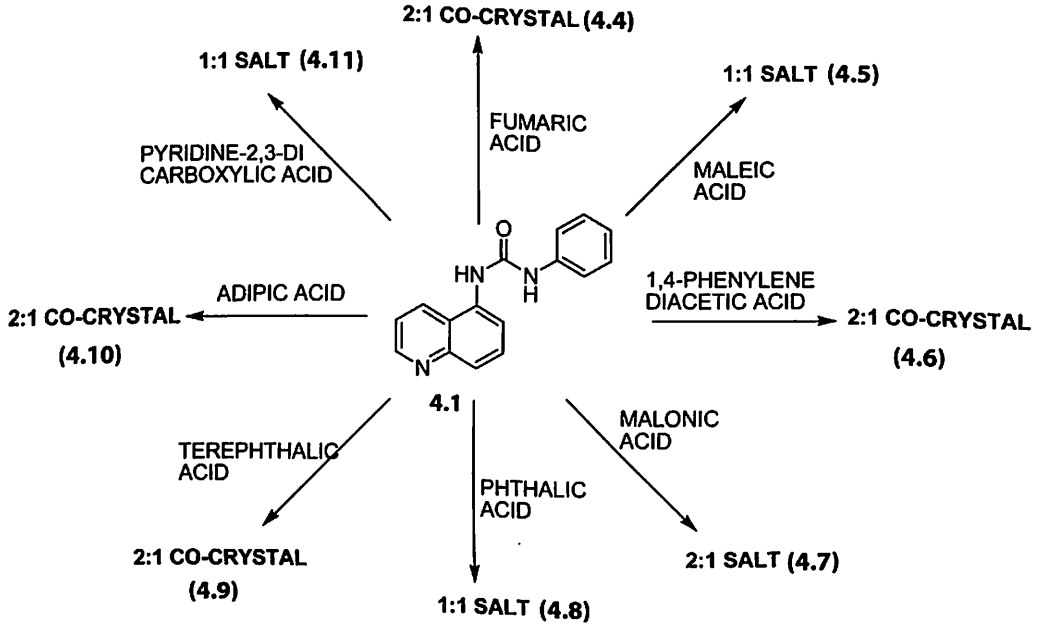

Scheme 3

In chapter five the synthesis, characterization and guest inclusion property of a diquinoline receptor (**5.2**) is presented. The diquinoline receptor **5.2** was synthesised

in multiple steps. In the first step an ester derivative of 8-aminoquinoline was prepared by reacting with methylbromo acetate and the ester group is reduced to obtain an alcohol **5.1**. The alcohol derivative **5.1** thus obtained, was treated with catalytic amount of manganese(II) acetate to give dimerised derivative **5.2** (scheme 4).

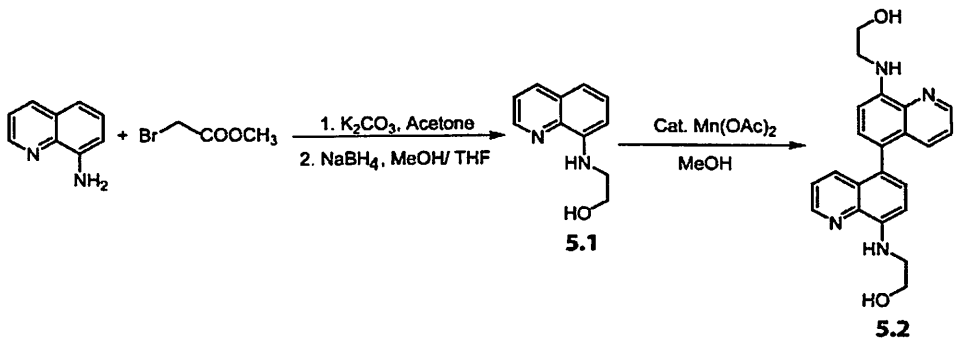

Scheme 4

The diquinoline receptor **5.2** is also crystallized and its crystal structure is studied. The crystal structure of **5.2** when viewed along 'a'-crystallographic axis we have observed that the molecule adopts a single helical structure. The receptor **5.2** is also crystalized with two mineral acids namely perchloric acid and nitric acid. The crystallographic structure shows that on treatment with perchloric acid, **5.2** forms a salt (**5.3**), where the two quinoline N atoms are protonated, whereas in the case of nitric acid a co-crystal (**5.4**) is formed. The helical structure of the molecule **5.2** is retained after the inclusion of the perchlorate anion in the fold of the helix. The perchlorate anion does not disturb the assembly of intermolecular hydrogen bonding of the molecule **5.2**; instead the anion is encapsulated inside the cavity formed by the helical arrangement of salt **5.3**. The co-crystal **5.4** also adopts a helical shape.

In chapter six the in-situ formation of co-ordination polymer and a dinuclear complex of sodium and cadmium with 2-(quinolin-8-yloxy)propionic acid are reported. The co-ordination polymer of sodium (**6.1**) was synthesized by the reaction of 8-hydroxyquinoline and 2-bromopropionyl bromide in presence of sodium hydroxide. The co-ordination polymer **6.1** on reaction with cadmium acetate gave another co-ordination polymer of cadmium (**6.3**). A dinuclear complex **6.2** was obtained by the reaction of dilute perchloric acid with co-ordination polymer **6.1** as illustrated in scheme 5. The crystal structures of all these complexes are studied. The co-ordination

polymer **6.1** and the dinuclear complex **6.2** are found to be a fluorescent sensor for selective detection of some metal ions.

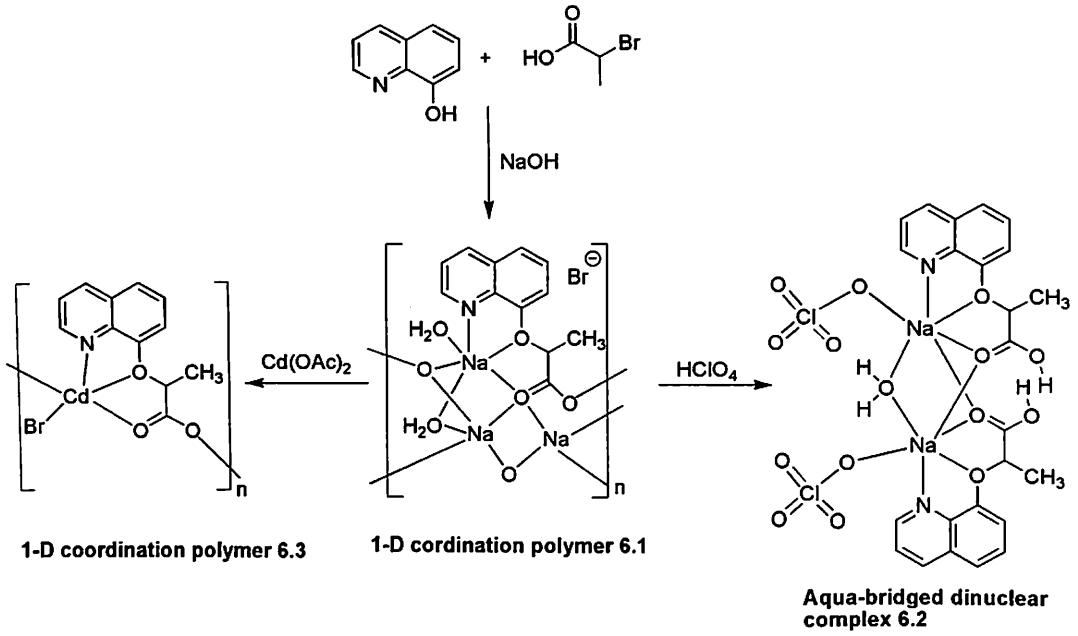

Scheme 5

Each chapter has the spectroscopic details of the compounds along with synthetic methodology. Pertaining literature are included at the end of each chapter. The crystallographic data for all the structures that have been discussed in this work, except those, which are used as references are tabulated in the appendix section towards the end of the thesis. Details of the instruments used are given at the appendix section. A brief summary on the finding of the presented work is compiled at the end of the thesis. The CIF of the crystal structures are presented in terms of electronic data in a CD.

Contents

Chapter 1

Introduction

1.1 General features of quinoline and its derivatives

Quinoline is an organic base first obtained from coal-tar in 1834 by F. Runge[1]. Later Gerhardt[2] extracted quinoline by distillation of cinchonine, quinine and other alkaloids reacting with caustic potash. It is a tertiary base with pKa 4.85[3]; has a resonance structure as shown in figure 1.1.

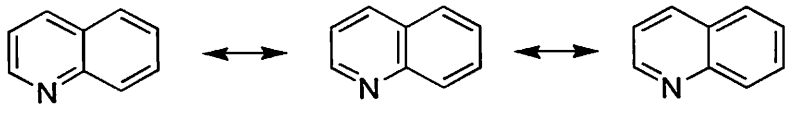

Figure 1.1: Resonance forms of quinoline molecule

The utility of quinoline derivatives in the areas of medicine, food, catalyst, dye, materials, refineries and electronics is well established. 8-Hydroxyquinoline is one of the most extensively studied derivatives of quinoline because of its unique structural properties. In neutral solution, the hydroxyl group is in the protonated form with pKa 9.89 and the nitrogen is not protonated with a pKa 5.13.[4] 8-Hydroxyquinoline is commonly used as chelating agent[5-7] and is also used in organic light emitting diodes (OLED).[8-10] The versatility in the structure of 8-hydroxyquinoline molecule is depicted in the figure 1.2.

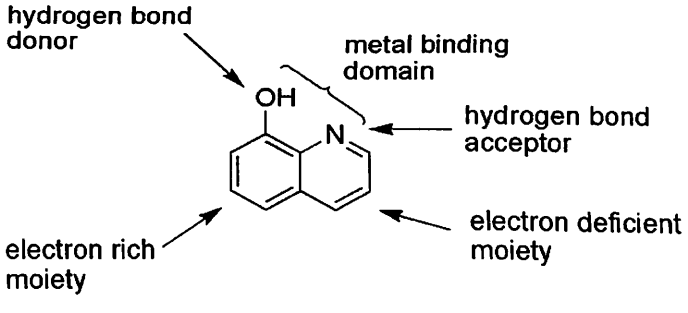

Figure 1.2: Versatility of the 8-hydroxyquinoline molecule

It is also used in fluorometric determination of metal ions. 8-Hydroxyquinoline does not show fluorescence in most of the solvents, and on complexation with some metal ions its fluorescence is enhanced. The poor fluorescence emission of 8-hydroxyquinoline is attributed to a photoinduced tautomerization reaction (Scheme 1.1) followed by deexcitation of the tautomer. Such process occurs mainly via a non-radiative route.[11]

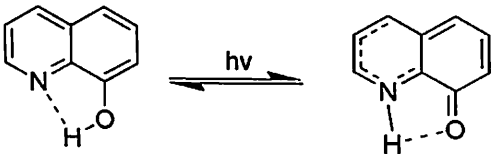

Scheme 1.1: Photoinduced tautomerization of 8-hydroxyquinoline

8-Aminoquinoline (**1.1**) is another important derivative of quinoline. 8-Aminoquinoline is a prototype for many antimalarial drugs[48-54] such as primaquine, tafenoquine and pamaquine.

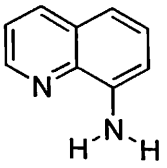

1.1

1.2 Synthesis and reactivity of quinoline derivatives

Quinoline derivatives are generally synthesized by various name reactions such as Friedlaender synthesis, Skraup synthesis, Combes synthesis etc.

The starting materials for Friedlaender synthesis of quinoline are *ortho*-aminoaryl aldehydes or ketones and a ketone possessing α-methylene group. After an initial amino-ketone condensation, the intermediate undergoes base- or acid-catalyzed cyclocondensation to produce a quinoline derivative as illustrated in scheme 1.2.[13-17]

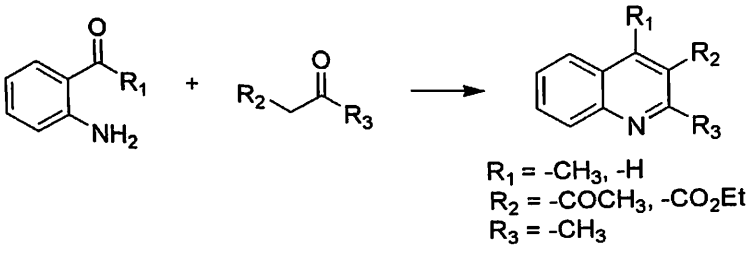

Scheme 1.2: Friedlaender synthesis of quinoline

In the Skraup synthesis of quinoline; aniline is heated with sulphuric acid, glycerol, and an oxidizing agent like nitrobenzene to yield quinoline (scheme 1.3).[18-19]

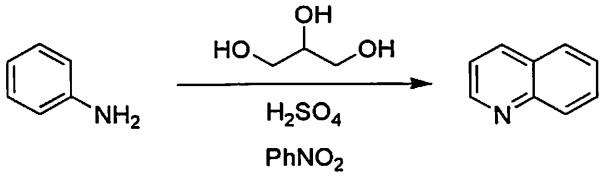

Scheme 1.3: Skraup synthesis of quinoline

Another method for synthesis of quinoline is the Combes synthesis, where unsubstituted aniline is condensed with a β-diketone to form substituted quinolines via an acid catalyzed ring closure of an intermediate Schiff-base (scheme 1.4).[20]

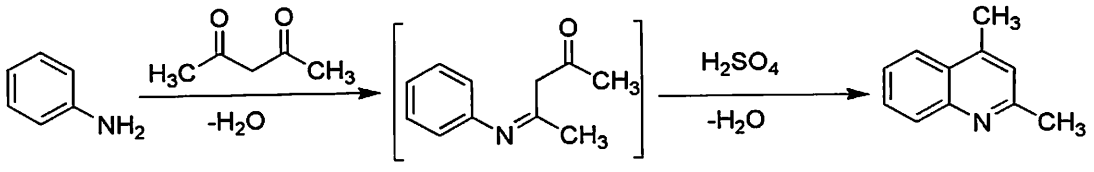

Scheme 1.4: Combes synthesis of quinoline

Based on these synthetic methods, Kouznetsov *et al.* mentioned that there are conceptually only two approaches towards the construction of quinoline. The first one relates to the use of the aromatic primary amine as the nucleophilic component providing nitrogen as the C-C-N unit whereas the second one employs the *ortho*-substituted anilines as the C-C-C-N unit.[12]

Quinoline is basic and therefore aromatic electrophilic substitution occurs on the homoaromatic ring as the heteroaromatic ring is deactivated due to protonation.[21] Substitution is preferred at C–5 and C–8 as the intermediates can profit from resonance stabilization without disrupting the aromaticity of the heteroaromatic ring. Some typical examples of aromatic electrophilic substitution reaction of quinoline are shown in scheme 1.5.[22]

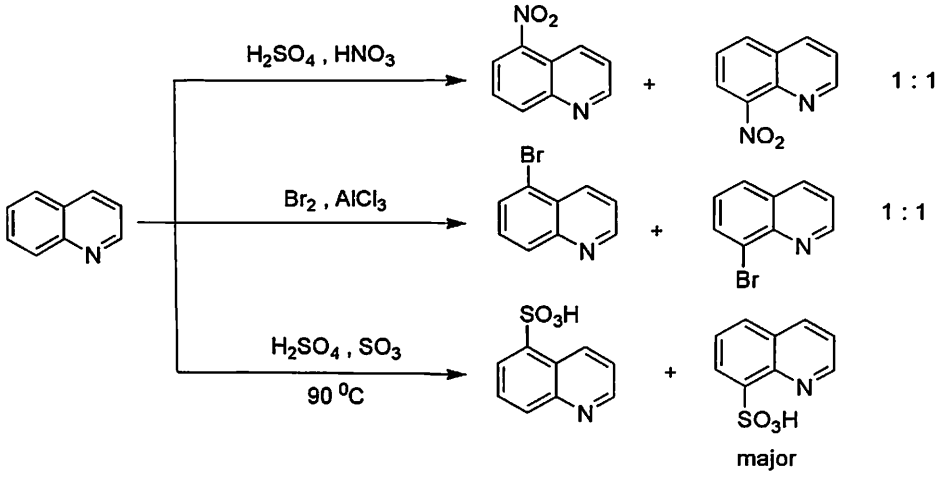

Scheme 1.5: Aromatic electrophilic substitution reaction of quinoline

Quinoline also undergoes nucleophilic aromatic substitution predominantly in the 2 position; such substitution with alkali metal amides to give 2-aminoquinoline is known as Chichibabin reaction (scheme 1.6).[23]

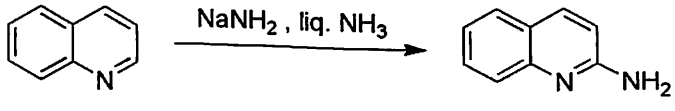

Scheme 1.6: Nucleophilic aromatic substitution of quinoline

Quinoline can be selectively reduced at 1,2-bond by reaction with lithium aluminium hydride but the 1,2-dihydro quinolines are unstable and disproportionate easily to give quinoline and 1,2,3,4-tetrahydroquinoline (scheme 1.7).[24]

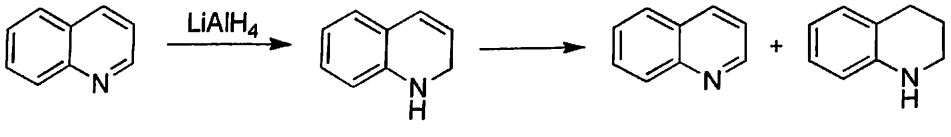

Scheme 1.7: Reduction of quinoline by $LiAlH_4$

Quinoline and its derivatives can be converted to 1,2,3,4-tetrahydroquinolines by catalytic hydrogenation with ruthenium complex. (scheme 1.8).[25]

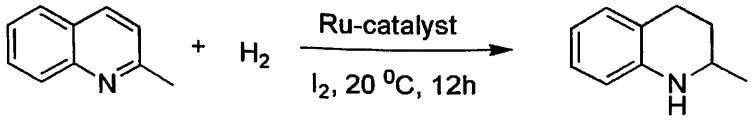

Scheme 1.8: Catalytic hydrogenation of quinoline

Quinoline also undergoes oxidative cleavage in alkaline $KMnO_4$ to give pyridine-2,3-dicarboxylic acid which further decarboxylates to give nicotinic acid (scheme 1.9).[26]

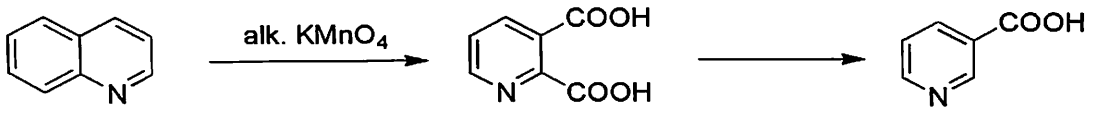

Scheme 1.9: Oxidative cleavage of quinoline

The nitrogen atom of the quinoline ring also can be protonated, alkylated or oxidized in order to modify the reactivity at the pyridine unit.[27]

1.3 Catalytic activity of quinoline complexes

Metal complexes of quinoline derivatives have wide applications as catalyst for different types of organic reactions. A few of the organic reactions catalyzed by quinoline based metal complex are discussed here.

Aerobic oxidative dehydrogenation of benzylamines to the corresponding benzonitriles is carried out by ruthenium complex of bezoquinoline under mild conditions (scheme 1.10).[28]

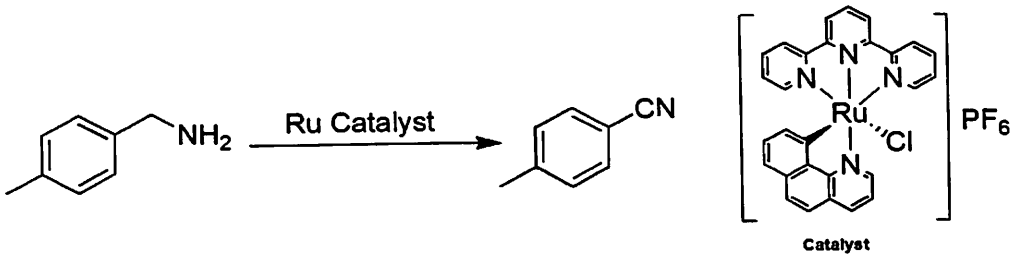

Scheme 1.10: Oxidative dehydrogenation using ruthenium complex of quinoline derivative

Polymer-supported heterogeneous catalysts in the form of complexes of 8-hydroxyquinoline with cobalt acetate is used for oxidation of alkenes (scheme 1.11).[29]

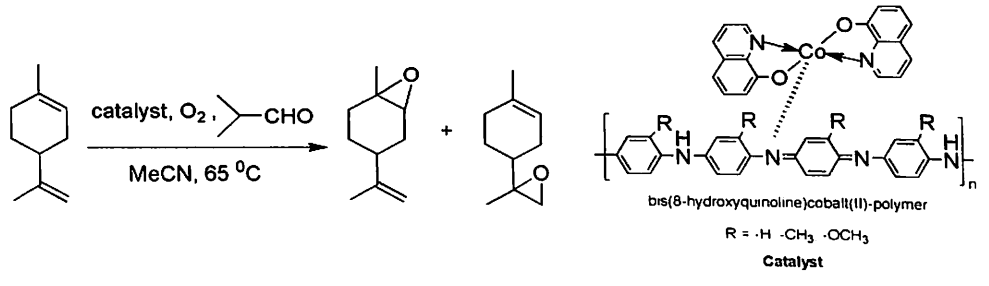

Scheme 1.11: Catalytic oxidation of alkenes

Ring-opening polymerization of ε-caprolactone and rac-lactide is catalyzed by zinc and aluminum complexes supported by quinoline-based N,N,N-chelate ligands (**1.2**).[30] Iron, cobalt and nickel complex of quinoline derivative (**1.3**) are reported to be very efficient catalyst for ethylene polymerization reactions.[31-32]

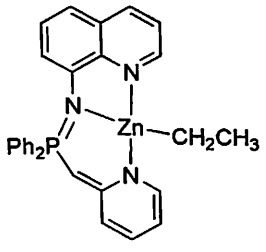

1.2

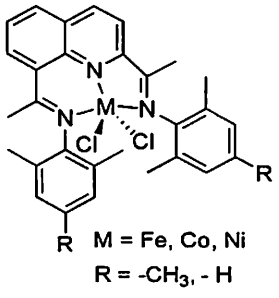

1.3

Palladium complex of 8-hydroxyquinoline is used as a catalyst for the Suzuki-Miyaura reaction as shown in scheme 1.12.[33]

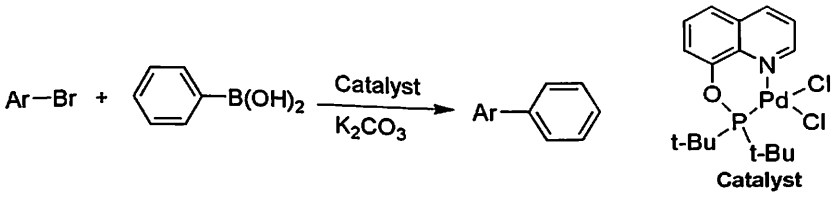

Scheme 1.12: Suzuki-Miyaura reaction

A quinoline-functionalized N-heterocyclic carbene complex of iridium is an active catalyst in the transfer hydrogenation of ketones to yield alcohols using 2-propanol as the hydrogen source.[34] Palladium complexes of 8-(di-tert-butylphosphinooxy) quinoline are efficient catalyst precursors in the coupling of the phenylboronic acid with aryl bromides and chlorides.[35]

The Sonogashira coupling reaction of terminal alkynes with aryl halides is also catalyzed by a quinoline-2-carboimine palladium complex[36] as shown in scheme 1.13.

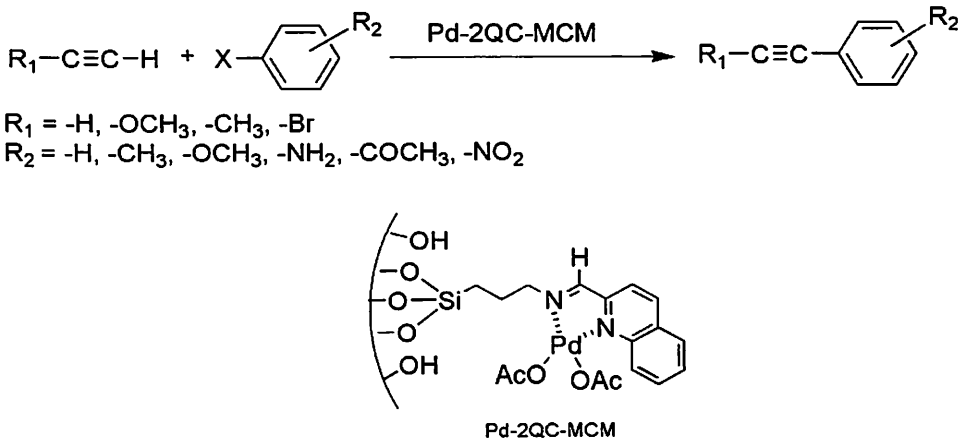

Scheme 1.13: Sonogashira coupling reaction of terminal alkynes

Ruthanium complex of quinoline derivative (**1.4**) is found to be an active catalyst for olefin metathesis reactions.[37] Olefin polymerization reactions are also efficiently catalyzed by chromium (III) complexes of quinoline derivative (**1.5**).[38]

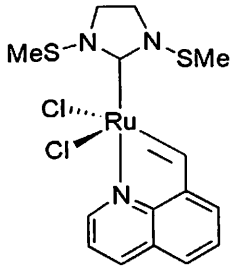

1.4

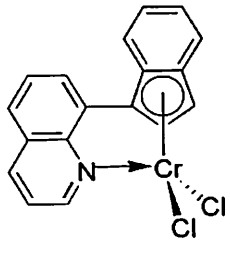

1.5

Organometallic complex of 8-methylquinoline and palladium is used as catalyst for carbon-carbon bond formation by Heck reaction.[39] Enantioselective hydrogenation of alkenes are catalyzed by Iridium complex of quinoline derivative (Scheme 1.14).[40]

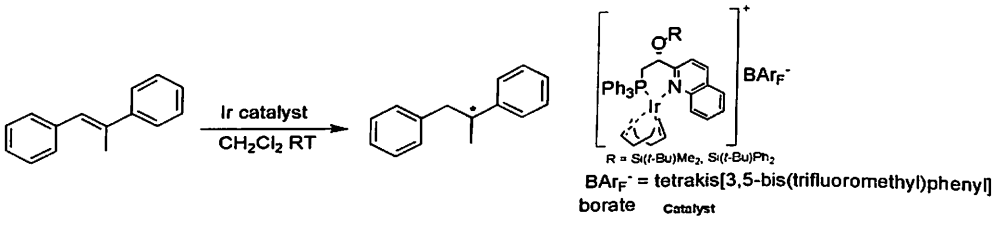

Scheme 1.14: Enantioselective hydrogenation of alkenes

Palladium complex of benzoquinine serves as an effective pre-catalyst for the selective halogenation of C-H bonds.[41] Electrochemical reduction of carbon dioxide is also catalysed by palladium and cobalt complexes of quinoline derivatives.[42]

Quinoline based Schiff-base complex of aluminium is a very good catalysts for ethylene polymerization reactions.[43]

1.4. Pharmaceutical application of quinoline derivatives

The bark of Cinchona plant containing quinine was utilized to treat palpitations, fevers and tertians since more than 200 years ago.[44] Compounds containing quinoline motif are most widely used as antimalarials, antibacterials, antifungals and anticancer agents. Additionally, quinoline derivatives find use in the synthesis of fungicides, virucides, biocides, alkaloids, rubber chemicals and flavouring agents.[45-47]

Quinoline containing antimalarial drugs, such as chloroquine, quinine, primaquine, quinacrine and mefloquine (figure 1.3) are the mainstays of chemotherapy against malaria.[48-54]

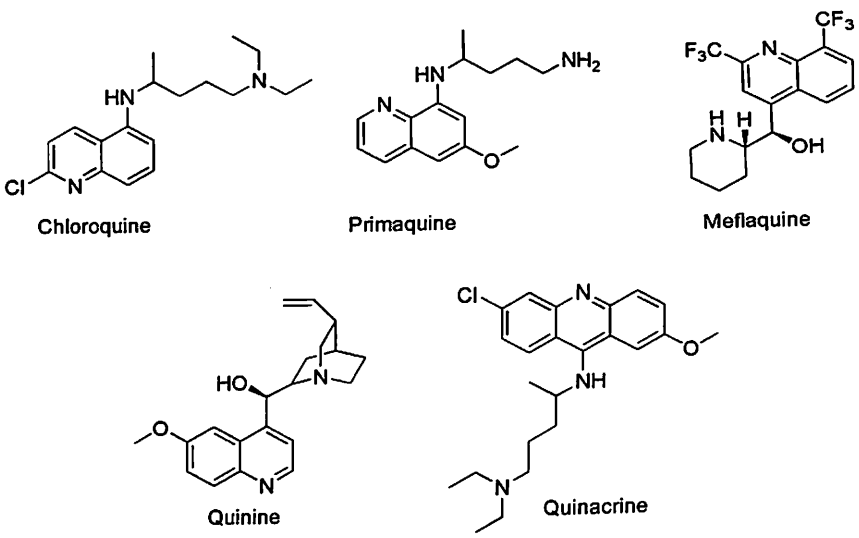

Figure 1.3: Some well known antimalarial drugs containing quinoline as structural back-bone.

Apart from these well known drugs a number of quinoline derivatives (**1.6, 1.7, 1.8, 1.9**) are being studied and their antimalarial activity is established.[55]

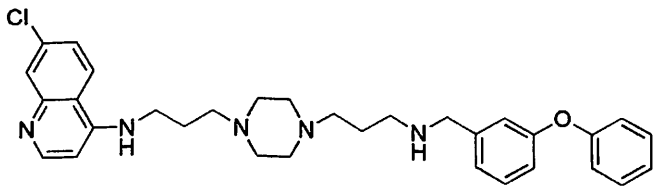

1.6

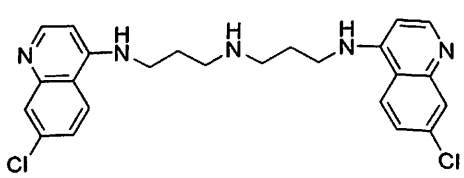

1.7

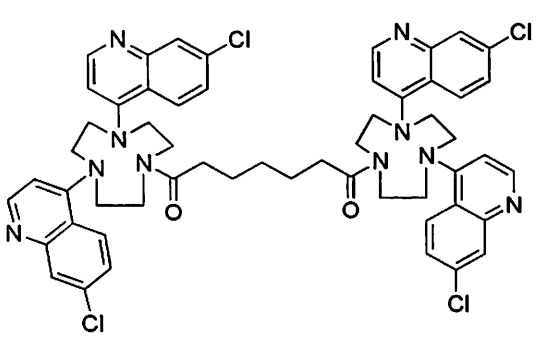

1.8

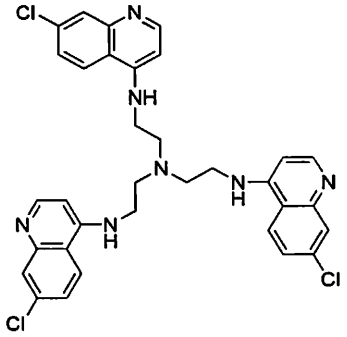

1.9

A number of quinoline compounds (**1.10, 1.11, 1.12**) have been used as anti bacterial drugs against various diseases such as tuberculosis etc.[56-59]

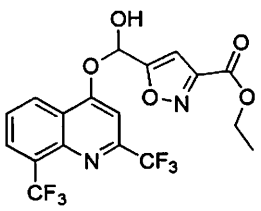

1.10

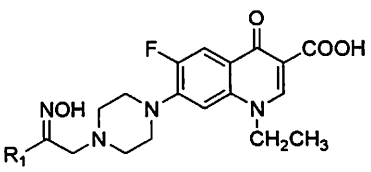

1.11

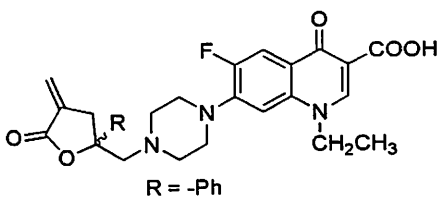

R = -Ph

1.12

Boron-containing quinoline compounds (**1.13, 1.14**) termed borinic acid quinoline esters are synthesized which shows remarkable antibacterial activity. These boron-containing compounds have broad-spectrum activity against several pathogenic strains of both Gram positive and Gram negative bacteria.[60]

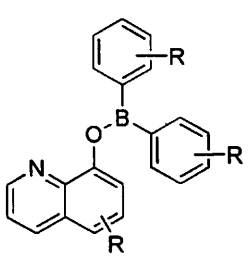

R = -4F, -4Cl, -3Cl, -4MeO

1.13

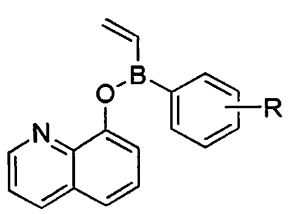

R = -H, -2Cl, -3Cl, -4Cl, -3F, -3CN

1.14

Quinoline derivatives are also used as antifungal agents.[61-62] A number of 2-substituted indoloquinolines (**1.15, 1.16**) have been synthesized and they are found to be very good antifungal agents.[63] Ring substituted 4-hydroxy-1*H*-quinolin-2-one derivatives (**1.17, 1.18**) are reported to be active as antifungal agents.[64] These compounds show a significant similarity to some novel antifungal agents such as homoallylamines, and therefore possess remarkable antifungal activity.[61]

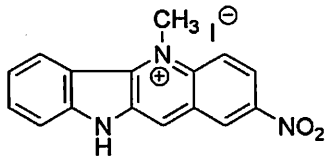

1.15

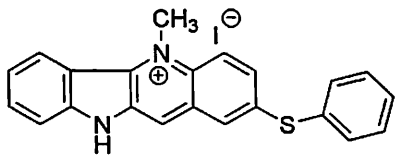

1.16

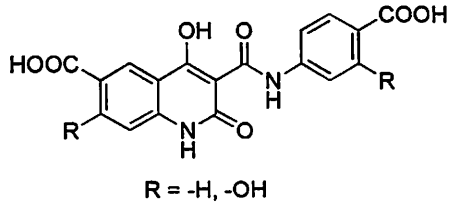

1.17

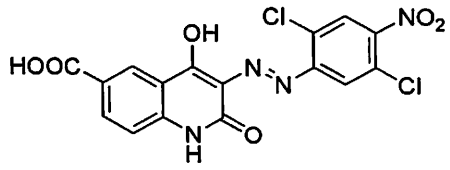

1.18

Many naturally occurring quinoline derivatives are also known for their anticancer activity.[65-66] Indoloquinoline alkaloids such as cryptolepine and neocryptolepine (**1.19** and **1.20**) are naturally occurring plant product that possess anti cancer activity.[67]

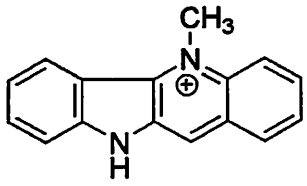

1.19

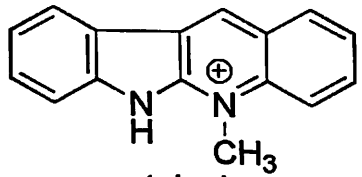

1.20

1.5. Supramolecular chemistry of quinoline derivatives

Apart from their various other important applications in chemistry and biology, quinoline derivatives find a wide range of applications in supramolecular chemistry. 8-hydroxyquinoline exists as a dimer in solid state by formation of bifurcated hydrogen bonds as shown in figure 1.4a.

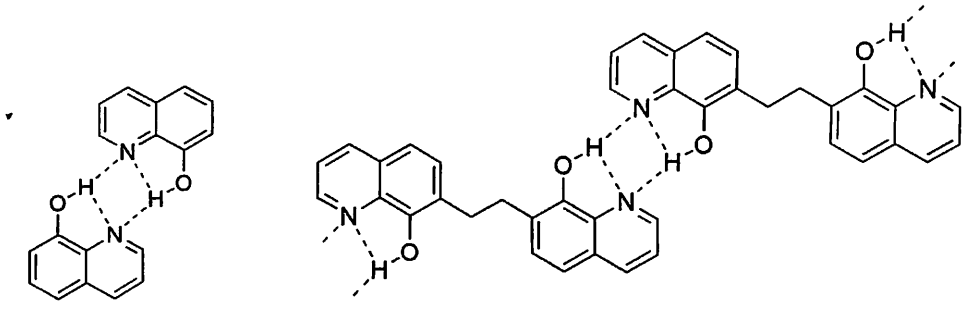

(a) **(b)**

Figure 1.4: Hydrogen bonding pattern in (a) 8-hydroxyquinolines and (b) alkyl-bridged bis-8-hydroxyquinolines

The alkyl-bridged bis-8-hydroxyquinolines forms hydrogen bonded polymers upon crystallization (figure 1.4b).[68] The conformation of the hydrogen bonded polymer can be influenced by introduction of spacers with either odd or with even numbers of carbon atoms in the bridge. With an odd numbers of carbon atoms, such polymers adopt zigzag conformation; while with even numbers polymers adopt a double-wound structure.[69-72]

Kemp's triacid binds selectively 8-substituted quinoline. For example it forms co-crystals with 8-aminoquinoline and 8-hydroxyquinoline through formation of intermolecular hydrogen bonds as depicted in figure 1.5.[73]

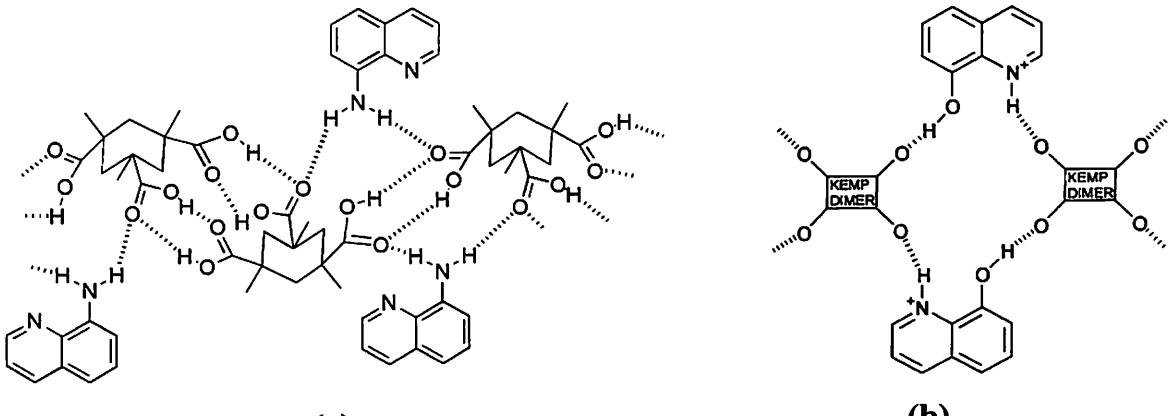

(a) **(b)**

Figure 1.5: Co-crystals of Kemp's triacid with (a) 8-aminoquinoline, and (b) 8-hydroxyquinoline

1.5.1 Ether linked quinolines

Ether linked quinoline derivatives have been used as podand-type receptors for the recognition of many metal cations since 1970s.[74] Attachment of rigid terminal groups bearing donor centres to oligoethylene glycol units affords neutral ligands which readily form stable crystalline complexes with alkali and alkaline earth metal ions in the same way as the cyclic crown ethers. Suitable terminal groups such as 8-quinolyloxy is used for the synthesis of such ligands (**1.21**).[75-76] Apart from the terminal group donor effect, geometrical and steric factors also play a role in guest encapsulation. For example, the compounds **1.22** (X = C-NO_2, and X = C-OCH_3) bearing an adequate number of proven donor atoms neither form crystalline complexes with alkali metal salts nor do they transfer alkali metal permanganates into

organic phases. This is because of the fact that the substituents apparently blocks approach of lignad for complexation.[75]

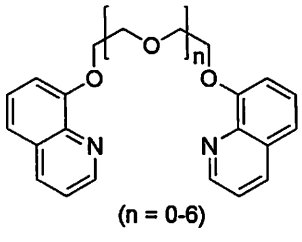

1.21

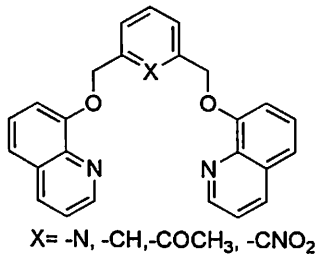

1.22

In case of ligand **1.23**, it is found that the terminal methyl group does not play a role in the complexation with metal ions; this is easily rationalized in terms of the helical structure of the ligand in the complex. The terminal quinoline moieties are also been attached by ester groups instead of ether groups (**1.24**).[77]

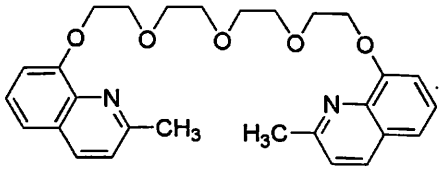

1.23

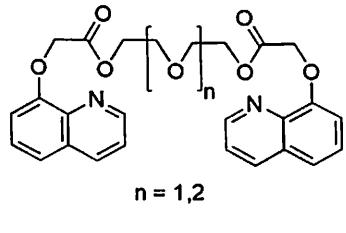

1.24

The podands **1.25**, which contain two pyridine rings as central unit and are therefore rigid enough to form crystalline complexes of alkali, alkaline earth, and transition metal ions. They can also form host-guest complex with urea and thiourea, with unusual ease.[74]

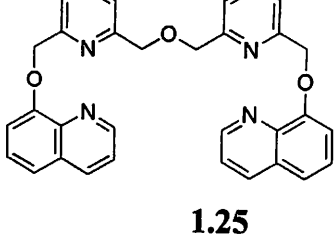

1.25

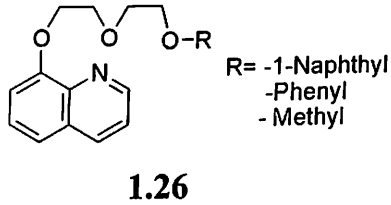

1.26

The tetra- to hexadentate neutral ligands containing a 8-quinolyloxy group, on the one side and a poor coordinating group such as naphthoxy, phenoxy, or methoxy group (**1.26**) on the other still can coordinate with various salts.[78]

Acyclic ligands having cryptand properties containing quinoline moiety (**1.27**) are reported to be excellent complexing agent for heavy metals. These types of neutral ligands have been designated as open-chain cryptands and they do indeed exhibit cryptand analogous complexation and phase transfer behaviour.[79] Quinoline based tetrapodand ligands (**1.28**) are also synthesized and their complexing ability is found to be lower than those tripodand ligands. This is because the four large terminal groups probably offer steric hindrance to complexation of small cations.[80]

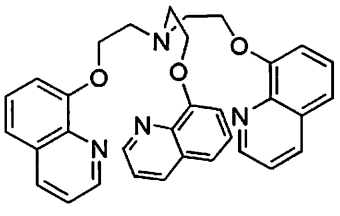

1.27

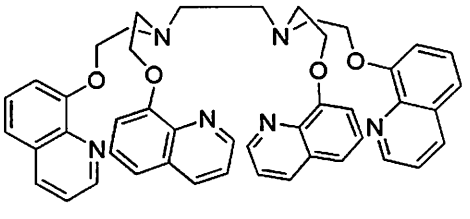

1.28

Tripodal hexadentate ligands (**1.29**), having three 2-methyl-8-hydroxyquinolyl groups as binding sites, binds to trivalent metal cations to form 1:1 complexes, and showed selective extractability for Ga^{3+} among trivalent cations of group 13 elements.[81]

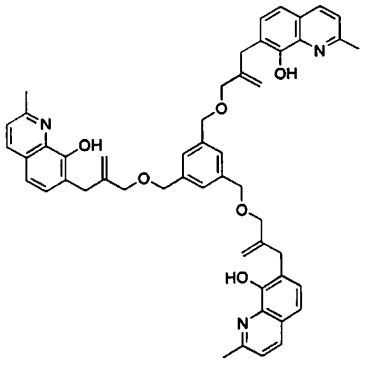

1.29

The synthesis and photophysical studies of a fluorescent sensors for Mg^{2+} ion based on diaza-18-crown-6 appended with two hydroxyquinoline groups bearing different substituents have been reported.[82-83] These molecules are effective chemosensors for different ions; in particular, some of them have high specificity for Mg^{2+} with negligible interference by Ca^{2+}. The macrocycle fluoresces in the presence of Mg^{2+} but not with other alkaline earth metal ions. The high sensitivity of the receptor **1.30** for magnesium and the strong response by fluorescence enable the use of this

compound for the detection of the divalent ion under strongly competing conditions. The magnesium ion is even sensed within the living cells.[84]

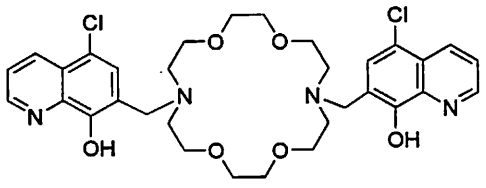

1.30

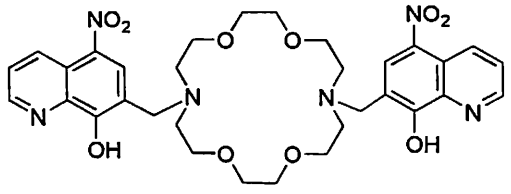

1.31

The replacement of the chlorine atoms on the 8-hydroxyquinoline moieties in **1.30** with nitro groups yields a compound **1.31** which is an effective fluorescent chemosensor for Hg^{2+} even in the presence of other metal cations, including Mg^{2+}. These types of crown ether conjugate of quinoline can stabilize metal ions through different modes of interactions as depicted in figure 1.6

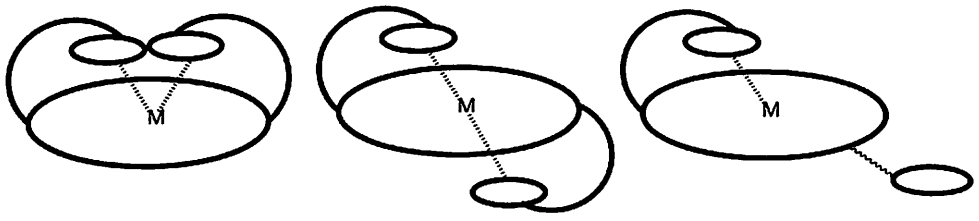

Figure 1.6: Different modes of interaction with metal ions of quinolinenate conjugate crown-ethers.

Meta-xylene spacer is used for the synthesis of receptors that can form compact, trinuclear circular helicate with silver (I) cations (scheme 1.15).[85]

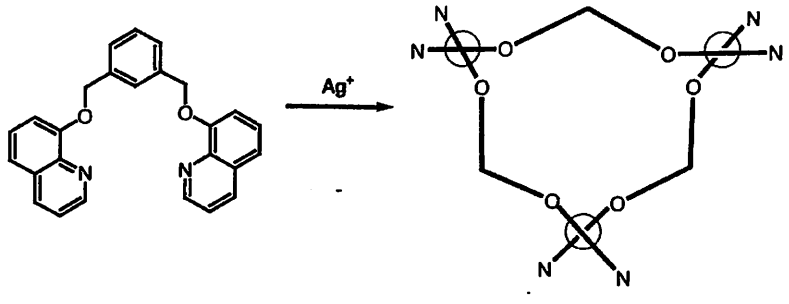

Scheme 1.15: Quinolinate ether ligands form a trinuclear circular helicate with silver ion (only schematic representation of the coordination compound is shown).

Ag(I) complexes containing the new highly flexible ligand *O,O*-bis(8-quinolyl)-1,8-dioxaoctane forms a linear polymeric structure with alternating configuration at the metal complex unit as shown in the scheme 1.16.[86]

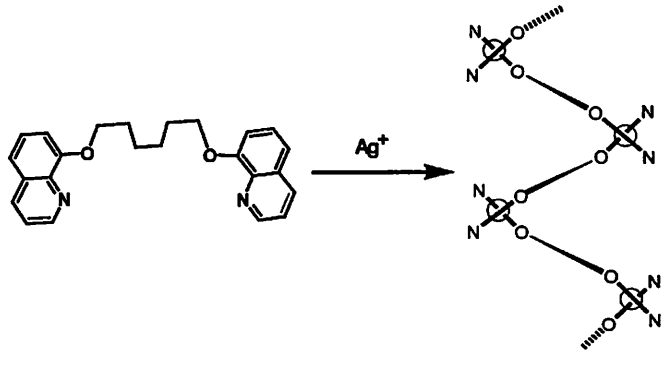

Scheme 1.16: Quinolinate ether ligands form a polymeric structure with silver ion (only schematic representation of the coordination compound is shown)

Calix[4]arene receptor modified with 8-hydroxyquinoline (**1.32**) through ether linkage exhibits luminescence and supramolecular energy transfer properties in the presence of coordinated Eu^{3+} and Tb^{3+} ions.[87]

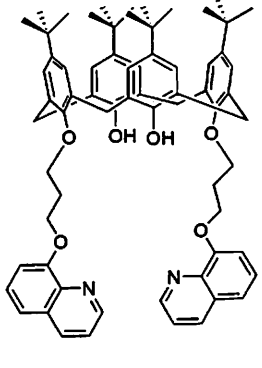

1.32

1.5.2. Amide based quinoline derivatives

Amide substituents are also added to hydroxyquinoline to introduce an additional hydrogen bond donor/acceptor units.[88] The introduction of a hydrogen bond donor/acceptor unit to 8-hydroxyquinoline as a substituent results in the formation of an intra-molecular hydrogen bonding and suppresses the formation of ten-membered rings as observed for 8-hydroxyquinoline. Thus, in this case a polymer is obtained which is connected by only one inter-molecular hydrogen bond between the amide NH and the aromatic nitrogen atom of quinoline as shown in figure 1.7.

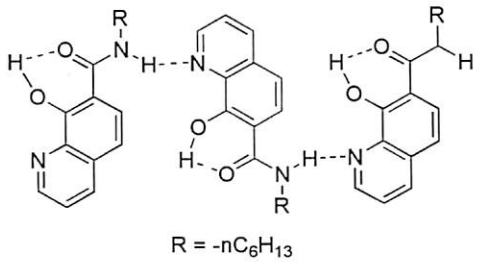

Figure 1.7: Hydrogen boned polymer of amide derivative of quinoline.

8-Hydroxyquinoline derived amides and study of their structural and acid recognition properties in solid and solution state are reported.[89] These types of receptors can adopt different orientations around the guest molecules; for instance one can encapsulate a guest anion by a head to head arrangement and other can adopt a head to tail arrangement as illustrated in figure 1.8. Various short range interactions that stabilize the host-guest complex are also described. These types of receptor can form either gel or a crystalline salt with different mineral acids.

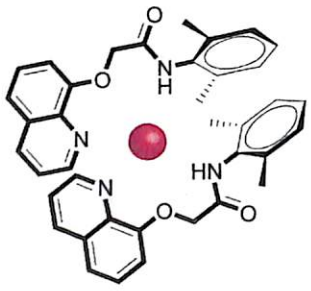

Head to Head arrangement

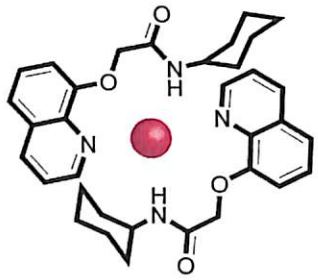

Head to Tail arrangement

Figure 1.8: Head to head and head to tail arrangement of receptors

Oligomers of the amide derivative of quinoline are synthesized and its helical orientation is established. When a (1S)-(-)-camphanyl moiety is introduced to such a oligomer (**1.31, 1.32**), helix handedness is completely shifts to right-handed helicity.[90]

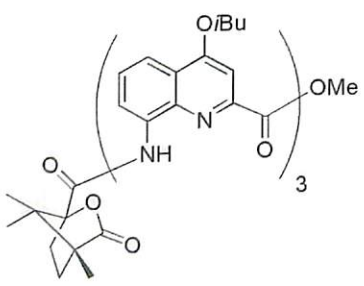

1.33

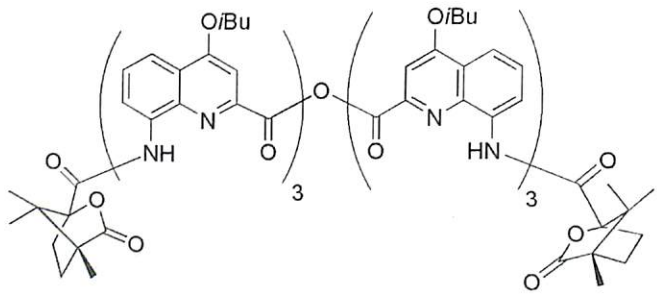

1.34

Both the oligomers are crystalline and their helical structures in solid state are illustrated. The helical orientation of the trimer (**1.33**) and the hexamer (**1.34**) are shown in figure 1.9.

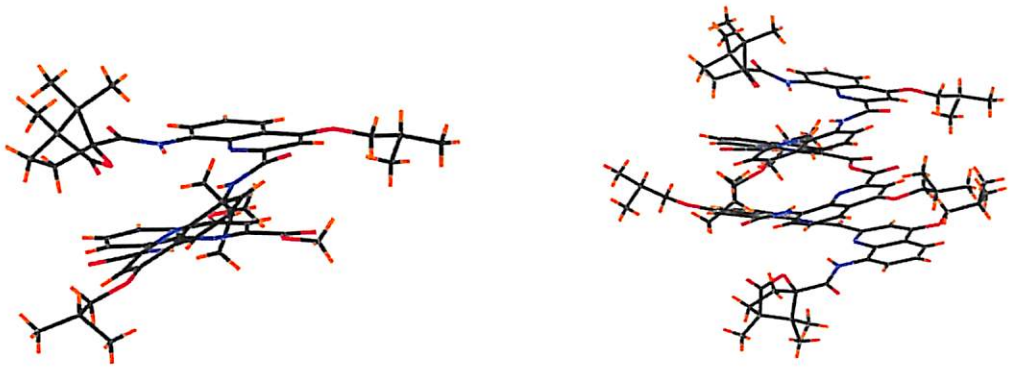

(a) (b)

Figure 1.9: Structures of (**a**) right-handed helical trimer and (**b**) hexamer.

Tetrapodal ligand containing 8-hydroxyquinoline (**1.35**) is reported which can form water soluble chelates with lanthanide ions such as Nd^{3+} and Yb^{3+}. Its lanthanide complexes are reported to be good sensitizer of the NIR luminescence.[91-92]

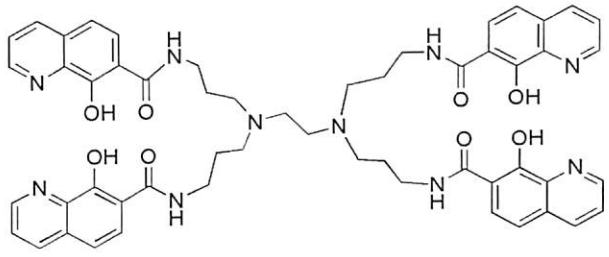

1.35

A copper complex of amide functionalized quinoline moiety as fluorophore has been used for anion recognition.

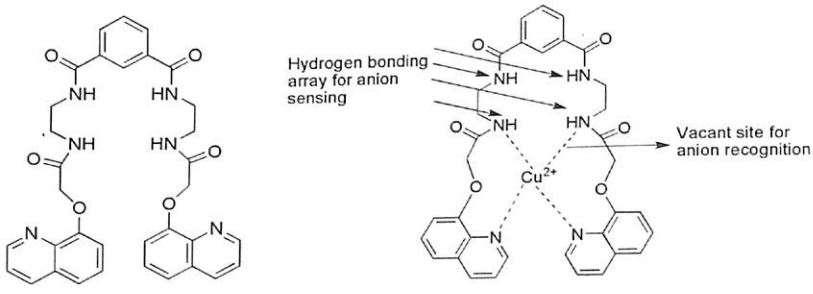

1.36 **1.37**

Figure 1.10: Structural modification of the receptor **1.36**, on coordination with copper.

The anion recognition behaviour of the receptor (**1.36**) and its copper complex (**1.37**) has been studied and the copper complex is found to shows high selectivity toward

acetate over other anions such as fluoride, chloride, bromide, iodide, DL-malate, L-mandelate, benzoate, isophthalate, phosphate, nitrate and sulphate.[93] The ligand undergoes structural modification on coordination with metal so that the anion binding is more favourable in its modified form (figure 1.10).

Another amide based quinoline receptor **1.38** bind anions with a selectivity of fluoride > cyanide > acetate and proved to be an efficient naked-eye detector for the fluoride and cyanide ion.[94]

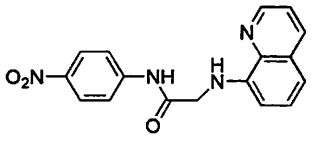

1.38

Boron complex appended with hydroxy and amide groups as proton donors and with quinolines having both proton acceptor and optical response (chromophore) properties has been synthesized. It's binding and the recognition ability with various anions is studied. The complex is found to be selective in recognizing phosphate anions.[95] The complex and its host-guest complex is shown in figure 1.11.

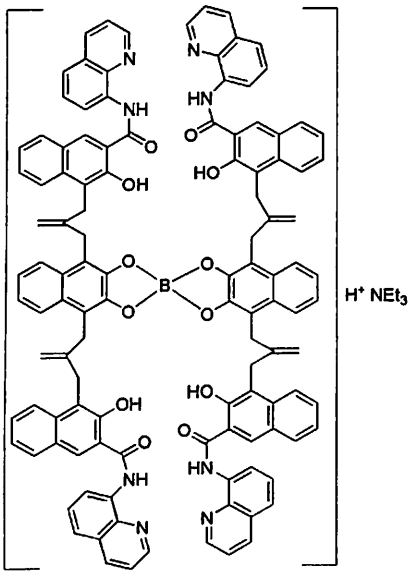

1.39

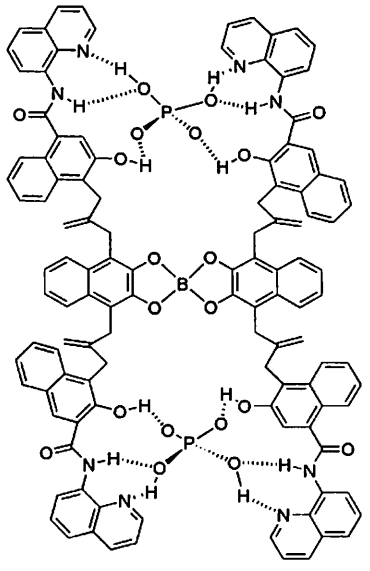

1.40

Figure 1.11: Boron complex having quinoline based amide derivative (**1.39**) and its host-guest complex with phosphate anion (**1.40**).

Quinoline containing receptors (**1.41, 1.42**) having multiple binding sites linked with both amide and ether linkage are also synthesized and their binding property with

various carboxylic acids are studied. Receptor **1.41** is able to distinguish hydroxy dicarboxylic acids from their non-hydroxy analogues and also aliphatic dicarboxylic acids from aromatic diacids.[96] Among various carboxylic acids, the receptor **1.42** shows high affinity towards tartaric acid and can be detected by fluorescence spectroscopy. The tartaric acid can be accommodated within the molecule **1.42** with numerous hydrogen bonding and forms a 1:1 host-guest complex **1.43**.[97]

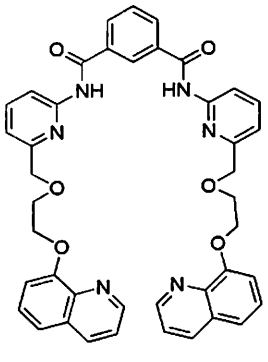

1.41

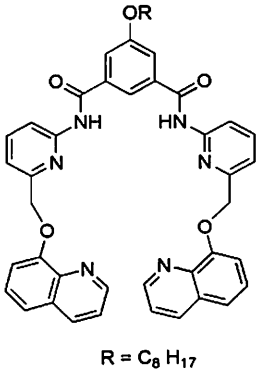

1.42

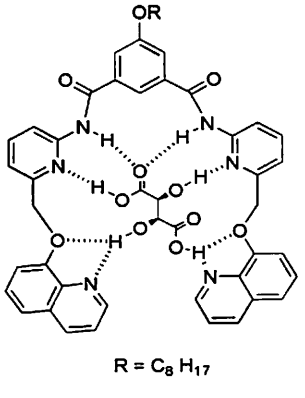

1.43

Dicationic receptors having amide functionality and quinoline moiety (**1.44**) have been synthesized and its anion binding abilities are compared with the neutral analogues. It is found that the cationic species binds anion much strongly than that of the neutral analogues; although the cationic species studied are relatively more hindered. The most important contribution to this stronger binding is the electrostatic attraction of anions to dicationic receptors.[98]

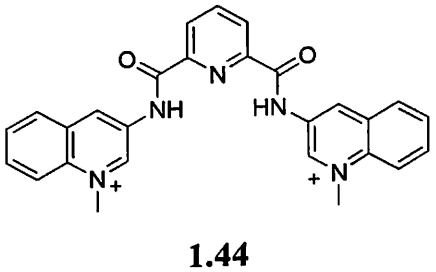

1.44

Amide based receptor of quinoline can be tuned to form nanocage structure which can be used as artificial chemosensors (scheme 1.17). This type of nanocage is used for fluorescent detection of nucleosides.[99-100]

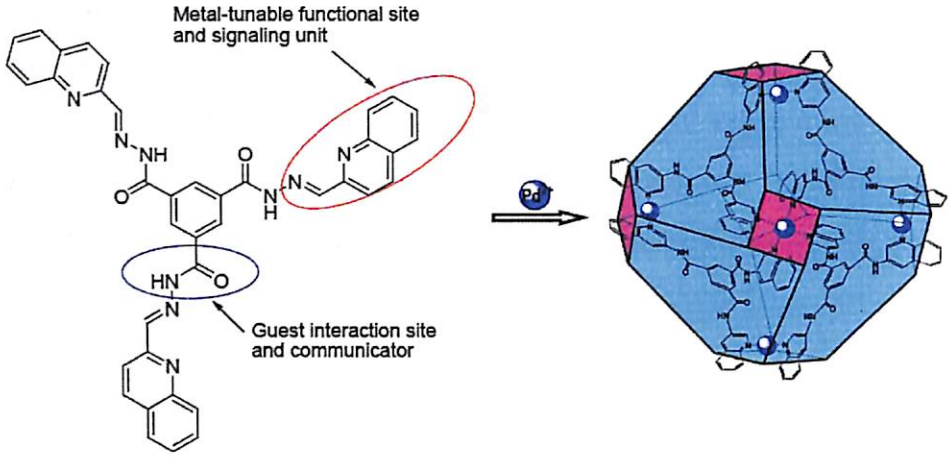

Scheme 1.17: Formation of nano cage from quinoline based amide receptor.

A new series of siderophore analogs based on the TREN (tris(2-aminoethyl)amine) spacer and related to sulfoxine subunits have been synthesized where the TREN backbone is connected through a trisamide moiety to the 2-position or the 7-position of sulfoxine. The structures of the two derivatives were named N-TRENSOX and O-TRENSOX, respectively (**1.45** and **1.46**). The O-TRENSOX is more selective towards iron than N-TRENSOX and it is used as iron sequestering agent.[101-102]

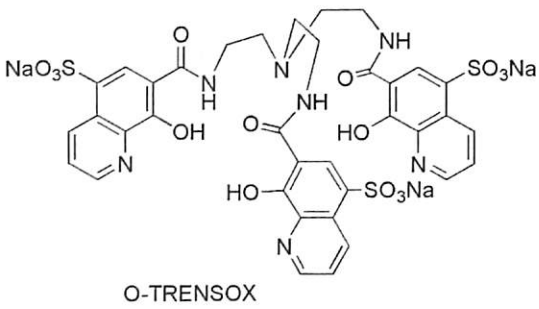

O-TRENSOX

1.45

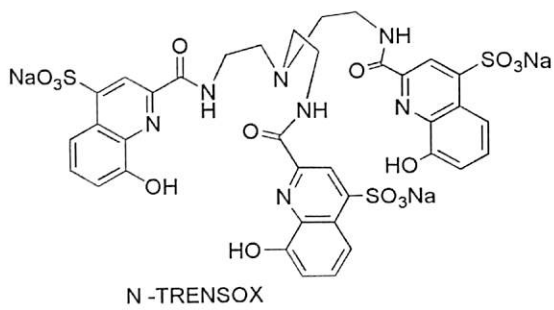

N -TRENSOX

1.46

1.5.3 Urea based quinoline derivatives

Urea and thiourea groups are excellent receptors for oxoanions such as carboxylates and phosphates to which they can donate two hydrogen bonds.[103] Receptors having both urea and amide functionality (**1.47**) have been synthesized and their anion binding property is explored (figure 1.12). These receptors are more selective towards small halide anions in comparison to the large halide anions.[104]

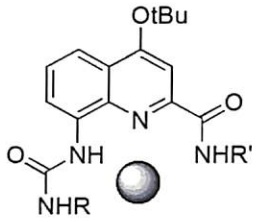

1.47

Figure 1.12: Encapsulation of spherical halide anion by a quinoline based urea derivative

The urea and amide derivative having quinoline moiety (**1.48**, **1.49**, **1.50**) have been compared for anion binding abilities. In all the derivatives, two acidic protons form intramolecular hydrogen bonds to the pyridine nitrogen atom and therefore are pre-orientated for an attractive interaction with anions. The amide receptor **1.48** binds chloride at room temperature in chloroform in a 1:1 ratio with very low association constant (Ka = 76 M^{-1}). In contrast to the amide derivative **1.48**, the urea derivatives **1.49**, **1.50** possess an additional hydrogen bond donor orientated toward the anion binding site. This one is not involved in hydrogen bonding and can strongly bind an anion, which is located "in front" of the receptor. Consequently, the binding constant increases. The urea receptor shows high affinity towards fluoride over other halides.[105]

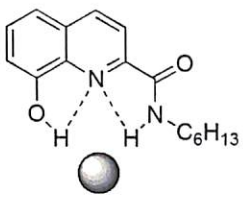

1.48

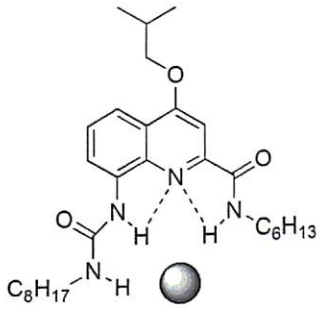

1.49

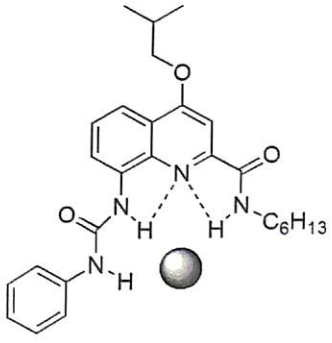

1.50

The fluorescent anion receptor **1.51** based on a quinoline backbone and on amide and urea side chains reveal a high affinity for fluoride over chloride and bromide.[106]

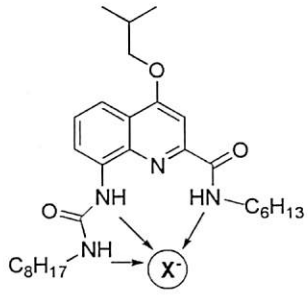

1.51

1.5.4. Diquinoline derivatives as host

Diquinoline molecules exhibit many interesting supramolecular features depending on the nature of the substituent present. For instance, the molecule **1.52** adopts a dimeric structure through a centrosymmetric edge-edge C-H···N interaction. However, in case of the molecule **1.53** such dimeric assemblies are not observed, instead a totally different π - halogen interaction stabilizes the structure (Figure 1.13).[107]

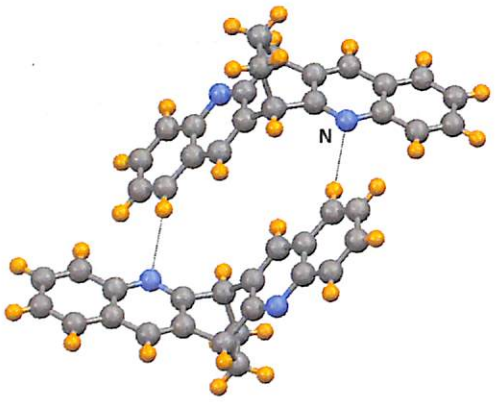

1.52

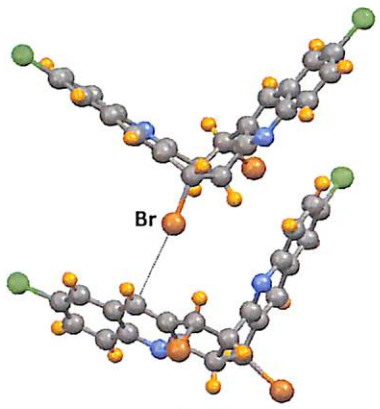

1.53

Figure 1.13: Examples of packing motifs commonly encountered among diquinoline compounds

The diquinoline hosts are generally consist of three basic structural sub-units: planar aromatic wings, central linker group, and exo-sensor groups as depicted in figure 1.14.[108-109]

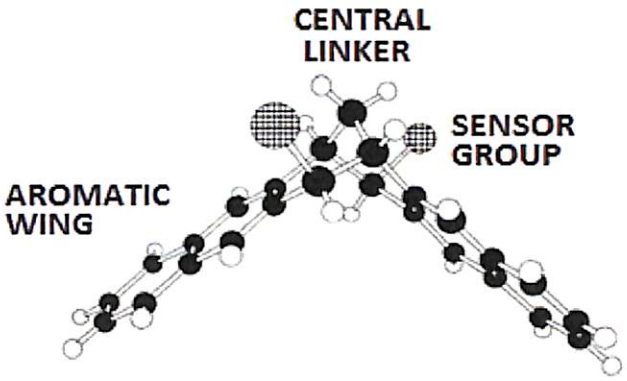

Figure 1.14: General features of diquinoline hosts

Many diquinoline derivatives have been synthesized and their host-guest chemistry is studied. Despite the close similarity of the host molecular structures, their supramolecular host-guest chemistry varies considerably.

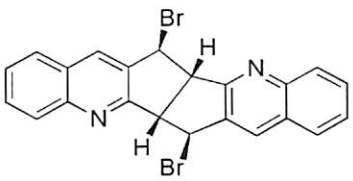

1.54

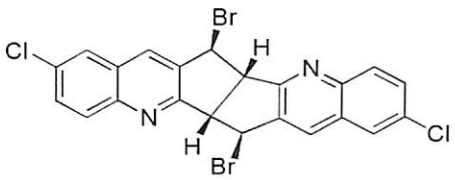

1.55

Compound **1.54**, for example, shows widespread inclusion behaviour in which two molecules of the host wrap around each guest enclosing it within a molecular pen (figure 1.15).[110] However, investigation of its chlorinated analogue **1.55** revealed an almost complete loss of inclusion properties.[107]

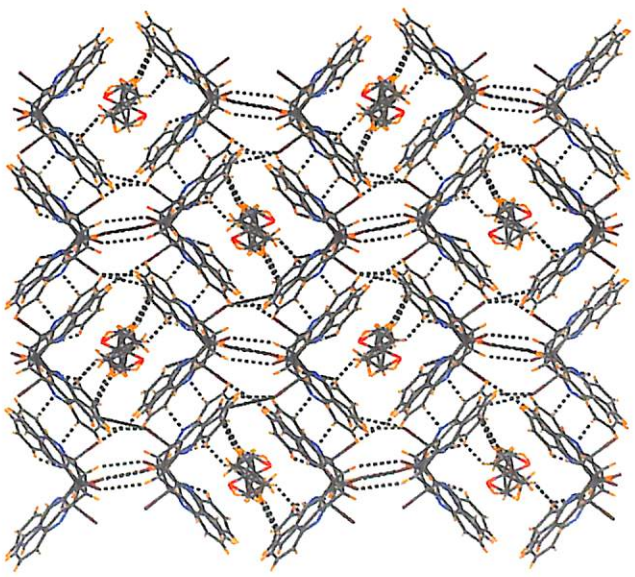

Figure 1.15: Encapsulation of acetone molecule by a diquinoline host **1.54**

When the central linker is modified to yield another chloro-substituted diquinoline dibromide **1.56**, its guest inclusion property remarkably changes. Diquinoline derivative **1.56** is a versatile host molecule that includes guest molecules of different functionality in several different ways. The inclusion properties of **1.56**, and the ways that it achieves these, are very different from those of its non-chlorinated parent, **1.57**.[111]

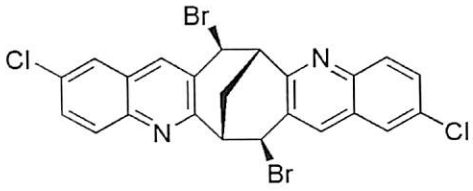

1.56

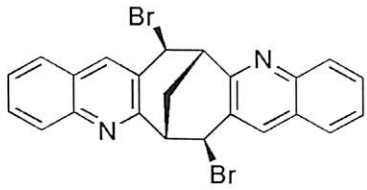

1.57

V-shaped diquinoline molecules are designed to have a degree of conformational flexibility and thereby allowing their compatibility with potential guest molecules or important intermolecular attractions. The sulphur-bridged compound **1.58** produces lattice inclusion compounds containing chloroform, dibromo-methane, water, and methanol which is in marked contrast to the non-inclusion characteristics shown by its corresponding oxygen analogues **1.59**. The inclusion of a dibromomethane molecule by two molecules of **1.58** is shown in figure 1.16.[112-113]

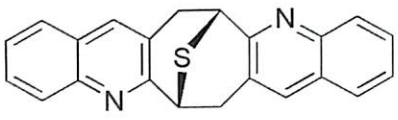

1.58

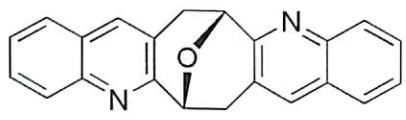

1.59

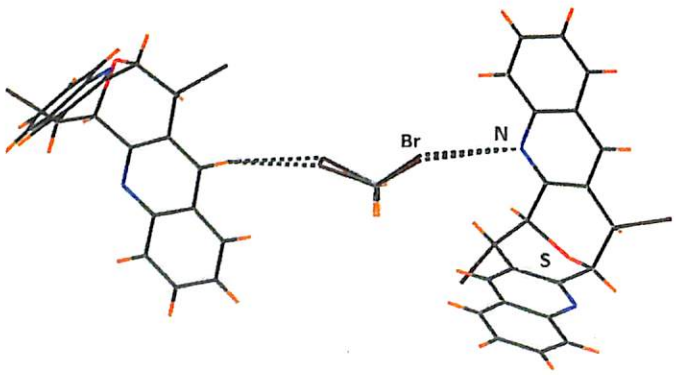

Figure 1.16: Encapsulation of dibromethane by sulphur-bridged diquinoline derivative

The tetrabromo (**1.60**) and tetraiodo (**1.61**) derivative of diquinoline has proved to be an excellent host for inclusion of a wide variety of small molecules such as dichloromethane, benzene, tetrahydrofuran, 1,1,2,2-tetrachloroethane, 1,1,1-trichloroethane, 1,1,2-trichloroethane, toluene, and ethyl acetate.[114] The inclusion of benzene molecule by **1.60** is shown in figure 1.17.

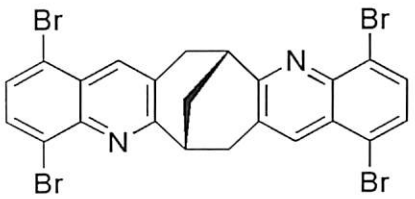

1.60

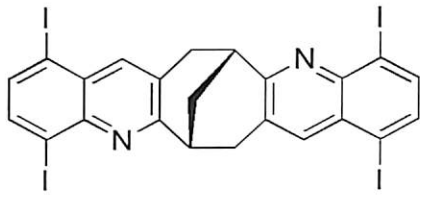

1.61

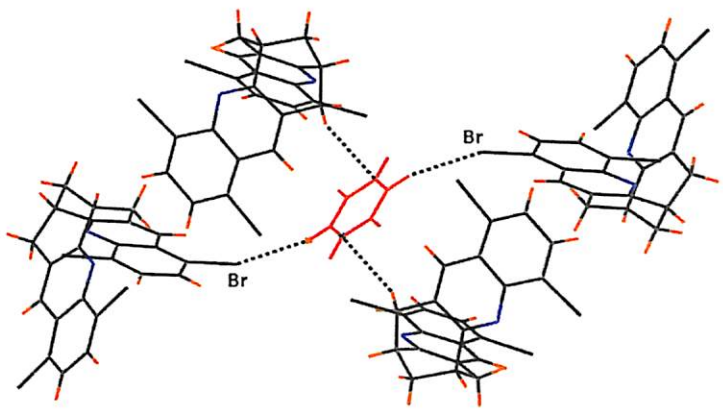

Figure 1.17: Encapsulation of a benzene molecule by a tetrabromo diquinoline host **1.60**.

Biquinoline linked β-cyclodextrin dimmers (**1.62**) have been synthesized and their metal complex are prepared (**1.63**). These receptors are found to be efficient fluorescent sensors for the molecular recognition of steroids.[115]

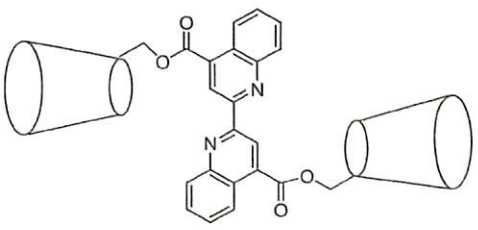

1.62

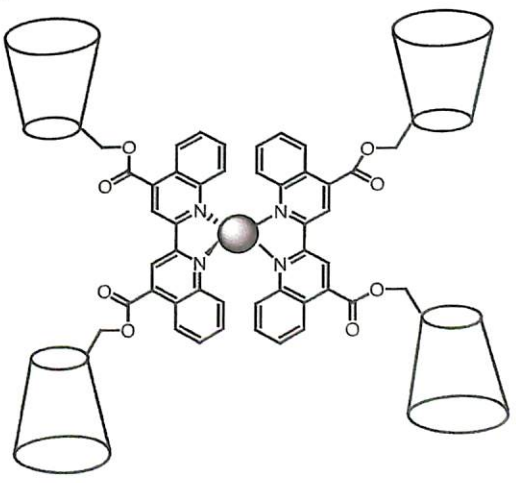

1.63

1.5.5. Schiff-base derivatives of quinoline as host

D-glucosamine group is linked with a quinoline moiety to form a receptor that can selectively recognize mercury(II) ion. The receptor in its free form shows a very weak fluorescence intensity which is enhanced drastically on addition of Hg^{2+} ion. The conformational change in the receptor on addition of mercury ion is shown in scheme 1.18. Further this receptor is used for fluorescence detection of Hg^{2+} ion in natural water.[116]

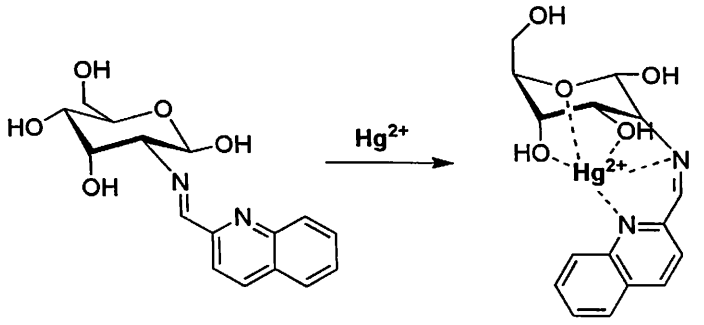

Fluorescence OFF **Fluorescence ON**

Scheme 1.18: Encapsulation of Hg^{2+} ion by the Schiff-base derivative of quinoline leading to fluorescence enhancement.

Quinoline based Schiff-base (**1.64** and **1.65**) are also used for selective fluorescent detection of Zn^{2+} ion which are highly selective for Zn^{2+} over biologically relevant alkali metals, alkaline earth metals and the first row transition metals such as Mn^{2+}, Fe^{2+}, Co^{2+} and Ni^{2+} in buffered aqueous DMSO solution.[117] Quinoline moiety is also linked with thiacalix[4]crown to sense Hg^{2+} and Zn^{2+} ions.[118]

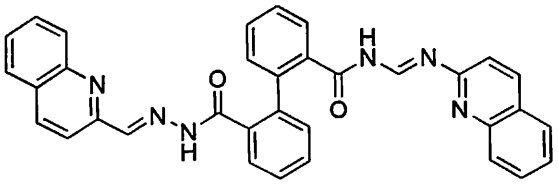

1.64

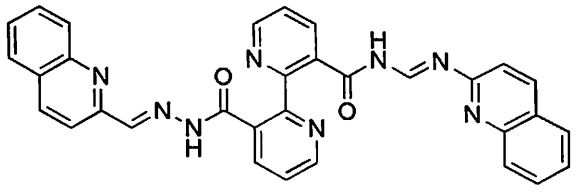

1.65

The Schiff-base receptor **1.66** is used as both visual and fluorescence sensors for Zn^{2+} ion. The receptor is capable of selectively recognize Zn^{2+} in presence of other metal ions such as Li^{+}, Na^{+}, K^{+}, Ag^{+}, Mg^{2+}, Ca^{2+}, Cu^{2+}, Co^{2+}, Cr^{2+}, Ni^{2+}, Fe^{2+}, Cd^{2+}, Hg^{2+}, Pb^{2+}. The addition of Zn^{2+} to a solution of **1.66** gives a yellow coloured solution, whereas other ions do not have effect on the colour of the parent solution.[119]

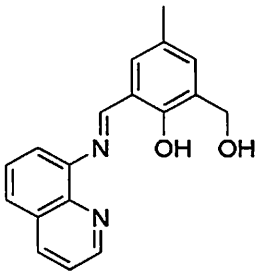

1.66

Enantiomerically pure Schiff-base of quinoline **1.67** and **1.68** can form double helices with a right or left handedness on complexation with copper (I) perchlorate. The copper complex adopts helical structure in solution; however, they can adopt both helical and non-helical structure in solid state.[120] Further the assembling/disassembling processes of the ligand **1.67** and **1.68** can be electrochemically controlled by a Cu(II)/Cu(I) couple.[121]

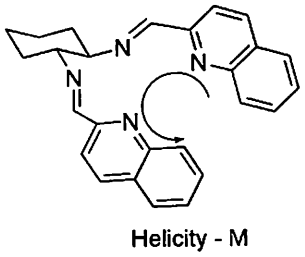

Helicity - M

1.67

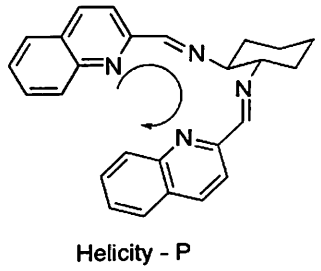

Helicity - P

1.68

A Schiff-base receptor of hydroxyquinoline (**1.69**) and its cobalt complex (**1.70**) are studied for recognition of various anions. The cobalt complex shows a dramatic colour change on coordination with anions. The selectivity and sensitivity of the receptor and its cobalt complex for sensing anions are also different.[122]

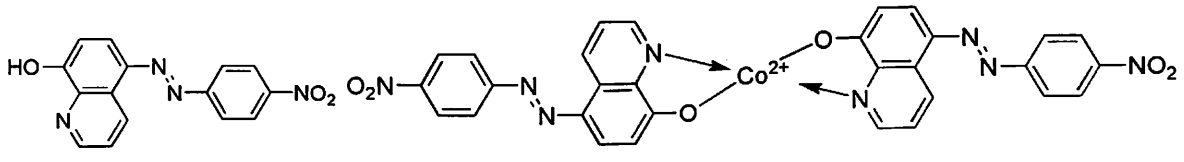

1.69 **1.70**

The host-guest interactions of **1.69** and a phosphate anion is shown in figure 1.18

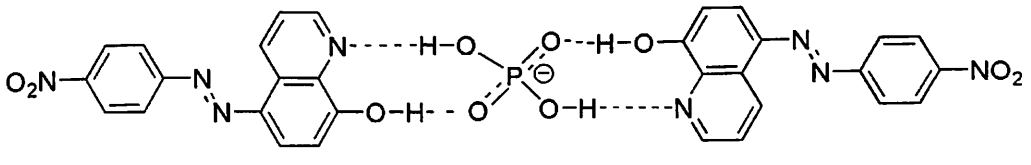

Figure 1.18: Host-guest complex of **1.69** with phosphate anion

1.6 pH sensing by quinoline derivative

Since the end groups of pyridyl N and -OH in the 8-hydroxyquinoline moiety are able to act as a weak acid and a weak base under acidic and basic conditions, respectively,[123] this moiety appears to be able to act as the pH indicator for both acidic and basic systems. Recently a series of 8-hydroxyquinoline-substituted boron-dipyrromethene derivatives have been synthesized which acts as OFF-ON-OFF type of pH-dependent fluorescent sensors. The receptors are highly fluorescent at neutral pH and the fluorescence is quenched on both acidic and basic medium. The quenching of fluorescence is due to the operation of a photoinduced electron transfer (PET) that take place in two opposite directions in acidic and basic conditions as illustrated in figure 1.19.[124]

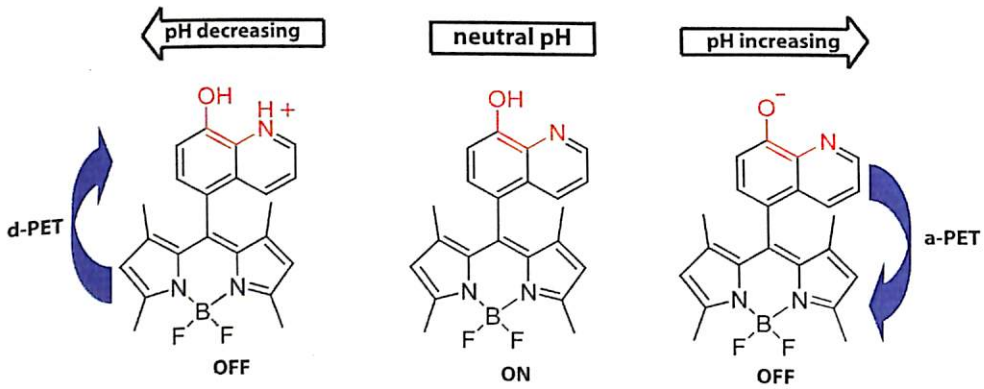

Figure 1.19: Photoinduced electron transfer mechanism in protonated quinolinium, neutral, and deprotonated quinolinate states

1.7 Co-ordination polymers of quinoline derivatives

Coordination compounds with infinite structures have been intensively studied, in particular, compounds with backbones constructed from metal ions as connectors and ligands as linkers, which is termed as coordination polymer. Similar supramolecular architectures are also called Metal-organic frameworks (MOFs).[125-133]

Pyridine carboxylic acids have been used as a good bridging ligand for the construction of metal organic polymers.[134-142] Another ligand having similar functional groups is quinoline carboxylic acid; which shows more structural diversity in the formation of metal organic frameworks.[143-150] This is because quinoline carboxylic acid has two primary structural characteristics that help in achieving such

structural diversity: quinoline carboxylic acid have larger conjugated π-systems, therefore π-π stacking interactions may play more important role in the formation of their complexes. Secondly, the larger conjugated π-systems as well as the steric hindrance of benzene rings probably weaken the coordination abilities of the quinoline N donors. The quinoline carboxylic acids can bind to metal centres in various modes which led to the formation of coordination polymers as illustrated in figure 1.20.

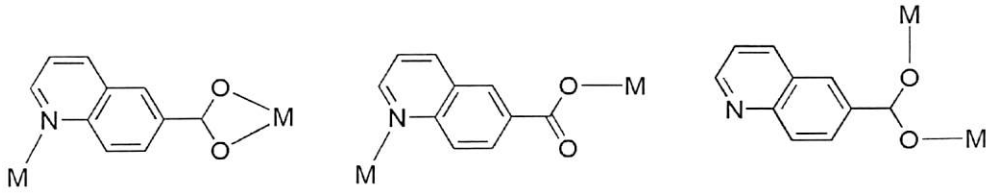

Figure 1.20: Binding modes of quinoline-6-carboxylic acid

Quinoline-6-carboxylic acid forms two dimensional coordination polymers with nickel(II), cobalt(II) and copper(II) salts with a wave like net structure (figure 1.21a). The coordination polymer forms uniform voids in its lattice as shown in the space fill model of figure 1.21b.[151]

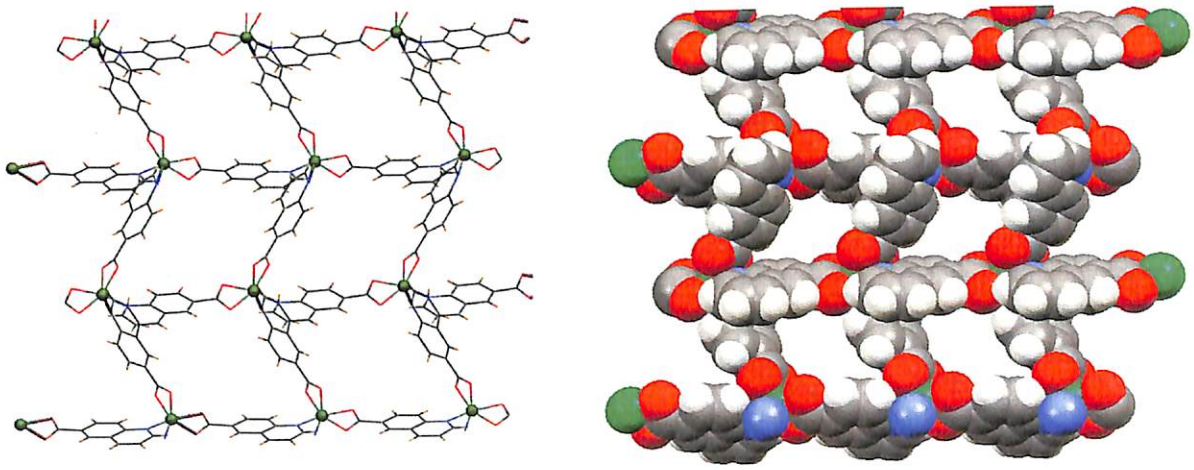

(a) **(b)**

Figure 1.21: (a) 2-D coordination polymer of quinoline-6-carboxylic acid with Nickel (II). (b) Space fill model showing uniform voids in the coordination polymer

Quinoline-4-carboxylic acid also forms a diverse range of coordination polymer ranging from one dimension to three dimensions with various metal salts.[149] Zn (II)

salts forms an one dimensional coordination polymer which is further extended to a three dimensional network through hydrogen bonding (figure 1.22).[147]

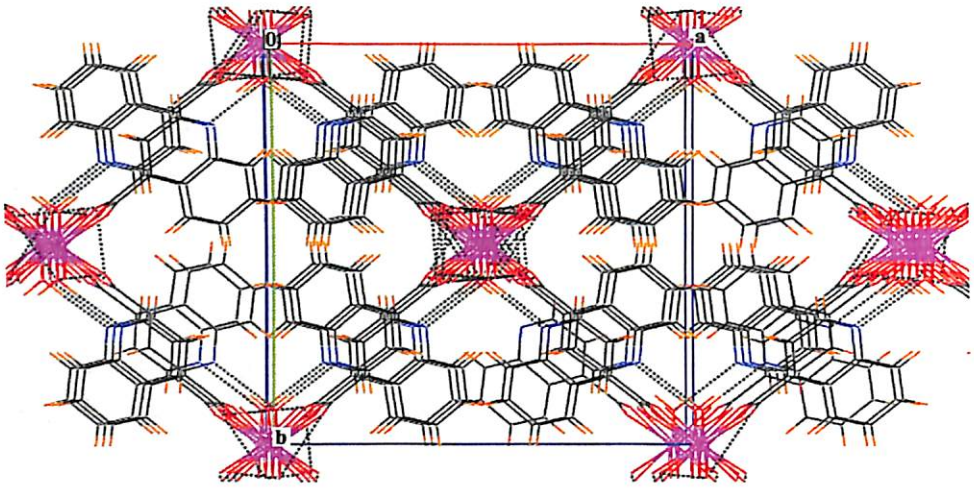

Figure 1.22: The 3D framework formed by hydrogen bonding interactions

Quinoline based chiral ligands with functional group other than carboxylic acid are reported to form homochiral coordination polymer. One example of such ligand and its coordination polymer with copper(II) is shown in figure 1.23.[152]

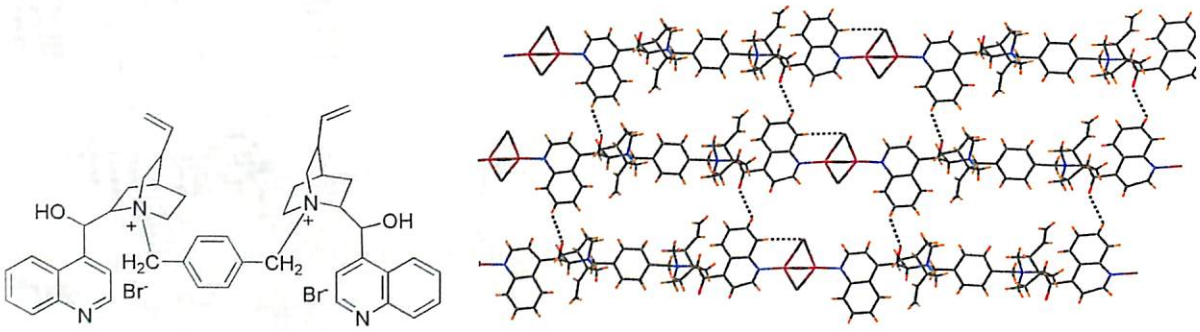

(a) **(b)**

Figure 1.23: (a) Quinoline based chiral ligand (b) 1-D coordination polymer extended to 2-D through hydrogen bonds

Another quinoline derivative; 8-quinolyloxy-acetic acid, with both a flexible and a rigid moiety, has multifunctional coordination sites which can form chelate as well as bridging complex through N, O atoms of quinolyl and carboxylate group (figure 1.24).[153-154]

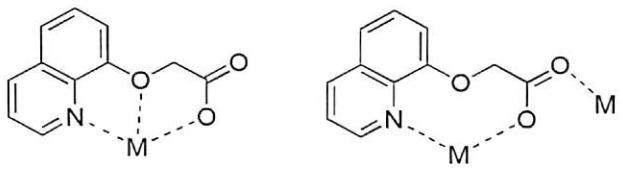

Figure 1.24: Binding modes of 8-quinolyloxy-acetate anion with metals

8-Quinolyloxy-acetic acid forms a helix chain polymer with copper(II) salt while it forms zig-zag chain polymers with nickel(II) and cobalt(II) salts (figure 1.24).[155] Under hydrothermal condition it forms 1-D, 2-D, and 3-D coordination polymers with lanthanide ions, namely Eu^{3+} and Gd^{3+} along with some other auxiliary ligand.[156]

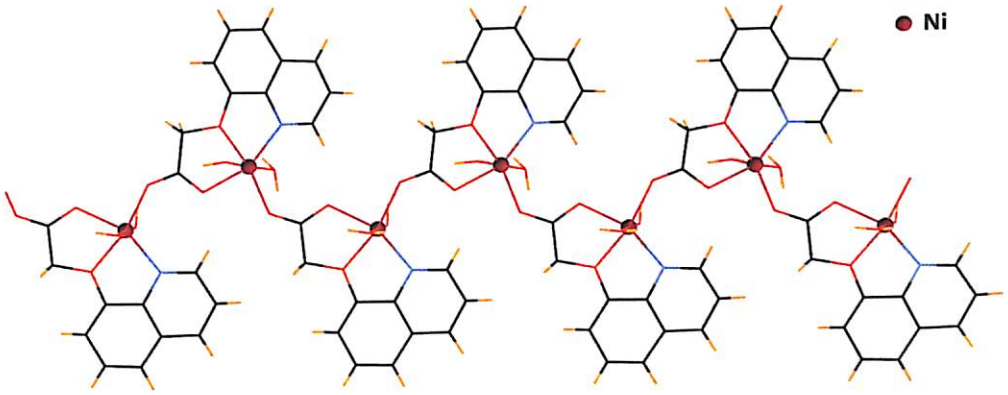

Figure 1.24: One dimensional zig-zag chain coordination polymer of 8-quinolyloxy-acetic acid with nickel (II)

In many quinoline carboxylic acids the N atom does not take part in the coordination with metal (figure 1.25) and hence coordination polymer is not observed.[157]

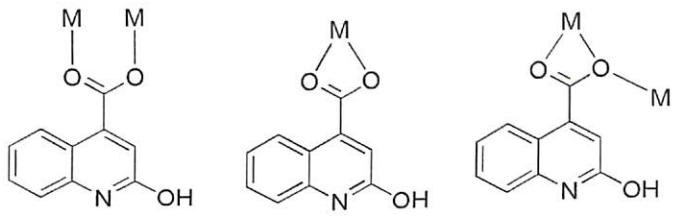

Figure 1.25: Binding modes of quinoline-2-hydroxy-6-carboxylic acid

1.8. Scope of the present work

Forgoing discussions describes the various applications of quinoline derivatives in the field of medicine, catalyst, materials, and electronics. Apart from these applications quinoline derivatives find versatile application as a supramolecular host in both anion and cation recognition. Among all the quinoline derivatives, 8-substituted quinolines such as 8-hydroxyquinoline and 8-aminoquinoline are the prototype for a large

number of supramolecular hosts. Functionalized 8-hydroxyquinoline and 8-aminoquinoline can form important supramolecular architecture such as podand, cryptand, lariat ethers etc[68-72,74]. These quinoline derivatives are also used as chelating agents for the separation of various metal ions.[5-7]

The quinoline derivatives have some additional advantages which make them molecules of choice for many supramolecular studies. They contain a readily available fluorophore, which makes the solution study much easier even in very trace concentrations. The quinoline group contains conjugated π-systems which provide an important contribution in stabilization of the supramolecular assemblies by π-π interactions. It is reported that 69% of 8-functionalised quinoline shows π-π interaction.[158] The quinoline N atom is basic in nature and thus can be easily protonated by various guest acids. The protonated form of quinoline provides an additional electrostatic interaction which can stabilize many anions thereby increasing the binding ability of the host. Further to this the quinoline ring is susceptible to both electrophilic and nucleophilic substitution reactions, which leaves a probability of some intra-molecular substitution reactions. These intra-molecular reactions in presence of some guests such as metal ions or some basic anions may lead to the formation of novel supramolecular architecture. The quinoline N atom can also be alkylated to increase the diversity of the receptors.

The amide and ester derivative of 8-amionoquinoline and 8-hydroxyquinoline provides a pre-organized cavity by adopting a cage-like structure that can hold various guest molecules. By applying appropriate spacer and receptors the orientation of the quinoline moiety can be controlled. A general feature of amide and ester linked supramolecular host in shown in figure 1.26.

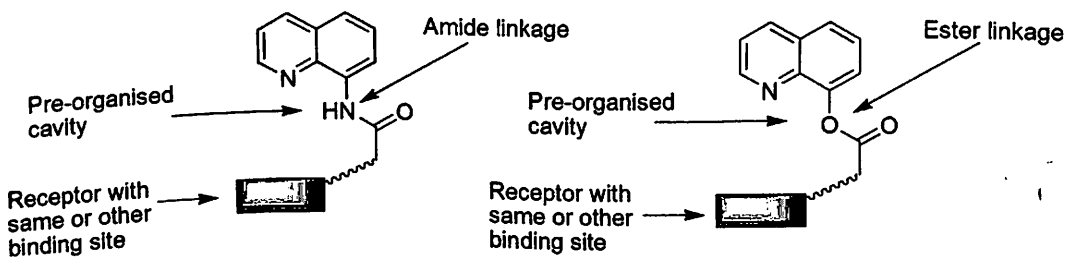

Figure 1.26: General features of ester and amide linked quinoline based supramolecular host

These types of receptors may form a monomeric assembly, dimeric assembly or a polymeric assembly depending on the nature of gust, spacer and the other receptor attached. A plausible mode of orientation of amide and ester derivative of quinoline is depicted in figure 1.27.

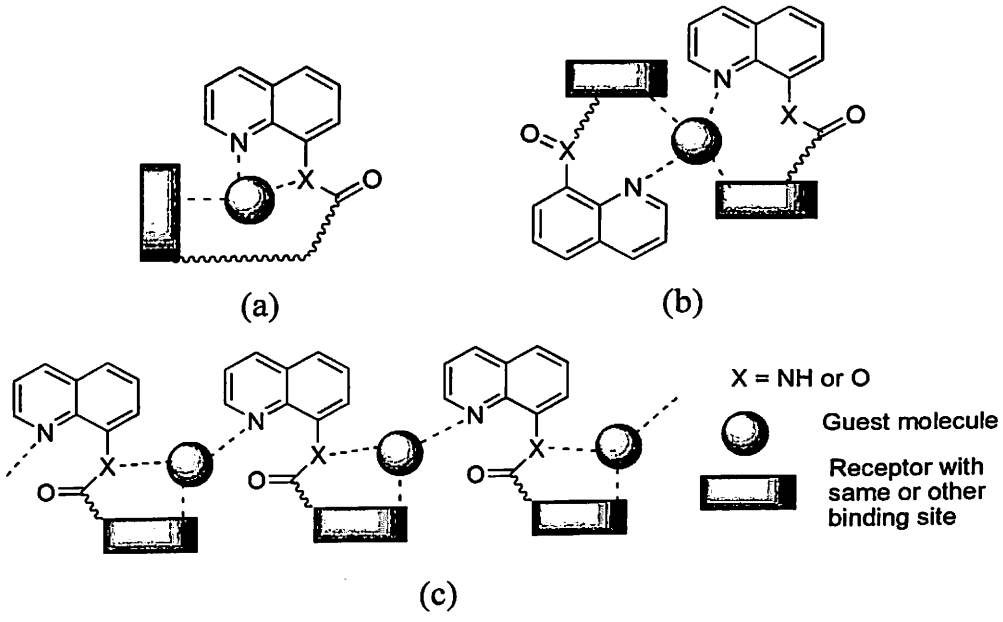

Figure 1.27: Plausible modes of interactions of amide and ester functionalized quinoline derivative with guest molecules; (a) monomeric assembly, (b) dimerci assembly, and (c) polymeric assembly

The rare-earth quinoline complexes are known for their near-infrared luminescence properties, hence they find a wide applications in optoelectronic devices.[159] The 8-hydroxyquinolinate complexes of neodymium (III), erbium (III), and ytterbium (III) are known to exhibit infrared luminescence[160-162] and they are also used for the fabrication of near-infrared-emitting OLEDs.[163-164] The tris(8-hydroxyquinolinato)-aluminum(III) complex exhibits intense green electroluminescence and is an active component in organic light-emitting diodes (OLEDs) operating in the visible region.[165-166]

Heterobinuclear lanthanide complexes with benzoxazole-substituted 8-hydroxyquinolines show bright near-infrared luminescence. These binuclear chelates display highest quantum yield of near-infrared luminescence for ytterbium complexes with organic ligand containing C-H bonds.[167]

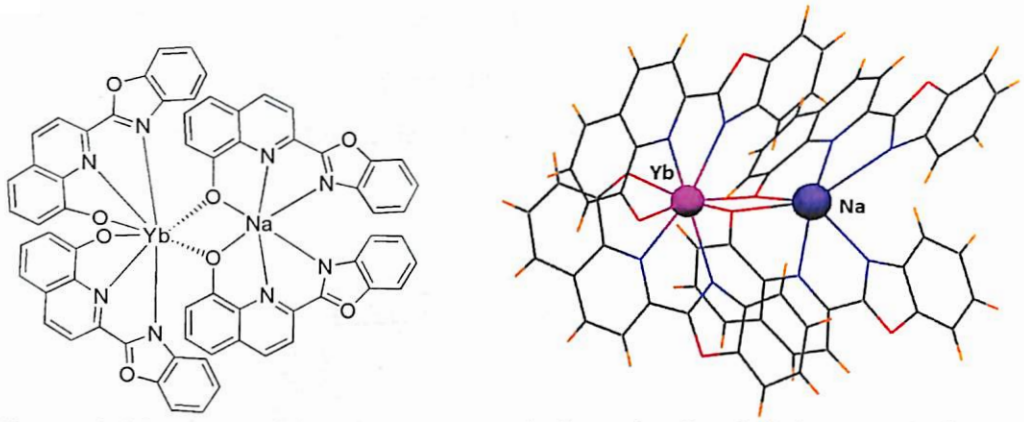

Figure 1.28: Hetero binuclear Yb-Na chelates having bright near-infrared luminescence

Thus, there is definite scope of the quinoline derivatives to study them as supramolecular assemblies, host-guest interactions and the reactivity of these derivatives under different conditions. With this background we have synthesized a number of quinoline derivatives and investigated their supramolecular assemblies, their guest inclusion properties in both solid and solution state. We have also investigated the reactivity of a series of quinoline derivatives under different conditions. The results obtained and the experimental details are discussed in the chapter followed.

References

1. F. F Runge, *Ann. Physik*, 1834, **31**, 68.
2. C. Gerhardt, *Annalen*, 1842, **42**, 310.
3. R. S. Hosmane and J. F. Liebman, *Struct. Chem.*, 2009, **20**, 693.
4. A. Albert and J. N. Phillips, *Journal of the Chemical Society (Resumed)*, 1956, 1294.
5. H. E. Zorel jr, C. A. Ribeiro and M. S. Crespi, *J. Mater. Sci. Lett.*, 2001, **20**, 621.
6. A. Y. Shen, C. P. Chenb and S. Raffler, *Life Sciences*, 1999, **64**, m-825.
7. F. Chang, S. Park and H. Kim, *Bull. Korean Chem., Soc.*, 2008, **29**, 1327.
8. R. Katakura and Y. Koide, *Inorg. Chem.*, 2006, **45**, 5730.
9. M. Cai, T. Xiao, R. Liu, Y. Chen, R. Shinar and J. Shinar, *Appl. Phys. Lett.*, 2011, **99**, 153303.

10. N. Rolfe, P. Desai, P. Shakya, T. Kreouzis and W. P. Gillin, *J. Appl. Phys.*, 2008, **104**, 083703.

11. E. Bardez, I. Devol, B. Larrey, and B.Valeur, *J. Phys. Chem. B*, 1997, **101**, 7786.

12. V. V. Kouznetsov, L. Y. V. Mendez and C. M. M. Gomez, *Curr. Org. Chem.*, 2005, **9**, 141.

13. C. S. Jia, Z. Zhang, S. J. Tu and G. W. Wang, *Org. Biomol. Chem.*, 2006, **4**, 104.

14. J. Wu, H. G. Xia and K. Gao, *Org. Biomol. Chem.*, 2006, **4**, 126.

15. J. S. Yadav, B. V. S. Reddy, P. Sreedhar, R. S. Rao and K. Nagaiah, *Synthesis*, 2004, 2381.

16. S. S. Palimkar, S. A. Siddiqui, T. Daniel, R. J. Lahoti and K. V. Srinivasan, *J. Org. Chem.*, 2003, **68**, 9371.

17. P. G. Dormer, K. K. Eng, R. N. Farr, G. H. Humphrey, J. C. McWilliams, P. J. Reider, J. W. Sager and R. P. Volante, *J. Org. Chem.*, 2003, **68**, 467.

18. R. H. F. Manske, *Chem. Rev.*, 1942, **30**, 113.

19. R. H. F. Manske and M. Kukla, *Org. React.*, 1953, **7**, 59.

20. F. W. Bergstrom, *Chem. Rev.*, 1944, **35**, 77.

21. G. Olahj, U. D. Olah and N. Overcchuk, *J. Org. Chem.*, 1965, **30**, 3373.

22. J. M. Khurana, *Chemistry of Heterocyclic Compounds*, 2006.

23. F. W. Bergstrom, H. G. Sturz and H. W. Tracy, *J. Org. Chem.*, 1946, **11**, 239.

24. A. R. Katritzky, C. A. Ramsden, J. A. Joule, V. V. Zhdankin, *Handbook of Heterocyclic Chemistry, 3rd Ed.*, 2010.

25. S. M. Lu, X. W. Han, Y. G. Zhou, *J. Organomet. Chem.*, 2007, **692**, 3065.

26. S. K. Roy, S. C. Roy and H. **S.** Rao, *J. appl. Chem. Biotechnol.*, 1973, **23**, 363.

27. M. Albrecht, M. Fiege and O. Osetska, *Coord. Chem. Rev.*, 2008, **252**, 812.

28. S. Aiki, A. Taketoshi, J. Kuwabara, T. Koizumi and T. Kanbara, *J. Organomet. Chem.*, 2011, **696**, 1301.

29. E. Błaż and J. Pielichowski, *Molecules* 2006, **11**, 115.

30. W. A. Ma and Z. X. Wang, *Organometallics*, 2011, **30**, 4364.

31. S. Zhang, W. H. Sun, T. Xiao and X. Hao, *Organometallics*, 2010, **29**, 1168.

32. W. H. Sun, Z. Li, H. Hu, B. Wu, H. Yang, N. Zhu, X. Leng and H. Wang, *New J. Chem.*, 2002, **26**, 1474.

33. A. Scrivanti, M. Bertoldini, U. Matteoli, S. Antonaroli and B. Crociani, *Tetrahedron*, 2009, **65**, 7611.
34. J. F. Sun, F. Chen, B. A. Dougan, H. J. Xu, Y. Cheng, Y. Z. Li, X. T. Chen and Z. L. Xue, *J. Organomet. Chem.*, 2009, **694**, 2096.
35. B. Crociani, S. Antonaroli, M. Burattini, F. Benetollo, A. Scrivanti and M. Bertoldini, *J. Organomet. Chem.*, 2008, **693**, 3932.
36. K. Komura, H. Nakamura and Y. Sugi, *J. Mol. Cat. A: Chemical*, 2008, **293**, 72.
37. M. Barbasiewicz, A. Szadkowska, R. Bujok and K. Grela, *Organometallics*, 2006, **25**, 3599.
38. M. Enders, P. Fernandez, G. Ludwig and H. Pritzkow, *Organometallics*, 2001, **20**, 5005.
39. P. Evans, P. Hogg,. R. Grigg, M. Nurnabi, J Hinsley, V. Sridharan, S. Suganthan, S. Korn, S. Collardb and J. E. Muirb, *Tetrahedron*, 2005, **61**, 9696.
40. W. J. Drury, N. Zimmermann, M. Keenan, M. Hayashi, S. Kaiser, R.Goddard and A. Pfaltz, *Angew. Chem. Int. Ed.*, 2004, **43**, 70.
41. P. L. Arnold, M. S. Sanford and S. M. Pearson, *J. Am. Chem. Soc.*, 2009, **131**, 13912.
42. A. G. M. M. Hossain, T. Nagaoka and K. Ogura *Electrochimica Acta.*, 1997, **42**, 2577.
43. P. A. Cameron, V. C. Gibson, C. Redshaw, J. A. Segal, M. D. Bruce, A. J. P. White and D. J. Williams, *Chem. Commun.*, 1999, 1883.
44. S. Levy and S. J. Azoulay, *Cardiovas. Electrophysiol.*, 1994, **5**, 635.
45. G. Jones, *Comprehensive Heterocyclic Chemistry II*; eds. A. R. Katritzky.
46. C. W. Rees and E. F. Scriven, Eds.; Pergamon: *Oxford* 1996, *5*, 167.
47. B. S. Holla, M. Mahalinga, M. S. Karthikeyan, P. M. Akberalib and N. S. Shettyc, *Bioorg. Med. Chem.* 2006, **14**, 2040.
48. O. Bilker, V. Lindo, M. Panico, A. E. Etiene, T. Paxton, A. Dell, M. Rogers, R. E. Sinden and H. R. Morris, *Nature*, 1998, **392**, 289.
49. G. Roma, M. D. Braccio, G. Grossi, F. Mattioli and H. Ghia, *Eur. J. Med. Chem.*, 2000, **35**, 1021.
50. Y. L. Chen, K. C. Fang, J. Y. Sheu, S. L. Hsu and C. C. Tzeng, *J. Med. Chem.* 2000, **44**, 2374.

51. P. A. Winstanley, *Parasitol Today*, 2000, **16**, 146.
52. V. P. Christopher, *The Journal of Experimental Biology*, 2003, **206**, 3745.
53. V. K. Zishiri, M. C. Joshi, R. Hunter, K. Chibale, P. J. Smith, R. L. Summers, R. E. Martin and T. J. Egan, *J. Med. Chem.*, 2011, **54** 6956.
54. M. Foley and L. Tilley, *Pharmacol. Ther.*, 1998, **79**, 55.
55. R. Klingenstein, P. Melnyk, S. R. Leliveld, A. Ryckebusch, and C. Korth, *J. Med. Chem.*, 2006, **49**, 5300.
56. K. C. Fang, Y. L. Chen, J. Y. Sheu, T. C. Wang and C. C. Tzeng, *J. Med. Chem.*, 2000, **43**, 3809.
57. J. Chevalier, S. Atifi, A. Eyraud, A. Mahamoud, J. Barbe and J. M. Pages, *J. Med. Chem.*, 2001, **44**, 4023.
58. L.T. Phan, T. Jian, Z. Chen, Y. L. Qiu, Z. Wang, T. Beach, A. Polemeropoulos and Y. S. Or, *J. Med. Chem.*, 2004, **47**, 2965.
59. R. Klingenstein, P. Melnyk, S. R. Leliveld, A. Ryckebusch and C. Korth, *J. Med. Chem.*, 2006, **49**, 5300.
60. S. J. Benkovic, S. J. Baker, M. R. K. Alley, Y. H. Woo, Y. K. Zhang, T. Akama, W. Mao, J. Baboval, P. T. R. Rajagopalan, M. Wall, L. S. Kahng, A. Tavassoli and L. Shapiro, *J. Med. Chem.*, 2005, **48**, 7468.
61. L. Y. Vargas, M. V. Castelli, V. V. Kouznetsov J. M., Urbina, S. N. Lopez, M. Sortino, R. D. Enriz, J. C. Ribas and S. Zacchino, *Bioorg. Med. Chem.*, 2003, **11**, 1531.
62. M. Singh, M. P. Singh and S. Y. Ablordeppey, *Drug Dev. Ind. Pharm.*, 1996, **22**, 377.
63. L. Dassonneville, K. Bonjean, M. C. De Pauw- Gillet, P. Colson, C. Houssier, J. Q. Leclercq, L. Angenot and S. Y. Ablordeppey, *Bioorg. Med. Chem.* 2002, **10**, 1337.
64. J. Jampilek, R. Musiol, M. Pesko, K. Kralova, M. Vejsova, J. Carroll, A. Coffey, J. Finster, D. Tabak, H. Niedbala, V. Kozik, J. Polanski, J. Csollei and J. Dohnal, *Molecules* 2009, **14**, 1145.
65. C. Bailly, *Biochemistry*, 1999, **38**, 7719.
66. C. Bailly, W. Laine, B. Baldeyrou, M. C. De Pauw-Gillet, P. Colson, C. Houssier, K. Cimanga, S. V. Miert, A. J. Vlietinck, L. Pieters, *Anti-Cancer Drug Des.*, 2000, **15**, 191.

67. L. Dassonneville, A. Lansiaux, A. Wattelet, N. Wattez, C. Mahieu, S. Van Miert, L. Pieters and C. Bailly, *Eur. J. Pharmacol.*, 2000, **409**, 9.
68. M. Albrecht, O. Blau, E. Wegelius and K. Rissanen, *New J. Chem.*, 1999, **23**, 667.
69. M. Albrecht, M. Fiege and O. Osetska, *Coord. Chem. Rev.*, 2008, **252**, 812.
70. M. Albrecht, O. Blau and R. Frohlich, *Chem. Eur. J.*, 1999, **5**, 48.
71. M. Albrecht, O. Blau, E. Wegelius and K. Rissanen, *New. J. Chem.*, 1999, **23**, 667.
72. M. Albrecht, O. Blau, K. Witt, E. Wegelius, M. Nissinen, K. Rissanen and R. Frohlich, *Synthesis*, 1999, 1819.
73. G. Smith, U. D. Wermuth and J. M. White, *Chem. Commun.*, 2000, 2349.
74. F. Vogtle and E. Weber, *Angew. Chem. Int. Ed. Engl.*, 1979, **18**, 753.
75. F. Vugfle and H. Sieger, *Angew. Chem.*, 1977, **89**, 410.
76. E. Weber and F. Vogrle, *Tetrahedron Lett.*, 1975, 2415.
77. W. Racshofer, W. M. Muller and F. Vogie, *ibid.* 1979, **112**, 2095.
78. U. Heimann and F. Vdgtle, *Angew. Chem. Int. Ed.*, 1978, **17**, 197.
79. F. Vogtk and W. M. Muller and E. Buhleier, *Angew. Chem. Int. Ed.*, 1977, **16**, 548.
80. F. Vigtle, W. M. Miiller, E. Buhleier and W. Wehner, *Chem. Ber.*, 1979, **112**, 899.
81. M. Hayashi, M. Ishii, K. Hiratani and K. Saigo, *Tetrahedron Lett.*, 1998, **39** 6215.
82. A. V. Bordunov, J. S. Bradshaw, X. X. Zhang, N. K. Dalley, X. Kou and R. M Izatt, *Inorg. Chem.*, 1996, **35**, 7229.
83. L. Prodi, F. Bolletta, M. Montalti, N. Zaccheroni, P. B. Savage, J. S. Bradshaw and R. M. Izatt, *Tetrahedron Lett.*, 1998, **39**, 5451.
84. G. Farruggia, S. Iotti, L. Prodi, M. Montalti, N. Zaccheroni, P. B. Savage, V. Trapani, P. Sale and F. I. Wolf, *J. Am. Chem. Soc.*, 2006, **128**, 344.
85. R.A. Muna, A, Mandhary and P. J. Steel, *Inorg. Chem. Commun.*, 2002, **5**, 954.
86. Y. P. Cai, H. X. Zhang, A. W. Xu, C. Y. Su, C. L. Chen, H. Q. Liu, L. Zhang and B. S. Kang, *J. Chem. Soc., Dalton Trans.*, 2001, 2429.
87. I. A. Bagatin and H. E. Toma, *New J. Chem.*, 2000, **24**, 841.

88. M. Albrecht, K. Witt, E. Wegelius and K. Rissanen, *Tetrahedron*, 2000, **56**, 591.

89. A. Karmakar, R. J. Sarma. and J. B. Baruah, CrystEngComm., 2007, **9**, 379.

90. A. M. Kendhale, L. Poniman, Z. Dong, K. L. Reddy, B. Kauffmann, Y. Ferrand and I. Huc, *J. Org. Chem.*, 2011, **76**, 195.

91. D. Imbert, S. Comby, A. S. Chauvin and J. C. G. Bunzli, *Chem. Commun.*, 2005, 1432.

92. S. Comby, D. Imbert, A. S. Chauvin and J. C. G. Bu1nzli, *Inorg. Chem.*, 2006, **45**, 732.

93. S. Goswami and R. Chakrabarty, *Tetrahedron Lett.*, 2009, **50**, 5994.

94. J. Kang , S. P. Jang , Y. H. Kim, J. H. Lee, E. B. Park, H. G. Lee, J. H. Kim, Y. Kim, S. J. Kim and C. Kim, *Tetrahedron Lett.*, 2010, **51**, 6658.

95. N. Kameta and K. Hiratani, *Chem. Commun.*, 2005, 725.

96. K. Ghosh, S. Adhikari1, A. P. Chattopadhyay and P. R. Chowdhury, *Beilstein Journal of Organic Chemistry*, 2008, **4**, 52.

97. K. Ghosh and S. Adhikari; *Tetrahedron Lett.*, 2006, **47**, 3577.

98. A. D. Gonzalez, H. Hopfl, F. Medrano and A. K. Yatsimirsky *J. Org. Chem.*, 2010, **75**, 2259.

99. C. He, Z. Lin, Z. He, C. Duan, C. Xu, Z. Wang, and C. Yan, *Angew. Chem. Int. Ed.* 2008, **47**, 877.

100. Y. Liu, X. Wu, C. He, R. Zhang and C. Duan, *Dalton Trans.*, 2008, 5866.

101. P. Baret, C. G. Beguin, H. Boukhalfa, C. Caris, J. P. Laulhtre, J. L. Pierre and G. Serratrice, *J. Am. Chem. Soc.*, 1995, **117**, 9760.

102. G. Serratrice, H. Boukhalfa, C. Beguin, P. Baret, C. Caris and J. L. Pierre, *Inorg. Chem.*, 1997, **36**, 3898.

103. P. A. Gale, S. E. G. Garrido and J. Garric, *Chem. Soc. Rev.*, 2008, **37**, 151.

104. M. Albrecht, Triyanti, S. Schiffers, O. Osetska, G. Raabe, T. Wieland, L. Russo and K. Rissanen, *Eur. J. Org. Chem.*, 2007, 2850.

105. M. Albrecht, *Naturwissenschaften*, 2007, **94**, 951.

106. M. Albrecht, T. M. Groot, M. Bahr and E. Weinhold, *Synlett*, 2005, 2095.

107. S. F. Alshahateet, A. N. M. M. Rahman, R. Bishop, D. C. Craig and M. L. Scudder, *CrystEngComm.*, 2002, **4** , 585.

108. A. N. M. M. Rahman, R. Bishop, D. C. Craig and M. L Scudder, *J. Supramol. Chem.* 2002, **2**, 409.
109. S. F. Alshahateet, R. Bishop, D. C. Craig and M. L. Scudder, *Cryst. Growth Des.*, 2004, **4**, 837.
110. A. N. M. M. Rahman, R. Bishop, D. C. Craig and M. L. Scudder, *Eur. J. Org. Chem.*, 2003, 72.
111. J. Ashmore, R. Bishop, D. C. Craig and M. L. Scudder, *Cryst. Growth Des.*, 2007, **7**, 47.
112. S. F. Alshahateet, R. Bishop, D. C. Craig and M. L. Scudder, *Cryst. Growth Des.*, 2010, **10**, 1742.
113. Solhe F. S. F. Alshahateet, R. Bishop, D. C. Craig and M. L. Scudder, *Cryst. Growth Des.*, 2011, **11**, 4474.
114. A. Noman, M. M. Rahman, R. Bishop, D. C. Craig, C. E. Marjo and M. L. Scudder, *Cryst. Growth Des.*, 2002, **2**, 421.
115. Y. Liu, Y. Song, Y. Chen, X.Q. Li, F. Ding and R.Q. Zhong, *Chem. Eur. J.*, 2004, **10**, 3685.
116. S. Ou, Z. Lin, C. Duan, H. Zhang and Z. Bai, *Chem. Commun.*, 2006, 4392.
117. D. Y. Wu, L. X. Xie, C. L. Zhang, C.Y. Duan, G. Zhao and Z. Guo, *Dalton Trans.*, 2006, 3528.
118. M. Kumar, A. Dhir and V. Bhalla, *Dalton Trans.*, 2010, **39**, 10122.
119. X. Zhou, B. Yu, Y. Guo, X. Tang, H. Zhang and W. Liu, *Inorg. Chem.*, 2010, **49**, 4002.
120. V. Amendola, L. Fabbrizzi, C. Mangano, P. Pallavicini, E. Roboli and M. Zema, *Inorg. Chem.*, 2000, **39**, 5803.
121. V. Amendola, L. Fabbrizzi, L. Linati, C. Mangano, P. Pallavicini, V. Pedrazzini and M. Zema, *Chem. Eur. J.*, 1999, **5**, 3679.
122. F. Y. Wu., X. F. Tan, Y. M. Wu and Y. Q. Zhao, *Spectrochimica Acta Part A*, 2006, **65**, 925.
123. E. Bardez, I. Devol, B. Larrey and B. J. Valeur, *Phys. Chem. B.*, 1997, **101**, 7786.
124. Y. Chen, H. Wang, L. Wan, Y. Bian and J. Jiang, *J. Org. Chem.*, 2011, **76**, 3774.

125. A. J. Blake, N. R. Champness, P. Hubberstey, W.S. Li, M. A. Withersby and M. SchrTder, *Coord. Chem. Rev.*, 1999, **183**, 117.
126. M. Eddaoudi, D. B. Moler, H. Li, B. Chen, T. M. Reineke, M. O'Keeffe and O. M. Yaghi, *Acc. Chem. Res.*, 2001, **34**, 319.
127. O. R. Evans and W. Lin, *Acc. Chem. Res.*, 2002, **35**, 511.
128. K. Kim, *Chem. Soc. Rev.*, 2002, **31**, 96.
129. S. Kitagawa, S. Kawata, *Coord. Chem. Rev.* 2002, **224**, 11.
130. B. Moulton, M. J. Zaworotko, *Chem. Rev.*, 2001, **101**, 1629.
131. O. M. Yaghi, H. Li, C. Davis, D. Richardson and T. L. Groy, *Acc. Chem. Res.*, 1998, **31**, 474.
132. M. J. Zaworotko, *Chem. Soc. Rev.*, 1994, **23**, 283.
133. S. L. James, *Chem. Soc. Rev.*, 2003, **32**, 276.
134. J. Y. Lu and A. M. Babb, *Chem. Commun.*, 2001, 821.
135. M. E. Chapman, P. Ayyappan, B. M. Foxman, G. T. Yee and W. B. Lin, *Cryst. Growth Des.*, 2001, **1**, 159.
136. S. L. Zheng, M. L. Tong, X. L. Yu and X. M. Chen, *J. Chem. Soc. Dalton Trans.*, 2001, 586.
137. K. S. Min and M. P. Suh, *Eur. J. Inorg. Chem.*, 2001, 449.
138. O. R. Evans and W. B. Lin, *Inorg. Chem.*, 2000, **39**, 2189.
139. O. R. Evans, R. G. Xiong, Z. Y. Wang, G. K. Wong and W. B. Lin, *Angew. Chem. Int. Ed.*, 1999, **38**, 536.
140. O. R. Evans, Z. Y. Wang, R. G. Xiong, B. M. Foxman and W. B. Lin, *Inorg. Chem.*, 1999, **38**, 2969.
141. R. G. Xiong, J. L. Zuo, X. Z. You, H. K. Fun and S. S. S. Raj, *New J. Chem.*, 1999, **23**, 1051.
142. R. G. Xiong, S. R. Wilson and W. B. Lin, *J. Chem. Soc., Dalton Trans.*, 1998, 4089.
143. X. H. Bu, M. L Tong, H. C. Chang, S. Kitagawa and S. R. Batten, *Angew. Chem., Int. Ed.* 2004, **43**,192.
144. H. S. Lin and P. A. Maggard, *Inorg. Chem.*, 2007, **46**, 1283.
145. D. Dobrzynska, L. B. Jerzykiewicz, J. Jezierska and M. Duczmal, *Cryst. Growth Des.*, 2005, **5**, 1945.

146. X. H. Bu, M. L. Tong, Y. B. Xie, J. R. Li, H. C. Chang, S. Kitagawa and J. Ribas, *Inorg. Chem.*, 2005, **44**, 9837.
147. X. H. Bu, M. L Tong, J. R. Li, H. C. Chang, L. J. Li and S. Kitagawa, *CrystEngComm.*, 2005, **7**, 411.
148. M. A. M. Abu-Youssef, A. Escuer and V. Langer, *Eur. J. Inorg. Chem.*, 2006, 3177.
149. M. A. M. Abu-Youssef and V. Langer, *Polyhedron*, 2006, **25**, 1187.
150. Z. F. Chen, P. Zhang, R. G. Xiong, D. J. Liu and X. Z. You, *Inorg. Chem. Commun.*, 2002, **5**, 35.
151. S. Hu, H. H. Zou, M. H. Zeng, Q. X. Wang and H. Liang. *Cryst. Growth Des.*, 2008, **8**, 2346.
152. Y. M. Song, Q. Ye, Y. Z. Tang, Q. Wu and R. G. Xiong, *Cryst. Growth Des.*, 2005, **5**, 1603.
153. X. N. Cheng, W. X. Zhang and X. M. Chen, *J. Am. Chem. Soc.*, 2007, **129**, 15738.
154. Z. H. Wang, J. Fan, W. G. Zhang and J. Wang, *Acta Crystallogr., Sect. E: Struct. Rep. Online*, 2008, **64**, m1446.
155. Y. H. Wang, R. F. Song and F. Y. Zhang, *J. Mol. Struct.*, 2005, **752**, 104.
156. J. Fan, Z. H. Wang, M. Yang, X. Yin, W. G. Zhang, Z. F. Huang and R. H. Zeng, CrystEngComm., 2010, **12**, 216.
157. R. Feng, F. L. Jiang, M. Y. Wu, L. Chen, C. F. Yan, and M. C. Hong, *Cryst. Growth Des*, 2010, **10**, 2306.
158. R. F. Semeniuc, T. J. Reamer and M. D. Smith, *New J. Chem.*, 2010, **34**, 439.
159. L. H. Slooff, A. van Blaaderen, A. Polman, G. A. Hebbink, S. I. Klink, F. C. J. M. Van Veggel, D. N. Reinhoudt and J. W. Hofstraat, *J. Appl. Phys.*, 2002, **91**, 3955.
160. R. Van Deun, P. Fias, K. Binnemans and C. Gorller-Walrand, *Phys.Chem. Chem. Phys.*, 2003, **5**, 2754.
161. W. P. Gillin and R. J. Curry, *Appl. Phys. Lett.*, 1999, **74**, 798.
162. S. W. Magennis, A. J. Ferguson, T. Bryden, T. S. Jones, A. Beeby and I. D. W. Samuel, *Synth. Met.*, 2003, **138**, 463.
163. R. J. Curry and W. P. Gillin, *Appl. Phys. Lett.*, 1999, **75**, 1380.
164. R. J. Curry and W. P. Gillin, *Synth. Met.*, 2000, **35**, 111.

165. W. E. Ohnesorge and L. B. Rogers, *Spectrochim. Acta* 1959, **15**, 27.

166. K. Sano, Y. Kawata, T. I. Urano and Y. Mori, *J. Mater. Chem.* 1992, **2**, 767.

167. N. M. Shavaleev, R. Scopelliti, F. Gumy and J.- C. G. Bunzli, *Inorg. Chem.* 2009, **48**, 7937.

Chapter 2

Synthesis, characterization and anion recognition properties of amide and ester derivatives of quinoline

Weak interactions play a vital role in most of the biological processes.[1-5] Among biological molecules the structural features of proteins are controlled by amide bonds and their weak interactions.[6-10] Inspired by the biological anion recognition process, different anion receptors having amide bonds are systematically studied.[11-18] Selective anion binding by amide receptors is very useful in the field of sensors.[19-25] The amide and ester derivatives of quinoline have been used as receptor for encapsulation of different guest anions.[26-31]

As the quinoline group is a Lewis base, the nitrogen atom of the ring can be easily protonated to form its salt and such hosts can be used as cationic receptors for anions, hence they are a very good receptor for acids. Acid recognition is a vital phenomenon in biology.[32] Amino acids are one of the most important class of biomolecules, hence their binding properties are of much importance. There are many receptors for recognition of amino acids; both organic and inorganic receptors synthesized for such purposes are studied in detail. Most of these receptors have structures that are relatively difficult to synthesize or they are used in the form of metal complexes.[33-38] Quinoline derivatives are known for their fluorescence properties, which can be used to study host-guest interactions.[39-42]

This chapter deals with the synthesis and characterization of a number of quinoline containing amide and ester receptors and the study on their comparative binding abilities towards different acids namely amino acids, mineral acids and carboxylic acids.

2.1 Synthesis and characterization of quinoline based receptors

A number of quinoline containing receptors illustrated in chart 2.1 (**2.1**, **2.2**, **2.3**, **2.4**, **2.5**, **2.6**, **2.7**, **2.8**) having amide and ester linkage are synthesized by simple synthetic methods.

is checked by TLC and IR of the intermediate product **2.5a**. The NH_2 signel of the diamine disappears upon complete conversion and amide streeching appears at 1643 cm^{-1}. The intermediate **2.5a** easily undergo substitution of the bromo group by 8-hydroxyquinoline.

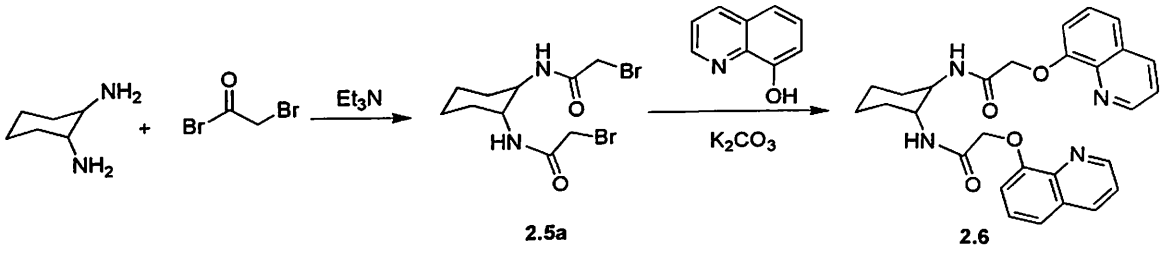

Scheme 2.5: Synthesis of receptor **2.6**

The receptor bis(2-(quinolin-8-yloxy)ethyl)isophthalate (**2.7**) was synthesized by reacting 8-hydroxy quinoline with bromomethylacetate followed by reduction of the ester formed by sodium borohydride to obtain an alcohol 2-(quinolin-8-yloxy) ethanol as an intermediate compound. The 2-(quinolin-8-yloxy) ethanol on further treatment with isophthaloyl dichloride resulted in the formation of receptor **2.7** (scheme 2.6).

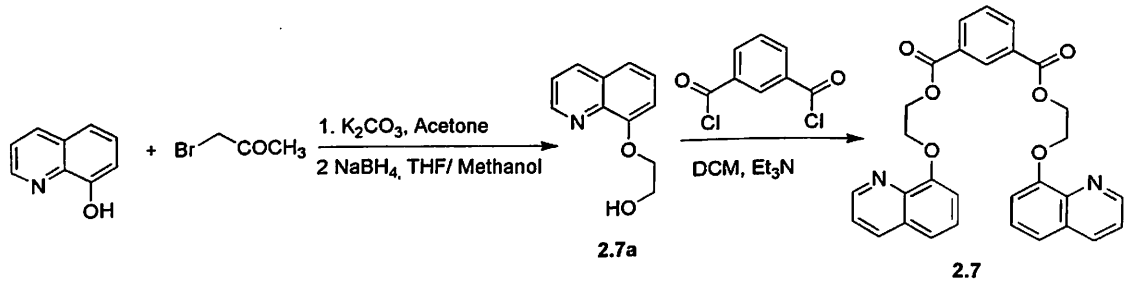

Scheme 2.6: Synthesis of receptor **2.7**

The receptor 2-(6,6'-dimethylbicyclo[3.1.1]hept-2-en-2-yl)ethyl 2-(quinolin-8-yloxy)acetate (**2.8**) was synthesized in two steps. In the first step bromoacetylbromide was reacted with (R)-(-)nopol in dichloromethane in the presence of base triethylamine to yield an intermediate ester derivative which is then reacted with 8-hydroxyquinoline in the presence of potassium carbonate (scheme 2.7).

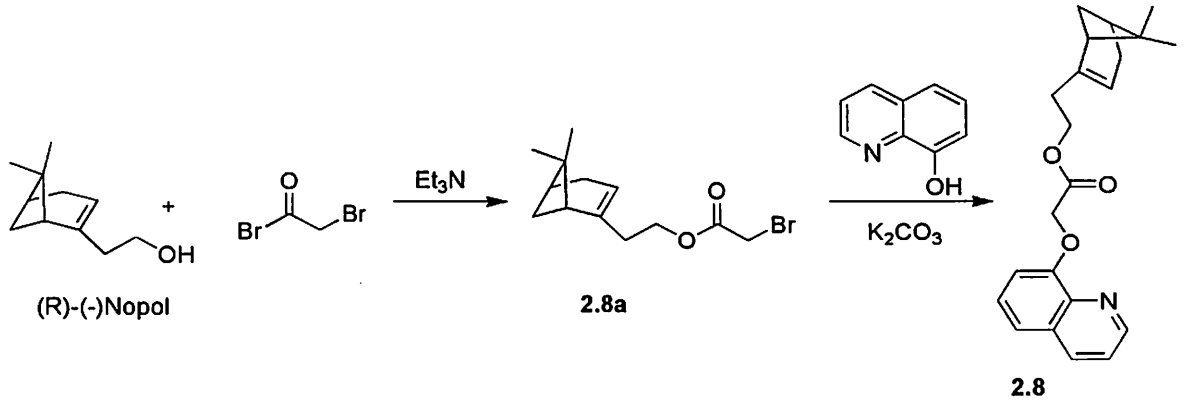

Scheme 2.7: Synthesis of receptor **2.8**

All these receptors were characterized by spectroscopic tools such as IR, NMR, LC-MS etc. As a representative case the ^{1}HNMR spectra of the receptor **2.2** is shown in figure 2.1.

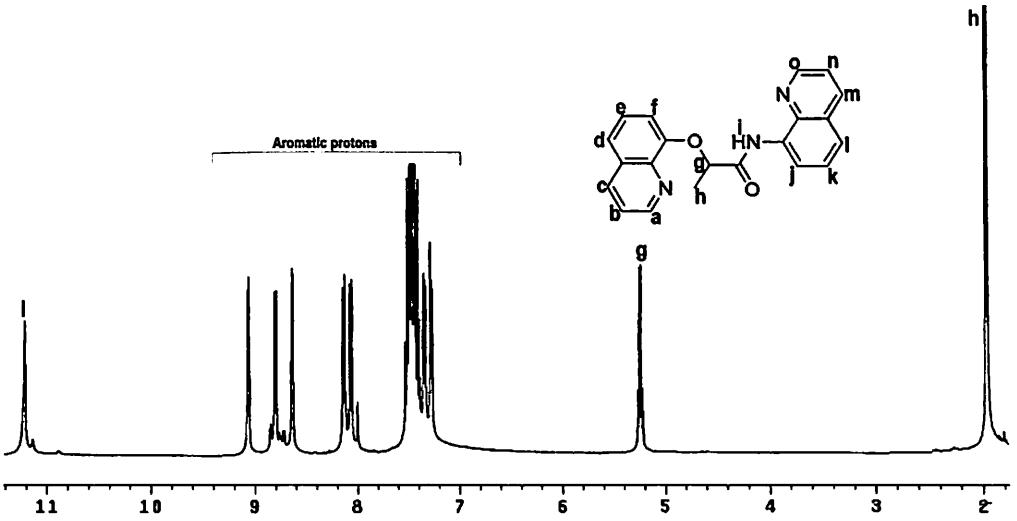

Figure 2.1: ^{1}H-NMR spectra of receptor **2.2**

2.2 Solution study of the interaction of the receptors with various acids

All the receptors shown in chart 2.1 bears quinoline unit; hence they are fluorescence active. The solution state studies are carried out by monitoring the changes in the fluorescence emission on gradual addition of various acid solutions. The fluorescence emission of quinoline derivatives such as densyl chloride is reported to be highly dependent on pH and sensitive to environment.[43] The visible absorption of each of these receptors with extinction co-efficients and fluorescence emission with quantum yields are listed in each case in table 2.1. The quantum yields are calculated by taking quinoline as reference compound.[44]

Table 2.1: The UV absorption and fluorescence emission data of the receptors

Receptor	λ max (nm)	ε (L $mol^{-1}cm^{-1}$)	Emission maximum (nm)	Quantum yield
2.1	302	3748	387	0.34
2.2	335	4647	510	0.24
2.3	301	2398	401	0.25
2.4	299	4047	387	0.16
2.5	298	3598	395	0.25
2.6	295	6146	390	0.38
2.7	301	4347	391	0.13
2.8	295	3148	392	0.23

Receptor **2.1** shows an emission maximum at 387 nm upon excitation at 280 nm. The fluorescence spectra of the receptor **2.1** are affected by mineral acids, amino acids, hydroxy acids, and simple carboxylic acids (figure 2.2). Here we have observed that the fluorescence intensity of **2.1** decreases on gradual addition of both mineral acids and amino acids. However, the change is very rapid in case of mineral acids than that of the amino acids. From these fluorescence titration curves we have calculated the binding constants of the various acids. The binding constant study clearly shows that receptor **2.1** binds mineral acids with much more affinity than the amino acids. The receptor **2.1** is also responsive to hydroxy acids such as ascorbic acid, mandelic acid and tartaric acid.

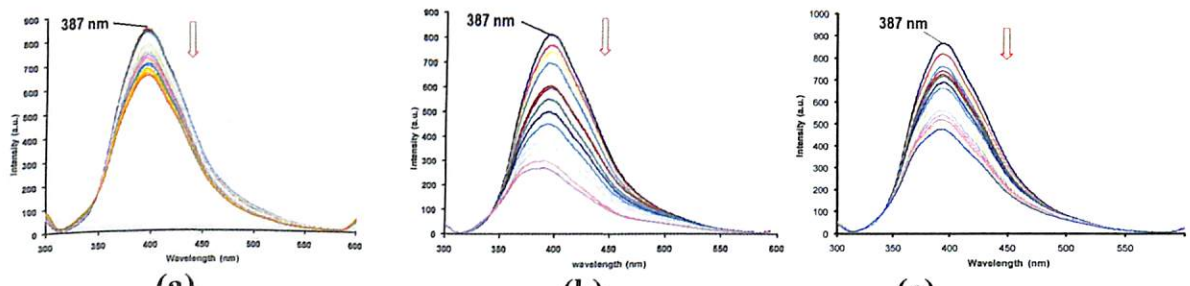

(a) **(b)** **(c)**

Figure 2.2 : Changes in fluorescence spectra of **2.1** (6.67 $\times 10^{-5}$ M in methanol) on addition of (a) glycine, (b) hydrochloric acid, (c) acetic acid (all 10^{-2} M in methanol, in 10 μl aliquot).

Receptor **2.2** shows an emission maximum at 510 nm upon excitation at 320 nm. The fluorescence emission spectra of receptor **2.2** were studied in presence of different

guests. On gradual addition of amino acids **2.2** shows a remarkable decrease in fluorescence intensity as shown in figure 2.3a. However, we have observed a mild enhancement of fluorescence emission intensity on addition of mineral acids to receptor **2.2** (figure 2.3b). It has been observed that receptor **2.2** is also responsive towards hydroxy acids, amino acids, mineral acids and to simple carboxylic acids. With simple carboxylic acid such as acetic acid it shows a gradual decrease in fluorescence (figure 2.3c).

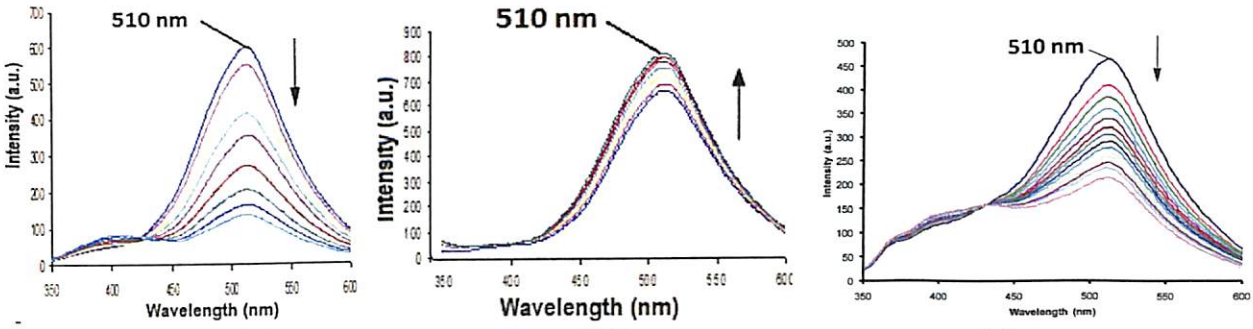

(a) **(b)** **(c)**

Figure 2.3: Changes in fluorescence spectra of **2.2** (6.67×10^{-5} M in methanol) on addition of (a) glycine (10^{-2} M in methanol), (b) hydrochloric acid (10^{-2} M in methanol), (c) acetic acid (10^{-2} M in methanol, in 10 µl aliquot).

On the other hand the fluorescence emission of receptor **2.3**, **2.4** and **2.6** is not responsive towards amino acids, however; the fluorescence significantly changes on addition of dicarboxylic acids such as maleic acid and fumaric acid. Receptor **2.4** shows an emission maximum at 387 nm upon excitation at 280 nm and the intensity of the peak decreases on gradual addition of maleic acid and it passes through an isoemissive point at 457 nm as shown in figure 2.4a. Receptor **2.6** shows an emission maximum at 390 nm upon excitation at 280 nm. The receptor **2.6** is responsive towards hydroxy acids such as ascorbic acid, mandelic acid and tartaric acid. Gradual decrease in fluorescence intensity of **2.6** is observed on addition of hydroxy acids (figure 2.4b).

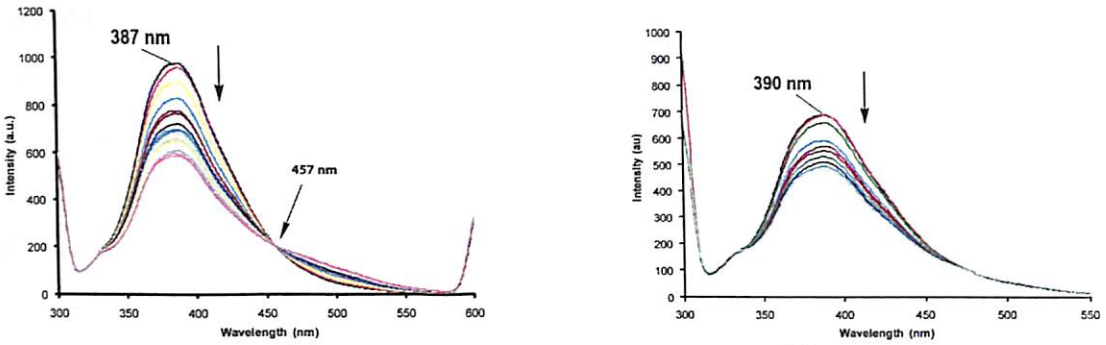

(a) (b)

Figure 2.4 : Changes in fluorescence spectra of (a) **2.4** (6.67×10^{-5} M in methanol) with maleic acid (10^{-2} M in methanol, in 10 µl aliquot), (b) **2.6** (6.67×10^{-5} M in methanol) on addition of D-mandelic acid (10^{-2} M in methanol, in 10 µl aliquot)

The ester receptor **2.7** is found to be responsive towards amino acids, mineral acids, and carboxylic acid but not responsive towards hydroxy acids such as ascorbic acid and mandelic acid. In order to differentiate the effect of amino acids over mineral acids on fluorescence emission, amino acid solutions viz. glycine or methionine were added gradually to a solution of receptor **2.7** and the fluorescence spectra were recorded. On addition of amino acids, receptor **2.7** shows enhancement of the fluorescence intensity at 391 nm (figure 2.5a). In case of mineral acids such as hydrochloric acid the initial fluorescence intensity at 391 nm is decreased with a simultaneous enhancement of fluorescence intensity at 486 nm thereby forming an isoemissive point (figure 2.5b). This difference in fluorescence spectra shows different types of supramolecular aggregation of receptor **2.7** with different guests. Comparing the study with mineral acids and with amino acids one can infer that the later case is not due to the simple protonation of **2.7.**

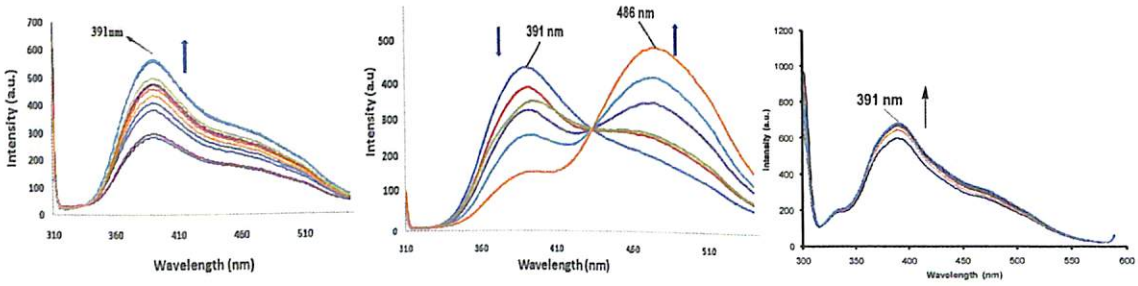

(a) **(b)** **(c)**

Figure 2.5: Changes in fluorescence spectra of **2.7** (6.7×10^{-5} M in methanol) on addition of (a) glycine (10^{-2} M in methanol), (b) hydrochloric acid (10^{-2} M in methanol).(c) Acetic acid (10^{-2} M in methanol, in 10µl aliquot).

Further we studied the binding properties of receptor **2.7** with various acids including simple carboxylic acids (figure 2.5c) and a few hydroxy acids. At this point we have observed that receptor **2.7** shows a very negligible affinity towards the hydroxy acids. However, receptor **2.7** shows good affinity towards dicarboxylic acids. Maleic acid behaves in a similar way to the mineral acids thereby passing through an isoemissive point whereas fumaric acid shows simple enhancement of fluorescence intensity as in the case of acetic acid. This may be because of the affinity of maleic acid to form salt whereas fumaric acid prefers to form hydrogen bonded co-crystal.

Receptor **2.7** is the only receptor where fluorescence intensity is enhanced on addition of amino acids and carboxylic acids. A plausible explanation for the enhancement of the fluorescence intensity is as follows.

The receptor **2.7** is the most flexible molecule in comparison to that of the other receptors studied. Hence, it can adopt different spatial orientations in order to interact with the solvent molecules as shown in scheme 2.8. In such spatial orientations its fluorescence intensity is partially quenched because of the hydrogen bonding of the quinoline moiety with the solvent molecules. When a guest molecule such as amino acids and carboxylic acids were added its structure becomes more regid due to the crown effect of the receptor **2.7** as depected in scheme 2.8. As a result the molecule adopts a conformation where the interaction with solvent molecule is less favoured and the overall observation is the enhancement of the fluorescence intensity. Among the carboxylic acids, dicarboxylic acids have more effect on the fluorescence enhancement as it can bind from both sides to enhance the crown effect of the receptor **2.7**.

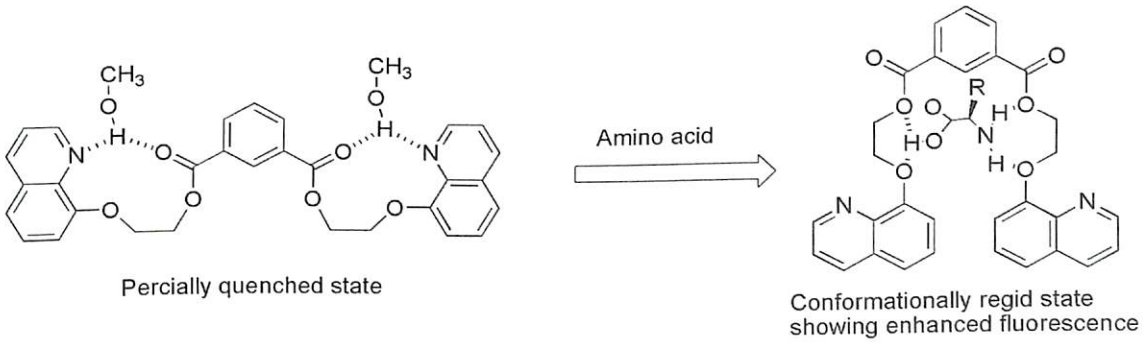

Scheme 2.8: Changes in the conformation of receptor **2.7** on coordination with amino acids.

In case of mineral acids which dissociates very rapidly, the protonation process dominates the crown effect. Hence, a decrease in the fluorescence intensity of the

original peak and a simultaneous enhancement of intensity at a different region is observed.

We have also studied the emission spectra in the presence of other amino acids such as serine, lysine, alanine etc. The relative intensity changes in the fluorescence emission of the receptor **2.7** with identical amount of amino acid (figure 2.6A) is found to vary whereas changes in the intensity pattern of the receptor **2.2** is found to be similar with all the amino acids (figure 2.6B). In general the addition of amino acids leads to enhancement of fluorescence emission intensity of receptor **2.7** and in case of such addition to receptor **2.2** fluorescence quenching occurs.

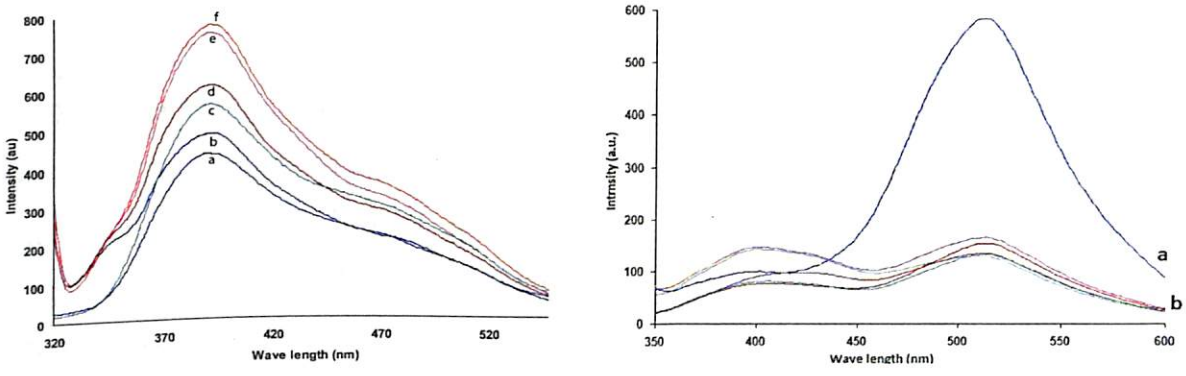

(A) (B)

Figure 2.6: (A) Fluorescence spectra of (a) **2.7** (6.67×10^{-5} M in methanol); and after addition of amino acid (b) serin, (c) lysine, (d) metheonine, (e) glycine and (f) alanine (100 μL of 10^{-2} M solution in methanol); (B) fluorescence spectra of (a) **2.2** (6.67×10^{-5} M in methanol), (b) Fluorescence quencing of **2.2** after addition of amino acid (100 μL of 10^{-2} M solution in methanol) viz. glycine, metheonine, alanine, serin, and lysine

From the relative changes in the fluorescence emission due to host-guest interactions, the binding constants for 1:1 host guest composition of all the systems are determined and these are listed in table 2.2. The calculation of binding constant is done with the assumptions that 1:1 host-guest complex are formed.

Table 2.2: Binding constant of different receptors calculated from fluorescence titration

	Binding constant ($mole^{-1}$)					
Guest	**2.1**	**2.2**	**2.3**	**2.4**	**2.6**	**2.7**
Glycine	8.058×10^{3}	3.825×10^{6}	***	***	***	6.478×10^{5}
Methionine	1.639×10^{3}	5.224×10^{6}	***	***	***	2.847×10^{5}
Hydrobromic acid	5.844×10^{5}	6.074×10^{5}	4.952×10^{5}	2.271×10^{6}	3.625×10^{6}	6.022×10^{6}
Hydrochloric acid	3.967×10^{5}	7.932×10^{5}	3.369×10^{5}	2.103×10^{6}	4.813×10^{7}	1.400×10^{7}
Perchloric acid	1.394×10^{6}	1.582×10^{5}	1.087×10^{6}	4.052×10^{6}	4.475×10^{7}	5.160×10^{6}
Acetic acid	1.22×10^{5}	1.388×10^{6}	1.055×10^{5}	***	***	$5.68\,0\times 10^{4}$
Fumaric acid	5.228×10^{5}	4.487×10^{4}	7.520×10^{4}	1.920×10^{5}	9.060×10^{5}	1.148×10^{5}
Maleic acid	9.811×10^{5}	1.464×10^{4}	1.329×10^{6}	4.963×10^{6}	2.399×10^{7}	2.822×10^{6}
L-Ascorbic acid	1.316×10^{5}	1.854×10^{4}	***	***	2.650×10^{5}	***
L-Mandelic acid	3.99×10^{5}	2.591×10^{4}	2.950×10^{4}	***	4.079×10^{6}	***
D- Mandelic acid	3.596×10^{5}	1.484×10^{5}	2.920×10^{4}	***	6.247×10^{6}	***
L-Tartaric acid	3.978×10^{5}	1.068×10^{5}	7.920×10^{4}	2.220×10^{5}	1.466×10^{6}	1.142×10^{5}

*** no changes in fluorescence spectra on addition of guest

Based on these results of binding constants a summary of comparative data on relative binding with respect to these hosts are shown in figure 2.7. It may be suggested that these quinoline derivatives binds to various amino acids, mineral acids, carboxylic acids and hydroxy acids, but the binding ability varies with structure of the parent receptor compound. Among all the receptors, receptor **2.7** shows enhancement of fluorscence on interaction with amino acids and carboxylic acids while the other receptors show quencing. This receptor is highly sensitive towards amino acid but it has also very high binding ability with mineral acid too, thus it is less selective in binding. Furthermore this receptor is insensitive to hydroxy carboxylic acids other than tartaric acid. Tartaric acid being a dicarboxylic acid; the binding behaviour of this acid should be analogous to other dicarboxylic acids such as maleic acid which bind to this receptor. The mineral acids have also similar effect on all the receptors other than receptor **2.2** and in each case fluorescence quencing is observed. The receptor N-(quinolin-8-yl)-2-(quinolin-8-yloxy) propanamide **2.2** has high affinity to bind to amino acids in comparision to mineral acids. This makes this receptor a promising candidate for recognising amino acid. However, the receptor **2.6** and **2.7** have higher affinity to bind to mineral acids.

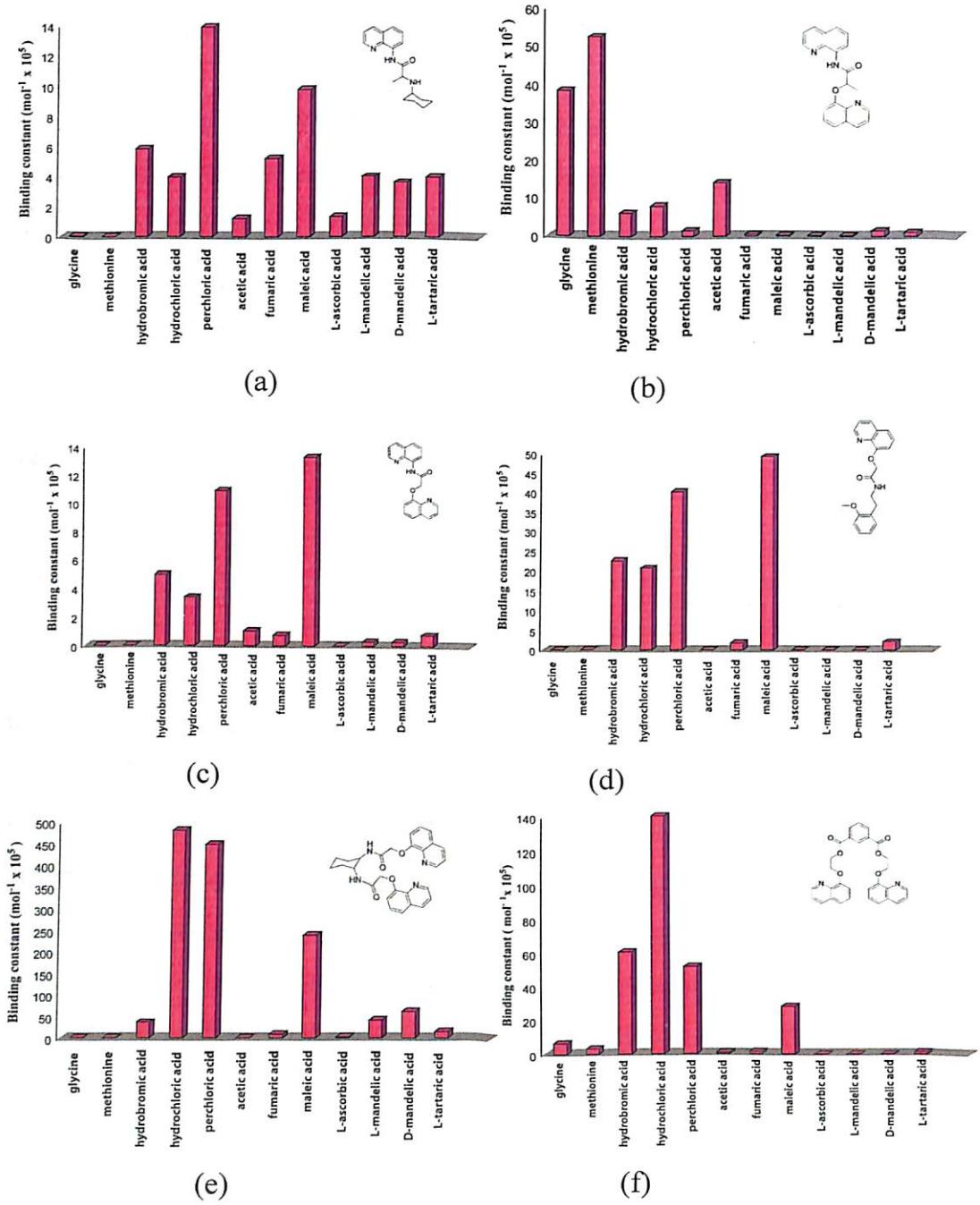

Figure 2.7: Comparisons of binding constant of receptor (a) **2.1,** (b) **2.2,** (c) **2.3,** (d) **2.4,** (e) **2.6,** (f) **2.7** with different acids.

One of the important observations is the greater binding ability of amino acids in the case of **2.2** over **2.3**. Both have similar structure other than an extra methyl group in **2.2**. So the steric effect of the methyl group is believed to make a transition state that is more favorable as illustrated in figure 2.8. Such state will be less favored in the case of **2.3** as the quinoline part will have equal preference for two oppositely directional

orientations. This is also reflected in the crystal structure which is described in the next section.

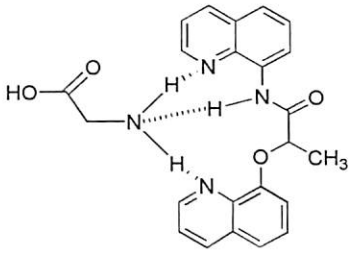

Figure 2.8: A schematic representration of H-bond interaction of receptor **2.2** with an amino acid.

Since these receptors can strongly bind to amino acids or hydroxy acids, there could be possibility of chiral recognition. With such point in mind we prepared and characterized a chiral receptor 2-(6,6-dimethylbicyclo[3.1.1]hept-2-en-2-yl)ethyl 2-(quinolin-8-yloxy)acetate (**2.8**) with an intension of chiral recognition of enantiomeric carboxylic acids. This receptor is also fluorescence active; hence the fluorescence spectra are studied in presence of different chiral acids. However, we found that this receptor is neither responsive to amino acids nor to hydroxy acids. A pair of enantiomeric carboxylic acid namely, R-(+)-2-bromopropionic acid and S-(-)-2-bromopropionic acid are found to be recognized by the receptor **2.8**. However, from fluorescence spectroscopy we could not ascertain chiral recognition as the fluorescence spectra of both the enantiomeric carboxylic acids are equally responsive to receptor **2.8**.

2.3 Structural study of the receptors and its inclusion compounds

All the receptors (**2.1–2.8**) forms crystalline product with different guest acids; however, only in few cases we could get diffraction quality crystals. Thus, we could determine solid state structures of several salts as well as cocrystals of these receptors with different types of acid molecules.

Receptor N-quinolin-8-yl-2-(quinolin-8-yloxy)-acetamide (**2.3**) is crystallized from methanol and it crystallizes in triclinic P-1 space group. The receptor **2.3** has a bent structure as shown in figure 2.9a. The dihedral angle between the two planes containing the two quinoline ring is found to be 83.13^0. This bent structure is stabilized by various weak interactions such as C-H···O interactions (C10-H10B···O2)

and C-H····N interactions (C10-H10B···N1). The short range interactions in **2.3** are shown in figure 2.9b and the hydrogen bond parameters are tabulated in table 2.3.

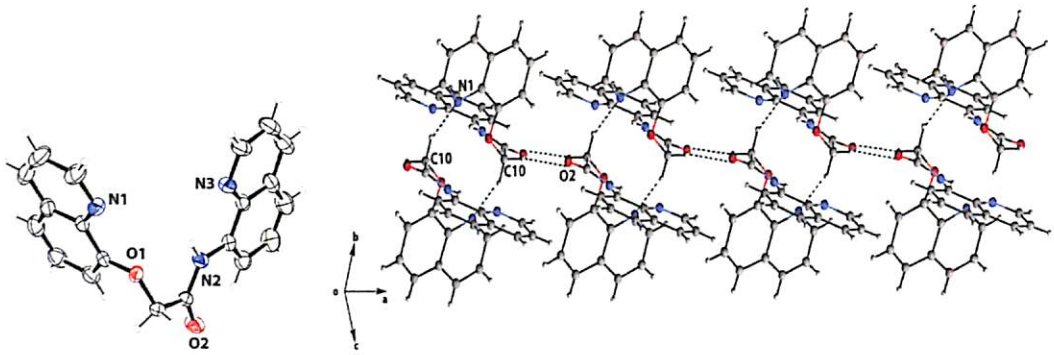

(a) **(b)**

Figure 2.9: (a) Short range interactions in **2.3**, (b) asymmetric unit of **2.3** (ORTEP drawn with 50% thermal ellipsoid probability).

Table 2.3: Hydrogen bond parameters of **2.3**

D-H····A	$d_{D\text{-}H}$(Å)	$d_{H\cdots A}$(Å)	$d_{D\cdots A}$(Å)	< D-H····A(°)
C(10) -H(10A) ····O(2) [-x,1-y,-z]	0.97	2.51	3. 48(2)	174
C(10)-H(10B) ····N1	0.97	2.63	3.33	138

The receptor **2.3** is crystallized with different guest acids as shown in scheme 2.9. Receptor **2.3** forms a quinolinium salt (**2.3a**) of tetrafluoroborate on reaction with fluoroboric acid (scheme 2.9). The same salt can be prepared via a hydrolytic reaction of sodium tetrafluoroborate with **2.3** in wet DMF.

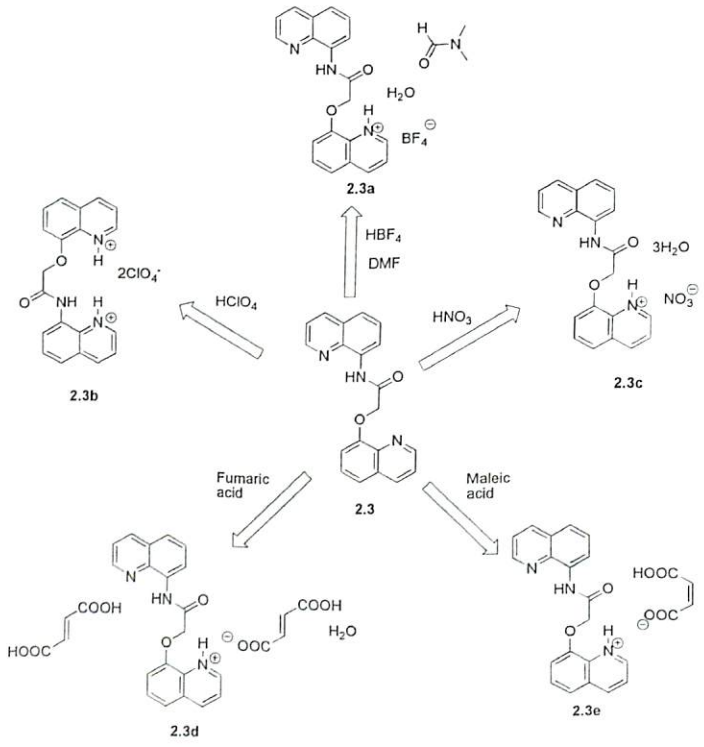

Scheme 2.9: Synthesis of the salts **2.3a**, **2.3b**, **2.3c**, **2.3d** and **2.3e**

The salt **2.3a** crystallizes in the space group orthorhombic $P2_12_12_1$ with a water and a dimethyl formamide molecule in the crystal lattice. The bent structure of the receptor **2.3** is changed to a planar structure on inclusion of the guest anion.

It is interesting to note that out of the two nitrogen atoms of the two different quinoline rings, only the nitrogen present in the ring of oxyquinoline gets protonated (figure 2.10a). The quinoline and quinolinium rings are disposed *trans* to each other. The N-H of protonated quinoline is involved in hydrogen bond with a water molecule (figure 2.10a). The *trans* disposition of two quinoline groups provides an S-shape geometry to the salt. The molecules adopting S-shaped geometries are π-staked in head to tail arrangements but in these stacks the nitrogen atoms of quinoline and quinolinium rings are on same side of the rings (figure 2.10b).

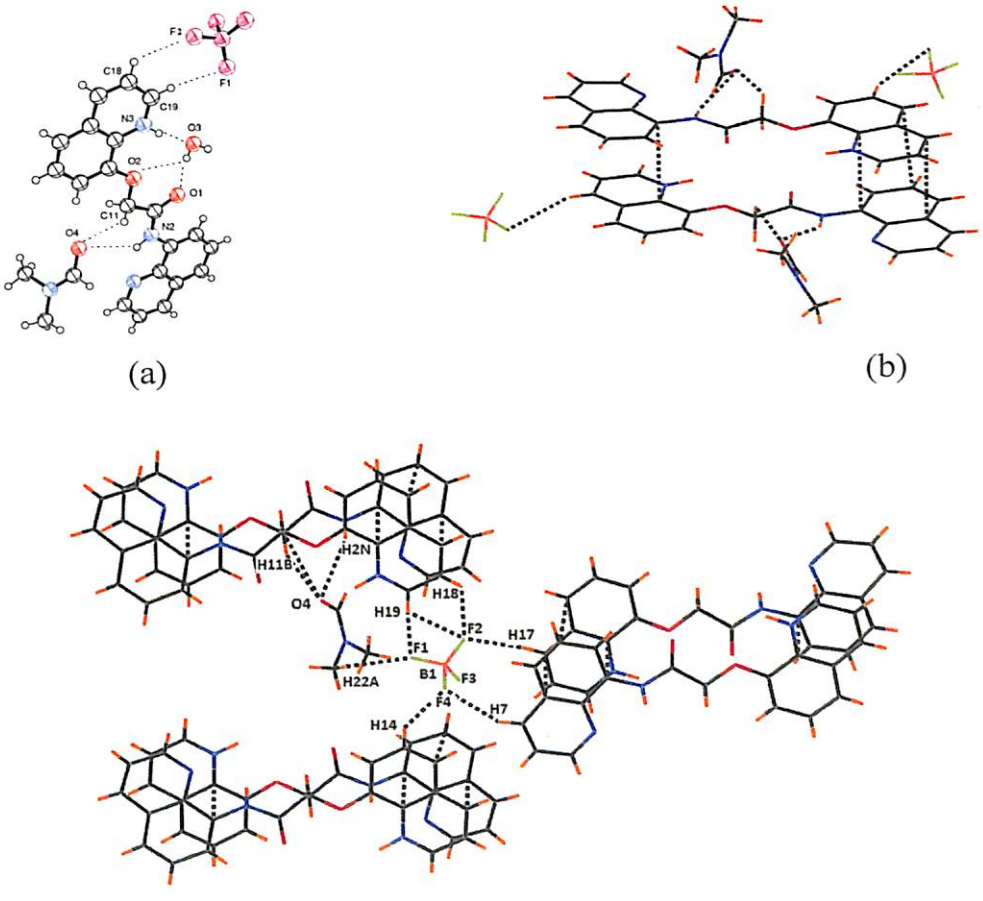

Figure 2.10: Structure of (a) tetrafluoroborate salt **2.3a** (ORTEP drawn with 50% thermal ellipsoid probability); (b) dimeric assembly of with π-π interactions, (c) environment around tetrafluoroborate anion in the lattice

The tetrafluoroborate anions are held at the edges of these rings through several C-H···F interactions namely (C14-H14···F4; d_{D-A}, 3.36Å; <D-H···A, 141.2°, C17-H17···F2, d_{D-A}, 3.45Å; <D-H···A, 157.5°; C18-H18···F2, d_{D-A}, 3.21Å; <D-H···A, 124.2°; C19-H19···F1, d_{D-A}, 3.36Å, <D-H···A, 163.0°; C19-H19···F2 d_{D-A}, 3.24Å, <D-H···A, 121.5° and C22-H22A···F1, d_{D-A}, 3.34Å, <D-H···A, 134.3°) which holds the anion. Each tetrafluoroborate anions are in seven coordination number. A dimethylformamide (DMF) molecule is held by weak C11-H···O4 (d_{D-A}, 3.07Å, <D-H···A, 117.4°) and a N2-H···O4 (d_{D-A}, 3.37Å, <D-H···A, 140.0°) interactions (figure 2.10c). The selected hydrogen bond parameters of **2.3a** are tabulated in table 2.4.

Table 2.4: Selected hydrogen bond parameters of **2.3a**

D-H····A	d_{D-H}(Å)	$d_{H\cdots A}$(Å)	$d_{D\cdots A}$(Å)	< D-H····A(°)
O(3)-H(3A) ····O(1) [1/2+x,1/2-y,-z]	0.91(6)	1.89(6)	2.79(4)	173(6))
O(3)-H(3A) ···· O(2) [1/2+x,1/2-y,-z]	0.91(5)	2.55(6)	3.01(4)	112(5)
O(3)-H(3B) ····O(4)	0.81(7)	1.99(7)	2.79(6)	169(7)
N(3)-H(3N) ····O(3) [-1/2+x,1/2-y,-z]	1.04(5)	1.71(5)	2.72(4)	163(4)
C(19)-H(19) ····F(1) [1/2-x,-y,-1/2+z]	0.93	2.44	3.34(6)	164

The N-quinolin-8-yl-2-(quinolin-8-yloxy)acetamide (**2.3**) gets easily protonoted by perchloric acid and we could easily crystallize the perchlorate salt (**2.3b**). The crystal structure of the salt shows it to be di-protonated salt as shown in figure 2.11a. The salt crystallizes in the monoclinic $P2_1/c$ space group and unlike **2.3a**; no solvent molecule is included in the crystal lattice. In this case also we have observed that the bent structure of the receptor **2.3** do not persist as the guest anions are encapsulated. The weak interactions holding the anions in the crystal lattice are shown in figure 2.11b. The di-protonated species adopts a concave shape; in which the nitrogen atoms at the two ends are disposed in the same side but away from each other making a non-planar structure; this observation is in contrast to the S-shape geometry observed in the case of the tetrafluoroborate salt (**2.3a**). The salt **2.3b** adopts non-planar structure to avoid repulsion between the two cationic charges on nitrogen atoms. The perchlorate anions are held in the lattice through N-H···O as well as C-H···O interactions, some of which are listed in table 2.5. The two perchlorate anions are in two different environments in the crystal lattice. One of them is placed at the concave site between the two quinoline rings. The amide hydrogen and proton on the quinoline nitrogen

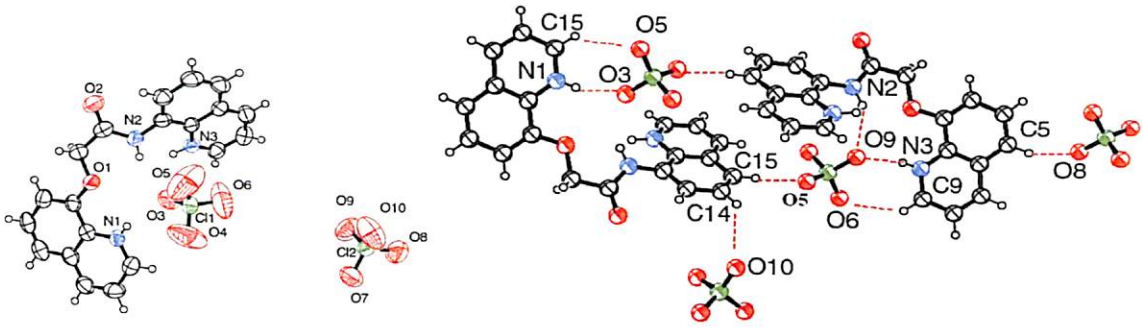

(a) (b)

Figure 2.11: Structure of (a) asymmetric unit of perchlorate salt **2.5**; (b) weak interactions in its lattice (ORTEP drawn with 50% thermal ellipsoid probability)

interact with oxygen atoms of the perchlorate anion (N3-H···O9; $d_{D\text{-}A}$, 2.87Å; <D-H···A, 170.9° and N2-H···O9; $d_{D\text{-}A}$, 3.09Å; <D-H···A, 122.1°). This same perchlorate anion is also held by two independent C-H···O interactions with the parent molecule (C9-H···O6; $d_{D\text{-}A}$, 3.35Å; <D-H···A, 131.3°). There is also another weak interaction of this perchlorate with a C15-H of neighboring molecule via C15-H···O5 ($d_{D\text{-}A}$, 3.23Å; <D-H···A, 168.6°) interactions. The other perchlorate anion is held in a four coordinated geometry through N2-H···O3 ($d_{D\text{-}A}$, 3.00Å; <D-H···A, 146.4°); N1-H···O3 ($d_{D\text{-}A}$, 2.81Å; <D-H···A, 152.0°); C14-H···O10 ($d_{D\text{-}A}$, 3.34Å; <D-H···A, 131.2°) and C5-H···O8 ($d_{D\text{-}A}$, 3.39Å; <D-H···A, 142.9°) interactions. Thus, the perchlorate ions are embedded in two sheets like structures arising from the perpendicular disposition of the quinoline rings.

Table 2.5: Hydrogen bonded parameter of **2.3b**.

D-H····A	$d_{D\text{-}H}$(Å)	$d_{H\cdots A}$(Å)	$d_{D\cdots A}$(Å)	< D-H····A(°)
N(1)-H(1)····O(3)	0.77(7)	2.10(7)	2.81(8)	154(6)
N(2)-H(2)····O(3)	0.86	2.25	3.00(8)	146
N(2)-H(2)····O(9) [1-x,-1/2+y,1/2-z]	0.86	2.55	3.09(8)	122
N(3)-H(3N)····O(9) [1-x,-1/2+y,1/2-z]	0.93(6)	1.95(6)	2.87(9)	171(5)
C(15)-H(15)····O(5)[1-x,1-y,-z]	0.93	2.32	3.23(12)	168
C(19)-H(19)····O(10)	0.93	2.49	3.26(9)	140

The receptor **2.3** is also crystallized with nitric acid from an aqueous methanol solution to yield a nitrate salt **2.3c**. In this case also we have observed planner geometry of the parent molecule **2.3**. The nitrate salt **2.3c** crystallizes in the

monoclinic space group $P2_1/c$ with three water molecules and one nitrate anion in the crystal lattice as shown in figure 2.12a. Similar to the tetrafluroborate salt (**2.3a**), out of the two quinoline group only the ring of oxyquinoline gets protonated. The molecule adopts planer geometry where the two quinoline rings are projected in a *trans* orientation. The protonated N atom forms a strong intermolecular hydrogen bond with one lattice water molecule.

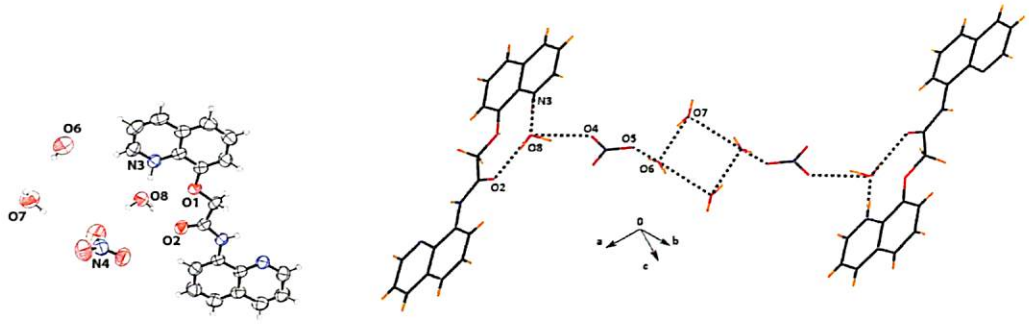

(a) **(b)**

Figure 2.12: (a) Asymmetric unit of **2.3c** (ORTEP drawn with 50% thermal ellipsoid probability) (b) hydrogen bonded self-assembly of **2.3c**

The lattice water molecules form a number of inter-molecular hydrogen bonding with the cationic and the anionic species and forms a dimeric assembly (figure 2.12b). One water molecule is held in the concave geometry formed around the protonated quinoline ring through inter-molecular hydrogen bonding (N3-H3N···O8 and O8-H8A···O2).

Table 2.6: Selected hydrogen bond parameters in **2.3c**

D-H····A	$d_{D\text{-}H}$(Å)	$d_{H\cdots A}$(Å)	$d_{D\cdots A}$(Å)	< D-H····A(°)
N(3)-H(3N) ···· O(8)	1.08	1.60	2.67(3)	168
O(6)-H(6A) ···· O(5) [x,-1+y,z]	0.84(3)	2.13(3)	2.93(3)	162(4)
O(6)-H(6B) ···· O(7)	0.82(7)	2.28(13)	2.85(3)	127(11)
O(7)-H(7A) ···· O(4)	1.00(5)	2.38(5)	3.11(3)	130(4)
O(7)-H(7A) ···· O(5)	1.00(5)	2.17(5)	3.15(3)	167(5)
O(7)-H(7B) ···· O(6) [-x,1-y,-z]	0.85(4)	1.97(4)	2.77(3)	159(5)
O(8)-H(8A) ···· O(2)	0.85(3)	1.95(3)	2.79(3)	172(2)
O(7)-H(7A) ···· O(5)	1.00(5)	2.17(5)	3.14(3)	167(5)

This water molecule is held in concave cavity further hydrogen bonds with the nitrate anion (O8-H8B···O4), thereby forming a bridge between the cationic and anionic species in the crystal lattice. The other two lattice water molecules form a self

assembly in the form of a four member hydrogen bonded ring (O7-H7B···O6 and O6-H6B···O7). This unit is again connected to the nitrate anion with another inter-molecular hydrogen bond (O6-H6A···O5). The hydrogen bond parameters are tabulated in table 2.6.

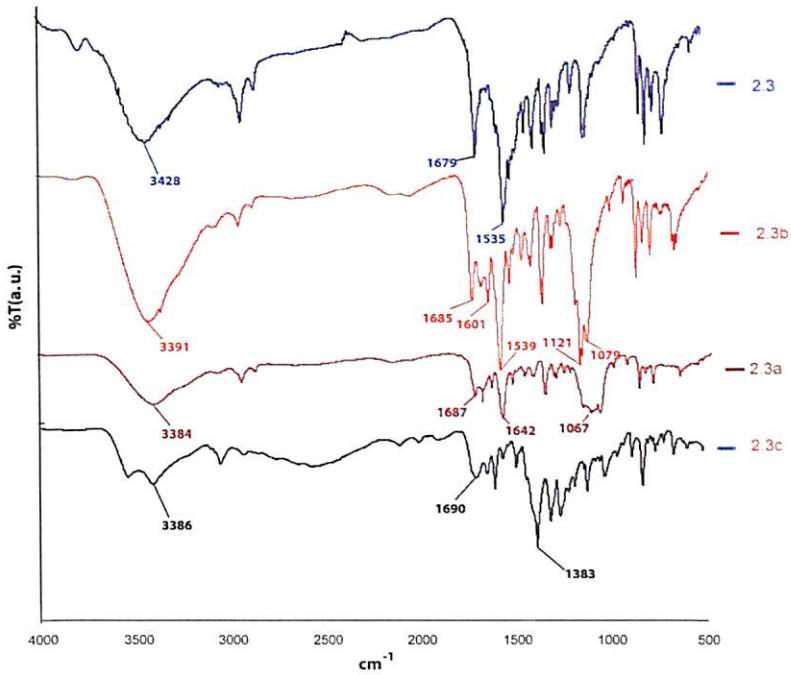

Figure 2.13: Comparison of the IR spectra of the receptor **2.3** and the salts **2.3a**, **2.3b**, **2.3c**.

The formation of the acid inclusion compounds can be easily identified from its IR spectra. The receptor **2.3** gives strong IR peak at 1679 cm^{-1} for amide C=O stretching and at 1535 cm^{-1} for aromatic C=C stretching. Apart from this two peak the salts **2.3a**, **2.3b**, and **2.3c** shows characteristic peaks for the anionic part. IR spectra of **2.3a** shows a broad peak at 1067 cm^{-1} characteristic of the tetrafluroborate anion; **2.3b** shows two strong peaks at 1121 cm^{-1} and 1079 cm^{-1} characteristic of the perchlorate anion, and the salt **2.3c** shows a strong peak at 1383 cm^{-1} for the nitrate anion (figure 2.13).

Receptor **2.3** is further crystallized with two carboxylic acids viz, fumaric acid (**2.3d**) and maleic acid (**2.3e**). The molecule **2.3d** crystallizes in the space group triclinic P-1 with one molecule of fumaric acid, one molecule of fumarate anion and one molecule of water in the asymmetric unit. The interesting feature of the structure is that one fumaric acid molecule remains in the protonated form whereas the other molecule remains as an anion. The fumaric acid molecule lies on an inversion centre with only

half of the molecule contained in the crystallographic asymmetric unit, whereas in case of the deprotonated fumaric acid molecule, the entire molecule lies in the asymmetric unit (figure 2.14c).

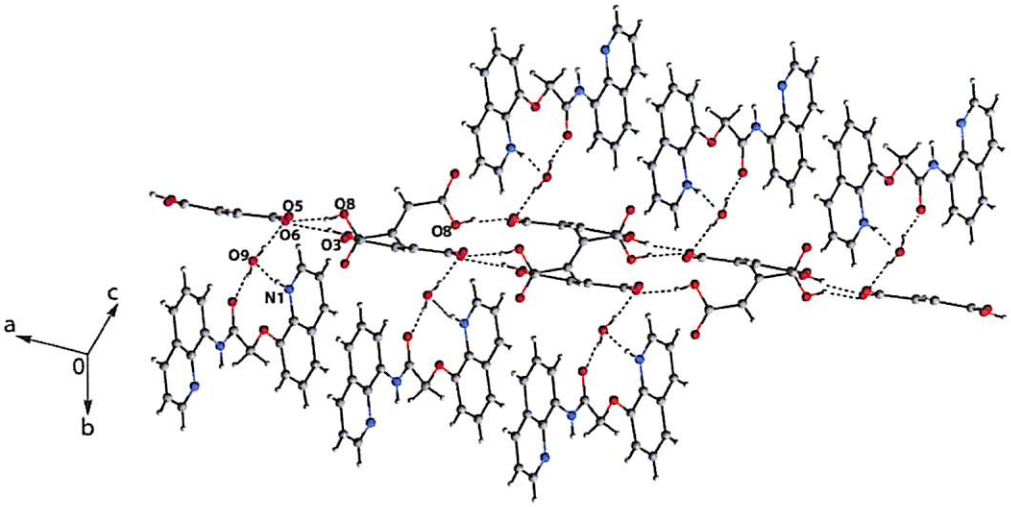

(a)

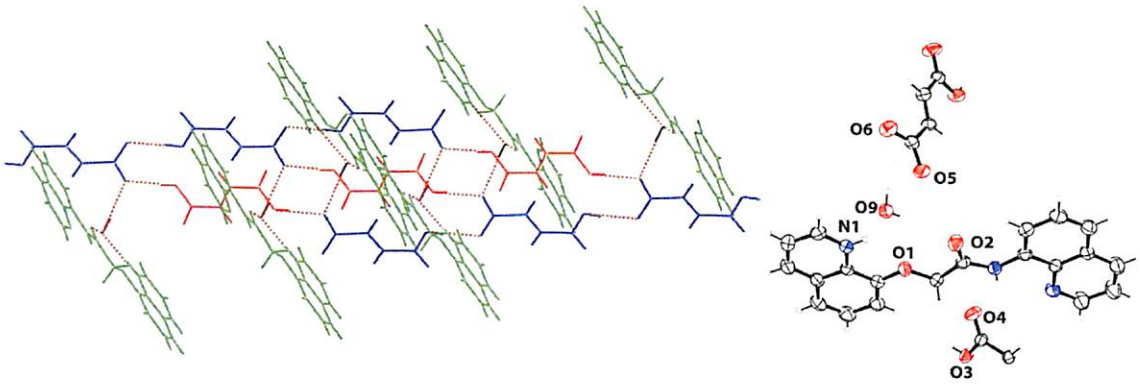

(b) (c)

Figure 2.14: (a) Short range interactions present in **2.3d**; (b) the presence of two different types of fumaric acid molecules is shown in different colour; (c) asymmetric unit of **2.3d** (ORTEP drawn with 50% thermal ellipsoid probability)

Table 2.7: Hydrogen bond parameters of **2.3d**.

D-H····A	d_{D-H}(Å)	$d_{H\cdots A}$(Å)	$d_{D\cdots A}$(Å)	< D-H····A(^{0})
N(1) -H(1N) ····O(9) [1-x,-y,1-z]	0.887(16)	1.748(16)	2.620(3)	167.2(19)
N(2)-H(2A) ····O(7)	0.86	2.60	3.373(2)	150
O(3)-H(3A)····O(5) [-1+x,y,z]	0.82	1.77	2.5854(18)	172
O(8)-H(8A) ····O(6) [-1+x,y,z]	0.82	1.75	2.554(2)	166
O(9 -H(9A) ····O(1) [1-x,-y,1-z]	0.841(17)	2.478(19)	2.983(2)	119(2)
O(9)-H(9A) ···· (2) [1-x,-y,1-z]	0.841(17)	1.867(18)	2.696(3)	168(2)
O(9)-H(9B) ····O(6)	0.83(2)	1.90(2)	2.729(2)	172(3)
C(2)-H(2) ····O(8) [x,-1+y,z]	0.93	2.52	3.445(3)	172
C(4)-H(4) ····O(4) [-x,-y,-z]	0.93	2.48	3.223(3)	137

The water molecule is held between one fumaric acid molecule and one molecule of receptor **2.3** through intermolecular hydrogen bonding (N1-H1N···O9, O9-H9A···O2 and O9-H9B···O6). Fumaric acid molecule and the fumarate anion forms a self assymbly through intermolecular hydrogen bonding (O8-H8A···O6 and O3-H3A···O5). The presence of two different types of fumaric acid molecules in the structure is shown in figure 2.14b. The component in blue colour is the fumarate anion and the one in red colour in the fumaric acid molecule. The hydrogen bond parameters are tabulated in table 2.7.

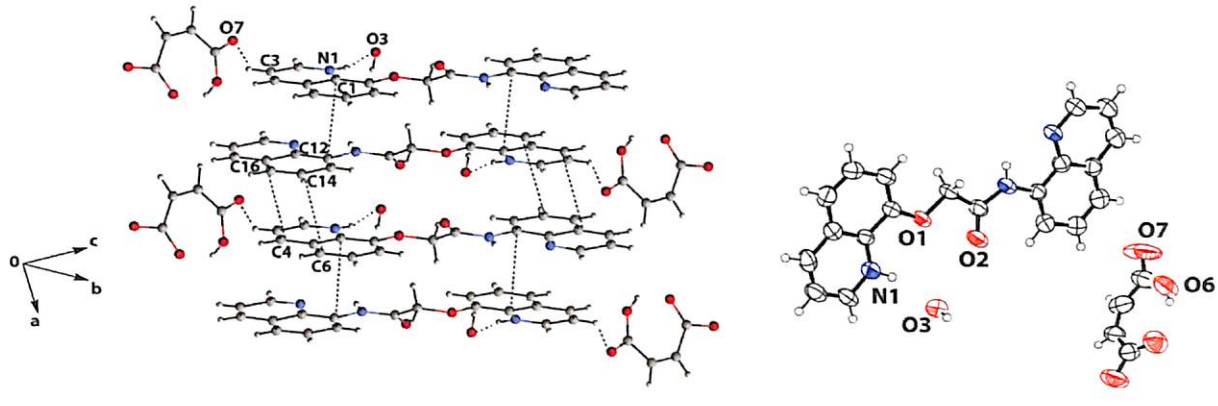

(a) (b)

Figure 2.15: (a) Short range interactions in **2.3e**; (b) asymmetric unit of **2.3e** (ORTEP drawn with 50% thermal ellipsoid probability)

Table 2.8: Hydrogen bond parameters of **2.3e**

D-H····A	$d_{D\text{-}H}$(Å)	$d_{H\cdots A}$(Å)	$d_{D\cdots A}$(Å)	< D-H····A(^{0})
N(1) -H(1N)···O(3) [3/2-x,-1/2+y,1/2-z]	0.87(3)	1.81(2)	2.667(5)	170(5)
N(2) -H(2A)···O(5) [1/2+x,1/2-y,-1/2+z]	0.86	2.45	3.242(5)	153
O(3) -H(3A) ···O(5)	0.82(2)	1.90(2)	2.724(7)	178(7)
C(3) -H(3)···O(7) [1/2+x,-1/2-y,-1/2+z]	0.93	2.55	3.203(7)	128
C(10)-H(10A)···O(5) [1/2+x,1/2-y,-1/2+z]	0.97	2.43	3.030(5)	120

Unlike fumaric acid, maleic acid crystallises in a 1:1 ratio to form a salt with receptor **2.3**. The salt of maleic acid **(2.3e)** crystallises in the space group monoclinic $P2_1/n$ with one maleate anion and one water molecule in its asymmetric unit (figure 2.15b). The receptor **2.3** is held together by number of π····π interactions ($d_{C12\text{-}C1}$, 3.358 Å; $d_{C16\text{-}C4}$, 3.361 Å; $d_{C14\text{-}C6}$, 3.473 Å). The maleate anion is involved in a C-H···O interaction (C3-H3···O7) and the water molecule is held by hydrogen bond (N1-H1N···O3). The short range interaction of **2.3e** are shown in figure 2.15a and the hydrogen bond parameters are given in table 2.8.

The ^{1}HNMR spectra of **2.3d** shows a broad singlet at 13.1 ppm for the proton of the carboxylic acid group of fumaric acid, however; in case of **2.3e** the peak for the carboxylic acid proton of maleic acid is not observed. The ratio of the fumaric acid and the maleic acid in the compounds **2.3d** and **2.3e** can also be determined from their ^{1}HNMR spectra. The ^{1}HNMR spectra of **2.3d** shows a singlet at 6.6 ppm corresponding to 3 protons, whereas in case of **2.3e** a singlet at 6.2 ppm corresponding to 2 protons is observed. Thus it can be infered that 1.5 molecule of fumaric acid is present per molecule of the receptor **2.3** and only 1 molecule of maleic acid is present per molecule of the receptor **2.3**. The comparison of the ^{1}H-NMR spectra of **2.3d** and **2.3e** is shown in figure 2.16.

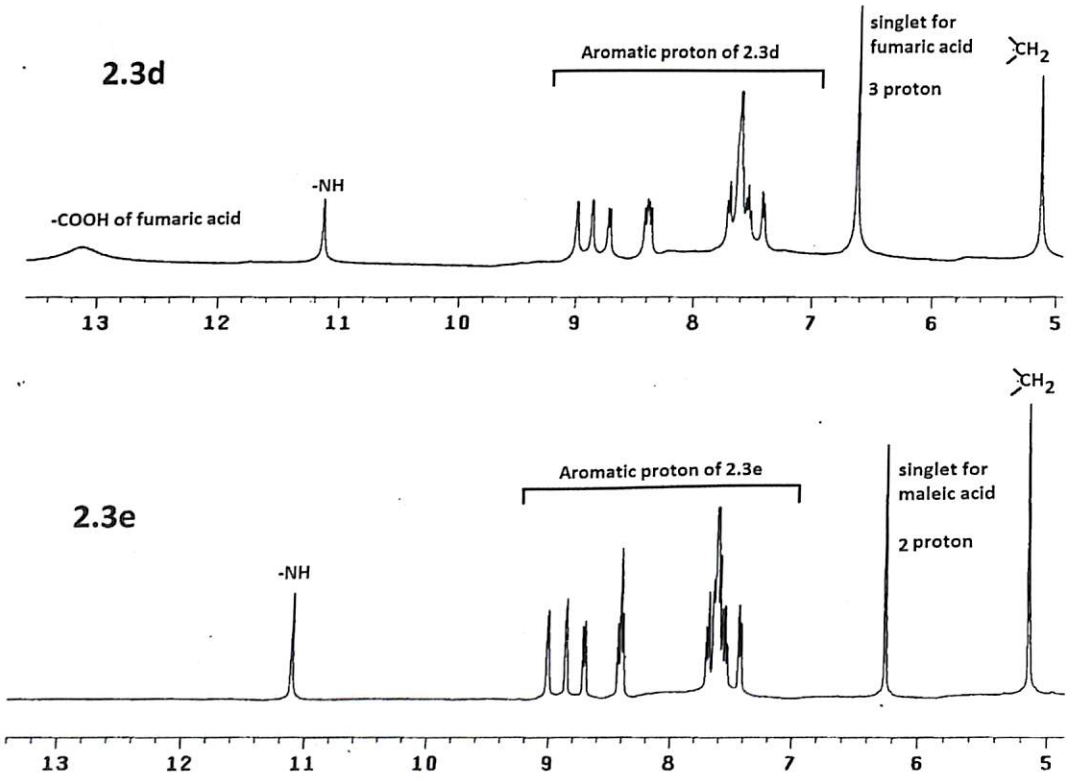

Figure 2.16: Comparison of ^{1}H-NMR spectra of **2.3d** and **2.3e**

The receptor N-(2-methoxyphenethyl)-2-(quinolin-8-yloxy)acetamide (**2.4**) crystallises in the space group triclinic P-1 with two molecules of water in its asymmetric unit (figure 2.17b). Four water molecules are held together in between two host molecules by hydrogen bonds (O4-H4A···O2, N2-H2N···O5, and O5-H5A···N1) as shown in figure 2.17a. The hydrogen bond parameters are tabulated in table 2.9.

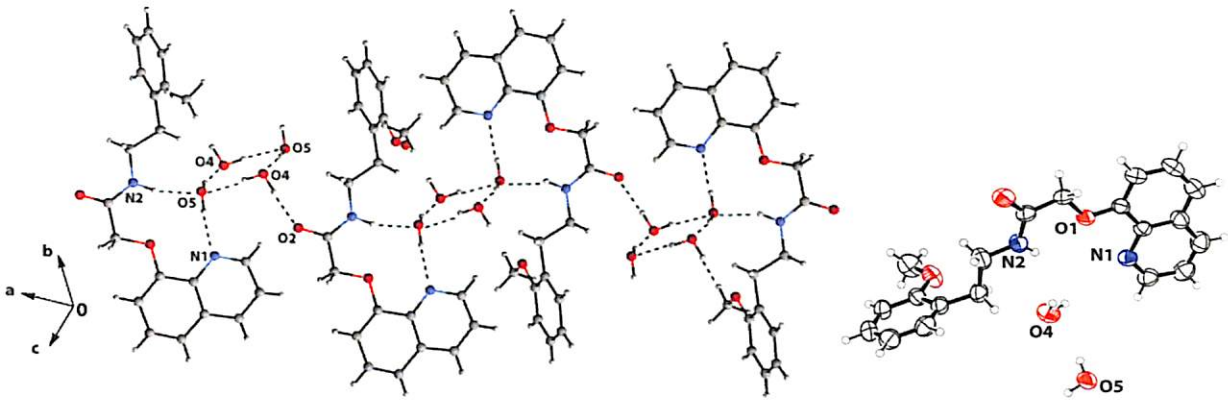

(a) (b)

Figure 2.17: (a) Short range interactions in **2.4**; (b) asymmetric unit of **2.4** (ORTEP drawn with 50% thermal ellipsoid probability)

Table 2.9: Hydrogen bond parameters of **2.4**

D-H····A	$d_{D\text{-}H}$(Å)	$d_{H\cdots A}$(Å)	$d_{D\cdots A}$(Å)	< D-H····A(^{0})
N(2)-H(2N)····O(5)	0.87(3)	2.09(3)	2.899(2)	155.0(19)
O(4)-H(4A) ····O(2) [-1+x,y,z]	0.91(3)	1.97(3)	2.874(2)	170(2)
O(4)-H(4B)····O(5)	0.82(4)	1.98(4)	2.794(2)	170(3)
O(5)-H(5A) ····N(1)	0.86(3)	1.91(3)	2.763(2)	173(3)
O(5)-H(5B) ····O(4) [1-x,1-y,-z]	0.88(4)	1.95(4)	2.813(2)	165(4)

The receptor **2.4** was than crystallised with two isomeric dicarboxylic acids namely, maleic acid and fumaric acid. It is reported that maleic acid prefers to form salt whereas fumaric acid prefers to form co-crystal with quinoline based receptors. In this case also we observed a 1:1 salt with maleic acid (**2.4a**) and a 1:2 co-crystals with fumaric acid (**2.4b**) (scheme 2.10).

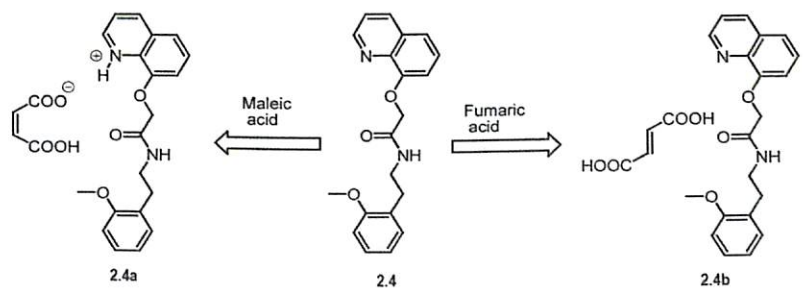

Scheme 2.10: Formation of the salt (**2.4a**) and cocrystal (**2.4b**) of **2.4**

The salt **2.4a** crystallises in the space group monoclinic $P2_1/n$. The protonated quinoline nitrogen atom forms hydrogen bond with the oxygen atom of maleate anion (N1-H1N···O4). The maleate anion is further involved in various types of weak

interactions (figure 2.18) such as C-H···O interaction (C2-H2···O5), and hydrogen bonding interaction (N2-H2N···O4). The hydrogen bond parameters are tabulated in table 2.10.

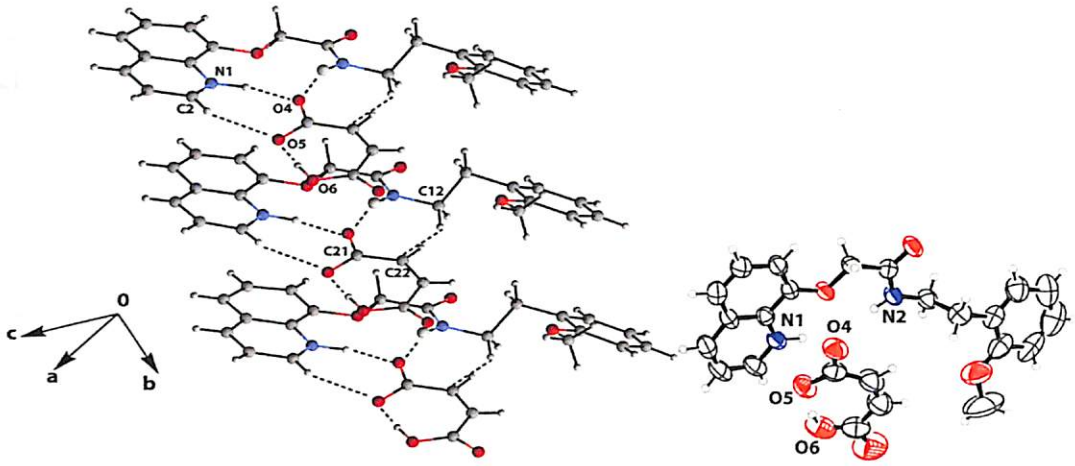

(a) (b)

Figure 2.18: (a) Short range interactions in **2.4a**; (b) asymmetric unit of **2.4a** (ORTEP drawn with 50% thermal ellipsoid probability)

Table 2.10: Hydrogen bond parameters of **2.4a**.

D-H····A	d_{D-}	$d_{H\cdots A}$(Å)	$d_{D\cdots A}$(Å)	< D-H····A(^{0})
N(1)-H(1N)····O(4) [x,1+y,z]	1.03(3)	1.73(3)	2.729(4)	163(3)
N(2)-H(2N)····O(4([x,1+y,z]	0.85(3)	2.11(3)	2.915(4)	157(2)
O(6)-H(6A) ····O(5)	0.84(3)	1.63(2)	2.461(4)	169(3)
C(2) -H(2)····O(5) [x,1+y,z]	0.93	2.40	3.138(4)	136
C(8)-H(8) ····O(2) [1-x,-y,-z]	0.93	2.38	3.296(4)	170
C(10)-H(10B) ····O(2) [1-x,1-y,-z]	0.97	2.59	3.258(4)	126

Likewise, when we have crystallised the receptor **2.4** with fumaric acid, we obtained a 1:2 cocrystal (**2.4b**) as shown in figure 2.19. The co-crystal **2.4b** crystallises in monoclinic space group $P2_1/c$, the fumaric acid molecule lies on an inversion centre with only half of the molecule contained in the crystallographic asymmetric unit (figure 2.19b). One molecule of fumaric acid is held in between two molecules of the receptor **2.4** through inter-molecular hydrogen bonding (O4-H4A···N1and N2-H2N···O4) as shown in figure 2.19a. The hydrogen bond parameters are tabulated in table 2.11.

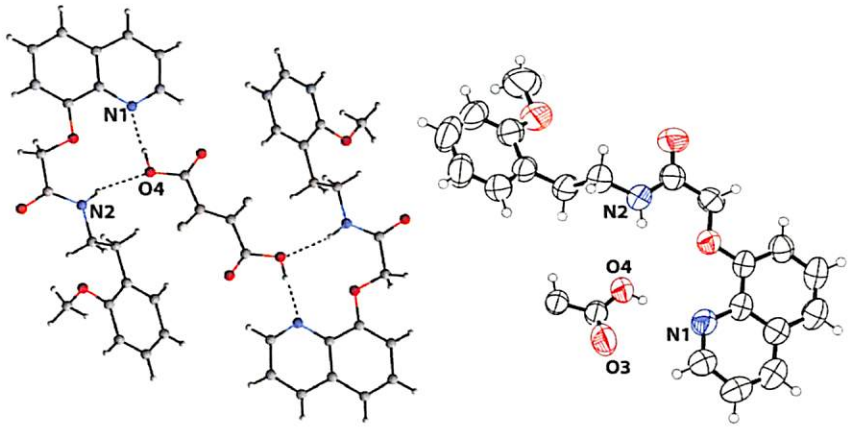

(a) (b)

Figure 2.19: (a) Hydrogen bonded structure of **2.4b** showing encapsulation of one fumaric acid molecule by two molecules of receptor **2.4**; (b) asymmetric unit of **2.4b** (ORTEP drawn with 50% thermal ellipsoid probability)

Table 2.11: Hydrogen bond parameters of **2.4b**.

D-H····A	$d_{D\text{-}H}$(Å)	$d_{H\cdots A}$(Å)	$d_{D\cdots A}$(Å)	< D-H····A(^{0})
N(2)-H(2A)····O(4) [x,3/2-y,-1/2+z]	0.86	2.22	3.052(6)	163
O(4)-H(4A)····N(1) [x,3/2-y,1/2+z]	0.82	1.84	2.651(5)	171

The receptor N-[2-(4-methoxy-pheny)-ethyl]-2-(quinolin-8-yl-amino)-acetamide (**2.5**) is crystallized from methanol and its crystal structure is studied. It crystallizes in the orthorhombic space group $Pna2_1$. Unlike receptor **2.3** which is of bent structure, **2.5** have a stretched structure as shown in figure 2.20a.

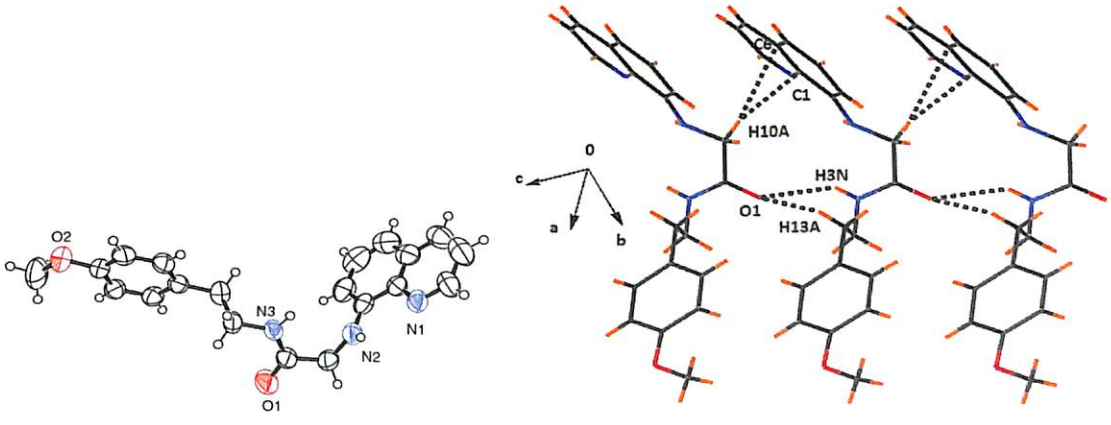

(a) (b)

Figure 2.20: (a) Asymmetric unit of receptor **2.5** (ORTEP drawn with 50% thermal ellipsoid probability); (b) short range interactions in **2.5**

The receptor **2.5** forms a one dimensional polymeric structure through some weak interactions namely, hydrogen bonding (N3-H3N···O1); C-H···O (C13-H13A···O1; d_{D-A}, 3.336 Å; <D-H···A, 132.3°) and C-H···π (C10-H10A···C1 and C10-H10A···C6) interactions as shown in figure 2.20b. The hydrogen bond paramers are tabulated in table 2.12.

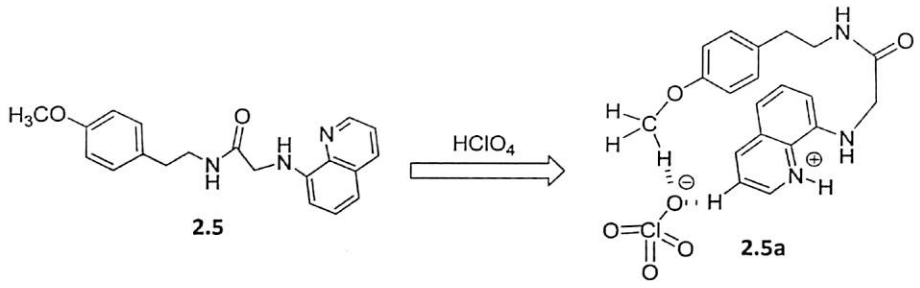

Scheme 2.11: Formation of the perchlorate salt **2.5a**

The receptor **2.5** is treated with perchloric acid (scheme 2.11) and the perchlorate salt (**2.5a**) is crystallized from an aqueous methanol solution. The perchlorate salt **2.5a** crystallizes in the space group trigonal R-3 with a perchlorate anion and the protonated molecule of receptor **2.5** in the asymmetric unit. The receptor **2.5** has a stretched structure, whereas its perchlorate salt has a tweezer-like geometry as illustrated in figure 2.21a. The folded structures of protein specially the hairpin models are greatly influenced by weak interactions.[45-48] To achieve particular property of enzymes, geometrical features governed by the weak interactions are important.[7-11] The tweezer-like geometry is held by very weak C-H···O interactions (C7-H···O4, d_{D-A} 3.45Å, <D-H···A, 147.3°; and C20-H···O4, d_{D-A} 3.28Å; <D-H···A, 124.9°). These interactions leads to self assembly formation which is shown in figure 2.21b. The structure of the perchlorate salt has π-π interaction among the aromatic quinoline rings, as evident from the distance of separation between the quinoline rings, which is 3.33Å. This distance is well within the limit for π-π interactions.[49-51] The crystal structure when viewed along the *c*-crystallographic axis as in figure 2.21c, it is clear that there are empty cylindrical channels with diameter 7.2 Å. Such channels are formed by the arrangement of the hydrophobic part containing the CH_2-CH_2-$C_6H_4OCH_3$ groups and these units are associated with weak C-H···π ($d_{C19-C20}$, 3.72 Å) and C-H···O (C18-H···O2 d_{D-A}, 3.48 Å; <D-H····A, 150.7°) interactions. Although the C-H···π interactions[52-53] and C-H···O interactions[54-56] are very weak, yet they are known to be responsible for changing reactivity and structural features in biology.

The structure of perchlorate salt **2.5a** is an illustrative example of organic channels with uniform voids and such materials with uniform patterns are important in material science.[57-58] The hydrogen bond parameters of **2.5a** are tabulated in table 2.12.

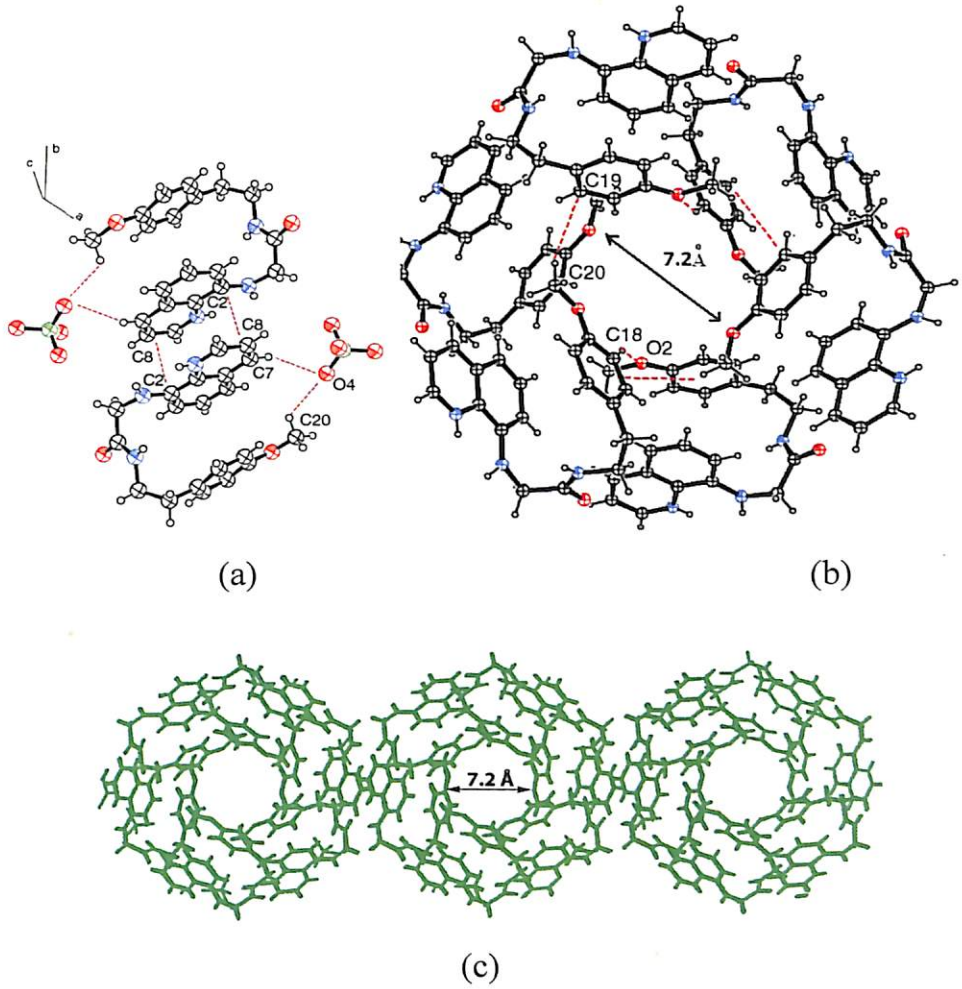

Figure 2.21: (a) Perchlorate salt (**2.5a**) showing the weak interactions (ORTEP drawn with 50% thermal ellipsoid probability); (b) self-assembly through weak C-H···π and C-H···O interactions (perchlorate anions are omitted); (c) channel like structure of **2.5a** viewed along *c*-crystallographic axis

Table 2.12: Hydrogen bond parameters for **2.5** and **2.5a**

D-H····A	$d_{D\text{-}H}$(Å)	$d_{H\cdots A}$(Å)	$d_{D\cdots A}$(Å)	< D-H····A(°)
For 2.5				
N(2)-H(2) ····N(1)	0.79(4)	2.22(4)	2.70(5)	120(4)
N(3)-H(3N) ····O(1) [x,y,1+z]	0.84(5)	2.50(5)	3.15(5)	135(4)
For 2.5a				
N(1)-H(1) ····O(1) [1/3-y,2/3+x-y,-1/3+z]	0.80(4)	1.99(4)	2.74(5)	157(4)
N(2)-H(2)····O(1) [1/3-y,2/3+x-y,-1/3+z]	0.87(4)	2.02(4)	2.86(4)	160(4)
N(3)-H(3N)····O6 [x-y,x,-z]	0.77(5)	2.43(4)	3.18(6)	164(5)
C(9)-H(9) ····O(5) [1/3-x+y,2/3-x,-1/3+z]	0.93	2.49	3.23(6)	145

Although channels with empty voids are not favored by thermodynamics,[57] the present case may be outcome of interplay of weak interactions with electrostatic interactions present in the lattice.

Conclusion

In conclusion we have synthesized a number of quinoline based amide and ester receptors having structural diversity. The acid recognition property of the receptors is established both in solution as well as in solid state. The receptors have different affinity towards different acids, for example receptors **2.1** and **2.2** are sensitive towards amino acids whereas receptors **2.3**, **2.4**, **2.5** are not responsive towards amino acids. Again receptor **2.7** shows an enhancement of fluorescence intensity on addition of amino acid but the receptor **2.1** and **2.2** shows a decrease of fluorescence intensity. The effect of different acids on the receptors is summarised in table 2.13.

Table 2.13: Effect of different acids on the receptors

Receptors	Suitable for substrates	Effect on fluorescence
2.1 and **2.2**	Amino acids, mineral acids, hydroxy acids and carboxylic acids	Quenching
2.3 and **2.6**	Mineral acids, hydroxy acids and carboxylic acids	Quenching
2.4	Mineral acids and carboxylic acids	Quenching
2.7	Amino acids, mineral acids, and carboxylic acids	Enhancement for amino acids and carboxylic acids; quenching for mineral acids

The anion binding and stoichiometry can change orientations of the flexible arm of an amide containing receptor. Such spatial arrangements also can decide the number/s of sites to protonate in case of substrates having multiple sites for protonation. On coordination with anion a bent molecule (**2.3**) can change its orientation to a planer one; whereas a planer molecule (**2.5**) can change its orientation to form tweezer like geometry. Again a receptor having closed packed structure can be modified to porous materials of uniform voids by coordination with anion having potential application as storage materials. These types of structural modification around an amide linkage

through weak interaction plays important role in functioning of the biological molecules especially in the peptides.

Experimental

Compound 2.1:

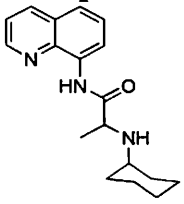

To a solution of 8-aminoquinoline (0.433 g, 3 mmol) in dry dichloromethane (20 mL) triethylamine (0.31 g, 3 mmol) was added. The solution was stirred at 0 ^{0}C for 15 min and 2-bromopropionylbromide (0.316 g, 3 mmol) was added over a period of 30 min. The reaction mixture was then stirred overnight at room temperature. To the reaction mixture 10 ml of water was added and the organic layer was separated using a separatory funnel. The solution was then dried over anhydrous sodium sulphate and the solvent was removed under reduced pressure to obtain a brown solid of 2-bromo-N-(quinolin-8-yl)propanamide. The crude product was then recrystallized from dichloromethane. In the second step, 2-bromo-N-(quinolin-8-yl)propanamide (0.834 g, 3 mmol), cyclohexylamine (0.297 g, 3 mmol) and potassium carbonate (0.5g, 3.7 mmol) were taken in dry acetone (20mL) and stirred at 70 ^{0}C for 9hs (progress of the reaction was monitored at regular intervals using TLC). After completion of the reaction, the product was filtered and the solvent was removed under reduced pressure. The product 2-(cyclohexylamino)-N-(quinolin-8-yl)propanamide was further purified by thin layer chromatography (silica gel; hexane/ethyl acetate 3:2).

Yield: 48%.

IR (KBr, cm^{-1}): 3329 (b), 2927 (m), 2851(m), 1672 (s), 1520 (s), 1486 (m), 1448 (w), 1423(w), 1382 (w), 1322 (m), 1130 (m), 1052 (m), 823 (m), 791 (m).

^{1}H NMR ($CDCl_3$, 400 MHz): 11.6 (1H, s), 8.8 (1H, d, J = 6.0Hz), 8.8 (1H, d, J = 7.2Hz), 8.1 (1H, d, J = 8.0Hz), 7.5 (2H, m), 7.4 (1H, m), 3.5 (1H, q, J = 6.8Hz), 2.5 (1H, d, J = 3.6Hz), 2.0 (1H, bs), 1.6 (4H, m), 1.4 (3H, d, J = 6.8Hz), 1.1 (6H, m).

^{13}C-NMR ($CDCl_3$, 100 MHz): 20.9, 25.2, 25.3, 26.2, 33.9, 33.3, 56.5, 57.1, 116.5, 121.7, 127.5, 128.3, 134.8, 136.3, 136.6, 139.4, 148.6, 175.3.

LC-MS [M+1]: 298.20.

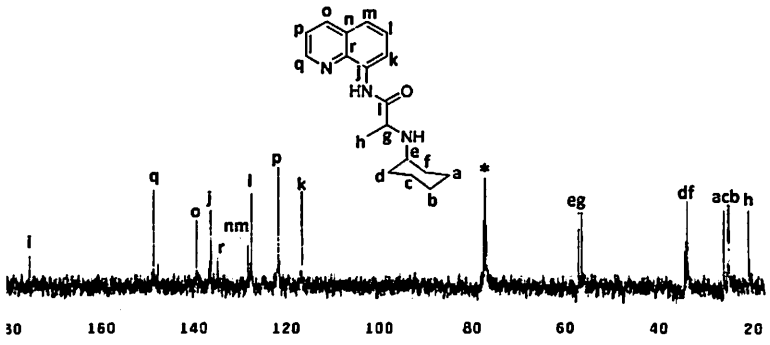

Figure 2.22: ^{13}C-NMR spectra of **2.1**

Compound 2.2:

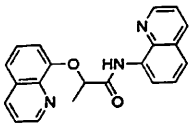

The 2-bromo-N-(quinolin-8-yl) propanamide (1.36 g, 5 mmol) was dissolved in dry acetone (30 ml). To the reaction mixture K_2CO_3 (1.0 g, 7.5 mmol) was added and stirred for 20 min. Then 8-hydroxyquinoline (0.725 g, 5 mmol) was added and the reaction mixture was refluxed at 70 ^{0}C for 10hs. (Progress of the reaction was monitored at regular intervals using TLC). After completion of the reaction, the reaction mixture was filtered to remove the K_2CO_3. The solvent from the filtrate was then removed under reduced pressure to obtain the crude product which was further purified by thin layer chromatography (silica gel; hexane/ethyl acetate 3:2).

Yield: 48%.

IR (KBr, cm^{-1}): 3432 (m), 3257 (s), 2764 (s), 1704 (s), 1637 (w), 1516 (s), 1420 (m), 1384(m), 1309 (m), 1281 (m), 1218(s), 1163 (m), 1063 (w), 993 (w), 873 (w), 821 (s),777 (w), 609 (m) .

^{1}H NMR ($CDCl_3$, 400 MHz): 11.2 (1H, s), 9.0 (1H, d, J = 4.0Hz), 8.8 (1H, d, J = 7.2Hz), 8.6 (1H, d, J = 4.4Hz), 8.1 (1H, d, J = 8.4Hz), 8.0 (1H, d, J = 8.4Hz,), 7.5-7.4 (5H, m), 7.3 (1H m), 7.2 (1H, d, J = 7.2Hz), 5.2 (1H, q, J = 6.8Hz), 1.9 (3H, d, J = 6.8Hz).

^{13}C-NMR (DMSO-d^6, 100 MHz): 169.9, 149.1, 147.9, 147.6, 145.9, 139.3, 133.0, 130.9, 130.4, 129.9, 128.0, 124.4, 123.7, 123.0, 122.0, 120.4, 115.9, 76.3, 18.9.

LC-MS [M+1]: 344.01

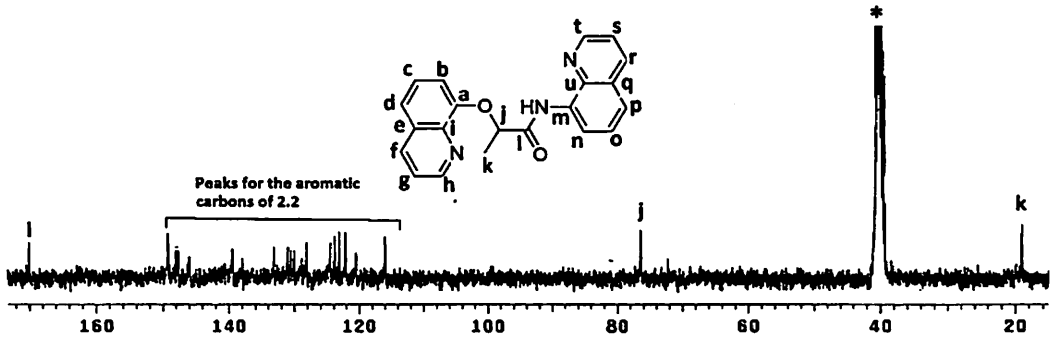

Figure 2.23: ^{13}C-NMR spectra of **2.2**

Compound 2.3:

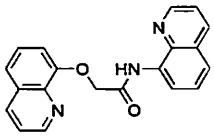

8-aminoquinoline (0.720 g, 5 mmol) was dissolved in dry dichloromethane (20 mL) and triethylamine (0.693 mL, 5 mmol) was added to it. The solution was stirred at 0^{0}C for 15 min and bromoacetylbromide (0. 434 mL, 5 mmol) was added to the stirred solution over a period of 30 min. The reaction mixture was stirred overnight at room temperature. It was then filtered to remove the hydrobromide salts, and the filtrate was removed under reduced pressure. The corresponding amide obtained was recrystallised from dichloromethane. In the next step, the amide obtained (1.3 g, 5 mmol), 8-hydroxyquinoline (0.72 g, 5 mmol) and potassium carbonate (1.0 g, 7.5 mmol) were taken in dry acetone (20 mL) under nitrogen atmosphere and the reaction mixture was stirred at 60 ^{0}C for 9 hs (progress of the reaction was monitored at regular intervals using TLC). After completion of the reaction, the solvent was removed under reduced pressure. The product N-(quinolin-8-yl)-2-(quinolin-8-yloxy)acetamide obtained was purified by column chromatography.

Yield: 63%.

IR (KBr, cm^{-1}): 3337 (s), 2924 (m), 2852 (w), 1682 (s), 1570 (w), 1537 (s), 1500 (m), 1423 (m), 1378 (m), 1315 (m), 1110 (s), 820 (m), 789 (m), 698 (m).

^{1}HNMR ($CDCl_3$, 400 MHz): 11.2 (1H, s), 9.0 (1H, d, J = 4.1Hz), 8.8 (1H, d, J = 6.8Hz), 8.7 (1H, d, J = 4.1Hz), 8.2 (1H, d, J = 8.4Hz), 8.1 (1H, d, J = 8.4Hz), 7.5 (5H, m), 7.4 (1H, m), 7.2 (1H, d, J = 7.2Hz), 5.0 (2H, s).

^{13}CNMR ($CDCl_3$, 100 MHz): 48.9, 105.4, 115.2, 115.8, 121.0, 121.1, 121.3, 126.4, 126.9, 127.2, 127.8, 133.4, 135.4, 135.5, 137.8, 137.9, 143.6, 146.7, 147.7, 168.8.

LC-MS [M+1]: 330.1361

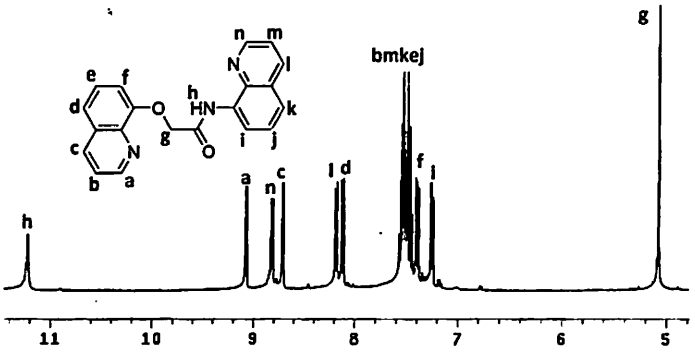

Figure 2.24: ^{1}H-NMR spectra of **2.3**

. **Compound 2.3a:**

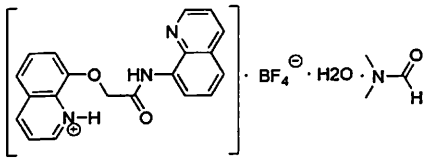

The compound **2.3** (0.33 g, 1 mmol) was dissolved in a mixture of methanol and dimethylformamide (3: 2). To this solution sodium tetrafluoroborate (0.11 g, 1 mmol) was added and stirred for 30 min. The solution was then kept for crystallization; brown colored crystals appeared after 17 days. Alternatively, same compound can be prepared from a solution of **2.3** in a mixed solvent of methanol and DMF by adding HBF_4.

Yield: 40%.

IR (KBr, cm^{-1}): 3398 (b), 2927 (m), 1689 (s), 1650 (m), 1604 (m), 1542 (s), 1492 (m), 1428 (m), 1377 (m), 1317 (s), 1261 (w), 1124 (s), 1083 (bs), 961 (w), 889 (m), 824 (s), 752 (m), 613 (m).

^{1}HNMR (DMSO-d^6, 400 MHz): 11.1 (1H, s), 8.9 (1H, s), 8.5 (2H, m), 8.2 (2H, m), 7.7 (1H, s), 7.5 (6H, m), 7.3 (1H, d, J = 7.6 Hz), 5.1 (2H, s), 2.8 (3H, s), 2.7 (2H, s).

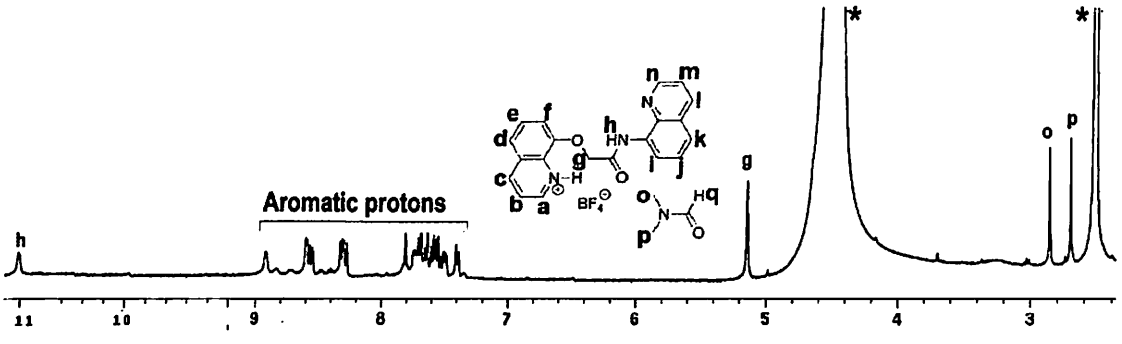

Figure 2.25: ^{1}H-NMR spectra of **2.3a** (* indicates the peaks for the solvent and water associated with solvent)

Compound 2.3b:

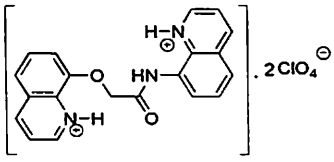

The perchlorate salt (**2.3b**) of protonated N-(quinolin-8-yl)-2-(quinolin-8-yloxy)acetamide was obtained by dissolving it in dilute perchloric acid solution (3M) followed by warming for 5 min to obtain a transparent solution. Brown colored crystals of **2.3b** appeared after 6 days.

Yield: 57%.

IR (KBr, cm^{-1}): 3401 (b), 2923 (m), 1688 (s), 1637 (m), 1603 (m), 1539 (s), 1490 (m), 1426 (m), 1377 (m), 1317 (s), 1274 (w), 1121 (s), 1080 (bs), 824 (s), 791 (m), 750 (m), 625 (m).

^{1}HNMR (DMSO-d^6, 400 MHz): 11.0 (1H, s), 9.0 (1H, s), 8.8 (1H, s), 8.6 (1H, d, J = 7.2 Hz), 8.5 (1H, d, J = 8.0 Hz,), 8.4 (1H, d, J = 7.6 Hz), 7.6 (6H, m), 7.4 (1H, d, J = 7.6Hz), 5.1(2H, s).

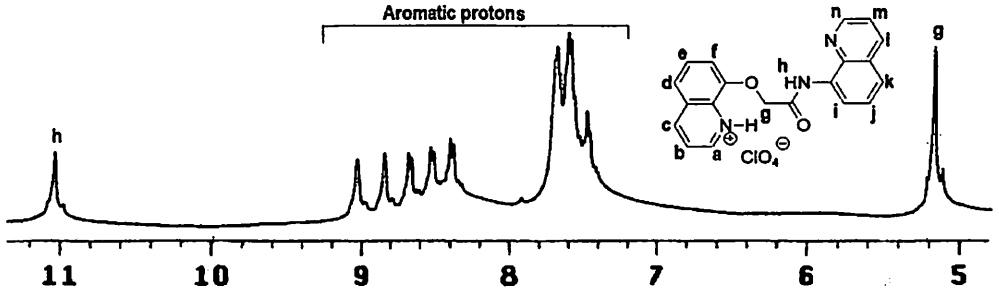

Figure 2.26: ^{1}H-NMR spectra of **2.3b**

Compound 2.3c:

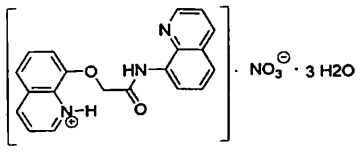

The nitrate salt (**2.3c**) of protonated N-(quinolin-8-yl)-2-(quinolin-8-yloxy)acetamide was obtained by dissolving it in dilute nitric acid solution (3M) followed by warming for 5 min to obtain a transparent solution. Brown colored crystals of **2.3c** appeared after 5 days.

Yield: 57%.

IR (KBr, cm^{-1}): 3486 (b), 3054 (w), 1690 (s), 1604 (s), 1491 (m), 1383 (s), 1313 (m), 1262 (m), 1186 (w), 1031 (m), 830 (m).

^{1}HNMR (DMSO-d^6, 400 MHz): 10.7 (1H, s), 9.2 (1H, d, J = 5.3Hz), 8.8 (1H, d, J = 8.0Hz), 8.5 (1H, d, J = 7.6Hz), 8.4 (1H, d, J = 8.4Hz), 7.9 (1H, d, J = 8.0 Hz), 7.8 (2H, m), 7.7(2H, m), 7.6(3H, m), 5.4(2H, s).

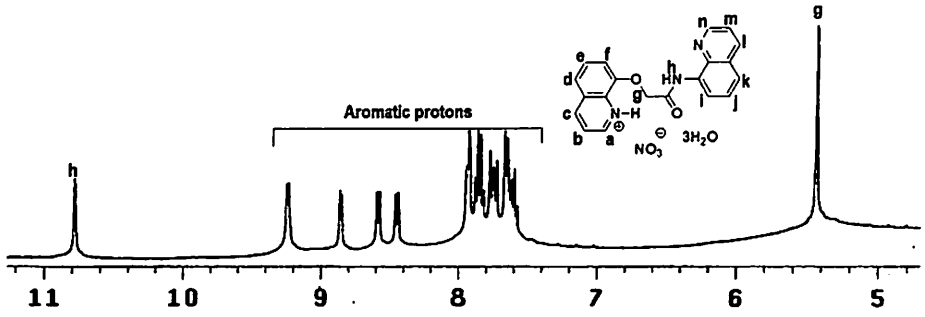

Figure 2.27: ^{1}H-NMR spectra of **2.3c**

Compound 2.3d:

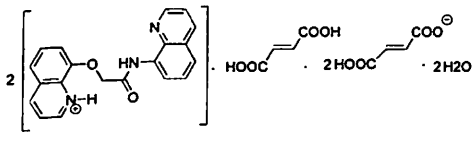

The compound **2.3** (0.33 g, 1 mmol) was dissolved in methanol. To this solution fumaric acid (0.12 g, 1mmol) was added and stirred for 20 min. The solution was then kept for crystallization, a brown coloured crystals appeared after 5 days.

Yield: 46%

IR (KBr, cm^{-1}): 3409 (bs), 1686 (s), 1545 (s), 1491(w), 1427 (m), 1318 (s), 1274 (s), 1218 (m), 1011(m), 825 (m), 645 (s).

^{1}HNMR (DMSO-d^6 , 400 MHz): 13.1(1H, s), 11.1 (1H, s), 9.0 (1H, s), 8.8 (1H, m), 8.7 (1H, d, J = 7.6Hz), 8.4 (2H, m), 7.7 (1H, d, J = 8.4Hz), 7.6 (5H, m), 7.4 (1H, d, J = 7.6Hz), 6.6 (3H, s), 5.1(2H, s).

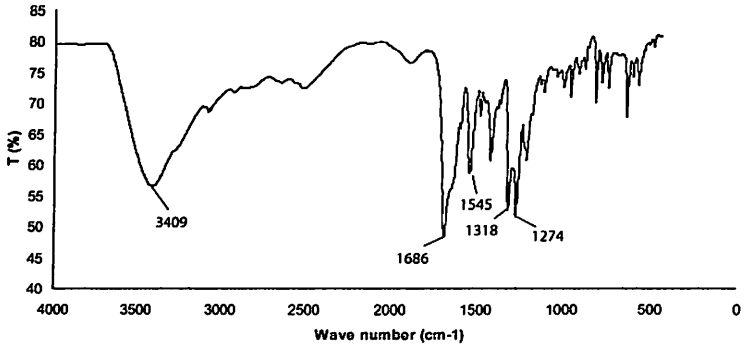

Figure 2.28: IR (KBr, cm^{-1}) spectra of **2.3d**

Compound 2.3e:

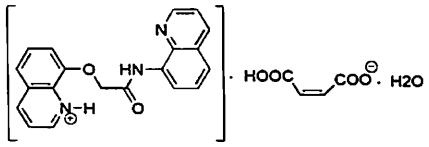

The compound **2.3** (0.33g, 1 mmol) was dissolved in methanol. To this solution maleic acid (0.12 g, 1mmol) was added and stirred for 20 min. The solution was then kept for crystallization, a brown coloured crystals of **2.3e** appeared after 3 days.

Yield: 66%

IR (KBr, cm^{-1}): 3393 (bs), 1684 (m), 1603 (m), 1543 (s), 1490 (s), 1427 (w), 1364 (m), 1353 (m), 1315 (m), 1274 (w), 1191 (w), 1120 (w), 961 (w), 873 (m), 824 (m), 793 (m), 745 (w), 611 (m).

^{1}HNMR (DMSO-d^6 400 MHz): 11.1 (1H, s), 9.0 (1H, s), 8.8 (1H, d, J = 4.0Hz), 8.7 (1H, d, J = 7.6Hz), 8.4 (2H, t, J = 8.4Hz), 7.7 (1H, d, J = 8.4Hz), 7.5 (5H, m), 7.4 (1H, d, J = 7.6Hz), 6.2 (2H, s), 5.1 (2H, s).

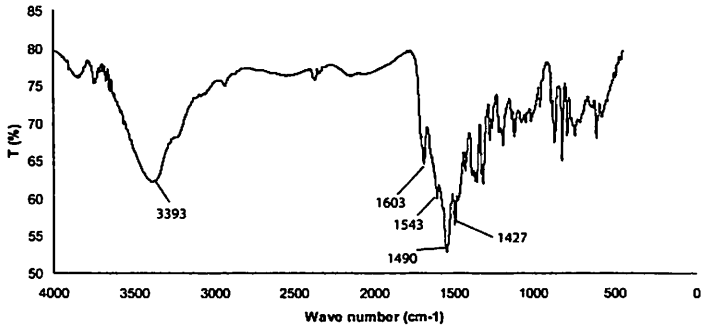

Figure 2.29: IR (KBr, cm^{-1}) spectra of **2.3e**

Compound 2.4:

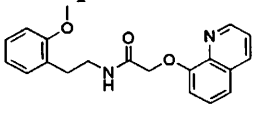

2-(2-Methoxyphenyl)ethylamine (0.755 g, 5 mmol) and triethylamine (0.505 g, 5 mmol) were dissolved in dry dichloromethane (20 mL). The solution was stirred at 0 ^{0}C for 15 min and bromoacetylbromide (0. 1.01 g, 5 mmol) was added to the solution over a period of 30 min. The reaction mixture was stirred overnight at room temperature. It was then filtered to remove the hydrobromide salts, and the filtrate was removed under reduced pressure. The corresponding amide obtained was recrystallised from dichloromethane. In the next step, the amide obtained (1.08 g, 5 mmol), 8-hydroxyquinoline (0.725 g, 5 mmol) and potassium carbonate (1.0 g, 7.5 mmol) were taken in dry acetone (20 mL) and the reaction mixture was stirred at 60

^{0}C for 9 hs (progress of the reaction was monitored at regular intervals using TLC). After completion of the reaction, the reaction mixture was filtered and the solvent was removed under reduced pressure. The product obtained was purified by column chromatography.

Yield: 54%.

IR (KBr, cm^{-1}): 3360 (bs), 3051 (s), 2968 (w), 1642 (s), 1601(m), 1552(s), 1504(s), 1497(s), 1469 (s), 1433 (m), 1380 (m), 1315 (s), 1264 (m), 1251(s), 1115(s), 1034 (m), 826 (m), 757 (s).

^{1}H NMR ($CDCl_3$, 400 MHz): 8.8 (1H, d, J = 4Hz), 8.2 (2H, d, J = 8.4Hz), 7.4 (2H, m), 7.0 (2H, d, J = 7.2Hz), 6.9 (1H, d, J = 7.2Hz), 6.7 (3H, m), 4.7 (2H, s), 3.7 (3H, s), 3.5 (2H, t, J = 6.8Hz), 2.8 (2H, t, J = 7.2Hz).

^{13}C-NMR ($CDCl_3$, 100 MHz): 30.3, 39.4, 55.3, 69.8, 110.4, 111.7, 120.5, 121.6, 122.1, 127.0, 127.5, 127.8, 129.7, 130.6, 136.5, 140.2, 149.4, 153.9, 157.7, 168.6.

LC-MS [M+1]: 337.17.

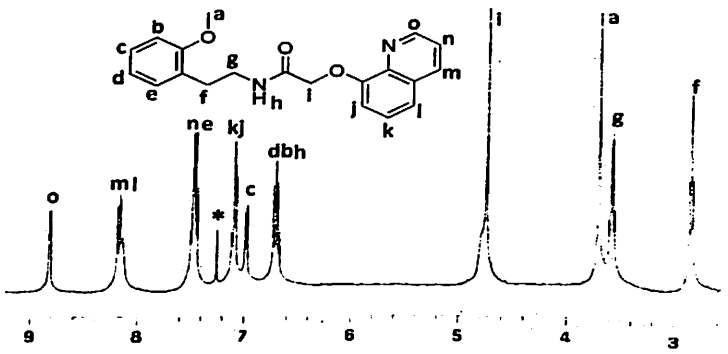

Figure 2.30: ^{1}H-NMR spectra of **2.4** (* indicates peak for the solvent)

Compound 2.4a:

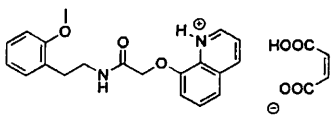

The compound **2.4** (0.34 g, 1 mmol) was dissolved in methanol. To this solution maleic acid (0.12 g, 1mmol) was added and stirred for 20 min. The solution was then kept for crystallization, colourless crystals of **2.4a** appeared after 3 days.

Yield: 74%.

IR (KBr, cm^{-1}): 3433 (bs), 3305 (s), 3056 (w), 3006 (w), 2940 (w), 1673 (s), 1618 (m), 1601 (m), 1495 (s), 1464 (s), 1348 (m), 1305 (m), 1280 (m), 1244 (m), 1111 (m), 1034 (w), 874 (w), 858 (m), 830 (m).

^{1}HNMR (DMSO-d^6 400 MHz): 8.9 (1H, d, J = 4.0Hz), 8.4 (2H, m), 7.6 (2H, m), 7.5 (1H, t, J = 8.0Hz), 7.2 (1H, d, J = 7.6Hz), 7.1(1H, t, J = 8.0Hz), 7.0 (1H, d, J = 7.2Hz), 6.9 (1H, d, J = 8.0Hz), 6.8 (1H. t, J = 7.6Hz), 6.2 (2H, s), 4.7 (2H, s), 3.7 (3H, s), 3.3 (2H, t, J = 6.8Hz), 2.7 (2H, t, J = 7.2Hz)

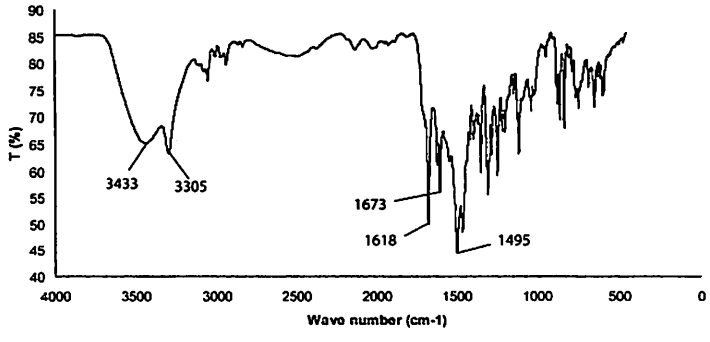

Figure 2.31: IR (KBr, cm^{-1}) spectra of **2.4a**

Compound 2.4b:

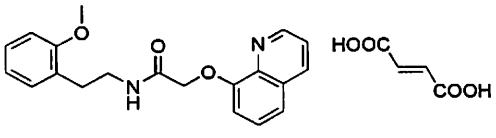

The compound **2.4** (0.34 g, 1 mmol) was dissolved in methanol. To this solution fumaric acid (0.12 g, 1 mmol) was added and stirred for 20 min. The solution was then kept for crystallization, colourless crystals of **2.4b** appeared after 5 days.

Yield: 77%.

IR (KBr, cm^{-1}): 3388 (s), 2941(w), 1703 (w), 1698 (w), 1672 (s), 1551 (m), 1508 (m), 1494 (m), 1424 (m), 1379 (m), 1296 (s), 1262 (s), 1245 (s), 1165 (m), 1111 (s), 1042 (m), 824 (m), 785 (m), 749 (s).

^{1}HNMR (DMSO-d^6 400 MHz): 8.9 (1H, d, J = 4.0Hz), 8.4 (2H, m), 7.5 (3H, m), 7.2 (1H, d, J = 7.6Hz), 7.1 (1H, t, J = 7.2Hz), 7.0 (1H, d, J = 7.6Hz), 6.9 (1H, d, J = 8.0Hz), 6.8 (1H, t, J = 7.6Hz), 6.6 (1H, s), 4.7 (2H, s), 3.7 (3H, s), 3.3 (2H, m), 2.7 (2H, t, J = 7.2Hz).

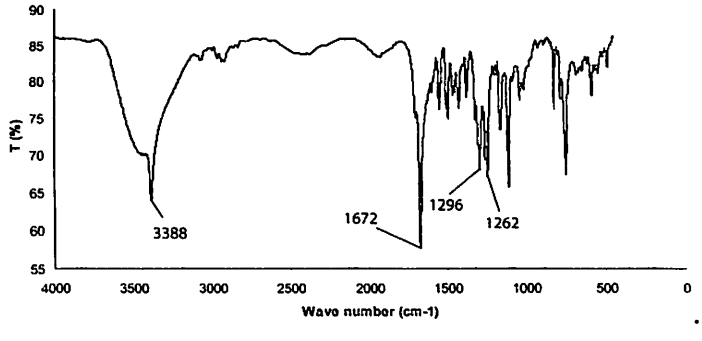

Figure 2.32: IR (KBr, cm^{-1}) spectra of **2.4b**

Compound 2.5:

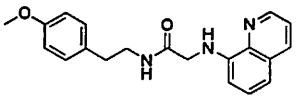

2-(4-Methoxyphenyl)ethylamine (0.735 mL, 5 mmol) and triethylamine (0.693 mL, 5 mmol) were dissolved in dry dichloromethane (20 mL). The solution was stirred at 0 ^{0}C for 15 min and bromoacetylbromide (0. 434 mL, 5 mmol) was added over a period of 30 min. The reaction mixture was stirred overnight at room temperature. It was then filtered to remove the hydrobromide salts, and the filtrate was removed under reduced pressure. The corresponding amide obtained was recrystallised from dichloromethane. In the next step, the amide obtained (1.08 g, 5 mmol), 8-aminoquinoline (0.72 g, 5 mmol) and potassium carbonate (1.0 g, 7.5 mmol) were taken in dry acetone (20mL) under nitrogen atmosphere and the reaction mixture was stirred at 60 ^{0}C for 9h (progress of the reaction was monitored at regular intervals using TLC). After completion of the reaction, the solvent was removed under reduced pressure. The product N-(4-methoxyphenethyl)-2-(quinolin-8-ylamino)acetamide obtained was purified by column chromatography.

Yield: 54%.

IR (KBr, cm^{-1}): 3300 (s), 3000 (m), 2922 (m), 1654 (s), 1613 (m), 1577 (m), 1549 (w), 1513 (s), 1478 (m), 1381 (s), 1325 (m), 1240 (s), 1182 (w), 1033 (m), 819 (m), 788 (m).

^{1}HNMR ($CDCl_3$, 400 MHz): 8.7 (1H, s), 8.1 (1H, d, J = 8.0Hz), 7.4 (2H, m), 7.2 (1H, m), 6.8 (3H, d, J = 8.4Hz), 6.5 (4H, m), 3.9 (2H, d, J = 6.4Hz), 3.6(3H, s), 3.4(2H, t , J = 6.8Hz), 2.6 (2H, t, J = 7.2Hz).

^{13}C-NMR ($CDCl_3$, 100 MHz): 35.3, 40.9, 49.0, 55.6, 106.6, 111.1, 114.3, 116.6, 122.2, 128.2, 130.1, 136.8, 141.4, 147.8, 170.7.

LC-MS [M+1]: 336.29

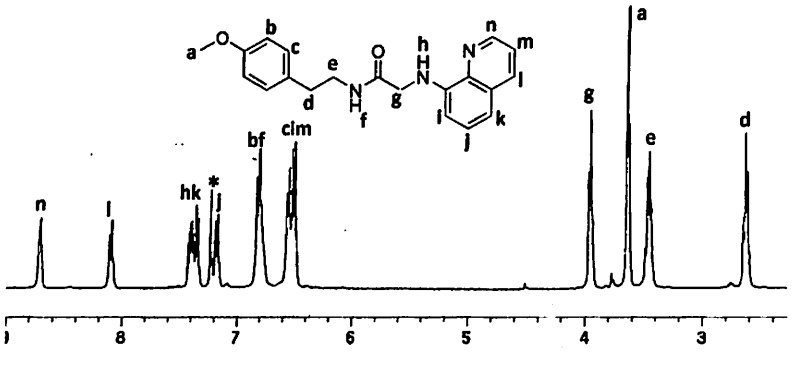

Figure 2.33: ^{1}H-NMR spectra of **2.5**

Compound 2.5a:

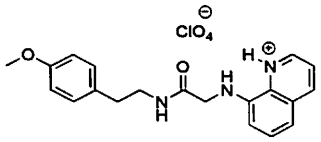

The perchlorate salt (**2.5a**) of protonated N-(4-methoxyphenethyl)-2-(quinolin-8-ylamino)acetamide) was obtained by dissolving it in dilute perchloric acid solution (3M) followed by warming for 10 min to obtain a transparent solution. The solution on standing led to brown crystals after 4 days.

Yield: 62%.

IR (KBr, cm^{-1}): 3335 (b), 3188 (m), 3119 (m), 3066 (m), 2928 (m), 1626 (s), 1557 (m), 1514 (s), 1475 (m), 1379 (s), 1250 (m), 1082 (bs), 812 (m), 622 (m).

^{1}HNMR (DMSO-d^6 400 MHz): 8.8 (1H, d, J = 4.0Hz), 8.5 (1H, d, J = 8.4Hz), 8.0 (1H, s), 7.6 (1H, m), 7.4 (1H, t, J = 8.4Hz), 7.2 (1H, d, J = 8.0Hz), 7.0 (2H, d, J = 8.0Hz), 6.7 (2H, d, J = 8.0Hz), 6.6 (1H, d, J = 8.0Hz), 3.9 (2H, s), 3.6 (3H, s), 3.3 (2H, m), 2.6 (2H, t, J = 6.8Hz).

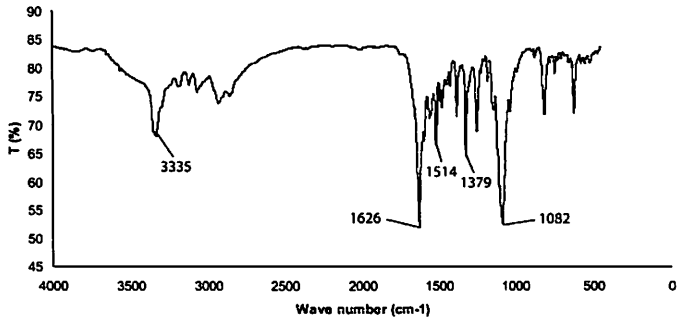

Figure 2.34: IR (KBr, cm^{-1}) spectra of **2.5a**

Compound 2.6:

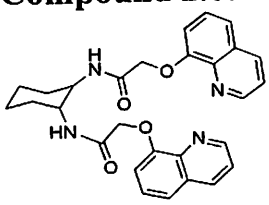

Trans-1,2-diaminocylohexane (0.342 g, 3 mmol) and triethylamine (0.61 g, 6 mmol) were taken in dry dichloromethane (20 mL). The solution was kept at 0 ^{0}C for 15 min and bromoacetylbromide (1.21 g, 6 mmol) was added over a period of 30 min so that the temperature does not rise above 10 ^{0}C. The reaction mixture was then stirred overnight at room temperature. To the reaction mixture 20 mL of water was added and the organic layer was separated using a separatory funnel. The solution was then dried over anhydrous sodium sulphate and decanted. The solvent was removed under

reduced pressure to obtain a brown solid. The crude product was then recrystallised from dichloromethane. The amide thus obtained (1.06 g, 3 mmol) along with 8-hydroxyquonoline (0.870 g, 6 mmol) and potassium carbonate (1.0 g, 7.4 mmol) were taken in dry tetrahydrofuran (20 mL) and stirred at 70 ^{0}C for 9 hs (progress of the reaction was monitored at regular intervals using TLC). After completion of the reaction, the product was filtered and the solvent was removed under reduced pressure. The product was further purified by thin layer chromatography.

Yield: 57%.

IR (KBr, cm^{-1}): 3465 (b), 2927 (m), 2856 (w), 1660 (s), 1551(m), 1504 (m), 1474 (w), 1437 (w), 1378 (m), 1318 (m), 1260 (m), 1184 (w), 1112 (m), 785 (m), 751(m).

^{1}H NMR ($CDCl_3$, 400 MHz): 8.9 (2H, d, J = 4.4Hz), 8.2 (2H, d, J = 8.4Hz), 7.5 (2H, m), 7.4 (2H, t, J = 8.4Hz), 7.3 (2H, t, J = 8.0Hz), 6.9 (2H, d, J = 7.6Hz), 4.6 (2H, d, J = 14.8Hz), 4.4 (2H, d, J = 15.2Hz), 3.9 (2H, bs), 2.0 (3H, m); 1.7 (3H, m); 1.2 (4H, m).

^{13}C-NMR ($CDCl_3$, 100 MHz): 25.0, 32.7, 52.5, 69.1, 102.2, 111.1, 121.4, 122.2, 126.9, 128.1, 129.8, 136.7, 149.4, 168.6.

LC-MS [M+1]: 485.24

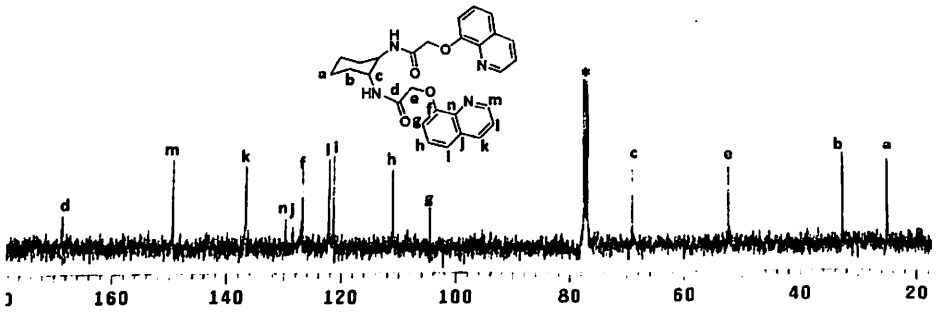

Figure 3.35: ^{13}C-NMR spectra of **2.6**

Compound 2.7:

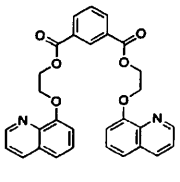

8-hydroxyquinoline (0.725 g, 5 mmol) was dissolved in dry acetone (20 ml) and potassium carbonate (1.0 g, 7.5 mmol) was added to it. The solution was stirred at room temperature for 15 min and then methyl bromoacetate (0.76 g, 5 mmol) was added and the reaction mixture was refluxed at 70 ^{0}C for 12 h (Progress of the reaction was monitored at regular intervals using TLC). After completion of the

reaction, the reaction mixture was filtered and the solvent was then removed under reduced pressure to obtain the ester as a yellow solid. In the next step, the ester was reduced to the corresponding alcohol [2-(quinolin-8-yloxy) ethanol] using a reported procedure.

Yield: 77%.

IR(KBr, cm^{-1}): 3405 (b), 3175 (b), 2923 (m), 2861(m), 1613 (w), 1505 (m), 1475 (m), 1381 (m), 1322 (m), 1266 (m), 1116 (m), 1075 (s), 904 (w), 823 (m).

^1H NMR ($CDCl_3$, 400 MHz): 8.8 (2H, d, J = 4.4Hz), 8.0 (2H, d, J = 8.4), 7.3 (3H, m), 7.0 (1H, d, J = 7.6Hz), 4.2 (2H, t, J = 4.8Hz), 4.1 (2H, t, J = 4.8Hz), 3.4(1H, bs).

The 2-(quinolin-8-yloxy) ethanol (0.756 g, 4 mmol) was dissolved in dry dichloromethane (20 ml) and triethylamine (0.404 g, 4 mmol) was added to it. The solution was stirred at 0 ^0C for 15 min and isophthaloyl dichloride (0.404 g, 2 mmol) was added. The reaction mixture was then refluxed at 40^0C for 8 hs (progress of the reaction was monitored at regular intervals using TLC). After completion of the reaction, 30 ml of water was added to reaction mixture and the organic layer was separated using a separatory funnel. The solvent was removed under reduced pressure to obtain a light yellow colour solid. The product was further purified by thin layer chromatography (silica gel; hexane/ethyl acetate 5:3).

Yield: 73%.

IR (KBr, cm^{-1}): 3422 (b), 2921(w), 1720 (s), 1608 (w), 1508 (m), 1474 (w), 1451(w), 1382 (m), 1259 (w), 1119 (m), 822 (w), 790 (w).

^1H NMR (DMSO-d^6, 400 MHz): 8.8 (2H, d, J = 2.8Hz), 8.4 (1H, s), 8.3(2H, d, J = 8Hz), 8.1(3H, t, J = 6.4Hz), 7.6 (2H, t, J = 7.6Hz), 7.5 (4H, m), 7.3 (2H, t, J = 5.2Hz), 4.7 (4H, s), 4.5(4H, s).

^{13}C-NMR (DMSO-d^6, 100 MHz): 166.5, 133.3, 131.1, 129.9, 129.3, 129.1, 122.5, 122.2, 112.3, 71.1; 54.8

LC-MS (M+1): 509.22

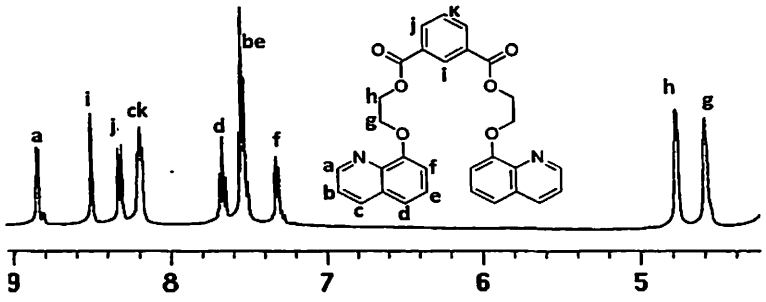

Figure 3.36: ^{1}H-NMR spectra of **2.7**

Compound 2.8:

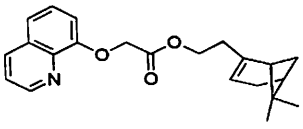

(1R)-(-)-Nopol (0.83g, 5 mmol) was dissolved in dry dichloromethane (20 mL) and triethylamine (0.61g, 6 mmol) was added to it. The solution was stirred at 0^{0}C for 15 min and bromoacetylbromide (1.01 g, 5 mmol) was added to the stirred solution over a period of 30 min. The reaction mixture was then stirred overnight at room temperature. To the reaction mixture 20 mL of water was added and the organic layer was separated using a separatory funnel. The solution was then dried over anhydrous sodium sulphate and the solvent was decanted. The solvent was removed under reduced pressure to obtain a yellow liquid product. The product thus obtained (1.4g, 5 mmol) together with 8-hydroxyquonoline (0.72g, 5mmol) and potassium carbonate (1.0g, 7.4 mmol) were taken in dry acetone (20mL) and the stirred at 70 ^{0}C for 9 hs (progress of the reaction was monitored at regular intervals using TLC). After completion of the reaction, the product was filtered and the solvent was removed under reduced pressure. The product was further purified by thin layer chromatography.

Yield: 63%.

IR (KBr, cm^{-1}): 3447 (bs), 2922 (m), 1747 (s), 1631 (s), 1502 (m), 1382 (m), 1242 (m), 1122 (s), 1040 (m), 824 (m).

^{1}H NMR ($CDCl_3$, 400 MHz): 8.9 (1H, s), 8.1 (1H, d, J = 8.0Hz), 7.4 (3H, m), 6.9 (1H, m), 5.1 (1H, s), 4.9 (2H, s), 4.6 (1H, m), 4.2 (2H, m), 3.7 (1H, m), 2.1 (2H, m), 2.0 (2H, m), 1.9 (2H, m), 1.1 (3H, s), 0.7 (3H, s).

^{13}C-NMR ($CDCl_3$, 100 MHz): 169.0, 153.8, 149.6, 143.8, 140.3, 136.1, 129.8, 126.5, 122.0, 121.1, 119.2, 109.6, 66.2, 63.7, 45.7, 40.8, 38.1, 35.9, 31.7, 31.4, 26.4, 21.2.

LC-MS [M+1]: 352.04

$[\alpha]_D^{25} = -17.3$

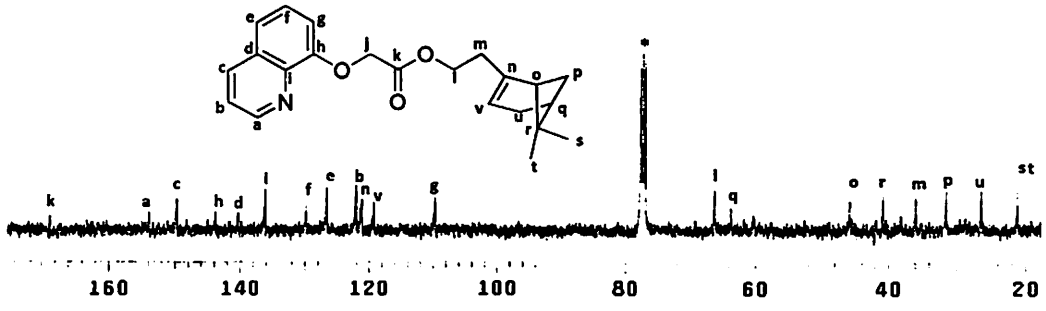

Figure 3.37: ^{13}C-NMR spectra of **2.8** (* indicates peaks for solvent)

Caution: Perchlorate salts are potentially explosive; however, our systems described here are stable and have not shown such property under ambient condition, it is advisable that care needs to be taken while dealing with perchlorate salts.

References

1. D. J. Kushner, *Bacteriological reviews,* 1969, **33**, 302.
2. Y. Ho, J-C. Hsiao, M-H. Yang, C-S. Chung, Y-C, Peng; T-H. Lin, W. Chang and D-L. Tzou, *J. Mol. Bio.,* 2005, **349**, 1060.
3. J-W. Kim, D. P. Carpenter and R. Deaton, *Nanomedicine: nanotechnology, biology and medicine,* 2005, **1**, 220.
4. A. M. Bittner, Eds. P. Behrens, E. Baeuerlein, *Handbook of Biomineralization: Biomimetic and Bioinspired Chemistry,* 2007, 335.
5. P. Ringler and G. E. Schulz, *Science*, 2003, **302**, 106.
6. K. Matsuura, K. Murasato and N. Kimizuka, *J. Am. Chem. Soc.*, 2005, **127**, 10148.
7. C-J. Tsai, J. Zheng, D. Zanuy, N. Haspel, H. Wolfson, C. Aleman and R. Nussinov, *Proteins: Structure, Function, and Bioinformatics,* 2007, **68**, 1.
8. Y. Furusho, Y.Tanaka, T. Maeda, M. Ikeda and E. Yashima, *Chem. Commun.*, 2007, 3174.
9. L-S. Li, H. Jiang, B.W. Messmore, S. R. Bull and S. I Stupp, *Angew. Chem. Int. Ed. Eng.*, 2007, **46**, 5873.

10. K. Bowman-James, *Acc. Chem. Res.*, 2005, **38**, 671.

11. *Supramolecular Chemistry of Anions*, Ed. A. Bianchi, K. Bowman-James, E. Garcia-España, Wiley-VCH, New York, 1997.

12. J. L. Sessler, S. Camiolo and P.A. Gale, *Coord. Chem. Rev.*, 2003, **240**, 17.

13. J. L. Sessler, E.A. Katayev, D.G. Pantos, P. Scherbakov, M.D. Reshetova, Y.N. Khurstalev, V.M. Lynch and Y.A. Ystaynyuk, *J. Am. Chem. Soc.*, 2005, **127**, 11442.

14. S.O. Kang, D. VanderVelde, D. Powell and K. Bowman-James, *J. Am. Chem. Soc.*, 2004, **126**, 12272.

15. C.A. Ilioudis and J.W. Steed, *Org. Biomol. Chem.* 2005, **3**, 2935.

16. P.D. Beer and P.A. Gale, *Angew. Chem. Int. Ed. Eng.* 2001, **40**, 486.

17. P.A. Gale, *Coord. Chem. Rev.*, 2001, **213**, 79.

18. J. Scheerder, J. F. J. Engbersen, A. Casnati, R. Ungaro and D. N. Reinhoudt, *J. Org. Chem.*, 1995, **60**, 6448.

19. R. C. Jagessar, M. Shang, W. R. Scheidt and D. H. Burns, *J. Am. Chem. Soc.*,1998, **120**, 11684.

20. B. H. M. Snellink-Ruel, M. M. G. Antonisse, J. F. J. Engbersen, P. Timmerman and D. N. Reinhoudt, *Eur. J. Org. Chem.*, 2000, 165.

21. M. Boiocchi, B. L. Del, D. E. Gomez, L. Fabbrizzi, M. Licchelli and E. Monzani, *J. Am. Chem. Soc.*, 2004, **126**, 16507.

22. D. A. Jose, D. K. Kumar, B. Ganguly and A. Das, *Inorg. Chem.* 2007, **46**, 5817.

23. D. A. Jose, D. K. Kumar, P. Kar, S. Verma, A. Ghosh, B. Ganguly, H. N. Ghosh and A. Das, *Tetrahedron*, 2007, **63**, 12007.

24. R. Custelcean, V. Sellin and B. A. Moyer, *Chem. Commun.*, 2007, 1541.

25. C. Zhao, P. L. Polavarapu, C. Das and P. Balaram, *J. Am. Chem. Soc.*, 2000, **122**, 8228.

26. A. Karmakar, R. J. Sarma and J. B. Baruah, *CrystEngComm.*, 2007, **9**, 379.

27. S. Goswami and R. Chakrabarty, *Tetrahedron Lett.*, 2009, **50**, 5994.

28. J. Kang , S. P. Jang , Y. H. Kim, J. H. Lee, E. B. Park, H. G. Lee, J. H. Kim, Y. Kim, S. J. Kim and C. Kim, *Tetrahedron Lett.*, 2010, **51**, 6658.

29. N. Kameta and K. Hiratani, *Chem. Commun.*, 2005, 725

30. K. Ghosh and S. Adhikari, *Tetrahedron Lett.*, 2006, **47**, 3577

31. W. Racshofer, W. M. Muller and F. Vogie, *ibid.*, 1979, **112**, 2095.

32. I. Tabushi, Y. Kuroda, and T. Mizutani, *J. Am. Chem. Soc.*, 1986, **108**, 4514.

33. A. Galan, D. Andreu, A. M. Echavarren, P. Prados and J. de Mendoza, *J. Am. Chem. Soc.*, 1992, **114**, 1512.

34. Y. Kuroda, Y. Kato, T. Higashioji, J. Hasegawa, S. Kawanami, M. Takahashi, N. Shiraishi, K. Tanabe and H. Ogoshi, *J. Am. Chem. Soc.*, 1995, **117**, 10950.

35. A. Metzger, K. Gloe, H. Stephan and F. P. Schmidtchen, *J. Org. Chem.*, 1996, **61**, 2051.

36. G. Arena, A. Casnati, A. Contino, A. Magr, F. Sansone and D. Sciotto, R. Ungaro, *Org. Biomol. Chem.*, 2006, **4**, 243.

37. I. Nicolas, S. Chevance, P. L. Maux and G. Simonneaux, *Tetrahedron: Asymmetry*, 2010, **21**, 1788.

38. R. Van Deun, P. Fias, K. Binnemans and C. Gorller-Walrand, *Phys.Chem. Chem. Phys.*, 2003, **5**, 2754.

39. S. Goswami and R. Chakrabarty, *Tetrahedron Lett.*, 2009, **50**, 5994.

40. J. Kang , S. P. Jang , Y. H. Kim, J. H. Lee, E. B. Park, H. G. Lee, J. H. Kim, Y. Kim, S. J. Kim and C. Kim, *Tetrahedron Lett.*, 2010, **51**, 6658.

41. N. Kameta and K. Hiratani, *Chem. Commun.*, 2005, 725.

42. Y. Umezawa, S. Tsuboyama, K. Honda, J. Uzawa and M. Nishio, *Bull. Chem. Soc. Jpn.*, 1998, **71**, 1207.

43. C. Cruces-Blanco, A. S. Carretero, S. F. Peinado and A. F.Gutierrez, *Mikrochim. Acta*, 2000, **134**, 107.

44. N. A. Masoud, *J. Chem. Soc. Pak.*, 2002, **24**, 171.

45. M. S. Searle, S. R. Griffiths-Jones and H. Skinner-Smith, *J. Am. Chem. Soc.*, 1999, **121**, 11615.

46. M. S. Searle, *Peptide Sci.*, 2004, **76**, 185.

47. M. S. Searle, *J. Chem. Soc. Perkin Trans.*, 2001, **2**, 1011.

48. M.R. Ghadiri and C. Choi, *J. Am. Chem. Soc.*,1990, **112**, 1630.

49. C. Janiak, S. Temizdemir, S. Dechert, W. Deck, F. Girgsdies, J. Heinze, M. J. Kolm, T. G. Scharmann and O. M. Zipffel, *Eur. J. Inorg. Chem.*, 2000, 1229.

50. M. Nishio, *CrystEngComm*, 2004, **6**, 130.

51. A. Nangia and G.R. Desiraju, *Supramolecular Synthons and pattern recognition: Design of organic solids;* ed. E.Weber Springer-Verlag, Berlin, 1998.

52. G. R. Desiraju, *Crystal design: Structure and function in Perspectives in Supramolecular chemistry*, **7**, 2003.

53. C. Janiak, *J. Chem. Soc. Dalton Trans.*, 2000, 3885.

54. S. L. Cockroft, C.A. Hunter, K.R. Lawson, J. Perkins and C. J. Urch, *J. Am. Chem. Soc.*, 2005, **127**, 8594.

55. M. E. Vazquez, J. B. Blanco, B. Imperiali, *J. Am. Chem. Soc.*, 2005, **127**, 1300.

56. S. Kitagawa and K. Uemura, *Chem. Soc. Rev.*, 2005, **34**, 109.

57. J. Y. Lu and A. M. Babb, *Chem. Commun.*, 2003, 1346.

58. L. J. Barbour, *Chem. Commun.*, 2006, 1163.

Chapter 3

Cyclisation reactions of amide derivatives of quinoline in presence of base and metal ions

Intra-molecular cyclisation processes are very useful in heterocycle synthesis.[1-6] Such cyclization reactions are used for synthesis of varieties of natural products and drugs. Among them N-acylinium ion cyclisation reactions are very attractive.[7-10] The intra-molecular reactions are generally carried out under catalytic conditions.[3] Several of these reactions require multiple steps.[1] Multi-component reactions to prepare heterocycles would help to reduce hassles[11-18] of product purification in each step and also would reduce the reaction time. Several naturally occurring compounds and drug molecules contain quinoline ring as their constituent.[19-24] Aminoquinoline derivatives are useful in cyclisation reactions for ring expansion[25-28] and for synthesis of steroid derivative.[29-30] Intramolecular cyclisation reactions of 8-aminoquinoline derivatives are very attractive as multiple possibilities to obtain cyclised products exist. For example, novel heterocyclic compounds through intra-molecular C-C bond formation by palladium catalysed reactions were observed in imine derivatives of 8-aminoquinoline.[31] Recently the coordination effects of amide functionalised 8-aminoquinoline derivatives are used for intramolecular cyclisation.[32] Further to this, the halo derivatives can also undergo conventional nucleophilic substitution by nucleophiles such as water, alcohol, amine etc. Thus, the competitive reactions of cyclisation versus nucleophilic substitution reactions in the presence or absence of metal catalyst are of interest. In this chapter the cyclization reactions of two quinoline based amide derivetives **3.1** and **3.2** under different reaction conditions are discussed.

3.1

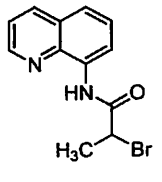

3.2

3.1 Reaction of the substrate 3.1 and 3.2 in presence of base

A three component reaction between 2-bromo-N-quinoline-8-yl-acetamide (**3.1**), 2-(4-Methoxyphenyl) ethylamine and acetone gives a fused ring heterocyclic compound **3.3** as illustrated in scheme 3.1. The compound is characterized from its spectroscopic properties. The compound has IR absorptions at 1676 cm^{-1} and at 1635 cm^{-1} due to carbonyl and C=N stretching. The mass spectrum of the compound shows the desired mass for the M^+ peak at 414.27.

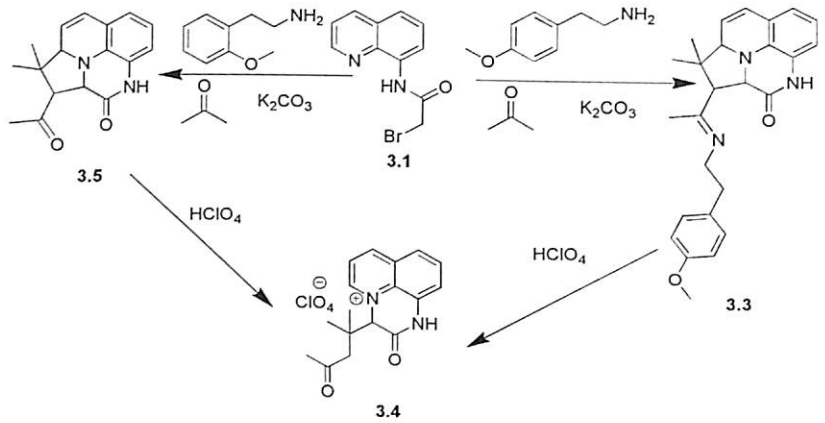

Scheme 3.1: Reaction leading to product **3.3** and **3.5** which reacts with perchloric acid to form salt **3.4**

The ^{1}H-NMR spectra of compound **3.3** shows three singlets at 1.0 ppm, 1.1 ppm and 1.7 ppm for the three methyl groups and another singlet at 3.7 ppm for the methoxy gropup.

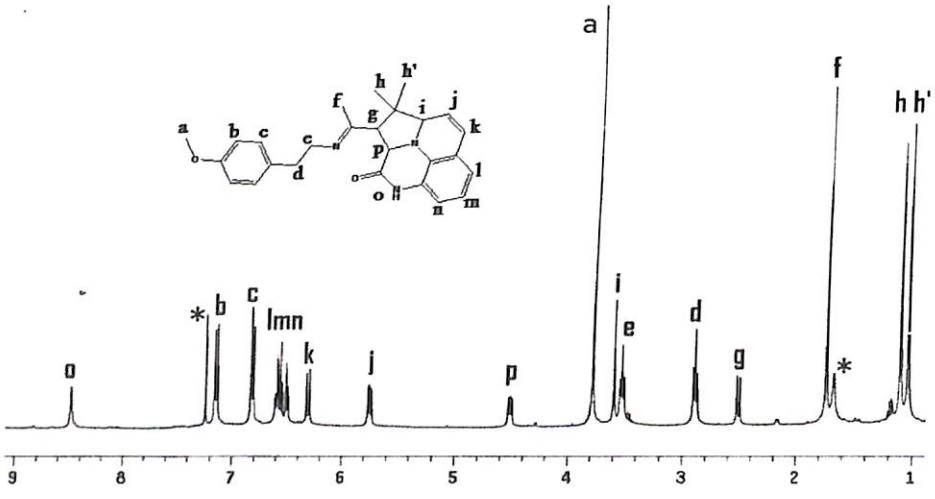

Figure 3.1: ^{1}H-NMR spectra of **3.3** (* indicates the peak for the solvent and water associated with solvent)

A singlet at 8.4 ppm represents the –NH proton. Apart from these charaterestic peaks the ^{1}HNMR spectra contains the desired peaks for compound **3.3** as shown in figure 3.1. Further, the ^{13}CNMR spectra of **3.3** also show the desired peaks for the aliphatic and aromatic carbons of compound **3.3**.

The compound is also characterized by X-ray crystallography and the structure of the compound is shown in figure 3.2.

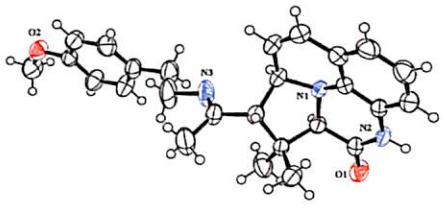

Figure 3.2: Crystal structure of **3.3** (ORTEP drawn with 50% thermal ellipsoid)

Plausible reaction paths (scheme 3.2) for the formation of the compound **3.3** may be through an initial condensation reaction of two molecules of acetone to form an aldol intermediate. The carbonyl group of the aldol gets condensed with 2-(4-methoxyphenyl)ethylamine to form an imine derivative as an intermediate species. The imine containing molecule has a hydroxy group, which is attached to a tertiary carbon and it would easily form C-C bond with the quinoiline ring through elimination of a water molecule. Presumably, this intermediate compound forms a bromide salt through cyclisation reaction. The cyclised product thus formed, undergo a hydride shift to form a derivative that is suitable for further nucleophilic attack of an anion generated next to the C=N group. It forms the desired product **3.3**. Thus, by these reaction steps, two additional rings over the quinoline rings are constructed. The added advantage of this reaction is that it does not stop at the stage of formation of one ring that is generally formed in intra-molecular cyclisation reactions.

This reaction proceeds in presence of a solid base viz. potassium carbonate. The excess of acetone serves the dual purpose of reactant as well as solvent. The formation of multiple rings provides a means to prepare compound **3.1** which otherwise would require multiple steps and use of less common reagents.

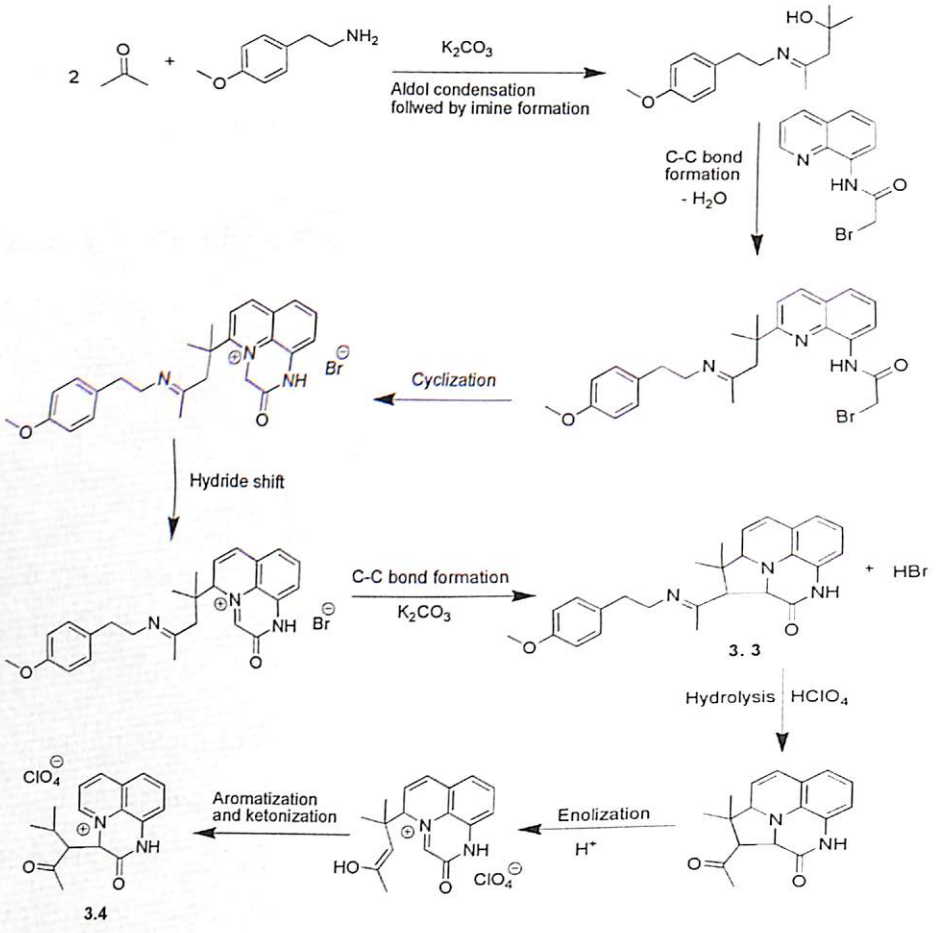

Scheme 3.2: Plausible paths for formation of **3.3** and **3.4**

The compound **3.3** undergoes hydrolysis cum ring opening reaction to give a quinaxalin derivative in the form of a perchlorate salt **3.4** as illustrated in scheme 3.1. The product **3.4** is characterized by conventional spectroscopic techniques as well as by X-ray single crystal structure (figure 3.3) determination. Formation of this salt can be explained by a three step mechanistic path as illustrated in scheme 3.2. The first step could be the generation of ketone from a hydrolytic reaction of perchloric acid from the conversion of imine to keto group. The keto compound thus formed would get protonated under acidic condition to give enolised form of a cationic species with perchlorate anion as counterion. This leads to opening of the five member ring of the parent compound. The enolic cation thus formed, on aromatisation leads to concomitant cleavage of a C-C bond along with the formation of a new C-C bond at a tertiary carbon. This new C-C bond formation along with enol to keto transformation of the enol form as illustrated in scheme 3.2 gives the final product **3.4**. The IR spectra of the salt **3.4** have characteristic sharp perchlorate absorption at 1100 cm^{-1} and it has carbonyl absorption at 1705 cm^{-1}.

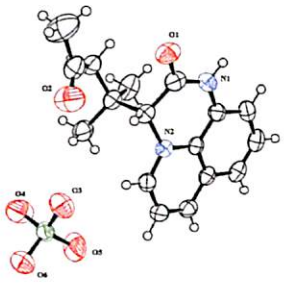

Figure 3.3: Crystal structure of **3.4** (ORTEP drawn with 50% thermal ellipsoid)

The ^{1}H-NMR spectra of compound **3.4** shows three singlets at 0.7 ppm, 1.0 ppm, and 2.1 ppm for the three methyl groups. The singlet peak for the –NH proton appears at 12.0 ppm. The ^{1}H-NMR spectra contains all the desired peaks for compound **3.4** as shown in figure 3.4.

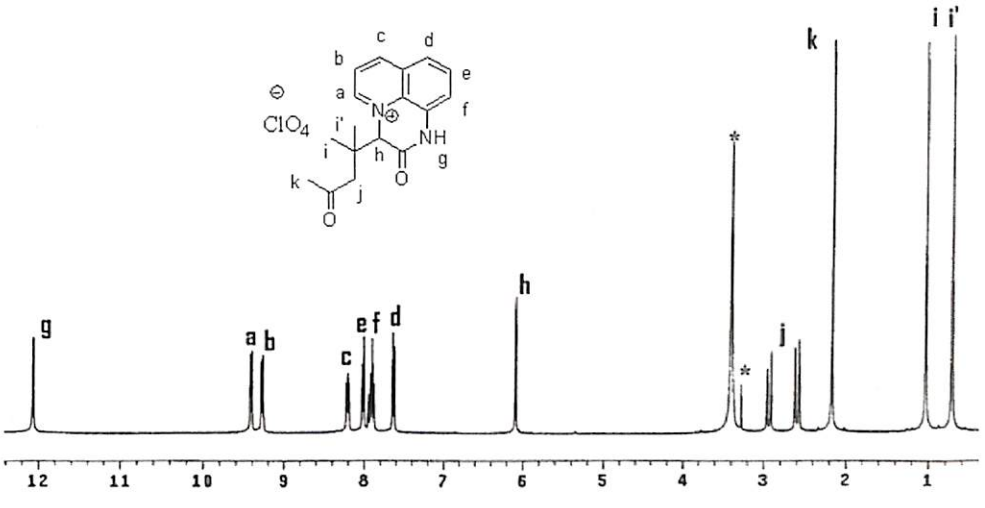

Figure 3.4: ^{1}H-NMR spectra of **3.4** (* indicates the peak for the solvent and water associated with solvent)

Further, we did not observe any aldol condensation and cyclisation reactions when we have reacted 2-bromo-N-quinoline-8-yl-acetamide with acetone in the presence of potassium carbonate without using an amine. When 2-(4-methoxyphenyl) ethylamine was reacted with acetone in the presence of potassium carbonate it led to an imine. However, this imine did not react with 2-bromo-N-quinoline-8-yl-acetamide to give product **3.3**. This suggests that the aldol condensation and the formation of imine took place concomitantly in the presence of 2-bromo-N-quinoline-8-yl-acetamide. When the same reaction was carried out with 2-(2-methoxyphenyl)ethylamine, we obtained the product **3.5**. The product **3.5** on further treatment with perchloric acid gives the product **3.4** (scheme 3.1). This shows that formation of **3.4** is an independent process,

but it depend on the type of amine used. The formation of a ketone instead of imine as the final product while using 2-(2-methoxyphenyl) ethylamine may be due to the possible hydrolysis of the imine formed from this reaction. We also carried out similar reactions of 2-bromo-N-quinoline-8-yl-acetamide (**3.1**) with other amines such as benzyl amine, picolyl amine and no reaction was observed under analogous reaction conditions. However, aromatic amines such as 8-aminoquinoline replaced the bromide of 2-bromo-N-quinoline-8-yl-acetamide to form C-N bonded derivative. Use of ethylmethyl ketone as solvent did not lead to the aldol condensation reaction; instead 2-(4-methoxyphynelamino)-N-(quinoline-8-yl)acetamide was formed as a product **3.6** by substitution of bromine (scheme 3.3) by 2-(4-methoxyphenyl) ethylamine.

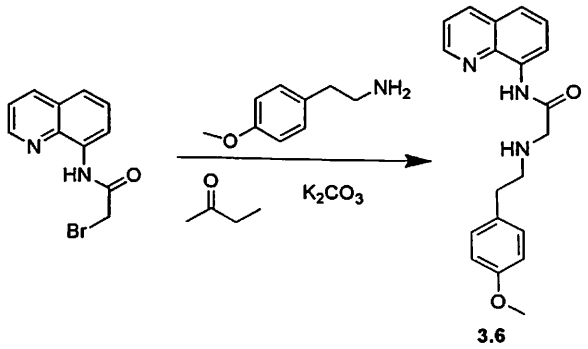

3.6

Scheme 3.3: Formation of product **3.6** in ethyl methyl ketone

When we have changed the substrate to 2-bromo-N-(quinolin-8-yl)propanamide (**3.2**) another product **3.7** is formed. In this case the aldol condensation took place without the formation of the cyclized product (scheme 3.4). This is attributed to the steric effect of the methyl group in the compound next to the carbonyl group.

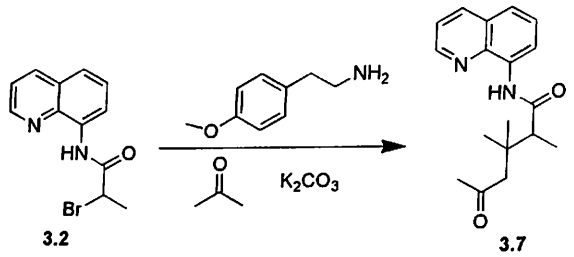

3.2 3.7

Scheme 3.4: Formation of product **3.7**

3.1 Reaction of the substrate 3.1 and 3.2 in presence of metal ion

The cyclization reactions of the two substrates **3.1** and **3.2** are also studied in presence of two metal ions namely copper(II) and nickel(II) salts.

The compound 2-bromo-N-(quinolin-8-yl)acetamide (**3.1**) on reaction with nickel(II) and copper(II) salts in methanol or in ethanol gives cyclised product through C-N bond formation (scheme 3.5). Depending on the counter anion on the metal salt used the cyclic amides **3.8a** and **3.8b** were formed. The products were characterized by different spectroscopic tools such as IR, NMR, LC-MS etc. In these reactions the bromide anion is replaced by the nitrate or perchlorate anions to form either the nitrate (**3.8a**) or the perchlorate salt (**3.8b**) of the cyclised product. However, when the reaction is carried out by the acetate salt of metal ions, the bromide anion is not replaced by the acetate anion thereby forming the bromide salt of the cyclised product.

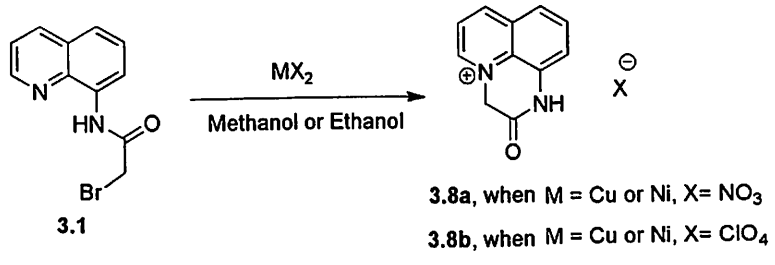

Scheme 3.5: Synthesis of compound **3.8a** and **3.8b**

The 2-bromo-N-(quinolin-8-yl)propanamide (**3.2**) also underwent cyclisation reactions through C-N bond formation reactions in methanol in the presence of different metal salts of copper(II) and nickel(II). The reactions were found to be highly solvent dependent and also metal dependent. When copper(II) salts were used in methanol exclusively cyclised product **3.9** in the form of the salt of the corresponding ions were obtained via C-N bond formation. When the cyclisation reactions were attempted in ethanol with copper(II) salts, no cyclisation of **3.2** was observed, but nucleophilic substitution leading to C-O bond gave compound **3.10**. It is also observed that the intra-molecular cyclisation reaction of **3.2** is promoted by nickel(II) salts and the compound **3.11** is formed in both methanol and ethanol. These observations clearly indicate that the reactions are highly sensitive towards both metal ions and solvent systems. The reactions are shown in scheme 3.6. These reactions

were found to be facilitated by metal ions as the simple dissolution of **3.2** in methanol or ethanol for two hours do not lead to products but presence of stoichiometric amount of copper(II) or nickel(II) ions in the reaction mixture gave the products within this time. Further, the counter anion has a role as the anions such as perchlorate and nitrate were found to be more suitable over ions like acetate, chloride or bromide. The intra-molecular cyclisation reactions leading to heterocyclic rings are very common in organic chemistry[33-34] and preferences of formation of thermodynamically favoured products are well documented.

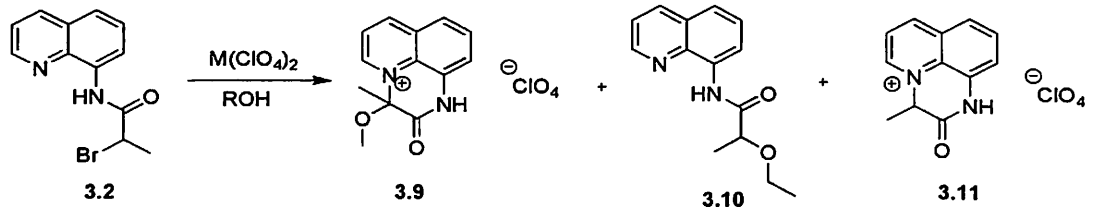

% ratio of product 3.9: 3.10: 3.11

M = Cu, R=CH_3 ;	100	0	0
M = Cu, R=CH_3CH_2 ;	0	100	0
M = Ni, R=CH_3CH_2, CH_3 ;	0	0	100

Scheme 3.6: Synthesis of product **3.9**, **3.10**, and **3.11**

Products obtained from each reaction were characterised by IR, ^{1}H-NMR, ^{13}C-NMR and LC-MS spectroscopy. The crystal structures of the products were also studied where good quality crystals could be obtained. Since the compound **3.9** and **3.11** are similar cyclic compounds with a difference in methoxy group and to show each products from these reactions varied a comparison of the ^{1}HNMR spectra of compound **3.9**, **3.10** and **3.10** is shown in figure 3.5. The compound **3.9** has signals at 3.5 ppm due to -OCH_3 group and the signal of methyl group at 1.9 ppm is a singlet. The compound **3.11** is devoid of –OCH_3 signal but has signals at 5.8 ppm as multiplet due to CH next to methyl group which shows signal at 1.8 ppm. The compound **3.10** has characteristic quartet and triplet from -OCH_2CH_3 group (3.4 and 1.0 ppm) and has doublet (1.8 ppm) and quartet (5.8 ppm) from CH and CH_3 groups.

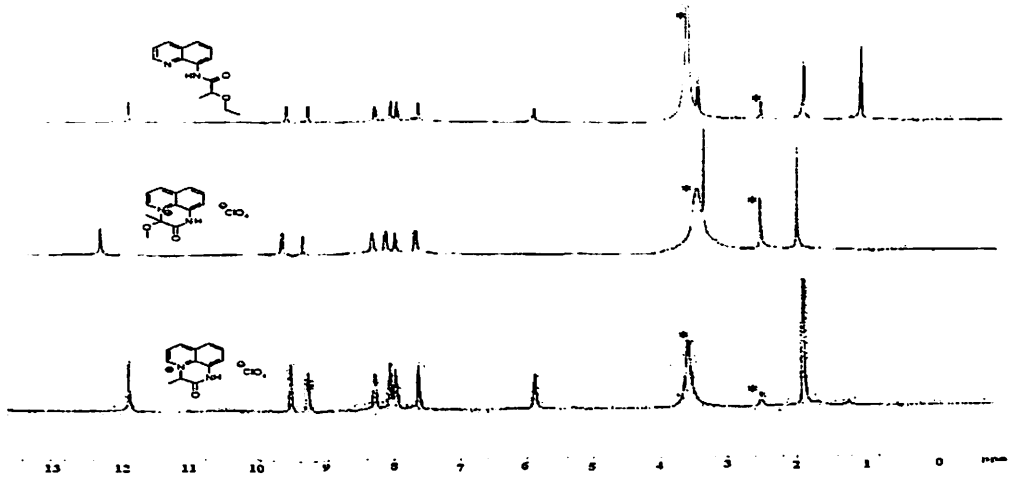

Figure 3.5: Comparison of ^{1}H-NMR spectra of **3.9, 3.10** and **3.11** (* indicates the peak for solvent and water associated with solvent)

In order to look at the role of solvent, in the intramolecular cyclisation of **3.2**, we have carried out the copper(II) perchlorate mediated reaction in a 1:1 mixed solvent of methanol and ethanol. From this reaction only compound **3.9** was obtained. To know the source of the incorporated methoxy group in compound **3.9** we carried out the copper(II) perchlorate mediated reaction of **3.2** in deuterated methanol. From this reaction we have isolated deuterium substituted product **3.9a** (scheme 3.7) showing

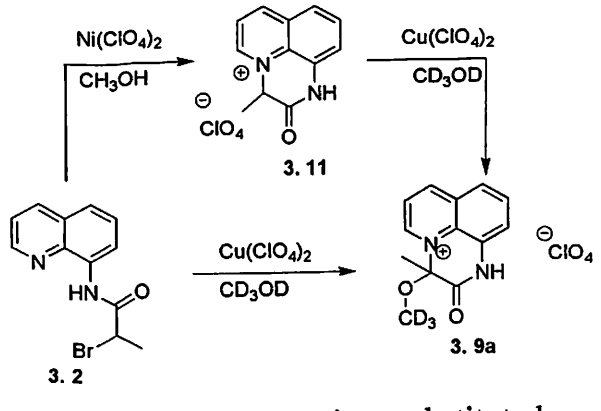

Scheme 3.7: Formation of deuterium substituted product **3.9a**

methanol solvent to be the source for the methoxy group. The mass spectra of **3.9** have m/e at 229.09 whereas the mass spectra of **3.9a** have m/e at 232.09 suggesting the later to have CD_3O- group. Further to this, when compound **3.9** was reacted with $Cu(ClO_4)_2$, in CD_3OD we obtained compound **3.9a** (scheme 3.7). This proves that in the case of copper(II) mediated reaction first the intra-molecular nucleophilic substitution takes place to form C-N bond, leads to product **3.11**, it further reacts with methanol in presence of copper to give product **3.9**. The $S_{RN}1$ mechanism for

coupling of nucleophile is well established in quinoline derivatives.[35] Thus it may be a methoxy radical that is introduced via a C-H bond cleavage of **3.11** to result into the formation of **3.9**, where the radical formation is initiated by the copper(II) ions. Copper(II) ions are good for radical generation[36] by interconversion to copper(I), in case of nickel, such redox couple is absent, thus donot lead to incorporation of methoxy group. In nutshell in case of copper(II) ion a nucleophilic cyclisation assisted by copper(II) followed by methoxy group incorporation to the cyclised product takes place.

These results suggest that there is an initial coordination of metal ion to the precursor **3.1** and **3.2** and as the bromide is abstracted by metal, a concomitant C-N bond formation takes place to form cation of three fused heterocyclic ring. In both the cases of copper and nickel ions the substitution is favoured by the coordination effect. This coordination effect is not favourable in case of the substrate **3.12**; hence we did not observe any nucleophilic substitution in **3.12** under ordinary condition (scheme 3.8).

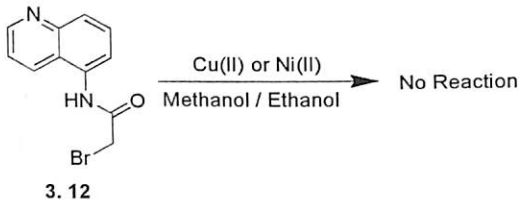

3. 12

Scheme 3.8: Substrate **3.12** does not undergo cyclisation or substitution reaction in ordinary condition

Quinoline based receptors have been identified to be sensitive to anion binding.[37-40] We have also studied the absorption and emission spectra of these compounds to see the spectral variation by the anion.

The compounds **3.1**, **3.8a** and **3.8b** show absorption maximum at 316 nm (figure 3.6a). In addition to peak at 316 nm compound **3.1** shows an absorption peak at 373 nm whereas compound **3.8a** and **3.8b** shows absorption at 386 nm. It shows that there is a 13 nm shift in the absorbance on formation of cyclised perchlorate or nitrate salt and the anion do not cause change in the absorption spectra of the products. All the compounds **3.1**, **3.8a** and **3.8b** are fluorescence active; similar to the UV-spectra the emission spectra of the products (**3.8a** and **3.8b**) are different from the starting material (**3.1**). Compound **3.1** shows an emission peak at 497 nm upon excitation at 380 nm, whereas the compounds **3.8a** and **3.8b** shows an emission peak at 510 nm

upon excitation at 380 nm. The emission spectra are shown in figure 3.6b. Thus, the trend in change in fluorescence emission is similar to the absorption spectra that upon cyclisation emission shift towards higher wavelength with enhancement of intensity.

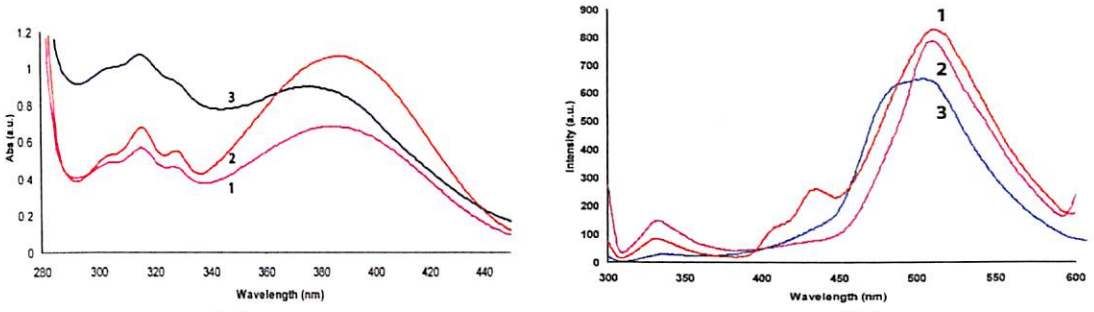

(a) (b)

Figure 3.6: (a) UV-Vis spectra of (1) compound **3.8a**, (2) compound **3.8b** and (3) compound **3.1**; (b) emission spectra (λ_{ex} = 380 nm) of (1) compound **3.8a**, (2) compound **3.8b** and (3) compound **3.1**. In all cases 10^{-4} M methanolic solution is used

The compound **3.2** shows an absorption maximum at 326 nm whereas the compounds **3.9**, **3.10** and **3.11** shows an absorption maximum at 316 nm (10 nm shift). In addition to peak at 316 nm the compound **3.9**, **3.10** and **3.11** shows a peak at 379 nm, 369 nm, and 395 nm respectively. The UV-Visible spectra are shown in figure 3.7a. All these compounds are fluorescence active except compound **3.9**. The emission spectra of compounds **3.2**, **3.9**, **3.10** and **3.11** are much different from each other as shown in figure 3.7b. Compound **3.2** shows an emission peak at 398 nm upon excitation at 310 nm (figure 3.7b).

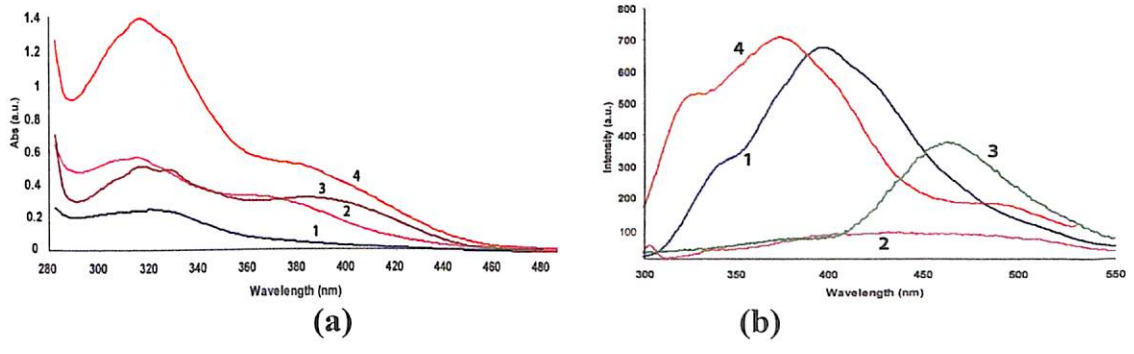

(a) (b)

Figure 3.7: (a) UV-Vis spectra of (1) compound **3.2**; (2) compound **3.9**; (3) compound **3.11** and (4) compound **3.10**; (b) emission spectra (λ_{ex} = 310 nm) of (1) compound **3.2**; (2) compound **3.9**; (3) compound **3.11** and (4) compound **3.10**. In all cases 10^{-4} M methanolic solution is used

The fluorescence emission intensity is very weak for compound **3.9** (figure 3.7b); however, the compound **3.10** shows an intense emission peak at 375 nm upon excitation at 310 nm (figure 3.7b). Unlike the other compounds, **3.11** shows an emission peak in a much different region i.e. at 463 nm upon excitation at the same wavelength (figure 3.7b).

3.3 Structural study of the compounds 3.8 and 3.11

The crystal structure of compound **3.8a** and **3.8b** shows that the similar molecule adopts different packing patterns guided by the anions. Compound **3.8a** crystallises in the orthorhombic space group Pnma whereas the compound **3.8b** crystallises in the monoclinic space group $P2_1/c$. In chapter 2 it has been reported that in quinoline based compounds the host molecule adopts different structural orientation depending on the nature of the guests. Hence, this difference in structural orientation is attributed to the effect of the size and structure of the counter anion. In case of **3.8a** the counter ion is a nitrate anion which is planar and in case of **3.8b** the counter ion is perchlorate anion which is of tetrahedral shape. Here, it is also observed that in case of compound **3.8a** only one half of the molecule is present in the asymmetric unit (figure 3.8b), whereas in compound **3.8b** the whole molecule and the perchlorate anion is present in the asymmetric unit (figure 3.9b).

The crystal structure of compound **3.8a** shows interesting crystallographic features; the asymmetric unit contains only one half of the molecule even though the molecule is not symmetric. It is observed that the two nitrogen atoms (N1 and N2) and the two carbon atoms (C2 and C7) are disordered and share 50% electron density each as shown in figure 3.8a. The presence of such disorder makes the molecule symmetric and forces it to crystallise in a more symmetric space group Pnma. The self assembly of the compound **3.8a** is also governed by a number of weak interactions such as C-H···O (C3-H3···O2; C5-H5···O1) and N-H···O interaction (N2-H2N···O3). These weak interactions lead to formation of a two dimensional wave like net structure as shown in figure 3.8c. The selected hydrogen bond parameters are tabulated in table 3.1.

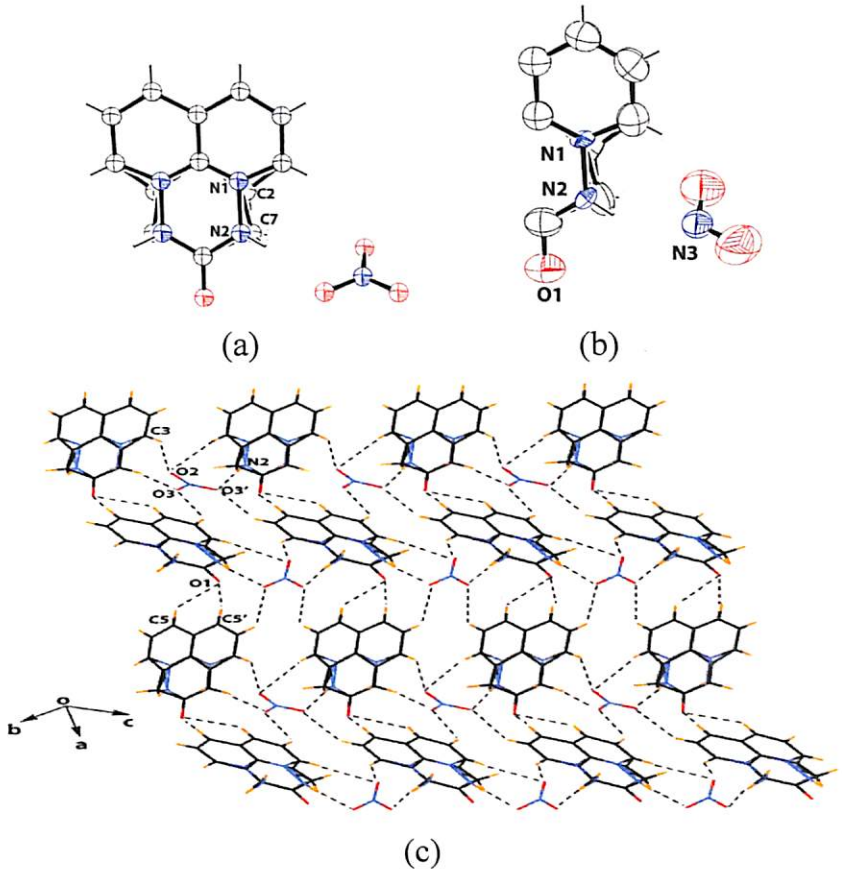

Figure 3.8: (a) Structure of **3.8a** (C, N atoms are disordered) (b) ORTEP diagram of the asymmetric unit of compound **3.8a** (drawn with 50% thermal ellipsoid) (c) short range interactions in **3.8a**

Table 3.1: Hydrogen bond parameters of **3.8a**

D-H····A	$d_{D\text{-}H}$(Å)	$d_{H\cdots A}$(Å)	$d_{D\cdots A}$(Å)	< D-H····A(°)
N(2)-H(7A)····O(3) [x, 1/2-y, z]	1.07	2.02	3.067(17)	164
N(2)-H(7B)····O(3) [1/2-x,1/2+y,1/2+z]	1.30	2.46	3.435(15)	129
C(3)-H(3)····O(1) [1/2-x, 1-y,-1/2+z]	0.93	2.55	3.172(3)	124

The compound **3.8b** forms a one dimensional chain with a C-H···O interaction (C4-H4···O1) which is further linked by other C-H···O interactions with the perchlorate anion (C8-H8···O2). The two one dimensional chains are further interlinked by a C-H···O interaction (C2-H2···O1) and a π···π interaction (C6-C6, 3.336 Å). The self assembly formation of compound **3.8b** is shown in figure 3.9b and the selected hydrogen bond parameters are tabulated in table 3.2.

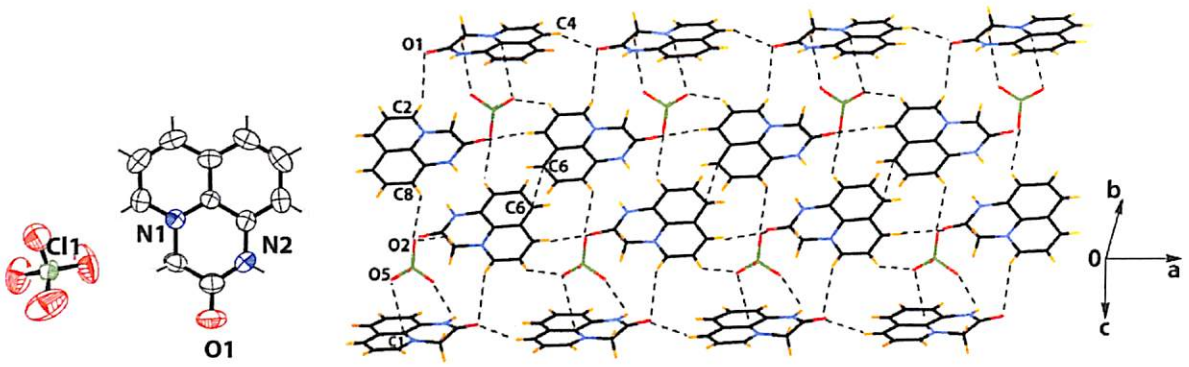

(a) (b)

Figure 3.9: (a) ORTEP diagram of the compound **3.8b**, (drawn with 50% thermal ellipsoid) (b) short range interactions in **3.8b**

Table 3.2: Hydrogen bond parameters of **3.8b**

D-H····A	$d_{D\text{-}H}$(Å)	$d_{H\cdots A}$(Å)	$d_{D\cdots A}$(Å)	< D-H····A(°)
N(2)-H(2N) ···O(4)[-x, 1/2+y, 1/2-z]	0.86	2.16	2.980(4)	159
C(3)-H(3)····O(5) [1-x,-1/2+y, 1/2-z]	0.93	2.44	3.262(6)	147
C(4)-H(4)····O(1) [1+x, y, z]	0.93	2.42	3.278(5)	152
C(8)-H(8)····O(2) [x, 3/2-y,-1/2+z]	0.93	2.56	3.274(5)	134
C(11)-H(11B)····O(2) [-x,-1/2+y, 1/2-z]	0.97	2.55	3.375(5)	144

The structure of the compound **3.11** is also determined by X-ray crystallography and is shown in figure 3.10a. The compound **3.11** crystallises in the space group monoclinic $P2_1/n$. Its asymmetric unit comprises of a cation of a three fused heterocyclic ring and one perchlorate anion. The molecules are self-assembled and the self-assembly is governed by $\pi\cdots\pi$ interactions (C8-C4, 3.370 Å) and C-H···O interactions (C6-H6···O1; C11-H11···O1). Presence of these interactions leads to arrangement of molecules in the form of one dimensional chain. The perchlorate anions are held between two such one dimensional chains through C-H···O (C4-H4···O4; C2-H2···O3) and N-H···O (N2-H2A···O5) interactions. The two methyl groups are projected away from each other which are expected and the methyl protons are further involved in a C-H···O interaction (C12-H12A···O2) with the oxygen atom of a perchlorate anion. The self assembly of the compound **3.11** is shown in figure 3.10b. The selected hydrogen bond parameters are tabulated in table 3.3.

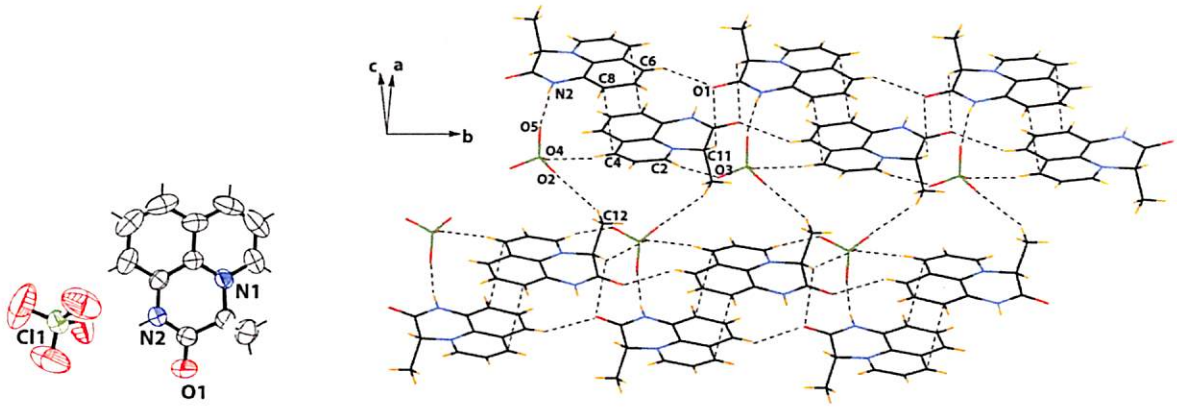

(a) (b)

Figure 3.8: (a) ORTEP diagram of the compound **3.11** (drawn with 50% thermal ellipsoid); (b) short range interactions in **3.11**

Table 3.3: Hydrogen bond parameters of **3.11**

D-H····A	d_{D-H}(Å)	$d_{H\cdots A}$(Å)	$d_{D\cdots A}$(Å)	< D-H····A(°)
N(2)-H(2A)····O(5) [1-x, 1-y,-z]	0.86	2.09	2.934(5)	167
C(2)-H(2)····O(3) [-1+x, 1+y, z]	0.93	2.46	3.384(7)	176
C(4)-H(4)····O(4) [-1+x, y, z]	0.93	2.39	3.305(7)	169
C(6)-H(6)····O(1) [x,-1+y, z]	0.93	2.49	3.309(6)	146
C(11)-H(11)····O(4) [-1+x, 1+y, z]	0.98	2.49	3.316(6)	141

Conclusion

In conclusion a three component reaction leading to a novel heterocyclic compound is established. The heterocyclic compound further rearranges to another heterocycle in presence of perchloric acid. The reactions are very specific to the solvent and the reactants. The cyclisation to form C-N bond formation reactions in in the same substrates **3.1** and **3.2** are also facilitated by copper(II) and nickel(II) ions. The copper(II) mediated intra-molecular cyclisation reactions are substrate dependent. In the case of **3.2** the initial cyclised product formed via C-N bond formation further undergoes C-H activation to give OMe substituted derivative. Thus, in the case of copper a mixture of mechanism involving cation and radical is favoured, whereas in the case of nickel it is an ionic mechanism leading to anion exchange. Further to this, the three fused ring heterocycles formed are fluorescence active. The structural study of the cyclised product shows that the counter anion changes the symmetry of the molecule.

This chapter definitely provides us a message that the use of the compounds **3.1** and **3.2** as receptor requires appropriate understanding of the reaction schemes taking

place either with solvent or with an anion. The anion binding to modified substrates can be used to distinguish between anions. The reactivity pattern of different metal ions with the compounds enables to distinguish the receptors as well as the metal ions. Thus it provides a scope for synthesis of new insitu generated receptors for recognition of metal ions and anions.

Experimental

The synthetic methodology of compounds **3.1** and **3.2** are already reported in chapter 2.

Synthesis of compound 3.3:

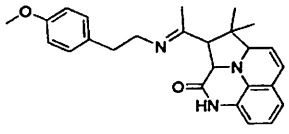

2-Bromo-N-quinoline-8-yl-acetamide (**3.1**) (1.4 g, 5 mmol), 2-(4-methoxyphenyl) ethylamine (0.735 mL, 5 mmol) and anhydrous potassium carbonate (1.03 g, 7.5 mmol) were added to dry acetone (20 mL) and the reaction mixture was stirred at 70°C for 12 hs (progress of the reaction was monitored at regular intervals by using TLC). The reaction mixture was filtered to remove the residue and the solvent was removed under reduced pressure. The product obtained was purified by preparative thin layer chromatography using silica gel with 30% ethylacetate in petroleum ether as eluant.

Yield: 41%.

IR (KBr, cm^{-1}): 3125 (w), 3059 (m), 3008 (m), 2960 (m), 2923 (m), 1676 (s), 1658 (w), 1635 (m), 1613 (m), 1584 (m), 1511 (s), 1482 (s), 1387 (s), 1369 (w), 1270 (m), 1246 (s), 1172 (m), 1028 (m), 798 (m), 724 (m).

^{1}H-NMR ($CDCl_3$, 400MHz): 8.4 (1H, s), 7.1 (2H, d, J = 8.4Hz), 6.8 (2H, d, J = 6.4Hz), 6.5 (3H, m), 6.3 (1H, d, J = 10Hz), 5.7 (1H, dd, J = 5.2, 10Hz), 4.5 (1H, dd, J = 5.2, 10Hz,), 3.7 (3H, s), 3.53 (1H, s), 3.50 (2H, t, J = 7.2Hz), 2.8 (2H, t, J = 7.2Hz), 2.5 (1H, d, J = 10.4Hz,), 1.7 (3H, s), 1.1 (3H, s), 1.0 (3H, s).

^{13}C-NMR ($CDCl_3$, 100MHz): 20.3, 24.7, 27.1, 36.6, 44.6, 53.2, 55.5, 59.5, 66.4, 71.5, 109.9, 113.9, 114.6, 118.7, 120.3, 121.8, 123.5, 124.8, 125.2, 129.0, 130.0, 132.9, 158.1, 166.5.

LC-MS [M^+]: 414.27.

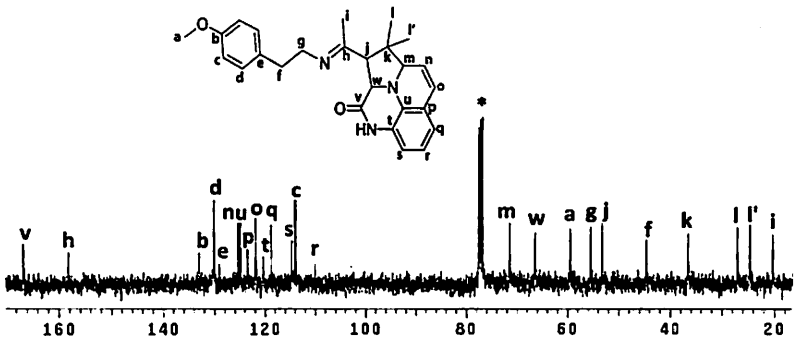

Figure 3.11: ^{13}C-NMR spectra of **3.3** (* indicates the peak for solvent)

Synthesis of compound 3.4:

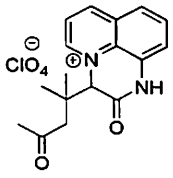

Compound **3.3** (0.41 g, 1 mmol) was dissolved in dilute perchloric acid (3 M) and heated for 10 min. The solution was kept undisturbed, yellow colour crystal of compound **3.4** appeared after 6 days.

Yield: 46%.

IR (KBr, cm^{-1}): 3258 (m), 3110 (w), 3083 (m), 2962 (m), 1705 (s), 1608 (w), 1587 (m), 1541 (s), 1471 (m), 1427 (s), 1384 (m), 1361(m), 1239 (w), 1177 (m), 1100 (s), 927 (m), 839 (s), 764 (m), 623 (s).

^{1}H-NMR ($CDCl_3$/DMSO-d^6, 400MHz): 12.0 (1H, s), 9.4 (1H, d, J = 6Hz), 9.2 (1H, d, J = 8.4Hz), 8.2 (1H, m), 8.0 (1H, d, J = 8.4Hz), 7.9 (1H, t, J = 8.0Hz), 7.6 (1H, d, J = 7.6Hz), 6.0 (1H, s), 2.9 (1H, d, J = 18.4Hz), 2.6 (1H, d, J =19.2Hz), 2.1 (3H, s), 1.0 (3H, s), 0.7 (3H, s).

^{13}C-NMR ($CDCl_3$/DMSO-d^6, 100MHz): 24.0, 24.7, 31.5, 51.2, 72.9, 118.9, 122.9, 123.2, 127.3, 129.8, 131.0, 131.5, 148.3, 149.8, 162.1, 206.9

LC-MS [M+]: 283.17.

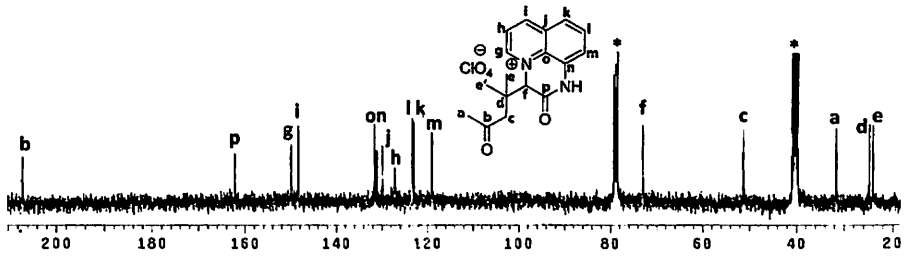

Figure 3.12: ^{13}C-NMR spectra of **3.4** (* indicates the peak for solvent)

Synthesis of compound 3.5:

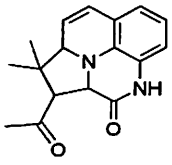

2-Bromo-N-quinoline-8-yl-acetamide (**3.1**) (1.4 g, 5 mmol), 2-(2-methoxyphenyl) ethylamine (0.735 mL, 5 mmol) and anhydrous potassium carbonate (1.03 g, 7.5 mmol) were added to dry acetone (20 mL) and the reaction mixture was stirred at 70 °C for 12 hs (progress of the reaction was monitored at regular intervals using TLC). The reaction mixture was filtered to remove the residue and the solvent was removed under reduced pressure. The product obtained was purified by preparative thin layer chromatography using silica gel with 30% ethylacetate in petroleum ether as eluant.

Yield: 25%.

IR (KBr, cm^{-1}): 3432 (b), 2924 (s), 2853 (m), 1681 (s), 1596 (m), 1527 (s), 1491 (m), 1458 (m), 1384 (m), 1325 (m), 1244 (s), 1174 (w), 1024 (m), 827 (m), 792 (m), 753(s).

^{1}H-NMR ($CDCl_3$, 400MHz): 8.2 (1H, s), 6.4 (2H, m), 6.3 (1H, d, J = 7.2Hz), 6.1 (1H, d, J = 10Hz), 5.5 (1H, m), 4.1 (1H, m), 3.3 (1H, s), 2.6 (1H, d, J = 10Hz), 1.9 (3H, s), 0.9 (6H, s).

^{13}C-NMR ($CDCl_3$, 100MHz): 24.7, 26.9, 33.1, 45.3, 59.8, 68.6, 71.3, 114.8, 116.7, 119.1, 120.7, 122.1, 123.3, 136.3, 148.7, 165.5

LC-MS [M^+]: 283.15.

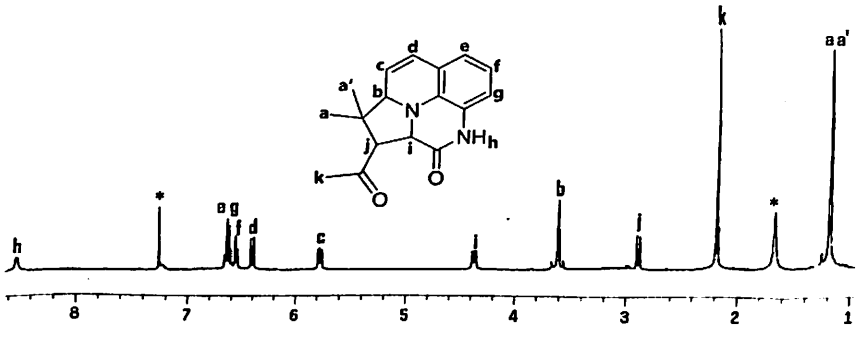

Figure 3.13: ^{1}H-NMR spectra of **3.5** (* indicates the peak for solvent and water associated with solvent)

Synthesis of compound 3.6:

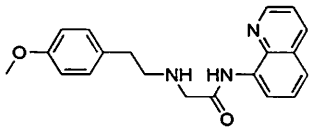

2-Bromo-N-quinoline-8-yl-acetamide (1.4 g, 5 mmol), 2-(4-methoxyphenyl) ethylamine (0.735 mL, 5 mmol) and anhydrous potassium carbonate (1.03 g, 7.5 mmol) were added to ethyl methyl ketone (20 mL) and the reaction mixture was stirred at 70 °C for 12 hs (progress of the reaction was monitored at regular intervals using TLC). The reaction mixture was filtered to remove the residue and the solvent was removed under reduced pressure. The product obtained was purified by preparative thin layer chromatography using silica gel with 30% ethylacetate in petroleum ether as eluant.

Yield: 55%.

IR (KBr, cm^{-1}): 3315 (m), 2925 (m), 2851 (w), 1655 (s), 1612 (w), 1579 (w), 1530 (s), 1488 (m), 1463 (m), 1424 (w), 1326 (s), 1245 (s), 1175 (m), 1033 (m), 786 (s), 750(m).

^{1}H-NMR ($CDCl_3$, 400MHz): 10.5 (1H, s), 8.7 (2H, m), 8.1 (1H, d, J = 6.8Hz), 7.5 (3H, m), 7.4 (1H, q, J = 4Hz), 7.1 (1H, d, J = 8.4), 6.8 (1H, d, J = 8.8), 4.3 (3H, s), 3.7 (2H, s), 3.5 (1H, s), 2.9 (2H, t, J = 6.8Hz,), 2.8 (2H, t, J = 6.0.Hz).

^{13}C-NMR (DMSO-d^6/$CDCl_3$, 100MHz): 28.8, 34.9, 62.0, 85.4, 115.5, 121.1, 121.2, 126.4, 127.3, 129.0, 133.3, 135.6, 137.6, 147.8, 170.6

LC-MS [M^+]: 336.17

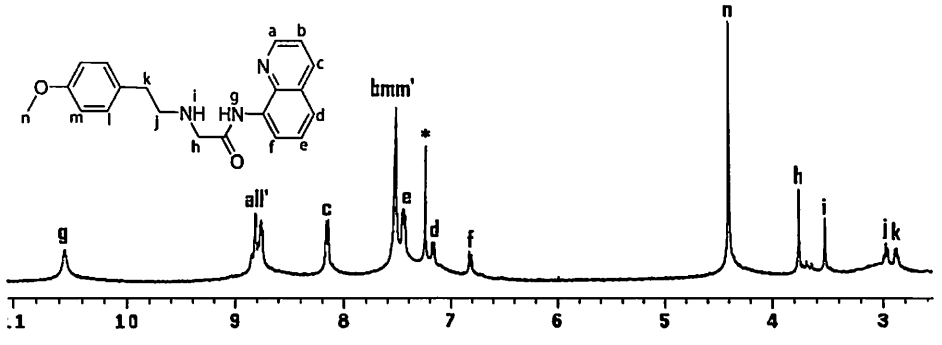

Figure 3.14: ^{1}H-NMR of spectra **3.6** (* indicates the peak for solvent)

Synthesis of compound 3.7:

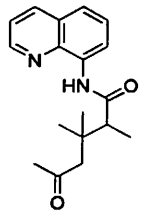

2-bromo-N-(quinolin-8-yl)propanamide (**3.1**) (1.5 g, 5 mmol), 2-(4-methoxyphenyl) ethylamine (0.735 mL, 5 mmol) and anhydrous potassium carbonate (1.03 g, 7.5 mmol) were added to dry acetone (20 mL) and the reaction mixture was stirred at 70 °C for 12 hs (progress of the reaction was monitored at regular intervals using TLC). The reaction mixture was filtered to remove the residue and the solvent was removed under reduced pressure. The product obtained was purified by preparative thin layer chromatography using silica gel with 25% ethylacetate in petroleum ether as eluant.

Yield: 46%

IR (KBr, cm^{-1}): 3431 (bs), 2923 (m), 1706 (m), 1637 (s), 1467 (m), 1405 (m), 1382 (m), 636 (m).

^{1}H-NMR ($CDCl_3$, 400MHz): 8.9 (1H, s), 7.5 (1H, d, J = 9.6Hz), 7.3 (1H, d, J = 9.6Hz), 7.1 (1H, d, J = 8.0Hz), 7.0 (1H, t, J = 7.6 Hz), 6.9 (1H, d, J = 7.6Hz), 6.8 (1H, m), 4.6 (1H, m), 3.8 (2H, s), 2.4 (3H, s), 1.7 (3H, s), 1.5 (3H, s), 1.4 (3H, s), 1.2 (3H, s).

^{13}C-NMR ($CDCl_3$, 100MHz): 16.5, 24.3, 27.1, 30.2, 47.6, 58.3, 113.5, 121.4, 124.3, 128.3, 131.4, 138.6, 139.7, 142.1, 151.3, 163.4, 203.2

LC-MS [M^+]: 298.15

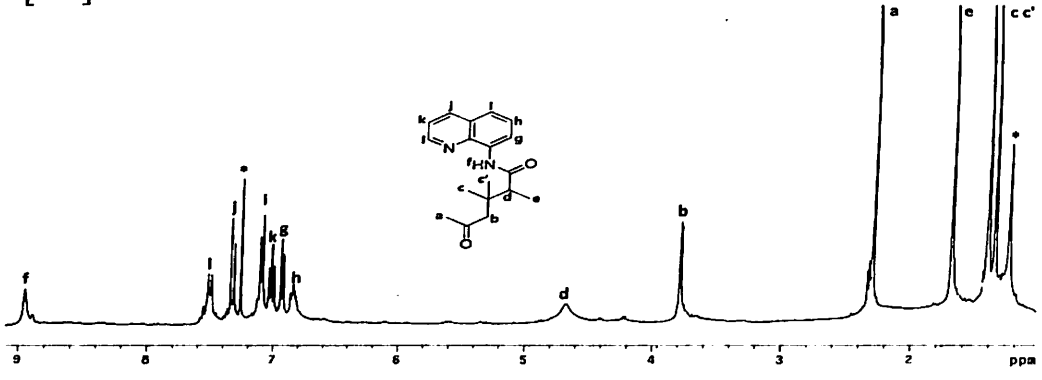

Figure 3.15: ^{1}H-NMR spectra of **3.7** (* indicates the peak for solvent and water associated with solvent)

Synthesis of compound 3.8a:

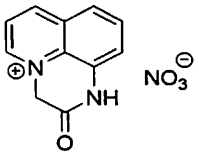

2-bromo-N-(quinolin-8-yl)acetamide (**3.1**) (1 mmol, 0.263 g) was dissolved in methanol (15 mL) and copper (II) nitrate (1 mmol, 0.241 g) was added. The solution was then stirred for 30 minutes in room temperature and kept undisturbed. Brown coloured crystals of compound **3.8a** were observed after 3 days. The solution is then filtered to isolate the product. The same reaction was also performed with nickel (II) nitrate which resulted in similar yield of compound **3.8a.**

Yield: 72%.

IR (KBr, cm^{-1}): 3434 (bm), 3043 (m), 3013 (m), 2929 (m), 2852 (w), 1698 (s), 1584 (m), 1543 (m), 1491 (w), 1384 (s), 1239 (w), 1154 (w), 1130 (w), 839 (m), 795 (w), 754 (w), 526 (w).

^{1}H-NMR (DMSO-d^6, 400MHz): 11.8 (1H, s), 9.2 (1H, d, J = 6.0Hz), 9.1 (1H, d, J = 8.4Hz), 8.2 (1H, t, J = 6.0Hz), 7.9 (2H, m), 7.5 (1H, d, J = 7.2Hz), 5.6 (2H, s).

^{13}C-NMR (DMSO-d^6, 100MHz): 56.2, 118.1, 122.8, 123.5, 126.7, 130.0, 131.4, 147.2, 147.7, 161.6.

LC-MS [M^+]: 185.09.

Vis: (λmax 386 nm), $\varepsilon = 6.5 \times 10^3\ M^{-1}\ cm^{-1}$.

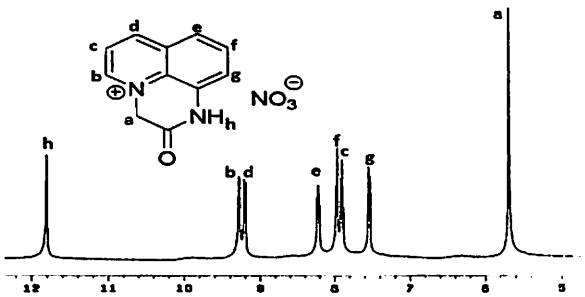

Figure 3.16: ^{1}H-NMR spectra of **3.8a**

Synthesis of compound 3.8b:

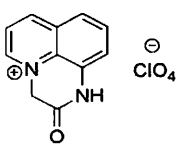

A similar procedure to **3.8a** was used for the synthesis of compound **3.8b**, only difference is that in this case copper (II) perchlorate was used instead of copper (II)

nitrate. The same reaction was also performed with nickel (II) perchlorate which resulted in similar yield of compound **3.8b.**

Yield: 74%.

IR (KBr, cm^{-1}): 3433 (bm), 3013 (m), 2928 (m), 2852 (m), 1698 (s), 1607 (w), 1584 (m), 1543 (s), 1428 (m), 1417 (m), 1385 (s), 1298 (w), 1240 (m), 1144 (s), 1115 (s), 1079(s), 909 (w), 838 (m), 754 (m), 624 (m).

Vis: (λmax 386 nm), $\varepsilon = 1.17 \times 10^4\ M^{-1}\ cm^{-1}$.

Synthesis of compound 3.9:

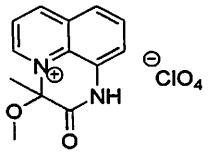

2-bromo-N-(quinolin-8-yl)propanamide (**3.2**) (1 mmol, 0.279 g) was dissolved in methanol (15 mL) and copper (II) perchlorate (1 mmol, 0.370 g) was added. The solution was then stirred for 30 minutes in room temperature and kept undisturbed. Brown coloured crystals of compound **3.9** were observed after 4 days. The solution is then filtered and the product is isolated.

Yield: 47%.

IR (KBr, cm^{-1}): 3433 (bs), 3006 (m), 2934 (w), 2890 (w), 2853 (m), 1704 (s), 1583 (w), 1545 (m), 1495 (w), 1469 (m), 1390 (m), 1275 (w), 1229 (m), 1174 (m), 1143 (s), 1114 (s), 1086 (s), 839 (m), 625 (m).

^{1}H-NMR (DMSO-d^6, 400MHz): 12.3 (1H, s), 9.6 (1H, d, J = 5.6Hz), 9.3 (1H, d, J = 8.0Hz), 8.3 (1H, d, J = 6.0Hz), 8.1(1H, d, J = 8.0Hz), 7.9 (1H, t, J = 8.0Hz), 7.6 (1H, d, J = 7.2Hz), 3.5 (3H, s), 1.9 (3H, s).

^{13}C-NMR (DMSO-d^6, 100MHz): 23.7, 48.8, 63.2, 118.0, 122.8, 123.6, 125.5, 129.9, 130.3, 131.0, 147.0, 147.3, 164.5.

LC-MS [M+]: 229.09.

Vis: (λmax 379 nm), $\varepsilon = 3.7 \times 10^3\ M^{-1}\ cm^{-1}$.

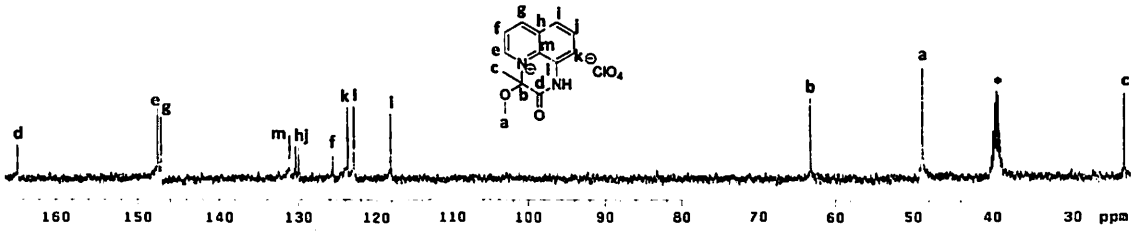

Figure 3.17: ^{1}H-NMR spectra of **3.9** (* indicates the peak for solvent and water associated with solvent)

Synthesis of compound 3.10:

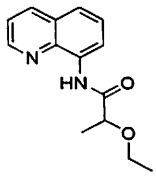

Compound **3.10** was synthesised by a procedure similar to compound **3.9**, except in this case ethanol was used as solvent instead of methanol.

Yield: 63%.

IR (KBr, cm^{-1}): 3444 (bs), 1627 (s), 1501 (m), 1467 (m), 1399 (m), 1121 (w), 1086 (w), 829 (w), 788 (w), 636 (w).

^{1}H-NMR (DMSO-d^6, 400MHz): 11.8 (1H, s), 9.5 (1H, d, J = 5.6Hz), 9.2 (1H, d, J = 8.4Hz), 8.2 (1H, t, J = 6.0Hz), 8.0 (1H, d, J = 8.4Hz), 7.9 (1H, t, J = 7.6 Hz), 7.6 (1H,d, J = 7.6 Hz), 5.8 (1H, q, J = 7.2 Hz), 3.4 (2H, m), 1.8 (3H, d, J = 7.6 Hz); 1.0 (3H, t, J = 8.8 Hz).

^{13}C-NMR (DMSO-d^6, 100MHz): 19.1, 24.1, 56.7, 63.5, 118.3, 123.2, 124.1, 125.9, 130.2, 130.7, 131.4, 147.3, 147.7, 164.9.

LC-MS [M-1]: 243.13.

Vis: (λmax 369 nm), $\varepsilon = 6.2 \times 10^3\ M^{-1}\ cm^{-1}$.

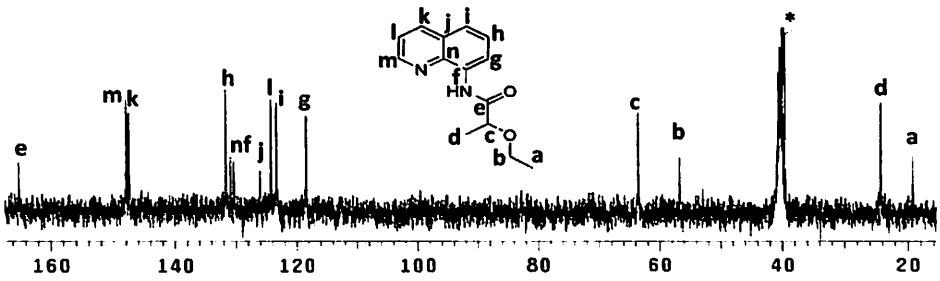

Figure 3.18: ^{13}C-NMR spectra of **3.10** (* indicates the peak for solvent)

Synthesis of compound 3.11:

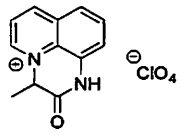

2-bromo-N-(quinolin-8-yl)propanamide (**3.2**) (1 mmol, 0.279 g) was dissolved in methanol (15 mL) and nickel (II) perchlorate (1 mmol, 0.365 g) was added. The solution was then stirred for 40 minutes in room temperature and kept undisturbed. Brown coloured crystals of compound **3.11** were observed after 3 days. The solution is then filtered to isolate the product.

Yield: 71%.

IR (KBr, cm^{-1}): 3424 (bs), 3043 (m), 2903 (w), 1694 (s), 1607 (w), 1587 (w), 1542 (m), 1492 (w), 1422 (m), 1392 (m), 1365 (m), 1241 (w), 1140 (s), 1116 (s), 1078 (s), 835 (m), 760 (w), 624 (m).

^{1}H-NMR (DMSO-d^6, 400MHz): 11.8 (1H, s), 9.5 (1H, s), 9.2 (1H, d, J = 7.6Hz), 8.2 (1H, d, J = 5.2Hz), 8.0 (2H, m), 7.5 (1H, d, J = 6.8Hz), 5.8 (1H, m), 1.8 (3H, s).

^{13}C-NMR (DMSO-d^6, 100MHz): 24.1, 63.5, 118.3, 123.1, 124.0, 125.9, 130.2, 130.6, 131.4, 147.3, 147.6, 164.9.

LC-MS [M+]: 199.03.

Vis: (λmax 395 nm), $\varepsilon = 4.3 \times 10^3\ M^{-1}\ cm^{-1}$.

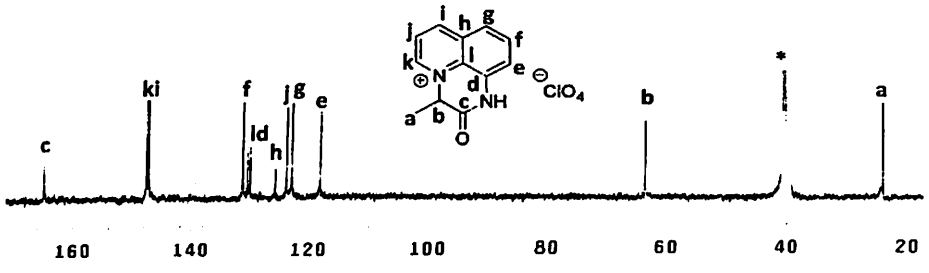

Figure 3.19: ^{13}C-NMR spectra of **3.11** (* indicates the peak for solvent)

Synthesis of 3.12:

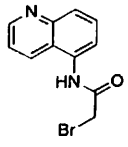

5-aminoquinoline (0.720 g, 5 mmol) was dissolved in dry dichloromethane (20 mL) and triethylamine (0.693 mL, 5 mmol) was added to it. The solution was stirred at 0^0C for 15 min and bromoacetylbromide (0. 434 mL, 5 mmol) was added to the stirred

solution over a period of 30 min. The reaction mixture was stirred overnight at room temperature. It was then filtered to remove the hydrobromide salts, and the filtrate was removed under reduced pressure. The corresponding amide obtained was recrystallised from dichloromethane.

Yield: 72%.

IR (KBr, cm^{-1}): 3438 (s), 2917 (m), 1688 (s), 1629 (s), 1629 (s), 1569 (s), 1533 (s), 1409 (m), 1368 (m), 1204 (m), 812 (m).

^{1}H-NMR (DMSO-d^{6}, 400MHz): 11.0 (1H, s), 9.5 (1H, d, J = 8.4Hz), 9.3 (1H, d, J = 5.2Hz), 8.2 (2H, d, J = 6.8Hz), 8.0 (2H, m), 4.3 (2H, s).

^{13}C-NMR (DMSO-d^{6}, 100MHz): 29.2, 117.4, 120.8, 123.8, 135.0, 138.1, 143.0, 144.1, 166.6

LC-MS [M+]: 265.01

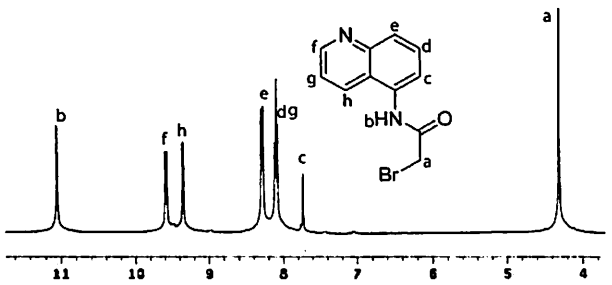

Figure 3.20: ^{1}H-NMR spectra of **3.12**

References

1. A. Katritzky and A.F. Pozhaskii, *Handbook of Heterocyclic Chemistry 2nd ed.* Pergamon Amsterdam, 2000.
2. S. E. Denmark and A. Thorarensen, *Chem Rev.*, 1996, **96**, 137.
3. J. D. Winkler, *Chem. Rev.*, 1996, **96**, 167.
4. 1,3-Dipolar Cycloaddition Chemistry, A. Padwa, Ed. Wiley-Interscience: New York, Vols. I and II. 1984.
5. H. Hiemstra, W. N. Speckamp, B. M. Trost and I. Fleming, *In Comprehensive Organic Synthesis, Eds.; Pergamon: Oxford*, 1991, **2**, 1047.
6. A. Kapat, P. S. Kumar and S. Baskaran, *Beilstein J. Org. Chem.*, 2007, **3**, 49.
7. A. Padwa and M. D. Weingarten, *Chem. Rev.*, 1996, **96**, 223.
8. A. Padwa, J. P. Jr Marino and M. H. Osterhout, *J. Org. Chem.*, 1995, **60**, 2704.
9. R. H. Hutchings and A. I. Meyers, *J. Org. Chem.*, 1996, **61**, 1004.

10. Y. Tsuda, S. Hosoi, A. Nakai, Y. Sakai, T. Abe, Y. Ishi, F. Kiuchi and T. Sano, *Chem. Pharm. Bull.*, 1991, **39**, 1365.

11. L. Joucla, A. Putey and B. Joseph, *Tettrahedron. Lett.*, 2005, **46**, 8177.

12. T. R. Hoye, C. J. Dinsmore, D. S. Johnson and P. F. Korkowski, *J. Org. Chem.*, 1990, **55**, 4518.

13. A. Padwa and S. L. Xu, *J. Am. Chem. Soc.*, 1992, **114**, 5881.

14. T. R. Hoye and C. J. Dinsmore, *J. Am. Chem. Soc.*, 1991, **113**, 4343.

15. P. H. Mueller, J. M. Kassir, M. A. Semones, M. D. Weingarten and A. Padwa, *Tetrahedron Lett.*, 1993, **34**, 4285.

16. H. M. L. Davies, M. J. McAfee and C. E. M. Oldenburg, *J. Org. Chem.*, 1989, **54**, 930.

17. H. M. L. Davies, C. E. M. Oldenburg, M. J. McAfee, J. G. Nordahl, J. P. Henretta and K. R.Romines, *Tetrahedron Lett.*, 1988, **29**, 975.

18. M. L. Deem, *Synthesis*, 1982, 701.

19. M. Foley and L. Tilley, *Pharmacol. Ther.*, 1998, **79**, 55.

20. J. Mao, H. Yuan, Y. Wang, B. Wan, M. Pieroni, Q. Huang, R. B. van Breemen, A. P. Kozikowski and S. G. Franzblau, *J. Med. Chem.*, 2009, **52**, 6966.

21. P. R. Verhoest, D. S. Chapin, M. Corman, K. Fonseca, J. F. Harms, X. Hou, E. S. Marr, F. S. Menniti, F. Nelson, R. O'Connor, J. Pandit, C. P. LaFrance, A. W. Schmidt, C. J. Schmidt, J. A. Suiciak and S. Liras, *J. Med. Chem.*, 2009, **52**, 5188.

22. G.X. Li, Z.Q. Liu and X.Y. Luo, *Eur. J. Med. Chem.*, 2010, **45**, 1821.

23. H. Zeng, R. Cao and H. Zhang, *Chem. Biol. Drug Des.*, 2009, **74**, 596

24. I. Deb, P. Paira, A. Hazra, S. Banerjee, P. K. Dutta, N. B. Mondal and S. Das, *Bioorg. Med. Chem.*, 2009, **17**, 5782.

25. R. B. Toche, B. P. Pagar, R. R. Zoman, G. B. Shinde and M. N. Jachak, *Tetrahedron*, 2010, **66**, 5204.

26. N. G. Kozlov and K. N. Gusak, *Russ. J. Org. Chem.*, 2010, **46**, 1074.

27. Z. Pruckova, A. Klasek, A. Lycka, I. Miksik and A. Ruzicka, *Tetrahedron*, 2009, **65**, 9103.

28. S. A. Worlikar and R. C. Larock, *J. Org. Chem.*, 2008, **73**, 7175.

29. I. Y. Tao and R. T. Blickenstaff, *J. Pharm. Sci.*, 1978, **67**, 283.

30. I. Y. Tao and R. T. Blickenstaff, *Steroids*, 1976, 205.

31. C. Rangheard, D. Proriol, H. Olivier-Bourbigou and P. Braunstein, *Dalton Trans,* 2009, 770.

32. Y. Feng, Y. Wang, B. Landgraf, S. Liu and G. Chen, *Org. Lett.*, 2010, **12**, 3414.

33. S. E. Denmark and A. Thorarensen, *Chem. Rev.*, 1996, **96**, 137.

34. J. D. Winkler, *Chem. Rev.*, 1996, **96**, 167.

35. R. Beugelmans and M. Bois-Choussy, *J. Org. Chem.*, 1991, **56**, 2518.

36. J. E. M. N. Klein, A. Perry, D. S. Pugh and R. J. K. Taylor, *Org. Lett.*, 2010, **12**, 3446.

37. M. A. Triyanti, S. Schiffers, O. Osetska, G. Raabe, T. Wieland, L. Russo and K. Rissanen, *Eur. J. Org. Chem.*, 2007, 2850.

38. A. M. Triyanti, G. Marita, B. de Matthias and W. Elmar, *Synlett*, 2005, 2095

39. A. Karmakar, R. J. Sarma and J. B. Baruah, *CrystEngComm*, 2007, **9**, 378.

40. A. Karmakar and J.B. Baruah, *Supramolecular Chemistry*, 2008, **20**, 667.

Chapter 4

Synthesis, characterization and anion recognition properties of urea and carbamide derivatives of quinoline

Urea derivatives find a wide range of applications in supramolecular chemistry due to their strong and directional hydrogen bonding. They form planar urea tap motifs and such motifs can break down in the presence of guest molecules or anions.[1] The anion recognition property of urea derivatives are well known in both in solid and in solution state.[2-4] As discussed in chapter 1, urea derivatives have higher binding affinity for anions than the corresponding amide derivatives. Receptors having urea motifs are useful for selective binding of carboxylic acids such as dibutylmalonic acid.[5] Owing to their versatile biological applications, design and synthesis of receptors for selective binding of carboxylic acids are of interest.[6-11] There are several examples of receptors for dicarboxylic acids and their binding properties are explored in details.[12-21] Troger's base analogues have been reported to recognise dicarboxylic acids.[22-27] Recently, it is shown that dicarboxylic acids form salts and co-crystals with pyridine receptors depending upon the orientation of the acid groups.[28-34] Further to this, conformational changes brought about in dicarboxylic acid by receptors have practical applications in memory devices.[35-36] Binding of the carboxylic acids to nitrogen containing receptors have great diversity[36-38] and such binding also leads to changes in the physical properties of the parent compounds.[39]

In the preceding chapter it is shown that the anion recognition properties of amide and ester derivatives of quinoline led to identifications of new receptors. So in continuation of search for new selective anion recognition properties, urea and carbamide derivatives of quinoline are synthesised and their anion binding abilities are discussed here.

4.1 Synthesis and characterization of urea and carbamide derivatives of quinoline

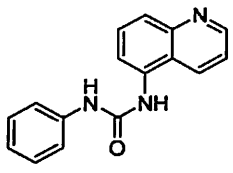

4.1

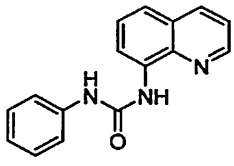

4.2

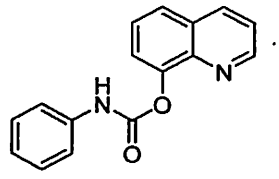

4.3

The urea derivatives **4.1**, **4.2** and the carbamide derivative **4.3** were synthesized by reacting phenylisocyanate with the corresponding amino or hydroxyquinoline as shown in scheme 4.1.

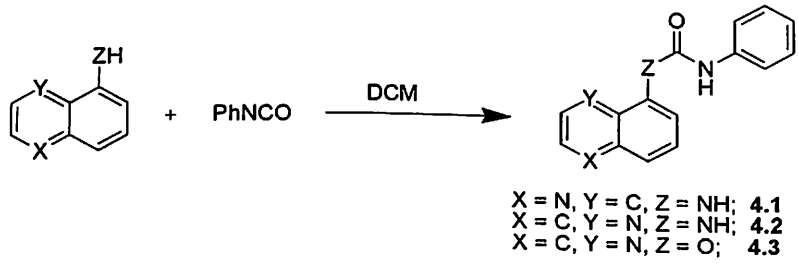

Scheme 4.1: Synthesis of compound **4.1**, **4.2**, **4.3**

The compounds were characterised by using various spectroscopic techniques such as NMR, IR, LC-MS etc. As a representative case the ^{1}HNMR spectra of the receptor **4.1** is shown in figure 4.1.

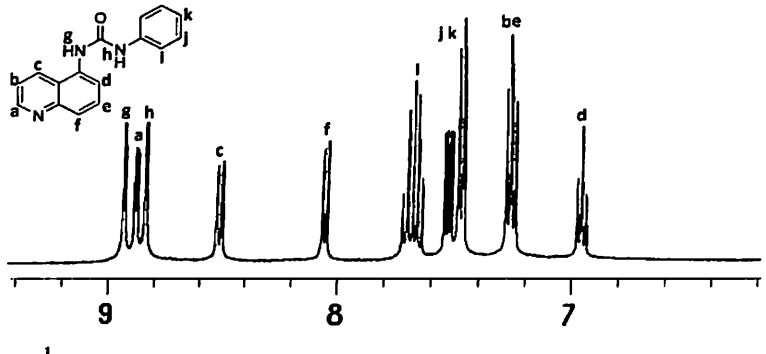

Figure 4.1: ^{1}H-NMR spectra of **4.1** (only the aromatic region is shown)

The urea and carbamide derivatives were further allowed to bind with different dicarboxylic acids. However, it is found that only receptor **4.1** interacts with dicarboxylic acids by forming either co-crystals or salts under ambient condition. This is confirmed by the visible, IR and the NMR spectra of the precipitate obtained from each mixture and comparing them with the starting compound.

The urea derivative, 1-phenyl-3-(quinolin-5-yl)urea (**4.1**) is crystallized with different dicarboxylic acids such as fumaric acid (**4.4**), maleic acid (**4.5**), 1,4-phenylenediacetic acid (**4.6**), malonic acid (**4.7**), phthalic acid (**4.8**), terephthalic acid (**4.9**), adipic acid (**4.10**) and pyridine 2,3-dicarboxylic acid (**4.11**) to obtain either the salt or co-crystal of the corresponding acid as shown in scheme 4.2.

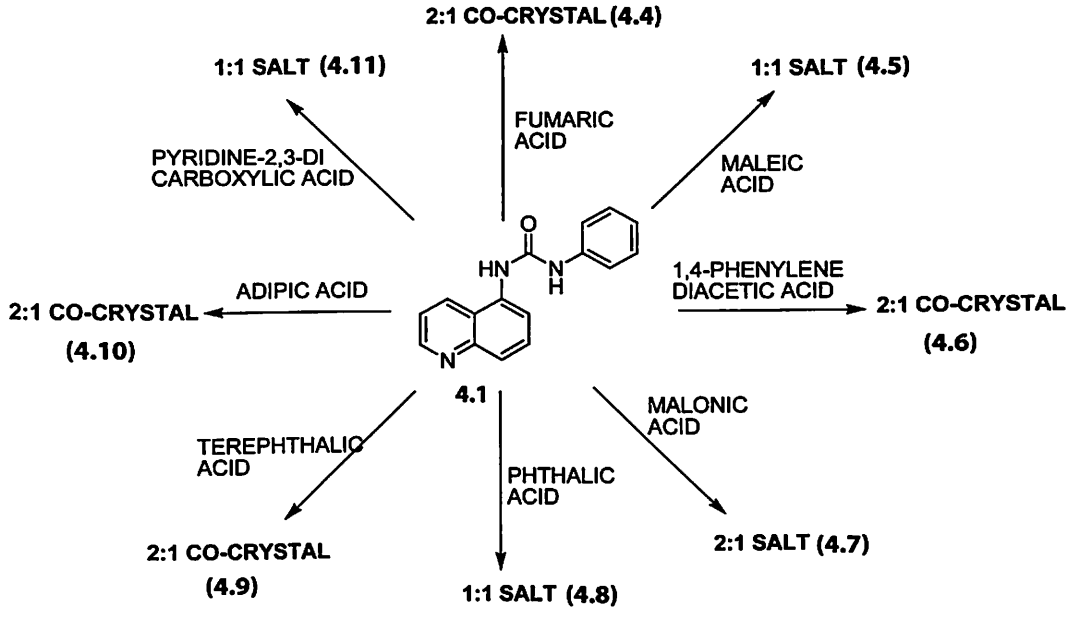

Scheme 4.2: Salts and co-crystals of **4.1**

4.2 Structural studies of the salts and co-crystals of 1-phenyl-3-(quinolin-5-yl)urea

The receptor **4.1** crystallizes in the space group monoclinic Pc with one molecule in the crystallographic asymmetric unit. The structure is featured by urea-urea interaction that leads to the formation of urea tape motif. The bifurcated N-H···O hydrogen bonding ($d_{D\text{-}H\cdots A}$ (Å), N1-H1A···O1, 2.05(19); N2-H2A···O1, 2.18(2), and <D-H···A (°), <N1-H1A···O1, 156.1(19); < N2-H2A···O1, 152(2) is the only weak interaction present in the lattice of the molecule. The structure of the hydrogen bonded tape motif of **4.1** is shown in figure 4.2.

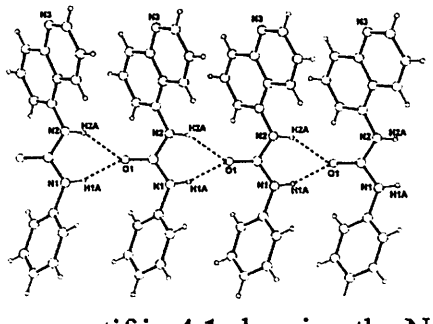

Figure 4.2: Urea tape motif in **4.1** showing the N-H···O interactions

The receptor **4.1** on treatment with fumaric acid forms a colourless co-crystal **4.4**. The co-crystal **4.4** crystallizes in the space group monoclinic $P2_1/c$. The fumaric acid molecule lies on an inversion centre with only half of the molecule contained in the crystallographic asymmetric unit (figure 4.3a). One molecule of fumaric acid is held in between two molecules of 1-phenyl-3-(quinolin-5-yl)urea through intermolecular hydrogen bonding (O3-H3A····N1 $d_{D\cdot\cdot A}$ 2.72 Å).

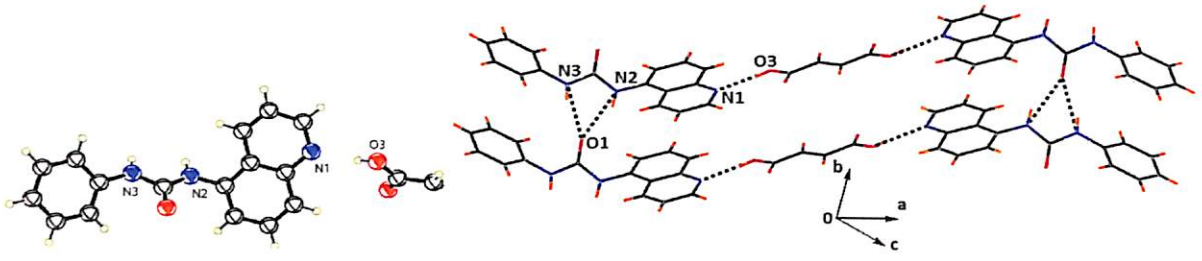

(a) (b)

Figure 4.3: (a) Asymmetric unit of **4.4** (ORTEP diagram drawn in 50% probability ellipsoid); (b) hydrogen bonding network in co-crystal **4.4**

Another important structural feature is the presence of urea-like $R_2^1(6)$ interactions (N2-H2N···O1 $d_{D\cdot\cdot A}$ 2.89 Å and N3-H3N···O1, $d_{D\cdot\cdot A}$ 2.80 Å) that leads to the growth of urea tape (figure 4.3b).The hydrogen bond parameters are listed in table 4.1.

Table 4.1: Hydrogen bond distances and angles for compound **4.4**

D-H····A	$d_{D\text{-}H}$(Å)	$d_{H\cdots A}$(Å)	$d_{D\cdots A}$(Å)	< D-H····A(°)
N(2)-H(2N) ····O(1) [x, y-1, z]	0.83(2)	2.12(2)	2.890 (2)	153(2)
O(3)-H(3A)···N(1) [x, -y+3/2, z-1/2]	0.82	1.91	2.716(2)	168
N(3)-H(3N) ····O(1) [x, y-1, z]	0.78(2)	2.07(2)	2.796(2)	155(2)

On treatment with maleic acid, receptor **4.1** forms a yellow coloured salt (**4.5**). The salt **4.5** crystallizes in the space group triclinic P-1with one protonated **4.1** cation and one maleic acid anion in the asymmetric unit (figure 4.4a). The urea tap motif is not maintained in this case instead a hydrogen bonding between the urea N-H and the carboxylate group (N2-H2N····O2 and N3-H3N····O2) (table 4.2) is observed. Another intra-molecular hydrogen bonding in the maleate anion (O3-H3A····O4) is also observed. The other carboxylate group of maleate anion forms hydrogen bonds with the protonated quinoline N (N1-H1N····O4). The hydrogen bonded assembly is shown in figure 4.4b.

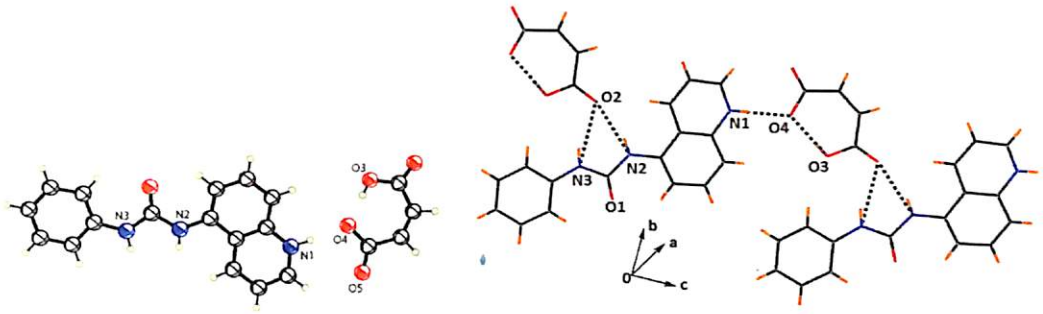

(a) (b)

Figure 4.4: (a) Asymmetric unit of the salt **4.5** (ORTEP diagram drawn in 50% probability ellipsoid); (b) hydrogen bond network in the salt **4.5**

Table 4.2: Hydrogen bond distances and angles for compound **4.5**

D-H····A	d_{D-H}(Å)	$d_{H\cdots A}$(Å)	$d_{D\cdots A}$(Å)	< D-H····A(°)
N(1)-H(1)····O(4)	0.89(4)	1.79(4)	2.679(4)	176(4)
N(2)-H(2N)····O(2) [x, y, z-1]	0.81(3)	2.11 (3)	2.881(4)	161(3)
N(3)-H(3N)····O(2) [x, y, z-1]	0.84(3)	2.25(3)	3.025(4)	154(3)
O3-H3A····O4	0.82	1.59	2.410(4)	177

A colourless co-crystal **4.6** is formed when receptor **4.1** is treated with 1, 4-phenylenediacetic acid. The co-crystal **4.6** crystallises in the space group monoclinic $P2_1/c$. In this case also the 1, 4-phenylenediacetic acid molecule lies at an inversion centre with only half of the molecule contained in the crystallographic asymmetric unit (figure 4.5a). It has a structure analogous to that of **4.4**. Accordingly, one molecule of 1,4-phenylenediacetic acid is held together by two molecule of 1-phenyl-3-(quinolin-5-yl)urea through intermolecular hydrogen bonding (O3-H3A····N1). The urea-urea tape hydrogen bonding (N3-H3N····O1 and N2-H2N····O1) is one of the major weak interaction (table 4.3) dominating the structural feature of **4.6** (figure 4.5b).

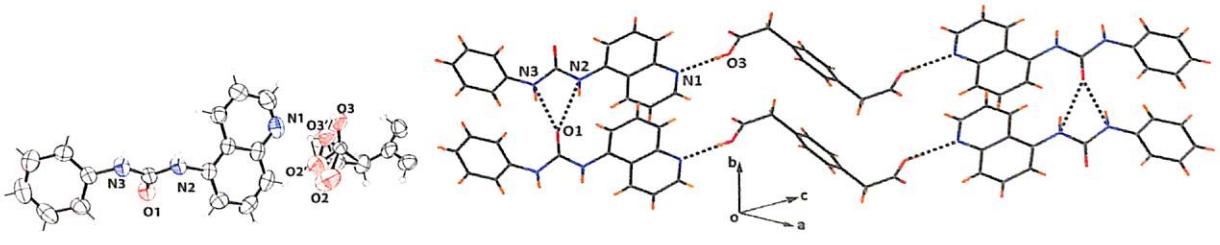

(a) (b)

Figure 4.5: (a) Asymmetric unit of **4.6** (ORTEP diagram drawn in 50% probability ellipsoid); (b) hydrogen bonding network in **4.6**

Crystal structure of the co-crystal shows disorder in the carboxyl group of the acid molecule as shown in figure 4.4a.

Table 4.3: Hydrogen bond distances and angles for **4.6**

D-H····A	$d_{D\text{-}H}$(Å)	$d_{H\cdots A}$(Å)	$d_{D\cdots A}$(Å)	< D-H····A(°)
N(2)-H(2N) ····O(1) [x,1+y,z]	0.86	2.12	2.897(2)	150
O(3)-H(3A) ····N(1) [x,1/2-y,1/2+z]	0.82	1.91	2.718(4)	166
N(3)-H(3N) ····O(1) [x,1+y,z]	0.86	2.01	2.817(2)	155

Receptor **4.1** on treatment with malonic acid forms a yellow coloured salt **4.7**. The salt **4.7** crystallizes in the space group monoclinic C2/c. In the crystal lattice the malonate ion lies on an inversion centre with only half of the anion contained in the crystallographic asymmetric unit (figure 4.6a). It has its central carbon atom on a twofold axis. Although we have got a salt with malonic acid the basic structural unit does not vary with those of the co-crystals. The malonate anions are held between two 1-phenyl-3-(quinolin-5-yl)urea molecule through intermolecular hydrogen bonding (N1-H1····O2) (table 4.4), however in this case the donor atom for hydrogen bonding is the nitrogen atom of the quinoline ring. The structure is also featured by the retention of hydrogen bond pattern of urea tape motif (N2-H2N····O1 and N3-H3N····O1) of its parent molecules. The carboxylate oxygen atoms are found to be disordered as in the case of salt **4.7** as shown in the figure 4.6a.

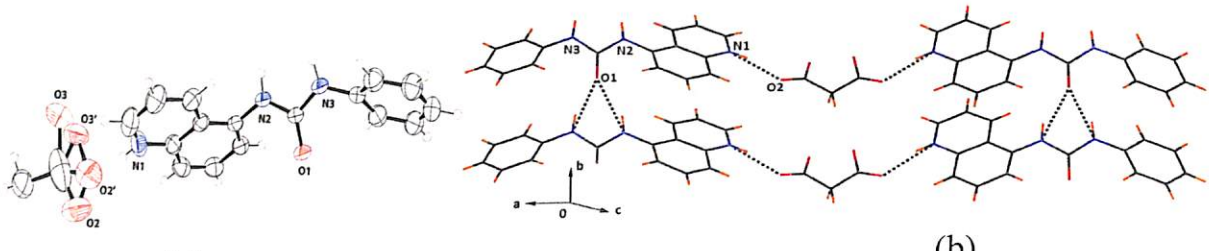

(a) (b)

Figure 4.6: (a) Asymmetric unit of **4.7** (ORTEP diagram drawn in 50% probability ellipsoid); (b) hydrogen bonding network in **4.7**

Table 4.4: Hydrogen bond distances and angles for compound **4.7**

D-H····A	$d_{D\text{-}H}$(Å)	$d_{H\cdots A}$(Å)	$d_{D\cdots A}$(Å)	< D-H····A(°)
N(1)-H(1) ····O(2) [x, -y+2, z+1/2]	0.86	1.88	2.724(5)	165.3
N(3)-H(3N)····O(1) [x, y-1, z]	0.86(2)	2.01(2)	2.812(2)	155(2)
N(2)-H(2N)····O(1) [x, y-1, z]	0.84(2)	2.13(2)	2.907(2)	154(2)

Phthalic acid forms a yellow coloured salt (**4.8**) with receptor **4.1**. The salt **4.8** crystallizes in the space group orthorhombic Pbcn with one protonated cation of **4.1** and a phthalate anion in the asymmetric unit (figure 4.7a). The urea tap motif is not observed in the structure of this salt, instead two hydrogen bond between the oxygen atom of the phthalate anion and the urea nitrogen atom is observed (N2-H2N····O4, N3-H3N····O5) (table 4.5). Another intermolecular hydrogen bond between the protonated nitrogen atom of the quinoline ring and the carboxylate group of phthalate anion (N1-H1N····O2) is also present in the crystal structure (figure 4.7b).

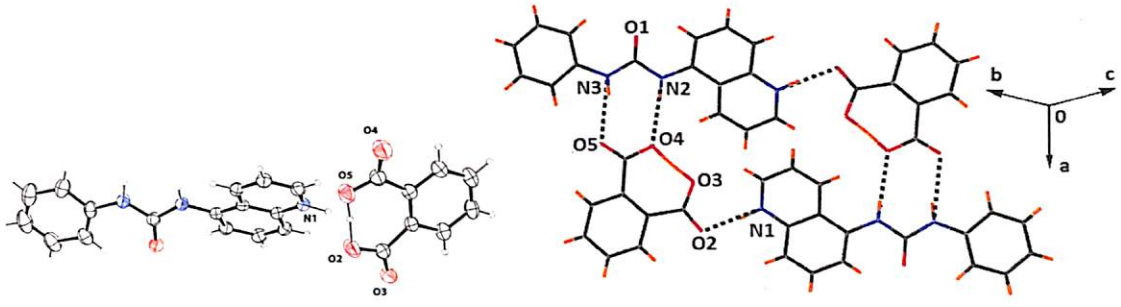

(a) (b)

Figure 4.7: (a) Asymmetric unit of **4.8** (ORTEP diagram drawn in 50% probability ellipsoid); (b) hydrogen bonding network in **4.8**

Table 4.5: Hydrogen bond distances and angles for compound **4.8**

D-H····A		$d_{D\text{-}H}$(Å)	$d_{H\cdots A}$(Å)	$d_{D\cdots A}$(Å)	< D-H····A(°)
N(1)-H(1N) ····O(2)	[x,-y,-1/2+z]	1.05(3)	1.68(3)	2.714(2)	168(2)
N(2)-H(2N) ····O(4)	[-x,y,1/2-z]	0.86	2.16	3.015(3)	177
N(3)-H(3N) ····O(5)	[-x,y,1/2-z]	0.86	2.14	2.970(3)	163
O(3)-H(4A) ····O(4)		1.25(4)	1.12(4)	2.367(3)	174(4)

Terephthalic acid forms a colourless co-crystal (**4.9**) with receptor **4.1**. The co-crystal **4.9** crystallizes in the space group monoclinic $P2_1/c$ where the terephthalic acid molecule lies on an inversion centre with only half of the molecule contained in the crystallographic asymmetric unit (figure 4.8a). The urea tap motif of the receptor molecule is maintained in the co-crystal (N2-H2N····O1, N3-H3N····O1). Another intermolecular hydrogen bonding between the quinoline N atom and the carboxylic acid (O2-H2····N1) forms a bridge between two receptor molecules as shown in figure 4.8b. The hydrogen bond parameters are shown in table 4.6.

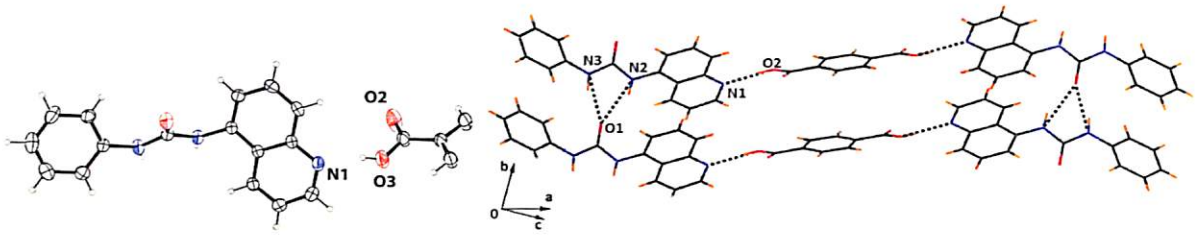

(a) (b)

Figure 4.8: (a) Asymmetric unit of **4.9**(ORTEP diagram drawn in 50% probability ellipsoid); (b) hydrogen bonding network in **4.9**

Table 4.6: Hydrogen bond distances and angles for compound **4.9**

D-H····A	$d_{D\text{-}H}$(Å)	$d_{H\cdots A}$(Å)	$d_{D\cdots A}$(Å)	< D-H····A(°)
N(2)-H(2N) ····O(1) [x,-1+y,z]	0.86	2.10	2.864(1)	148
N(3)-H(3N) ····O(1) [x,-1+y,z]	0.86	1.98	2.779(2)	155
O(2)-H(2A) ····N(1) [x,3/2-y,1/2+z]	0.82	1.89	2.697(2)	168

The receptor **4.1** forms a colourless co-crystal with adipic acid (**4.10**). The co-crystal **4.10** crystallizes in the space group monoclinic $P2_1/c$ with half of the adipic acid molecule and a molecule of receptor **4.1** in the crystallographic asymmetric unit (figure 4.9a). The co-crystal **4.10** forms an analogous structure with the other co-crystals by maintaining the urea tap hydrogen bonding interaction (N2-H2N····O1, N3-H3N····O1) (table 4.7). The carboxylic acid group of adipic acid form hydrogen bonds with the quinoline N atom (O3-H3····N1). The hydrogen bonded self assembly of the co-crystal is shown in figure 4.9b.

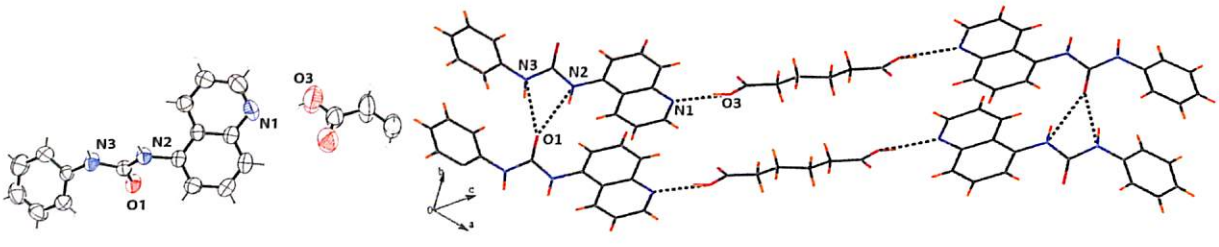

(a) (b)

Figure 4.9: (a) Asymmetric unit of **4.10** (ORTEP diagram drawn in 50% probability ellipsoid); (b) hydrogen bonding network in **4.10**

Table 4.7: Hydrogen bond distances and angles for compound **4.10**

D-H····A	$d_{D\text{-}H}$(Å)	$d_{H\cdots A}$(Å)	$d_{D\cdots A}$(Å)	< D-H····A(°)
N(2)-H(2N) ····O(1) [x,-1+y,z]	0.85(2)	2.10(2)	2.870(3)	150(2)
N(3)-H(3N) ····O(1) [x,-1+y,z]	0.90(3)	1.98(3)	2.798(4)	150(2)
O(3)-H(3A) ····N(1) [x,3/2-y,1/2+z]	0.82	1.92	2.707(5)	162

We have extended our result to a pyridine dicarboxylic acid namely pyridine-2, 3-dicarboxylic acid, to understand the changes in bonding pattern as well as the deprotonation process. Accordingly the salt **4.11** was prepared and it is found to crystallize in the space group triclinic P-1. It is observed that only one of the carboxylate group of pyridine-2,3-dicarboxylic acid gets deprotonated and remains hydrogen bonded with the protonated quinoline N-H (N1-H1N····O3). The H-atom attached to the quinoline nitrogen is also hydrogen bonded with the nitrogen atom of pyridine-2,3-dicarboxylic acid (N1-H1N····N4). Due to the presence of the two carboxylate groups similar to that of maleic acid and phthalic acid we did not observe the urea tape motif. The deprotonated carboxylic acid group forms intermolecular hydrogen bonds with the urea hydrogens (N2-H2N····O3 and N3-H3N····O2), which is responsible for the breakdown of the hydrogen bond urea tape motif present in the structure of the original molecule. Another interesting structural feature of the salt is the presence of intermolecular hydrogen bonding (O5-H5····O4) between two carboxylic acid groups which leads to formation of a dimeric assembly of mono deprortonated pyridine-2,3-dicarboxylic acid. In the assembly of the salt **4.11**, intra-molecular hydrogen bond (O5-H5····O4) between the one carboxylate anion and a carboxylic acid group is also observed (figure 4.10 and table 4.8).

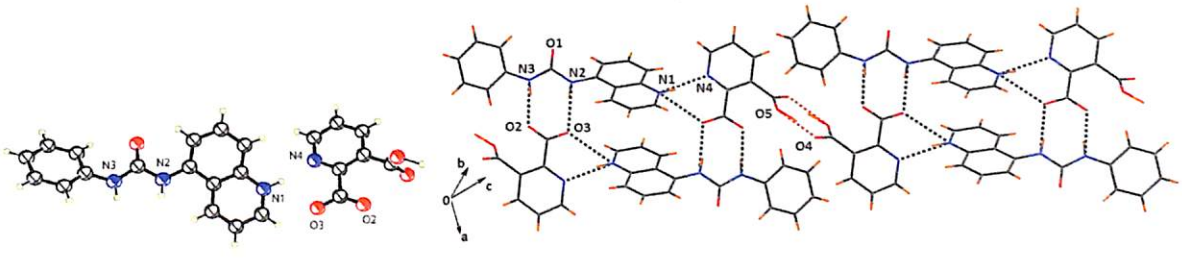

(a) (b)

Figure 4.10: (a) Asymmetric unit of **4.11** (ORTEP diagram drawn in 50% probability ellipsoid); (b) hydrogen bonding network in **4.11**

Table 4.8: Hydrogen bond distances and angles for compound **4.11**

D-H····A	$d_{D\text{-}H}$(Å)	$d_{H\cdots A}$(Å)	$d_{D\cdots A}$(Å)	< D-H····A(°)
N(1)-H(1N) ····N(4) [x+1, y, z]	0.94(2)	1.97(2)	2.888(2)	167(2)
N(2)-H(2N) ····O(3) [-x+1, -y+1, -z+1]	0.89(2)	1.95(2)	2.832(2)	168(2)
N(3)-H(3N) ····O(2) [-x+1, -y+1, -z+1]	0.88(2)	1.90(2)	2.773(2)	172(2)
O(5)-H(5) ····O(4) [-x+1, -y+2, -z+2]	1.24(4)	1.40(4)	2.622(2)	169(3)

From crystal design and engineering viewpoint the above structures (**4.4-4.11**) can be divided into two categories. First one, those with urea····urea and acid····pyridine H bonding (**4.4**, **4.6, 4.7, 4.9** and **4.10**) and secondly, those with urea····COOH/COO$^-$ H bonding (**4.5**, **4.8** and **4.11**).

The solid state NMR spectra of the co-crystal **4.4** and the salt **4.5** are also studied which shows a difference in the chemical shift value of the carboxylic acid carbons. Solid-state ^{13}C CPMAS NMR of co-crystal **4.4** shows that the peak for the carboxylic acid carbon of fumaric acid is at 156 ppm (figure 4.11).

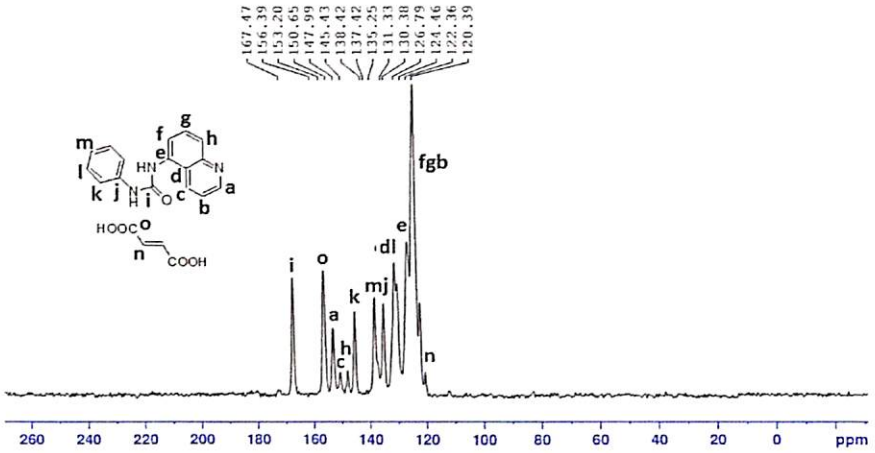

Figure 4.11: Solid-State ^{13}C CPMAS NMR of co-crystal **4.4**

In case of the salt **4.5** the peak for the carboxylate carbon of maleate anion is at 169 ppm (figure 4.12). The peak for the urea carbon is at 167 ppm for both the co-cryatal (**4.4**) and the salt (**4.5**). Thus the distinction of the salt and co-crystals can be done from their respective solid state NMR spectra.

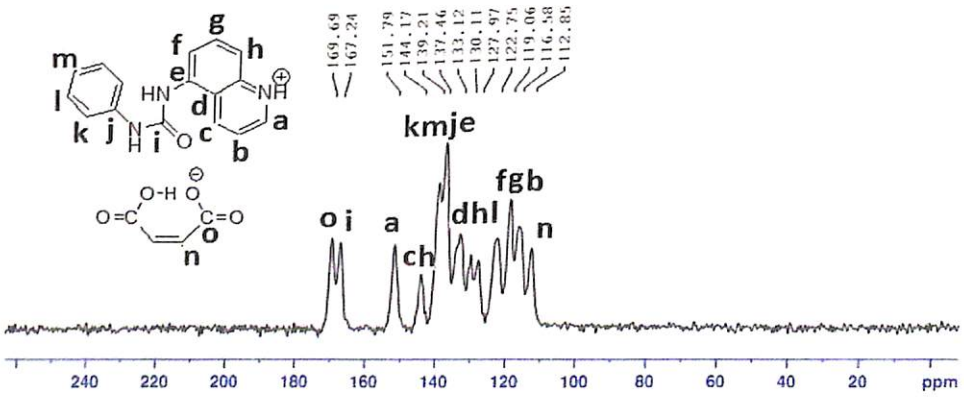

Figure 4.12: Solid-State ^{13}C CPMAS NMR of salt **4.5**

4.3 Visual distinction of the salts and co-crystals

The interesting features of these salts or co-crystals are that they can be distinguished from each other by looking at their colour morphology and from their optical spectra. Generally the co-crystals are colourless whereas the salts are yellow in colour. As an illustrative example, the crystal morphology of co-crystal **4.4** and salt **4.5** are shown in figure 4.13. The co-crystal **4.4** is a colourless needle shape crystal whereas the salt **4.5** is a yellow coloured blocks.

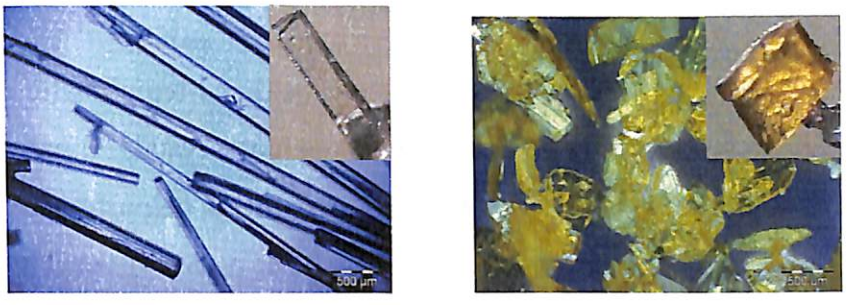

(a) (b)

Figure 4.13: Colour morphology of crystals distinguishing regioisomers (a) co-crystal with fumaric acid; (b) salt with maleic acid with **4.1**; Inset: photograph of the single crystals

The compound 1-phenyl-3-(quinolin-5-yl)urea (**4.1**) has an absorption maximum at 320 nm in methanol. While on subsequent addition of a maleic acid solution to a solution of 1-phenyl-3-(quinolin-5-yl)urea leads to corresponding salt which shows an absorption maximum at 400 nm, and from a titration of the receptor with maleic acid solution leads to an isosbestic point (figure 4.14). The peak at 400 nm is indicative of a protonated 1-phenyl-3-(quinolin-5-yl) urea. This peak is observed from interaction of **4.1** with any mineral acid also; thus, we can attribute to the formation of salt, as this peak is observed by protonation with other mineral acids. However, in the case of co-crystals of acids with **4.1,** we did not observe the peak at 400 nm.

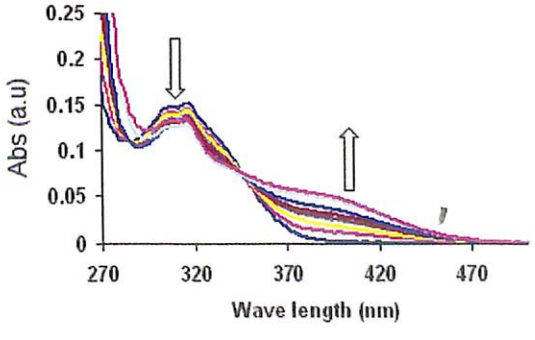

Figure 4.14: Changes in absorption spectra of **4.1** (10^{-5} M in methanol) on addition of maleic acid (10^{-2} M in methanol in 20 μL aliquot each)

Fumaric acid forms co-crystals with compound **4.1** whereas its stereoisomer maleic acid forms a salt. On the basis of this we have done control experiment by adding a solution of maleic acid to co-crystals of fumaric acid and vice-versa and found that the compound **4.1** binds preferentially to maleic acid in presence of fumaric acid. To prove this we have prepared a methanolic solution of compound **4.1** and fumaric acid (1:1) and to it constant aliquot of maleic acid was added. On gradual addition of acid solution a peak at 400 nm appears which suggests the binding of maleic acid to compound **4.1**.

Another pair of positional isomer namely phthalic acid and terephthalic acid can also be distinguished by virtue of the formation of salt and co-crystal. Phthalic acids forms a yellow coloured salt whereas terephthalic acid forms a colourless co-crystal. We have also studied the UV-visible spectra of the parent carboxylic acids i.e., phthalic acid and terephthalic acid (figure 4.15). Phthalic acid absorbs at 273 nm and on addition of base such as triethyl amine no absorbance in the visible region is observed. Similarly in the case of terephthalic acid which absorbs at 285 nm, no absorbance at the visible region is observed on addition of triethyl amine. Hence, the yellow colour of the salts is only because of the protonated form of the receptor **4.1**. Further, the mineral acid salts of **4.1** are also yellow coloured.

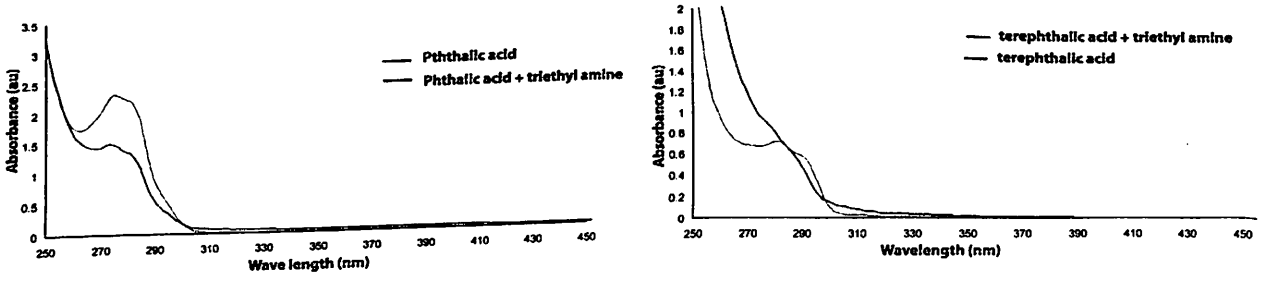

(a) (b)

Figure 4.15: Changes in the absorption spectra of (a) phthalic acid (10^{-4} M in methanol) and (b) terephthalic acid (10^{-4} M in methanol) on addition of 20 μL of triethyl amine

It has been shown in literature that the n-π^* and π-π^* levels in quinoline derivatives are very close. Thus the protonation and hydrogen bonding make the difference in the observation of colour change. This may be quantitatively explained as follws. For

example, in receptor **4.1** in the usual condition it has the broad absorption maximum at 320 nm (figure 4.14) due to the n-π* and π-π* transition.

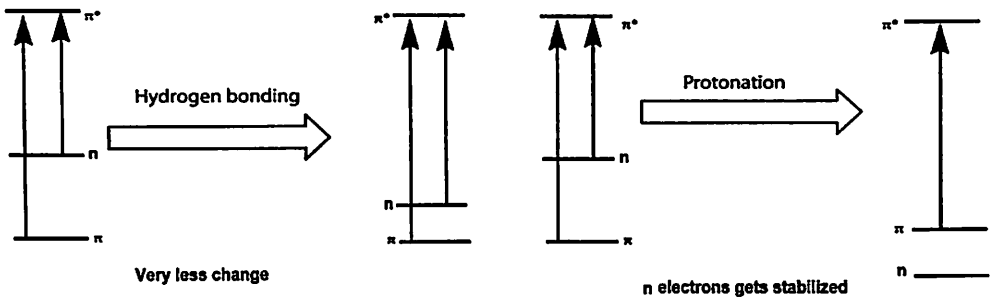

Figure 4.16: Qualitative energy level diagram to show the changes in the elrctronic spectra of **4.1**

In the case of weak hydrogen bonding tha n electrons are slightly effected whereas upon protonation it gets stabilized and the π-π* transition dominates which is reflected in the UV-visible spectra (figure 4.16).

4.4 Structural study of the mineral acid salt of 4.1, 4.2, and 4.3

We have tried preparation of similar salt/co-crystals with other receptors such as 1-phenyl-3-(quinolin-8-yl)urea (**4.2**) and quinoline-8-yl phenylcarbamate (**4.3**) having slightly different structures than **4.1**. These molecules are found to be poor in binding to the dicarboxylic acid. However, the mineral acids, such as perchloric acid binds rapidly to compound **4.1, 4.2** and **4.3**. Hence, the compound **4.2** and **4.3** are selective only for the mineral acids. The receptors **4.1**, **4.2**, and **4.3** were treated with different mineral acids. Unfortunately no good diffraction quality crystals were obtained from acids other than perchloric acid. The mineral acid binding of these receptors lead to the formation of symmetry non-equivalent molecules i.e., the existence of more than one molecule in the crystallographic asymmetric unit. The number of molecules in the asymmetric unit is represented by the symbol Z′.

The receptor **4.1** crystallizes with only one molecule in its asymmetric unit (Z′=1). The compound **4.12**, perchlorate salt of **4.1** crystallizes in the space group monoclinic $P2_1/c$. This structure is featured by three symmetry independent molecules (Z′=3) with a total of eight molecules (Z″=8) in the crystallographic asymmetric unit. The asymmetric unit is shown in figure 4.17a. It consists of three protonated **4.1** cations,

three perchlorate anions and two molecules of water of crystallization. The H- atoms of one of the waters of crystallization could not be located due to poor crystal quality.

The structure **4.12** exhibits extensive supramolecular interactions viz. H-bonding interactions, C-H···O interactions, N-H···O interactions, C-H···π interactions and π···π interactions between the aromatic rings. It is noteworthy that the presence of the guest anion, ClO_4^-, imparts some supramolecular features to the host so that it can be involved in a number of short range interactions. The presence of two waters of crystallization in fact further increases this possibility. It is these short range interactions as a result of which **4.12** acquires a Z′=3 structure. Unlike the parent compound **4.1**, **4.12** do not possess a urea tape motif through simple N-H···O hydrogen bonding. **4.1** on treatment with perchloric acid solution undergo protonation at the quinoline-N. This proton then involves in N-H···O hydrogen bonding with the perchlorate anion. All the three asymmetric molecules in the structure thus become protonated and remains hydrogen bonded to perchlorate ions. Apart from this all the perchlorate anions are also involved in C-H···O interactions with ring protons. The second type of N-H···O hydrogen bonding is exhibited by the urea O-atoms O2 and O3 ($d_{D\text{-}H\cdots A}$ (Å), N8-H8A···O2, 2.26(5); N2-H2A···O3, 2.25(3), and <D-H···A (°), <N8-H8A···O2, 159(5); <N2-H2A···O3, 173(3)). The remaining oxygen atom viz. O1 is hydrogen bonded to one of the waters of crystallization. The oxygen atom of this water is again involved in a bifurcated H-bonding to the urea N-H atoms of an adjacent molecule ($d_{D\text{-}H\cdots A}$ (Å), N5-H5A···O16, 2.22(4); N6-H6A···O16, 1.96(5) and <D-H···A (°), <N5-H5A···O16, 158; <N6-H6A···O16, 160(3)). Apart from all these interactions face to face π···π interactions are also there among the quinoline rings of the three asymmetric molecules. The structure of **4.12** with the short range interactions are shown in figure 4.17b. It should be noted here that the presence of the anion imparts some twist in the molecules. Consequently the conformation of each of the three symmetry independent molecules changes from each other, as the angle between the planes of the aromatic rings viz. quinoline and phenyl rings in each molecule differs significantly from each other as well as from that in the parent compound **4.1**.

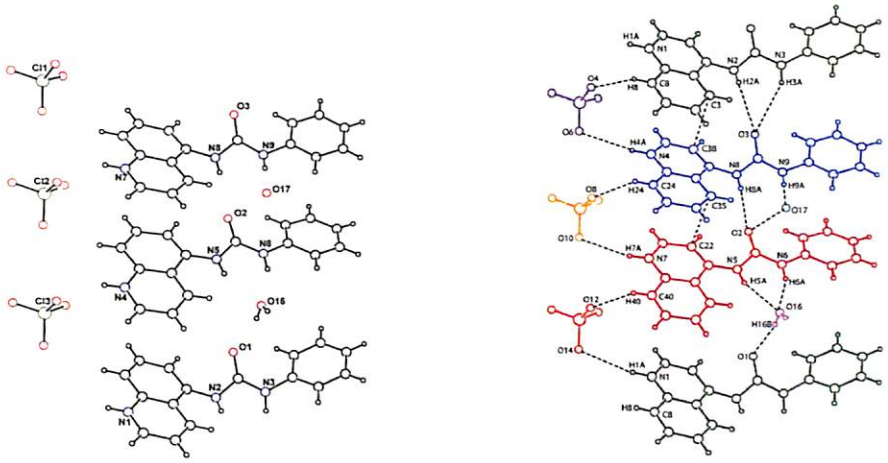

(a) (b)

Figure 4.17: (a) Asymmetric unit of **4.12**; (b) short range interactions in **4.12**

Apart from perchloric acid, receptor **4.1** also crystallizes with *p*-tolunesulphonic acid to give a salt (**4.13**); however, in this case we did not observed any change in the Z′ value on co-ordination with anion. Hence the changes in the number of molecule in the asymmetric unit (Z′) are selective to anions.

The salt **4.13** crystallizes in the space group monoclinic C2/c and exists as a Z′=1 structure with a total of two molecules in the crystallographic asymmetric unit (Z″=2). The asymmetric unit consists of a *p*-tolunesulphonate anion and a protonated **4.1** cation. In this structure also the urea tap motif is not observed, instead the urea H atoms are involved in an intermolecular hydrogen bond with the O atom of the *p*-tolunesulphonate anion ($d_{D\text{-}H\cdots A}$ (Å), N2-H2N···O2, 2.904(2); N3-H3N···O4, 3.050(2) and <D-H···A (°), < N2-H2N···O2, 167(2); < N3-H3N···O4, 153(1)).

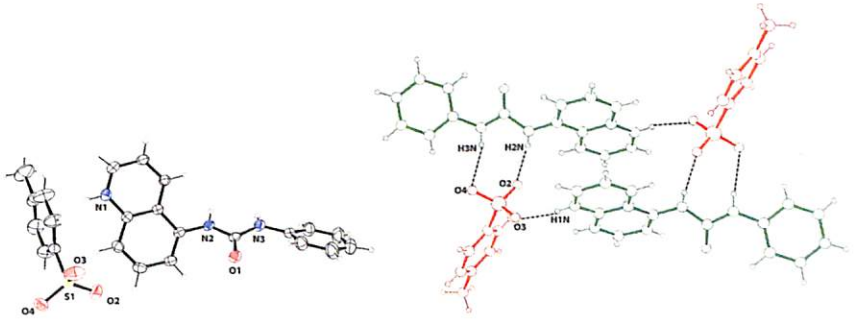

(a) (b)

Figure 4.18: (a) Asymmetric unit of **4.13**; (b) short range interactions in **4.13**

Another oxygen atom O3 of the *p*-tolunesulphonate anion forms a hydrogen bond with the protonated quinoline nitrogen atom ($d_{D-H\cdots A}$ (Å), N1-H1N··· O3, 2.698(2) and < N1-H1N··· O3, 156(2)). The asymmetric unit of **4.13** is shown in figure 4.18a along with the short range interactions in figure 4.18b.

The salts of receptor **4.1** can be easily be distinguished from their IR spectra. The receptor **4.1** gives strong IR peak at 1641 cm^{-1} for amide C=O stretching and at 1557 cm^{-1} for aromatic C=C stretching. Apart from these two peaks the salts **4.12** and **4.13** shows characteristic peaks for the anionic part. The perchlorate salt **4.12** shows two sharp peaks at 1120 cm^{-1} and 1080 cm^{-1} characterestic of the perchlorate anion. The *p*-tolunesulphonate salt **4.13** shows a sharp peak at 1212 cm^{-1} characterestic of the *p*-tolunesulphonate anion. The comparison of the IR spectra of the two salts **4.12** and **4.13** with the receptor **4.1** is shown in figure 4.19.

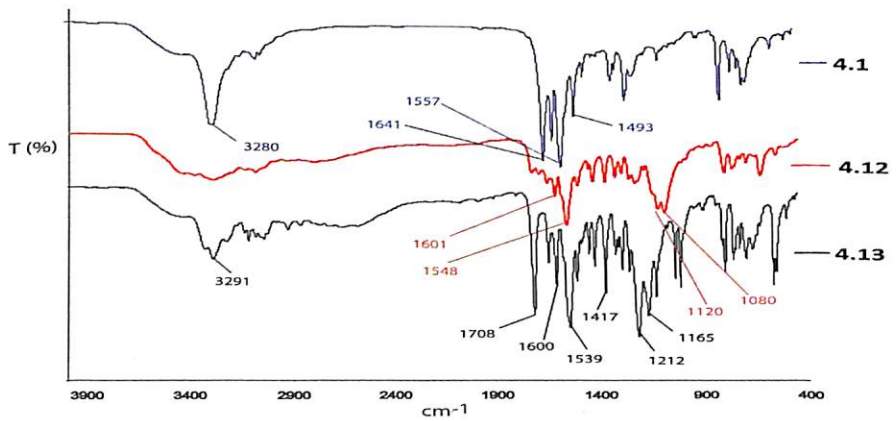

Figure 4.19: Comparison of the IR spectra of **4.1**, **4.12** and **4.13**

Unlike **4.1**, the urea derivative of 8-aminoquinoline, **4.2,** exists as a Z′=2 structure and crystallizes in the space group monoclinic $P2_1/c$. This structure exhibits a helical packing arrangement through the N-H···O hydrogen bonding and π···π interactions available therein. All the urea oxygens are involved in a bifurcated hydrogen bonding interaction with the N-H of the other symmetrically non equivalent molecule ($d_{D-H\cdots A}$ (Å), N5-H5N···O1, 2.29(3); N6-H6N···O1, 2.06(3); N3-H3N···O2, 2.02; N2-H2N···O2, 2.19(3) and <D-H···A (°), <N5-H5N···O1, 141; <N6-H6N···O1, 160(3); <N3-H3N···O2, 163; <N2-H2N···O2, 150(3)). The face to face π···π interaction between the quinoline rings (C8···C17= 3.36 Å) further facilitates the formation of the

helical structure. The short range interactions in **4.2** are shown in figure 4.20a along with the helical structure in figure 4.20b.

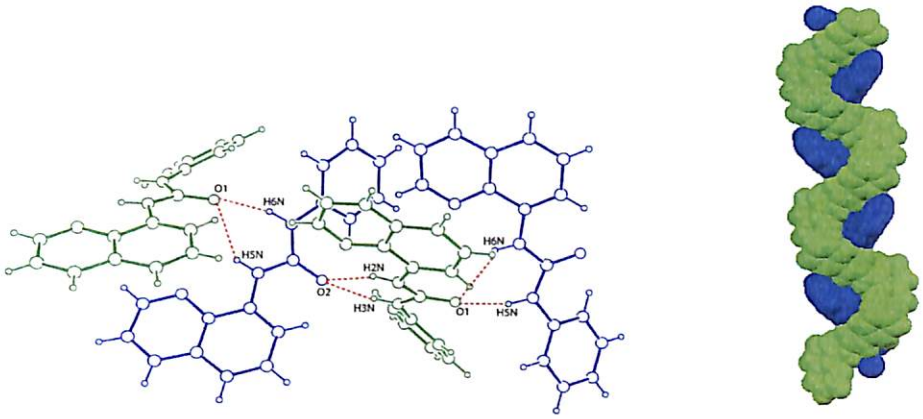

(a) (b)

Figure 4.20: (a) Short range interactions in **4.2**; (b) helical packing arrangement in **4.2**

The perchlorate salt of **4.2**, viz. **4.14**, crystallizes in the orthorhombic space group $Pna2_1$ and exists as a $Z'=2$ structure with a total of four molecules in the crystallographic asymmetric unit ($Z''=4$). On treatment with $HClO_4$, **4.2** undergo protonation at the quinoline-N to result in the cationic **4.2**. Like the parent compound **4.2**, **4.14** also exhibit N-H···O hydrogen bonding and π···π interactions as the only available short range interactions. The perchlorate ions are bound to the host cation through N-H···O hydrogen bonding as well as C-H···O interactions ($d_{D\text{-}H\cdots A}$ (Å), N4-H4A···O18, 2.28(4); N3-H3A···O14, 1.93(6); C17-H17···O20, 2.70; C1-H1···O19, 2.48; C7-H7···O8, 2.67; C23-H23···O15, 2.69 and <D-H···A (°), < N4-H4A···O18, 159(4); < N3-H3A···O14, 170(5); < C17-H17···O20, 119; < C1-H1···O19, 138, < C7-H7···O8, 138; < C23-H23···O15, 139). The urea N-H are H-bonded to the urea oxygen atoms thereby forming hydrogen bonded tape ($d_{D\text{-}H\cdots A}$ (Å), N1-H1A···O2, 2.24; N2-H2A···O2, 2.22(5); N6-H6A···O1, 2.29(5); N5-H5A···O5, 2.28(5) and <D-H···A (°), < N1-H1A···O2, 151; < N2-H2A···O2, 163(4); < N6-H6A···O1, 151(4); < N5-H5A···O5, 151(4)). Apart from these there exist face to face π···π interactions between the quinoline ring of one and the phenyl ring of another molecule (C6···C28= 3.33 Å; C22···C16= 3.36 Å). The structure of **4.14** is shown in figure 4.21.

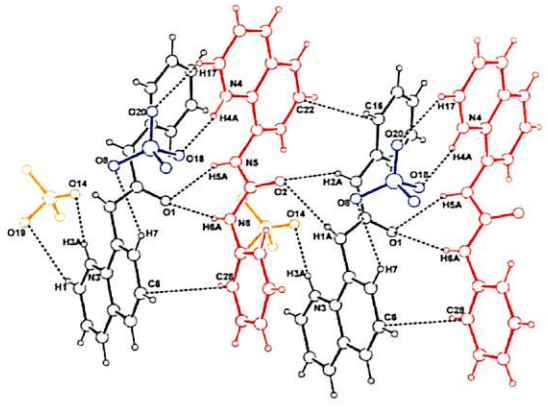

Figure 4.21: Short range interactions in **4.14**

The carbamate derivative **4.3** crystallizes in the space group orthorhombic $P2_12_12_1$ with only one molecule in the crystallographic asymmetric unit. The molecule self assembles through N-H···O hydrogen bonding, C-H···O interactions as well as through π···π interactions. The N-H atoms of the carbamate functionality are involved in N-H···O hydrogen bonding with the carbonyl oxygen atoms of an adjacent molecule ($d_{D-H\cdots A}$ (Å), N3-H3A···O1, 2.18). The other oxygen O2 remains hydrogen bonded to the H6

atom in a relatively weak C-H···O interaction ($d_{D-H\cdots A}$ (Å), C6-H6···O2, 2.70). It may be noted here that the conformation of the molecule is such that the two rings viz. the quinoline and the phenyl ring in the same molecule are almost orthogonal to each other. This conformation is actually facilitated by the edge to face π ···π interactions between the phenyl ring and quinoline ring on adjacent atoms ($d_{D-H\cdots A}$ (Å), C5-H5···C10, 2.83). These short range interactions ultimately results in chain like self assembly of the molecule growing along the 'a' crystallographic axis. The interactions in **4.3** are shown in figure 4.22.

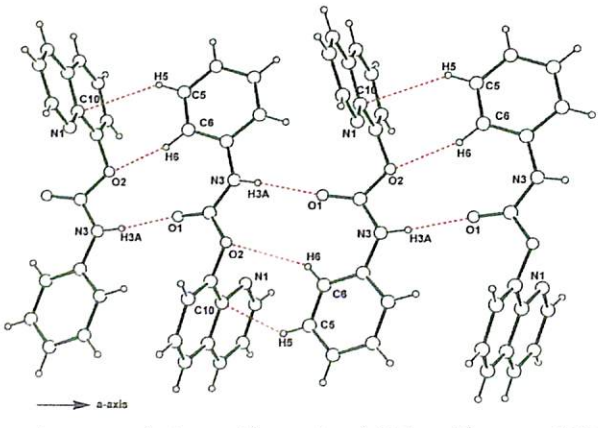

Figure 4.22: Short range interactions in **4.3** leading to 1D self assembly.

The perchlorate salt of **4.3**, namely **4.15**, crystallizes in the space group triclinic P-1. This structure have two symmetry independent molecules (Z′=2) in the crystallographic asymmetric unit. One water of crystallization is also there along with two symmetry independent cations of the carbamate derivative and two perchlorate anions. Thus there are a total of five molecules (Z′′=5) in the crystallographic asymmetric unit. The two symmetry independent molecules are involved in different short range interactions. The water of crystallization is engaged with only one among the two types of symmetry independent molecules. Like the previous two compounds **4.1** and **4.2**, **4.3** also get protonated at the quinoline-N atom. The quinolinium hydrogen on one of the two symmetry independent molecules is hydrogen bonded to a perchlorate anion ($d_{D\text{-}H\cdots A}$ (Å), N3-H3···O8, 2.08 and <D-H···A (°), <N3-H3···O8, 142). However the same on the other congener is now not hydrogen bonded to any perchlorate anion but remains H-bonded to the oxygen atom of the water molecule ($d_{D\text{-}H\cdots A}$ (Å), N1-H1···O11, 1.91 and <D-H···A (°), < N1-H1···O11, 160) and one of the hydrogen atom of the water molecule is hydrogen bonded to a perchlorate O-atom ($d_{D\text{-}H\cdots A}$ (Å), O11-H11A···O5, 1.95(15) and <D-H···A (°), <O11-H11A···O5, 156(11)). Interestingly unlike in the urea derivatives, the carbonyl oxygen on both the symmetry independent molecules possesses no significant supramolecular interactions. However the N-H atom of the carbamate functionality in both the molecules is involved in N-H···O hydrogen bonding with perchlorate anions ($d_{D\text{-}H\cdots A}$ (Å), N2-H2A···O3, 2.21; N4-H4···O7, 2.06 and <D-H···A (°), <N2-H2A···O3, 167; <N4-H4···O7, 176). It is noteworthy here that in one of the two symmetry independent molecules in **4.15** the planes of the two rings viz. the phenyl and the quinoline ring lie almost orthogonal to each other. However, in the other congener the two rings are almost parallel to each other. It is the presence of the perchlorate anion which changes the conformations of the molecules from that in **4.3**. Thus in the orthogonal molecules in **4.15** the quinoline rings are involved in π···π interactions (C3···C7 = 3.39 Å). However, no π···π interactions are observed in the other molecules. The asymmetric unit of **4.15** is shown in figure 4.23a along with the short range interactions in figure 4.23b.

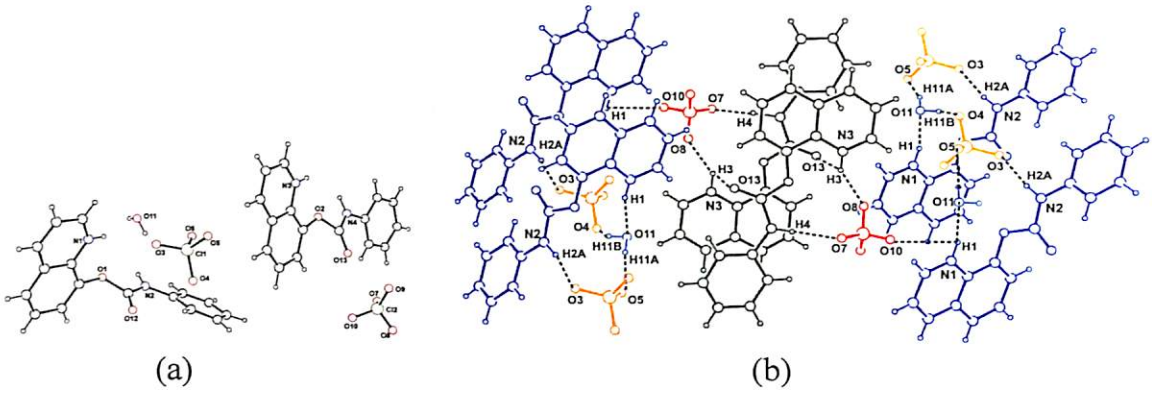

(a) (b)

Figure 4.23: (a) Asymmetric unit of **4.15**; (b) short range interactions in **4.15**

Conclusions

In conclusion a number of salts and co-crystals of 1-phenyl-3-(quinolin-5-yl) urea (**4.1**) with different dicarboxylic acids are synthesised and their crystal structures are studied. These salts and co-crystals can be distinguished from their colour morphology; the salts are of yellow coloured while the co-crystals are colourless. The salts and co-crystals can also be distinguished in solution state from their UV-visible spectra. A pair of diastereomer namely maleic acid and fumaric acid and a pair of positional isomer phthalic acid and terephthalic acid upon interaction with receptor **4.1** can easily be distinguished by virtue of the formation of salt and co-crystal. The well organized urea tap motif is maintained in the co-crystals whereas the urea tap motif is not maintained in the salts. The receptor **4.1** interacts easily with mineral acid or carboxylic acid; whereas receptor **4.2** and **4.3** binds only to mineral acids.

Perchlorate anion changes the planar arrangement of the two rings of protonated **4.1**, **4.2** and **4.3** and leads to structures with multiple Z′ value. It is clear from these observations that the anions placed in the lattice determines the orientation of the rings and changes the weak interactions significantly. This in turn causes the symmetry non equivalent structures leading to high Z′ value. The effect of anions on the Z′ value of the receptors is also sensitive to both the receptors as well as anions.

Experimental

Synthesis of 1-phenyl-3-(quinolin-5-yl)urea, (4.1):

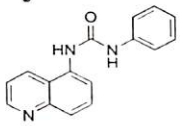

5-aminoquinoline (0.721 g, 5 mmol) was dissolved in dry dichloromethane (10 mL) and to this, another solution of phenylisocyanate (0.54 mL, 5 mmol) in dichloromethane was added drop wise and the mixture was stirred at room temperature for 3 hs. The product formed was filtered and recrystallized from methanol.

Yield: 78%.

IR (KBr, cm^{-1}): 3280 (s), 3062 (m), 1641 (s), 1599 (s), 1557 (s), 1493 (s), 1449 (m), 1315 (m), 1249 (s), 1091 (w), 799 (m), 748 (m), 694 (m).

^{1}H-NMR (DMSO-d_6, 400MHz, ppm): 8.8 (3H, m), 8.4 (1H, d, J = 8.8 Hz), 8.0 (1H, d, J = 7.2 Hz), 7.6 (2H, m), 7.4 (3H, m), 7.2 (2H, m), 7.0 (1H, t, J = 7.2 Hz).

^{13}C-NMR (DMSO-d_6, 100MHz, ppm): 118.3, 118.9, 121.4, 121.9, 122.7, 124.5, 129.5, 130.1, 130.8, 135.4, 140.2, 148.8, 150.9, 153.5.

LC-MS [M+1]: 264.13

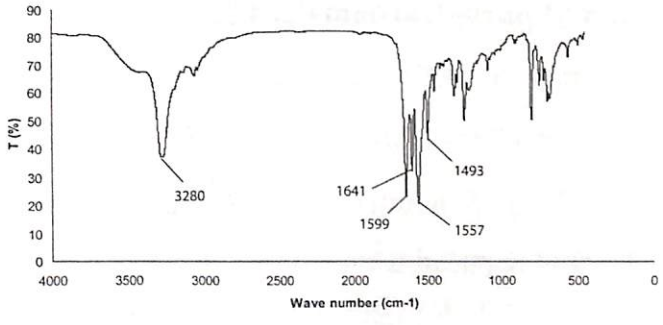

Figure 4.24: IR-spectra of receptor **4.1**

Synthesis of 1-phenyl-3-(quinolin-8-yl)urea, 4.2:

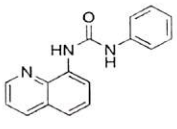

To a well stirred solution of 8-aminoquinoline (0.721 g, 5 mmol) in dry dichloromethane, a solution of phenylisocyanate (0.54 mL, 5 mmol) in dichloromethane was added and the mixture was refluxed for 4 hs. Solvent was evaporated and the residue obtained was recrystallized from methanol.

Yield: 74%.

IR (KBr, cm^{-1}): 3268 (s), 3140 (w), 3092 (w), 1658 (s), 1597 (m), 1549 (s), 1499 (m), 1487 (m), 1445 (m), 1423 (m), 1385 (m), 1312 (s), 1251 (s), 1219 (m), 1107 (m), 894 (w), 820 (w), 786 (w), 749 (s), 692 (w).

^{1}H-NMR ($CDCl_3$, 400 MHz, ppm): 9.3 (1H, s), 8.7 (1H, s), 8.6 (1H, d, J = 8.0 Hz), 8.1 (1H, d, J = 8.0 Hz), 7.4 (5H, m), 7.3 (2H, m), 7.1 (2H, m).

^{13}C-NMR ($CDCl_3$, 100MHz, ppm):109.9, 115.8, 120.4, 121.0, 121.5, 124.0, 127.7, 128.3, 129.3, 135.5, 136.6, 138.5, 148.0, 153.3.

LC-MS [M+1] 264.11

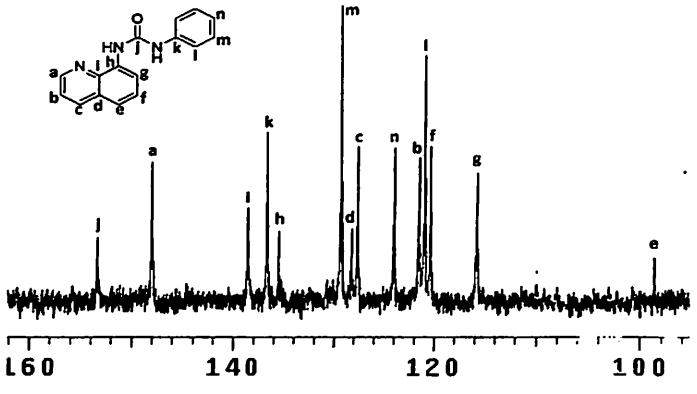

Figure 4.25: ^{13}C-NMR spectra of **4.2** (only the aromatic region is shown)

Synthesis of quinolin-8-yl phenylcarbamate, 4.3:

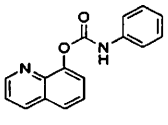

8-hydroxyquinoline (0.725 g, 5 mmol) was dissolved in dry dichloromethane and stirred for 10 min. To this solution a dichloromethane solution of phenylisocyanate (0.54 mL, 5 mmol) was added and the mixture was refluxed for 7 h. Solvent was removed and the product obtained was recrystallized from methanol.

Yield: 72%

IR (KBr, cm^{-1}) : 3337 (s), 3074 (w), 1721 (s), 1600 (s), 1542 (s), 1499 (m), 1446 (m), 1314 (m), 1216 (s), 1180 (m), 1164 (m), 1092 (s), 1004 (w), 835 (m), 758(s), 695 (m).

^{1}H-NMR ($CDCl_3$, 400 MHz, ppm) : 8.8 (1H, s), 8.2 (2H, d, J = 8.2 Hz), 7.7 (1H, d, J = 8.2 Hz), 7.6 (2H, m), 7.4 (3H, m), 7.2 (2H, m), 7.0 (1H, t, J = 7.2 Hz).

^{13}C-NMR ($CDCl_3$, 100MHz, ppm): 119.0, 121.9, 122.2, 123.7, 124.9, 125.7, 126.5, 129.1, 129.7, 136.5, 138.0, 141.7, 146.9, 150.4.

LC-MS [M+1]: 266.84

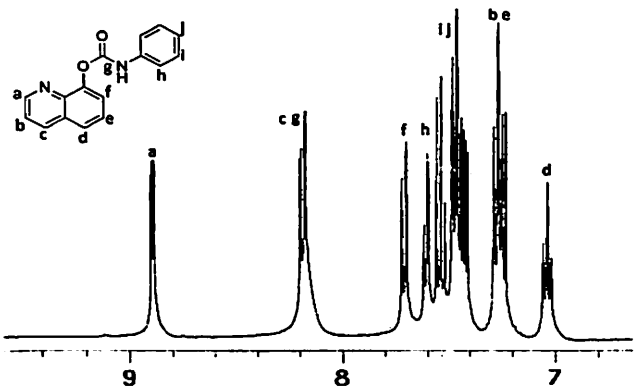

Figure 4.26: ^{1}H-NMR spectra of **4.3** (only the aromatic region is shown)

Synthesis of the salts and co-crystals of 4.1:

The compound **4.1** and the dicarboxylic acids (1:1) were dissolved in aqueous methanol. Slow evaporation of the solution results in colourless crystals of the co-crystals whereas in case of salts yellow colored crystals were observed.

Co-crystal of compound 4.1 with fumaric acid (4.4):

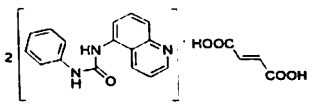

Isolated Yield: 73%

IR (KBr, cm^{-1}): 3271 (s), 3061 (w), 2926 (w), 1700 (s), 1680 (w), 1640 (s), 1599 (s), 1563 (s), 1496 (m), 1446 (m), 1399 (s), 1252 (m), 1168 (m), 1097 (m), 1015 (w), 806 (m), 747 (m), 723 (m), 692 (m), 632 (w).

^{1}H-NMR (DMSO-d_6, 400MHz, ppm): 9.0 (1H, s), 8.9 (2H, m), 8.5(1H, d, J = 8.4Hz), 8.1(1H, d, J = 6.8Hz), 7.7 (2H, m), 7.6 (1H, m), 7.4 (2H, d, J = 8.0Hz), 7.3 (2H, t, J = 7.6Hz), 6.9 (1H, t, J = 7.2Hz), 6.6 (1H, s).

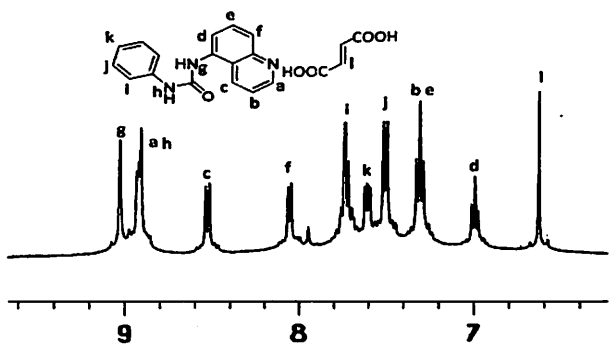

Figure 4.27: ^{1}H-NMR spectra of **4.4** (only the aromatic region is shown)

Salt of compound 4.1 with maleic acid (4.5):

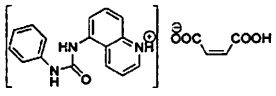

Isolated Yield: 68%

IR (KBr, cm^{-1}): 3361 (s), 3067 (w), 2925 (m), 1720 (m), 1637 (w), 1601 (m), 1572 (m), 1541 (m), 1502 (m), 1439 (m), 1423 (s), 1362 (s), 1313 (m), 1281 (m), 1241 (m), 1191(m), 1074 (w), 859 (m), 795 (m), 757 (m), 608 (m)

^{1}H-NMR (DMSO-d_6, 400MHz, ppm): 9.0 (1H, s), 8.9 (2H, m), 8.6 (1H, d, J = 8.0Hz), 8.0 (1H, m), 7.7 (2H, m), 7.6 (1H, m), 7.5 (2H, m), 7.3 (2H, t, J = 7.6Hz), 7.0 (1H, t, J = 6.4Hz), 6.2 (2H, s)

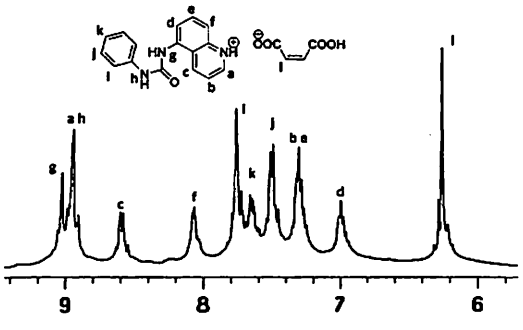

Figure 4.28: ^{1}H-NMR spectra of **4.5** (only the aromatic region is shown)

Co-crystal of compound 4.1 with 1,4-phenylenediacetic acid (4.6):

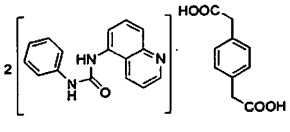

Isolated Yield: 65%

IR (KBr, cm^{-1}): 3274 (s), 3041 (w), 2924 (w), 1716 (s), 1641 (s), 1598 (s), 1558 (s), 1496 (m), 1446 (m), 1422 (w), 1309 (m), 1236 (m), 1140 (m), 1096 (m), 1024 (w), 804 (m), 747 (m), 723 (m), 692 (m).

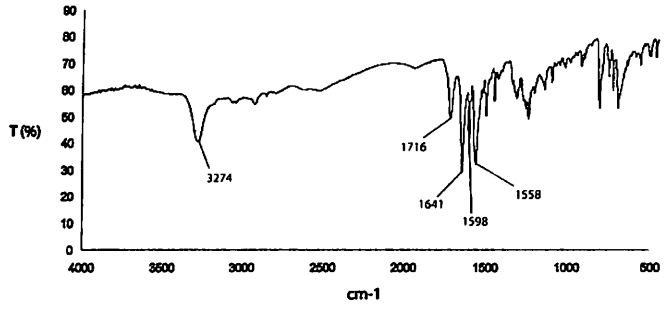

Figure 4.29: IR spectra of **4.6**

Salt of compound 4.1 with malonic acid (4.7):

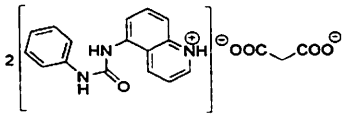

Isolated Yield: 76%

IR (KBr, cm^{-1}): 3275 (s), 3065 (w), 2927 (w), 1736 (m), 1712 (m), 1642 (s), 1598 (s), 1558 (s), 1496 (m), 1446 (m), 1316 (m), 1252 (m), 1214 (m), 1165 (m), 1098 (w), 916 (w), 805 (m), 748 (m), 723 (m), 692 (m).

^{1}H-NMR (DMSO-d_6, 400MHz, ppm): 9.0 (1H, s), 8.9 (2H, m), 8.5 (1H, d, J = 8.4Hz), 8.0 (1H, d, J = 6.8Hz), 7.7 (2H, m), 7.6 (1H, m), 7.5 (2H, d, J = 7.6Hz), 7.3 (2H, t, J = 8.0Hz), 7.0 (1H, t, J = 7.6Hz), 3.2 (1H, s).

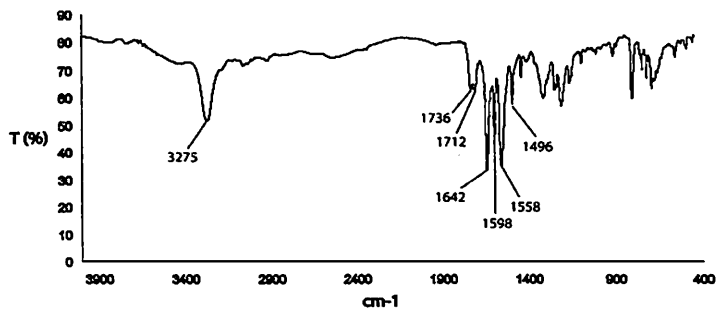

Figure 4.30: IR spectra of **4.7**

Salt of compound 4.1 with phthalic acid (4.8):

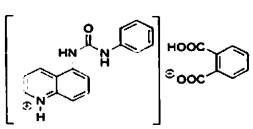

Isolated Yield: 69%

IR (KBr, cm^{-1}): 3444 (w), 2924 (w), 1695 (s), 1587 (m), 1535 (m), 1406 (m), 1284 (s), 1072 (m), 737 (m).

^{1}H-NMR (DMSO-d_6, 400MHz, ppm): 9.0 (1H, s), 8.9 (2H, m), 8.5 (1H, d, J = 7.6Hz), 8.0 (2H, m), 7.6 (5H, m), 7.5 (3H, m), 7.3 (2H, d, J = 7.6Hz), 7.0 (1H, d, J = 6.8Hz)

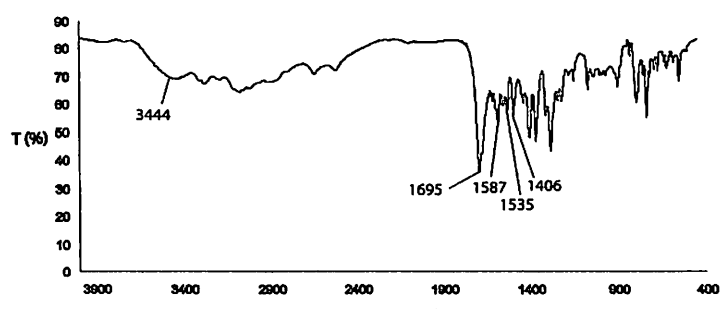

Figure 4.31: IR spectra of **4.8**

Co-crystal of compound 4.1 with terephthalic acid (4.9):

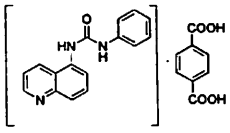

Isolated Yield: 67%

IR (KBr, cm^{-1}): 3444 (w), 3266 (s), 2925(w), 1698 (s), 1637 (s), 1599 (s), 1562 (s), 1496 (m), 1275 (s), 1253 (m), 807 (m), 729 (m)

^{1}H-NMR (DMSO-d_6, 400MHz, ppm): 9.0 (1H, s), 8.9 (2H, m), 8.5 (1H, d, J = 8.8Hz), 8.0 (5H, m), 7.7 (2H, m), 7.6 (1H, m), 7.5 (2H, d, J = 7.6Hz), 7.3 (2H, t, J = 7.2Hz), 7.0 (1H, t, J = 7.2Hz)

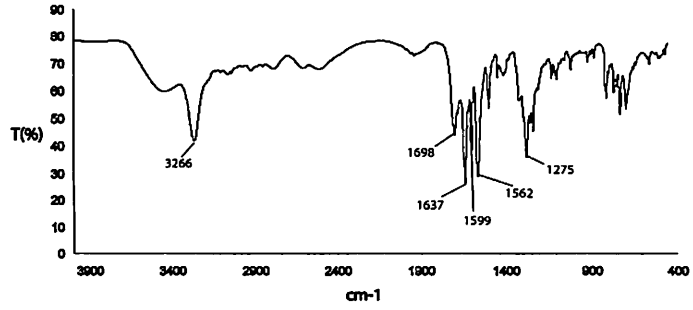

Figure 4.32: IR spectra of **4.9**

Co-crystal of compound 4.1 with adipic acid (4.10):

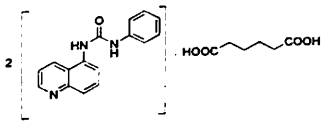

Isolated Yield: 74%

IR (KBr, cm^{-1}): 3436 (w), 3270 (s), 2945 (w), 1716 (s), 1639 (s), 1598 (s), 1561 (s), 1496 (m), 1258 (m), 1173 (m), 805 (m).

^{1}H-NMR (DMSO-d_6, 400MHz, ppm): 9.0 (1H, s), 8.9 (2H, m), 8.5 (1H, d, J = 8.4Hz), 8.0 (1H, d, J = 6.8Hz), 7.7 (2H, m), 7.6 (1H, m), 7.5 (2H, d, J = 8.0Hz), 7.3 (2H, t, J = 8.0Hz), 7.0 (1H, t, J = 7.2Hz), 2.2 (2H, m), 1.5 (2H, m).

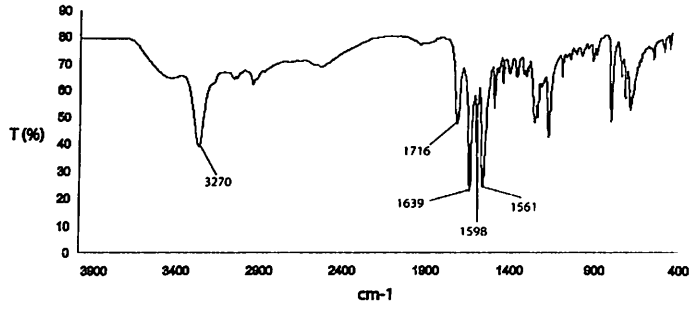

Figure 4.33: IR spectra of **4.10**

Salt of compound 4.1 with pyridine-2,3-dicarboxylic acid (4.11):

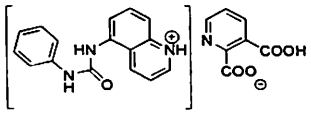

Isolated Yield: 71%

IR (KBr, cm^{-1}): 3430 (b), 3096 (w), 2926 (m), 1698 (s), 1638 (s), 1598 (s), 1573 (s), 1498 (m), 1444 (m), 1413 (m), 1382 (s), 1368 (m), 1314 (m), 1283 (m), 1255 (m), 1229 (m), 1092 (m), 993 (w), 852 (w), 810 (m), 798 (m), 758 (m), 694 (w), 655 (w)

^{1}H-NMR (DMSO-d_6, 400MHz, ppm): 9.0 (1H, s), 8.9 (2H, m), 8.7 (1H, d, J = 4.8Hz), 8.5 (1H, d, J = 7.6Hz), 8.2 (1H, d, J = 8.4Hz), 8.0 (1H, d, J = 7.2Hz), 7.7 (2H, m), 7.6 (2H, m), 7.5 (2H, d, J = 8.8Hz), 7.3 (2H, t, J = 7.6Hz), 7.0 (1H, t, J = 7.6Hz)

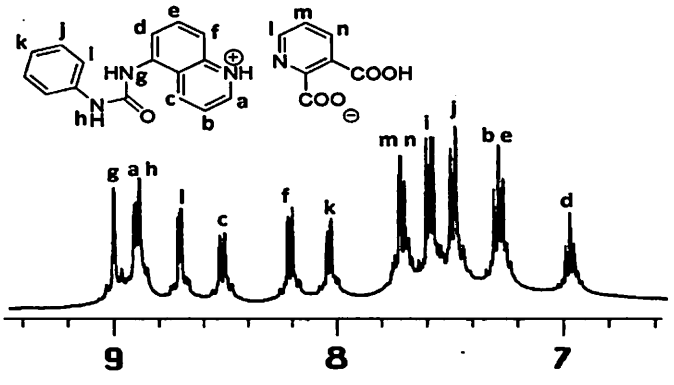

Figure 4.34: ^{1}H-NMR spectra of **4.11**(only the aromatic region is shown)

Typical procedure for preparation of the perchlorate salts of the compounds

The perchlorate salts of the compounds **4.1, 4.2, 4.3** were obtained by slow evaporation of the dilute acid solutions (0.3M) containing the host compounds.

Perchlorate salt of 4.1 (4.12):

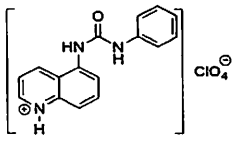

Isolated Yield: 67%

IR (KBr, cm^{-1}): 3446 (bs), 3071 (w), 2923 (w), 1637 (m), 1601 (m), 1548 (s), 1497 (m), 1443 (w), 1423 (m), 1365 (m), 1318 (m), 1285 (m), 1248 (m), 1120 (s), 1080 (s), 796 (m), 763 (m).

^{1}H-NMR (DMSO-d_6, 400MHz, ppm): 9.3 (2H, s), 9.1 (1H, d, J = 8.4Hz), 9.0 (1H, s), 8.3 (1H, d, J = 7.6Hz), 8.1 (2H, m), 7.9 (1H, d, J = 8.4Hz), 7.5 (2H, d, J = 8.0Hz), 7.3 (2H, t, J = 7.6Hz), 7.0 (1H, t, J = 7.2Hz).

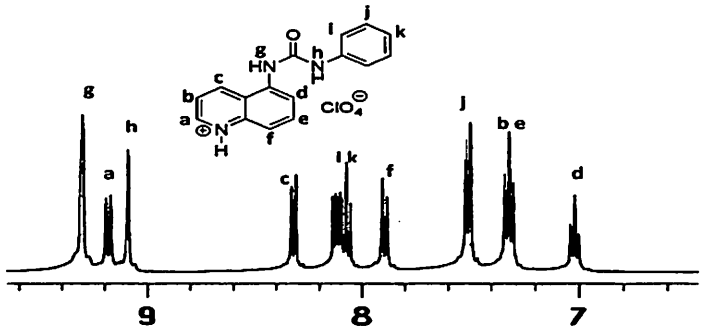

Figure 4.35: ^{1}H-NMR spectra of **4.12** (only the aromatic region is shown)

_p_-tolunesulphonate salt of 4.1 (4.13):

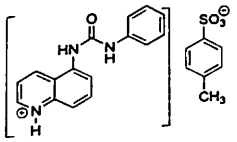

The compound **4.1** and *p*-tolunesulphonic acids (1:1) were dissolved in aqueous methanol. Slow evaporation of the solution results in yellow colored crystals of salt **4.13**.

Isolated Yield: 64%

IR (KBr, cm^{-1}): 3291 (w), 2922 (w), 1708 (s), 1637 (m), 1600 (m), 1539 (s), 1417 (m), 1366 (m), 1212 (s), 1165 (m), 1126 (m), 1033 (m), 1009 (m), 795 (m).

^{1}H-NMR (DMSO-d_6, 400MHz, ppm): 9.4 (1H, s), 9.2 (2H, m), 8.2 (1H, d, J = 7.6Hz), 8.0 (2H, m), 7.8 (1H, d, J = 8.0Hz), 7.5 (5H, m), 7.3 (2H, m), 7.1 (2H, d, J = 7.6Hz), 7.0 (1H, t, J = 7.2Hz), 2.2 (3H, s).

Perchlorate salt of 4.2 (4.14):

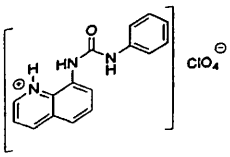

Isolated Yield 71%

IR (KBr, cm^{-1}): 3324 (b), 2921 (s), 2851 (m), 1693 (m), 1638 (s), 1597 (s), 1556 (s), 1499 (m), 1382 (m), 1296 (m), 1240 (m), 1217 (m), 1120 (s), 1086 (m), 760 (m), 695 (m).

^{1}H-NMR (DMSO-d_6, 400MHz, ppm): 9.8 (1H, s), 9.6 (1H, s), 8.9 (1H, d, J = 4.0Hz), 8.5 (1H, m), 8.4 (1H, d, J = 8.4Hz), 7.6 (2H, m), 7.5 (3H, m), 7.3 (2H, t, J = 7.6Hz), 7.0 (1H, t, J = 6.8Hz)

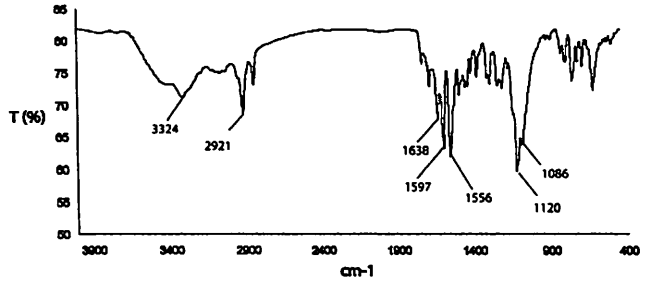

Figure 4.36: IR spectra of **4.14**

Perchlorate salt of 4.2 (4.15):

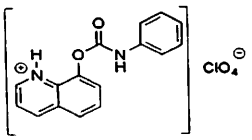

Isolated Yield 63%

IR (KBr, cm^{-1}): 3337 (m), 3169 (w), 1762 (s), 1643 (w), 1601 (s), 1548 (s), 1500 (w), 1444 (m), 1418 (m), 1301 (s), 1202 (m), 1112 (s), 1089 (m), 971 (m), 840 (m), 751 (s)

^{1}H-NMR (DMSO-d_6, 400MHz, ppm): 10.5 (1H, s), 9.0 (1H, d, J = 4.4Hz), 8.8 (1H, d, J = 8.4Hz), 8.0 (1H, d, J = 8.4Hz), 7.8 (3H, m), 7.5 (2H, d, J = 8.4Hz), 7.3 (2H, t, J = 7.2Hz), 7.0 (1H, t, J = 7.2Hz)

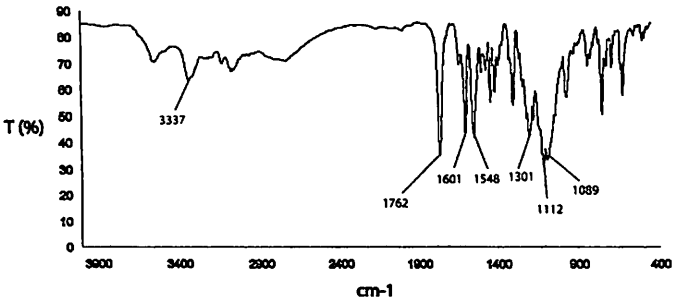

Figure 4.37: IR spectra of **4.15**

References

1. A. M. Todd, K. M. Anderson, P. Byrne, A. E. Goeta and J. W. Steed, *Cryst. Growth Des.*, 2006, **6**, 1750
2. P. Byrne, D. R. Turner, G.O. Lloyd, N. Clarke and J. W. Steed, *Cryst. Growth Des.*, 2008, **8**, 3335.

3. J. M. Russell, A, D. M. Parker, I, R.-Evans, J. A. K. Howard and J. W. Steed, *CrystEngComm*, 2006, **8**, 119.
4. V Amendola, L Fabbrizzi and Lorenzo Mosca, *Chem. Soc. Rev.*, 2010, **39**, 3889.
5. C. Raposo, C. Crego, A. Partcarroyo, M. L. Mussons, M. C. Caballero and J. R. Moran, *Tetrahedron Lett.*, 1993, **34**, 1995.
6. R. J. Fitzmaurice, G. M. Kyne, D. Douheret and J. D. Kilburn, *J. Chem. Soc. Perkin Trans.*, 2002, **1**, 841.
7. T. Shimizu, T. Usui, K. Machida, K. Furuya, H. Osadab and T. Nakata, *Bioorg. Med. Chem. Lett.*, 2002, **12**, 3363.
8. R. G. Almquist, W.R. Chao and C. J. White, *J. Med. Chem.*, 1985, **28**, 1067.
9. M. J. A. Bowker, P.H. Stahl and C.G. Wermuth, *Procedure for salt selection and optimisation, in handbook of Pharmaceutical salts Eds.*, Wiley-VCH, New-York 2002.
10. P.H. Schlesinger, R. Ferdani, J. Liu, J. Pajewska, R. Pajewki, M. Saito, H. Shabany and G.W. Gokel, *J. Am. Chem. Soc.*, 2002, **124**, 1848.
11. M. Almaraz, M. Martín, J. Hernández, M. C. Caballero and J. R.Morán, *Tetrahedron Lett.*, 1998, **39**, 1811.
12. M. S. Goodman, A. D. Hamilton and J. Weiss, *J. Am. Chem. Soc.*, 1995, **117**, 8447.
13. I. L. Karle, D. Ranganathan and V. Haridas, *J. Am. Chem. Soc.*, 1997, **119**, 2777.
14. J.H.G. Steinke, I.R. Dunkin, D.C. Sherrington, *Trends in analytical chemistry*, **18**, Elsevier, Amsterdam 1999.
15. I. P. Halter, T. J. Smith, and J.Weiss, *Tetrahedron Lett.*, 1996, **37**,1201.
16. C. Vicent, S. C. Hirst, F. Garcia-Tellado and A. D. Hamilton, *J. Am. Chem. Soc.*, 1991, **113**, 5466.
17. M. Almaraz, C. Rapuso, M. Martin, C. Caballero and J. R. Moran, *J. Am. Chem. Soc.*, 1998, **120**, 3516.
18. J. V. Hernandez, M. Almaraz, C. Raposo, M. Martin, A. Lithgow, M. Crego, C. Caballero and J. R. Moran, *Tetrahedron Lett.*, 1998, **39**, 7401.
19. R. Prohens, M. C. Rotger, M. N. Pina, P. M. Deya, J. Morey, P. Ballester and A. Costa, *Tetrahedron Lett.*, 2001, **42**, 4933.

20. M.W. Hosseini and J.M. Lehn, *J. Am. Chem. Soc.*, 1982, **104**, 3525.

21. J. Rebek, Jr., D. Memeth and P. Ballester, F.T. Lin, *J. Am. Chem. Soc.*, 1987, **109**, 3474.

22. J. Trogers, *J. Prakt. Chem.*, 1887, **36**, 225.

23. S.B. Larson and C.S. Wilcox, *Acta Cryst. C42*, 1986, 224.

24. C.S. Wilcox, J.C. Adrian, T.H. Webb and F.J. Zawacki, *J. Am. Chem. Soc.*, 1992, **114**, 10189.

25. S. Goswami, K. Ghosh and S. Dasgupta, *J. Org. Chem.*, 2000, **65**, 1907.

26. S. Goswami and K. Ghosh, *Tetrahedron Lett.*, 1997, **38**, 4503.

27. Y-S. Zheng and C. Zhang, *Org. Lett.*, 2004, **6**, 1189.

28. S. Mohamed, D. A. Tocher, M. Vickers, P. G. Karamertzanis and S. L. Price, *Cryst. Growth Des.*, 2009, **9**, 2881.

29. W. M. Singh, N. Barooah and J. B. Baruah, *J. Mol. Struct.*, 2008, **875**, 329.

30. D.A. Haynes, W. Jones and W.D.S. Motherwell, *CrystEngComm*, 2006, **8**, 830.

31. M.K. Stanton and A. Bak, *Cryst. Growth Des.*, 2008, **8**, 3856.

32. B.R. Bhogala, S. Basavoju and A. Nangia, *CrystEngComm*, 2005, **7**, 551.

33. S. L. Childs, G. P. Stahly and A. Park, *Molecular Pharmaceutics*, 2007, **4**, 323.

34. B. Sarma, N. K. Nath, B. R. Bhogala and A. Nangia, *Cryst. Growth Des.*, 2009, **9**, 1546.

35. K. Kishikawa, C. Iwashima, S. Kohmoto, K. Yamaguchi, M. Yamamoto, *J.Chem. Soc. Perkin. Trans. I*, 2000, 2217.

36. J.M. Lavin and K.D. Shimizu, *Org. Letters.*, 2006, **8**, 2389.

37. T., Steiner, *Angew. Chem. Int. Ed. Eng.*, 2002, **47**, 48.

38. N. Shan, E. Batchelor and W. Jones, *Tett. Letters*, 2002, **43**, 8721.

39. P. Vishweshwar, A. Nangia and V.M. Lynch, *Cryst. Growth Des.*, 2003, **3**, 783.

Chapter 5

Synthesis, characterization and anion recognition properties of diquinoline derivatives

As the name implies diquinolines are derived from quinoline molecules, formed by joining two rings. Diquinoline molecules exhibit many interesting supramolecular features depending on the nature of the substituent. Despite the close similarity of the host molecular structures, their supramolecular host-guest chemistry varies considerably.[1-7] The rotation around the single bond of the diquinoline derivative leaves a probability to adopt helical conformation. Further, many biological macromolecules containing nitrogenous bases adopt helical structures.[8-9] The structure of deoxyribose nucleic acid proposed by Watson and Crick in 1953 is one of the important discoveries of helical structure.[10] Inspired by commonly available helical conformations in biological macromolecules, there is a challenge to synthesize artificial systems having helical chain like structures.[11-13] Helical structures are generally guided by hydrogen bonds,[14-15] van der Waals interactions,[16-17] and dative bond to metal ions.[18-20] The quinoline moiety is known to adopt different orientations in the crystal lattice that contribute to the helical structure of many organic,[21-22] and inorganic[23-24] molecules. Further to this, molecules with the diquinoline moiety are used in the field of molecular recognition[25] and as optical materials.[26-27] Despite of interesting properties and wide synthetic protocols of 2,2'-diquinoline derivatives, there is limited synthetic methodology and study on 5,5'-diquinoline derivatives.[28] Thus, a diquinoline derivative is chosen such that it has hydroxy functional groups with flexible ethylene tethers which would help in self assembling to form extended structure. It would also get easily protonated or hydrogen bonded to an acid and expected to hold the anions. Hence we felt that the helical molecules will have ready empty spaces in the folds of the extended helix to accommodate anions. With this background we synthesized a new 5,5'-diquinoline derivative with alcohol pendent

group, namely *bis*-5,5'-[2-(quinolin-8-ylamino)ethanol] (**5.2**) and studied its anion binding properties.

This chapter includes the synthetic methodology and anion recognition property of the 5,5'-diquinoline host *bis*-5,5'-[2-(quinolin-8-ylamino)ethanol.

5.1 Synthesis and characterization of diquinoline receptor 5.2

The diquinoline derivative *bis*-5,5'-[2-(quinolin-8-ylamino)ethanol] **5.2** was synthesized in multiple steps. In the first step methyl 2-(quinolin-8-ylamino)acetate which is an ester derivative of 8-aminoquinoline was prepared by reacting with methyl bromo acetate. The ester group of methyl 2-(quinolin-8-ylamino)acetate on reduction gave an alcohol namely, 2-(quinolin-8-ylamino)ethanol **5.1**. The 2-(quinolin-8-ylamino)ethanol (**5.1**) thus obtained, was treated with catalytic amount of manganese (II) acetate to give dimerised derivative **5.2** (scheme 5.1). It may be noted that 8-aminoquinoline does not form C-C bond by manganese (II) acetate and the reaction is very specific for coupling of **5.1**. All these compounds formed in different steps are characterised by spectroscopic techniques such as IR, NMR, mass spectra. The compound **5.2** has desired proton signals for aromatic protons besides signals correspond to the two methylene groups flanked by oxygen and nitrogen at 3.7 ppm and 3.2 ppm respectively.

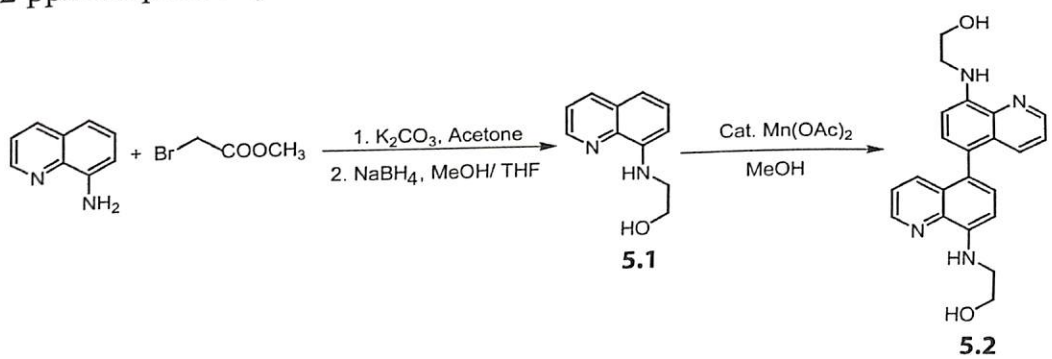

Scheme 5.1: Synthesis of receptor **5.2**

The comparison of the ^{1}HNMR spectra of **5.1** and **5.2** in the aromatic region (figure 5.1) clearly depicts the formation of the diquinoline derivative. The ^{1}HNMR spectra of **5.1** shows signals for six aromatic protons, whereas the ^{1}HNMR spectra of **5.2** shows signals for five protons indicating the formation of the dimmerized product.

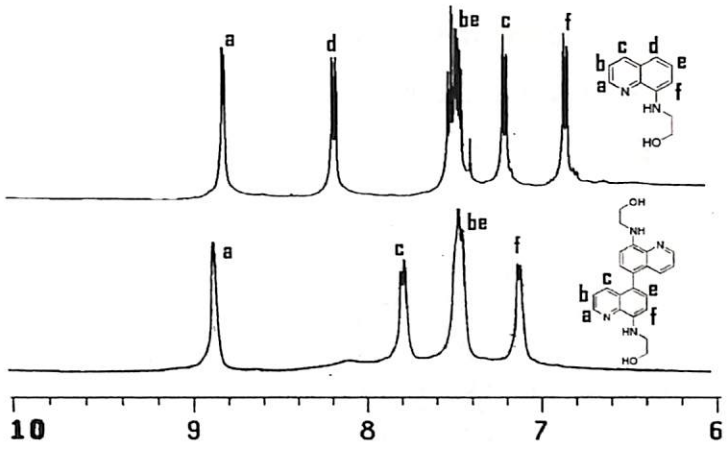

Figure 5.1: Comparison of the ^{1}H-NMR spectra of the aromatic protons of **5.1** and **5.2**

Further the diquinoline compound **5.2** is also confirmed by determining the crystal structure as shown in figure 5.2.

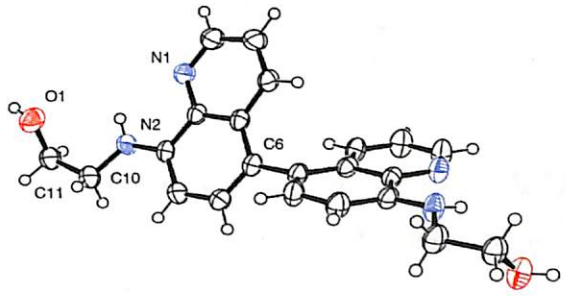

Figure 5.2: Crystal structure of **5.2** (ORTEP diagram drawn with 50% elipsoid probability)

5.2 Structural study of the receptors 5.2 and its inclusion compounds

The diquinoline receptor **5.2** is crystallized and its crystal structure is studied. The compound **5.2** crystallizes in a monoclinic C2/c space group, with only one half of the molecule appearing in the crystallographic asymmetric unit (figure 5.3a). The molecule has a twisted conformation with a dihedral angle of 60.08^{0} between the planes of two quinoline rings. Generally binol derivatives have dihedral angles[29] between the naphthalene rings in the range of $78\text{-}79^{0}$. The presence of hydroxyl group and the basic nitrogen atoms in quinoline ring allows the molecule to have self assembled structure through different weak interactions. The crystal structure of **5.2** when viewed along 'a'-crystallographic axis we have observed that the molecule adopts a single helical structure (figure 5.3b). The short range interactions that stabilize the helical arrangement of **5.2** include two intermolecular hydrogen bonds of

the hydroxy group with the quinoline N atom and the amine N atom (figure 5.4). A space-fill model of **5.2** shows that the helical orientation of the molecule is a closed packed without any kind cavity in the crystal lattice (figure 5.3c).

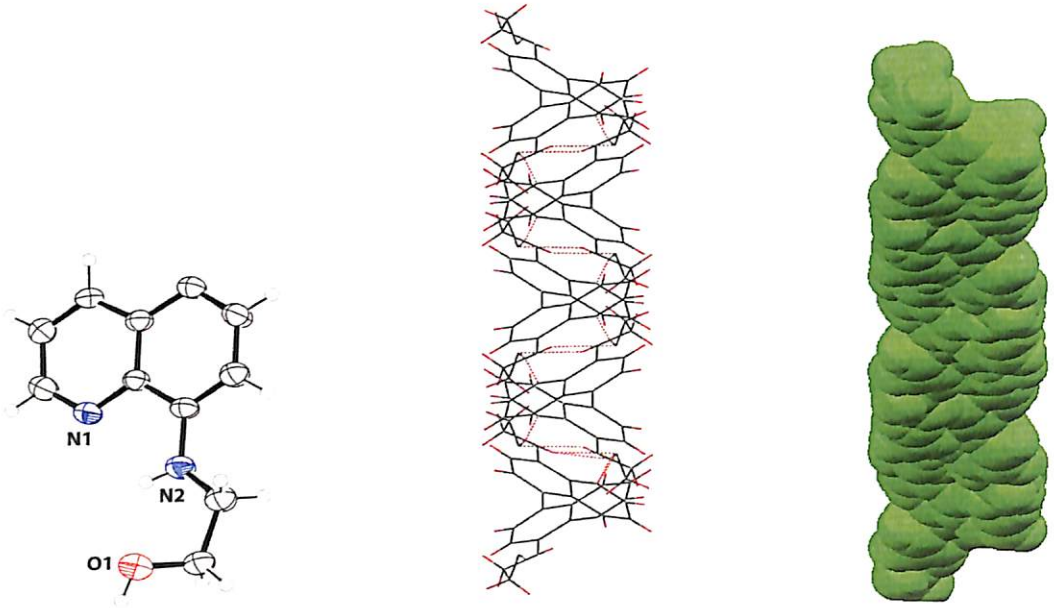

(a) (b) (c)

Figurre 5.3: (a) ORTEP diagram of the asymmetric unit of **5.2** (50% elipsoid probability); (b) view of molecule **5.2** along 'a'-crystallographic axis; (c) space-fill model of **5.2**

The crystal structure of compound **5.2** also reveals that two such single helix are held together by a T-type C-H···π interaction as shown in figure 5.4. The distance between C3-H3 and the centroid of the neighbouring ring (C1-C5-C6-C7-C8-C9) is found to be 2.713 Å. These helical structures self assembles to make a two dimensional sheet. The hydrogen bond parameters of **5.2** are tabulated in table 5.1.

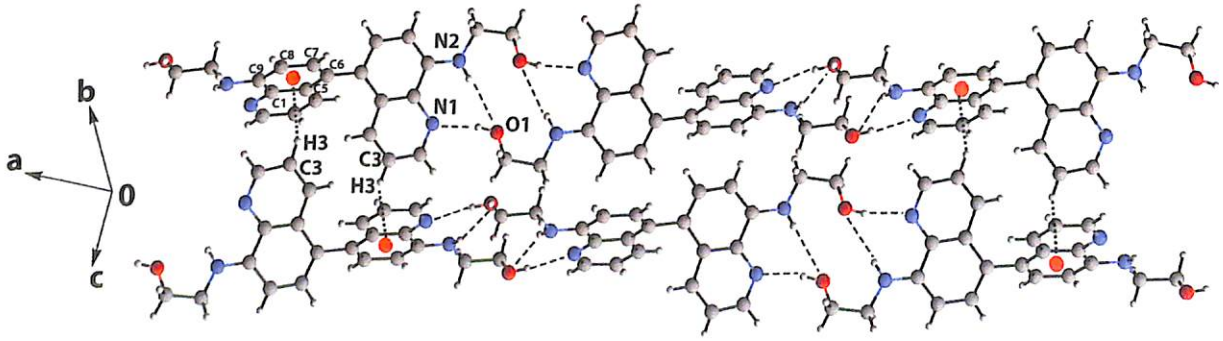

Figure 5.4: Short range interactions of molecule **5.2**

Table 5.1: Hydrogen bond parameters of **5.1**

D-H····A	d_{D-H}(Å)	$d_{H\cdots A}$(Å)	$d_{D\cdots A}$(Å)	< D-H····A(^{0})
O(1) - H(1) ···· N(1) [1/2-x, 1/2-y, 1-z]	0.82	2.07	2.875(3)	167.0
N(2) - H(2N) ···· O(1)	0.82(2)	2.46(2)	2.769(3)	103.8(17)

The IR-spectra (figure 5.5) of the molecule **5.2** shows a strong peak at 3394 cm^{-1} for the OH-stretching frequency and another peak at 1603 cm^{-1} and 1578 cm^{-1} characterestic of C=C and C=N. In case of the perchlorate salt (**5.3**) we have observed three strong peaks at 1144 cm^{-1}, 1111 cm^{-1} and 1088 cm^{-1} that are characterestic of the perchlorate anion in addition to the peaks of the parent molecule **5.2**. Generally an ionic perchlorate gives a braod single perchlorate absorption peak around 1100 cm^{-1}. The splitting of the perchlorate peak may be attributed to its possible distortion in an supramolecular environment. In the case of the co-crystal with nitric acid (**5.4**) a strong peak at 1384 cm^{-1} characterestic of the nitrate group of nitric acid molecule is observed.

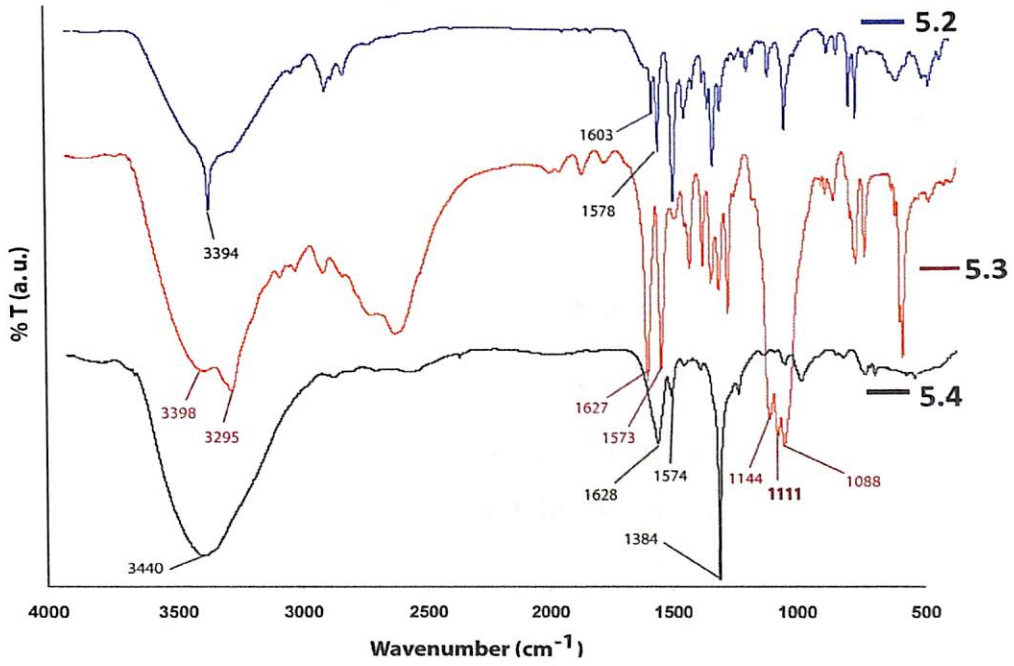

Figure 5.5: IR-spectra of **5.2**, **5.3**, and **5.4**

However, the crystallographic structure shows that on treatment with perchloric acid, molecule **5.2** forms a salt (**5.3**) where the two quinoline N atoms are protonated, whereas in the case of nitric acid a co-crystal (**5.4**) is formed. The salt **5.3** crystallizes in an orthorhombic space group Fddd. Its asymmetric unit contains one half of the

protonated molecule **5.2** and a perchlorate anion (figure 5.6a). The helical structure of the molecule **5.2** is retained after the inclusion of the perchlorate anion in the fold of the helix (figure 5.6b). The perchlorate anion does not disturb the assembly of intermolecular hydrogen bonding of the molecule **5.2**; instead the anion is encapsulated inside the cavity formed by the helical arrangement of salt **5.3** as shown in figure 5.6c. In this case also the molecule adopts a twisted geometry with a dihedral angle of 67.04^0 between the planes of two quinoline rings. One of the oxygen atoms of the perchlorate anion is found to be disordered and a disorder model is fixed by sharing the occupancy between two atoms as shown in figure 5.6a.

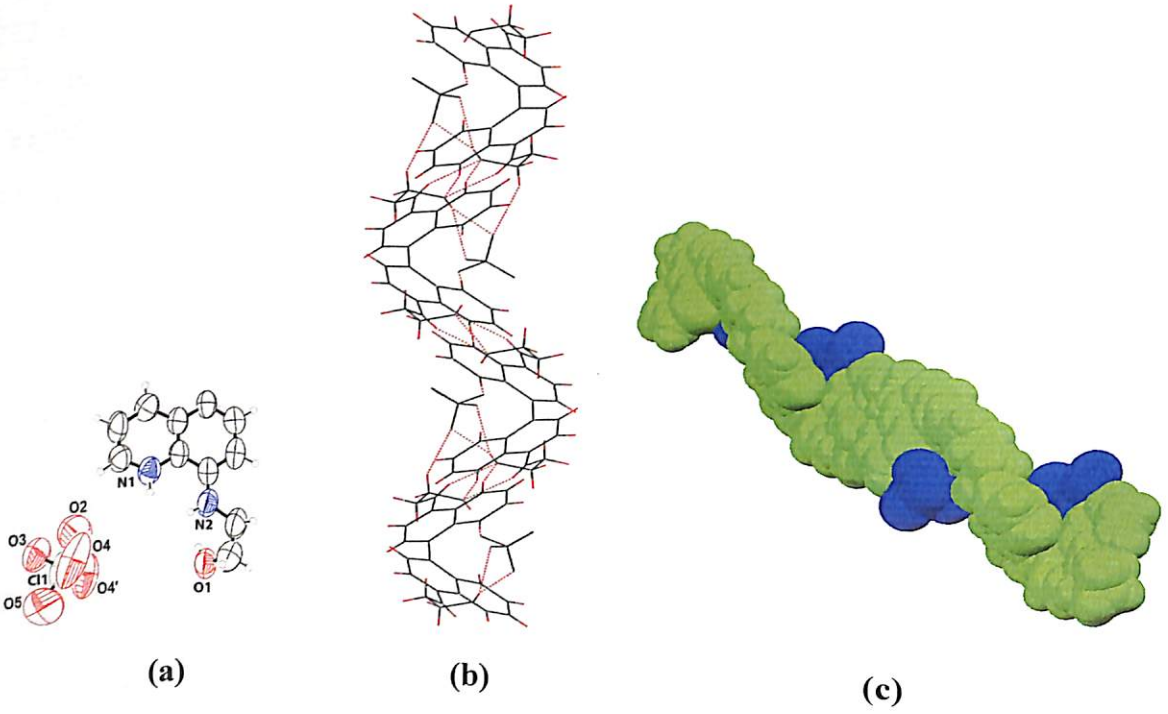

(a) **(b)** **(c)**

Figure 5.6: (a) ORTEP diagram of the asymmetric unit of salt **5.3** (50% elipsoid probability); (b) helical structure of salt **5.3**; (c) space-fill model of **5.3** showing the encapsulation of the perchlorate anion

In case of the salt **5.3** the hydroxy group of the molecule acts as a hydrogen atom acceptor in a strong intermolecular hydrogen bond with the protonated quinoline N atom (N1-HN···O1). The perchlorate anion is held together by a number of C-H···O interactions (C4-H4···O2 and C11-H11B···O4) and hydrogen bonding interaction (O1-H1···O5 and O1-H1···O3) as shown in figure 5.7. The hydrogen bond parameters are tabulated in table 5.2.

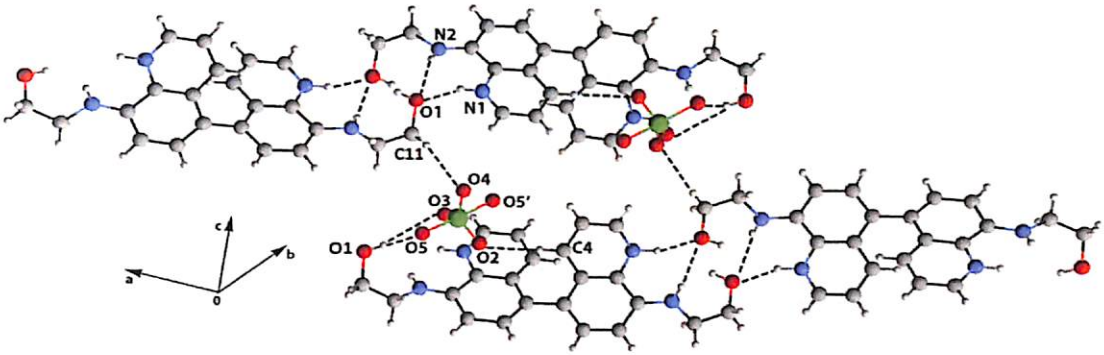

Figure 5.7: The short range interactions in **5.3**

Table 5.2: Hydrogen bond parameters of **5.3**

D-H····A	d_{D-H}(Å)	$d_{H\cdots A}$(Å)	$d_{D\cdots A}$(Å)	< D-H····A(^{0})
O(1) - H(1) ···· O(5)	0.82	1.78	2.584(18)	166.0
O(2) - H(2A) ···· N(1)	0.82	1.99	2.808(12)	173.0
N(2) - H(2N) ···· O(2)	0.86	2.17	3.030(13)	178.0
N(2) - H(2N) ···· N(1)	0.86	2.41	2.740(12)	103.0
C(2) - H(2) ···· O(4)	0.93	2.49	3.140(2)	127.0
C(4) - H(4) ···· O(3) [1/2-x, 1/2+y, 1/2-z]	0.93	2.56	3.446(13)	160.0

The co-crystal **5.4** crystallizes in the orthorhombic space group $C222_1$ with one half of the molecule **5.2**, a nitric acid molecule and a water molecule in the crystallographic asymmetric unit (figure 5.8a). The co-crystal **5.4** also adopts a helical shape although we did not observe the same type of intermolecular hydrogen bonding as we observed in the case of molecule **5.2** (figure 5.8b). The nitric acid and the water molecule are held in between the parent molecules as shown in the space fill model in the figure 5.8c.

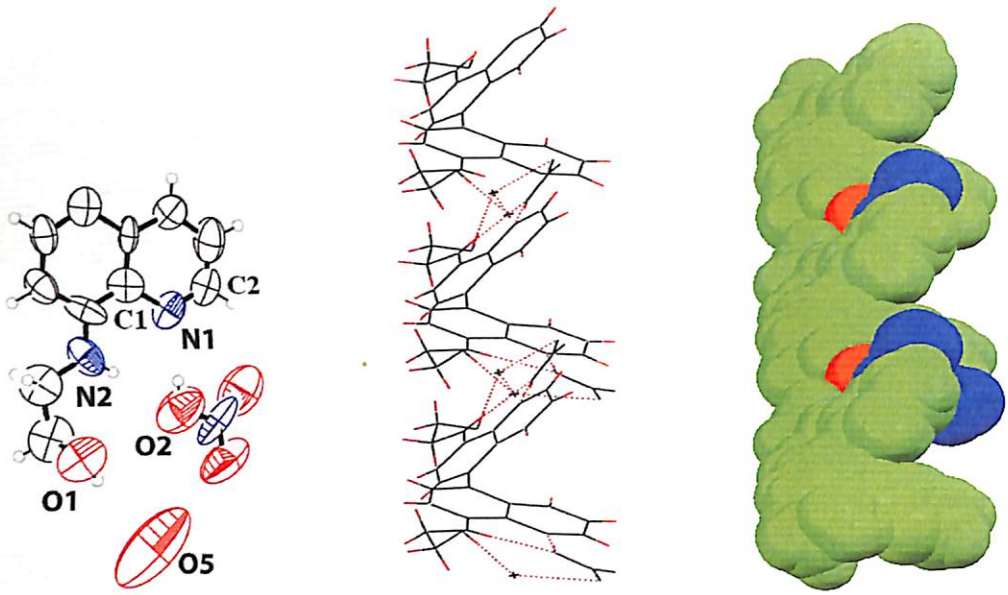

(a) (b) (c)

Figure 5.8: (a) ORTEP diagram of the asymmetric unit of **5.4** (50% elipsoid probability); (b) helical structure of **5.4**; (c) spacefill model showing the encapsulation of nitric acid and water molecule

Two nitric acid and two water molecules are encapsulated in between the parent molecules through intermolecular hydrogen bonds (O2-H2A···N2, N2-H2N···O2) and C-H···O interactions (C2-H2···O4) as shown in figure 5.9. The helical chains are further held together by weak C-H···N interactions (C8-H8···N3). The hydrogen bond parameters of the co-crystal **5.4** are shown in table 5.3.

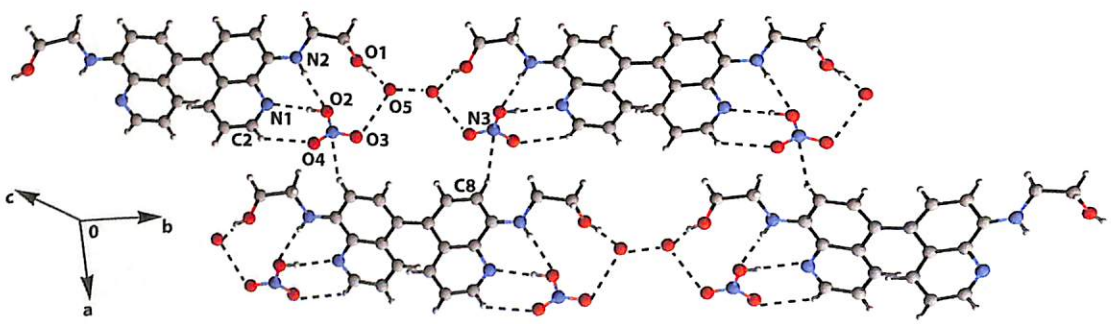

Figure 5.9: Short range interaction of co-crystal **5.4**

Table 5.3: Hydrogen bond parameters of **5.4**

D-H····A	$d_{D\text{-}H}$(Å)	$d_{H\cdots A}$(Å)	$d_{D\cdots A}$(Å)	< D-H····A(^{0})
O(1) - H(1) ···· N(2)	0.82	2.58	2.906(10)	105.0
O(1) - H(1) ···· O(5) [x, 1/4-y, 1/4-z]	0.82	2.57	3.225(18)	138.0
N(1) - H(1N) ···· N(2)	0.93(3)	2.45(7)	2.771(11)	101.0(5)
N(1) - H(1N) ···· O(1) [-x, 1/2-y, 1/2-z]	0.93(3)	1.85(3)	2.750(10)	164.0(7)
N(2) - H(2N) ···· N(1)	0.86	2.46	2.771(11)	102.0
N(2) - H(2N) ···· O(1) [-x, 1/2-y, 1/2-z]	0.86	2.26	3.084(9)	160.0
C(2) - H(2) ···· O(4) [x, 1/4-y, 1/4-z]	0.93	2.43	3.157(14)	135.0
C(4) - H(4) ···· O(2) [1/4-x, y, 1/4-z]	0.93	2.55	3.424(11)	157.0
C(11) - H(11B) ···· O(4) [-x, 1/2-y, 1/2-z]	0.97	2.43	3.309(19)	151.0

The formation of co-crystal with nitric acid by **5.2** can be justified from the crystallographic evidences. The bond angle <C1-N1-C2 (figure 5.8a) of the quinoline ring of **5.4** is found to be 119.21^0; however this bond angle is 124.43^0 in the case of the salt **5.4** where the quinoline N atom is protonated which is in accordance with the bond angles of protonated and unprotonated reported quinoline derivatives.[30-31] This suggests that the quinoline N atom is not protonated in the case of **5.4**. Further, while refining the X-ray crystal structure the hydrogen atom was located in the difference Fourier maps and the residual electron density was observed near the O atom and assigned to a proton accordingly, suggests it to be a nitric acid instead of nitrate anion. The N-O bond distances of the nitrate molecule are also not same ($d_{N\cdots O}$ (Å), N3···O2, 1.26; N3···O3, 1.15; N3···O4, 1.16), which suggests it to be nitric acid; however, these bond distances do not match exactly the structure of free nitric acid derived from microwave spectra where the bond distances are reported as 1.40 Å, 1.19 Å, 1.21 Å.

The comparison of the structures of **5.2**, **5.3** and **5.4** shows that the intermolecular hydrogen bonding between two molecules of **5.2** is maintained in the perchlorate salt **5.3**. However, this intermolecular hydrogen bond is not maintained in the co-crystal of nitric acid (**5.4**). In case of the perchlorate salt **5.3** the perchlorate anion is not involved in hydrogen bonding with the quinoline N, whereas in the case of the co-crystal **5.4** the nitric acid molecule is involved in hydrogen bond with the quinoline N thereby breaking the intermolecular hydrogen bonds of the two receptor molecules. A comparison of the structures of **5.2**, **5.3** and **5.4** is shown in figure 5.10.

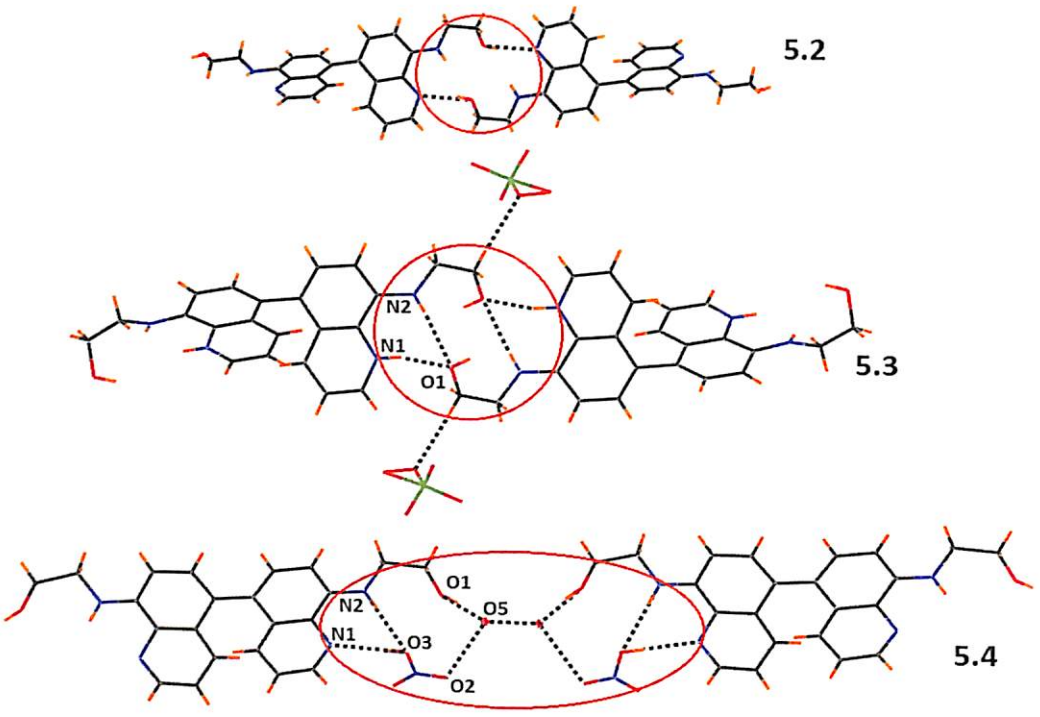

Figure 5.10: Comparison of the structures of **5.2**, **5.3** and **5.4**

5.3 Solution study of the diquinoline receptor 5.2

The solid state structural study shows that the receptor **5.2** can distinguish between nitric acid and perchloric acid. This observation encouraged us to study the effect of these two acids on receptor **5.2** in solution state. Hence, the effect of nitric acid and perchloric acid on the UV-visible spectra of receptor **5.2** is studied.

The UV spectra of compound **5.2** shows two absorption maxima at 253 nm ($\varepsilon = 1.79 \times 10^4$ $M^{-1}cm^{-1}$) and 368 nm ($\varepsilon = 4.51 \times 10^3$ $M^{-1}cm^{-1}$). On gradual addition of perchloric acid (10^{-2} M in methanol) to a solution of **5.2** (6.7×10^{-5} M in methanol); both the absorption maxima decreases which results in the formation three isosbestic point at 268 nm, 324 nm, and 417 nm (figure 5.11). The formation of the isosbestic points clearly suggests the existence of two chemical species at equilibrium in the solution state. A mild increase in the absorbance at 469 nm is also observed on gradual increase in the anion concentration (figure 5.11, Inset).

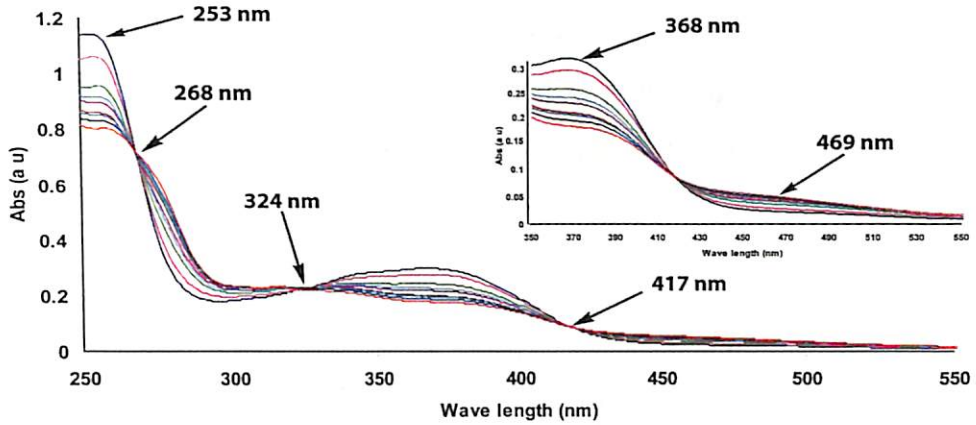

Figure 5.11: Changes in absorption spectra of **5.2** (6.7×10^{-5} M in methanol) on addition of perchloric acid (10^{-2} M in methanol). Inset: Expansion in the vissible region showing the small increase in absorption at 469 nm

Similarly, in the case of titration of **5.2** with nitric acid we have observed that the absorption spectra of **5.2** on gradual addition of nitric acid passes through three isosbestic point at 268 nm, 325 nm, and 423 nm as shown in figure 5.12. Thus it is seen that in both cases the changes observed in solution are similar, or in other word there is no recognition of the two acids used.

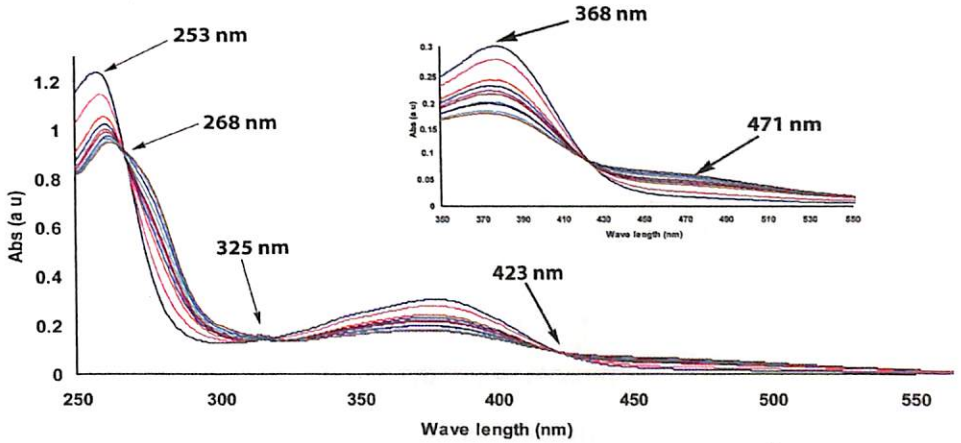

Figure 5.12: Changes in absorption spectra of **5.2** (6.7×10^{-5} M in methanol) on addition of nitric acid (10^{-2} M in methanol); Inset: Expansion in the vissible region showing the small increase in absorption at 471 nm

From the above observations it is clear that the salt or co-crystal formation from two strong acids could not be distinguished in solution; whereas in the solid state structure of **5.3** and **5.4** differs. The formation of co-crystal and salt are related to pKa[32-35] but from the present study we observe that two strong acids result in either of them. Thus,

it is the packing preference in solid state that favours the state as protonated or molecule of crystallization, but finally they are in the lattice due to electrostatic interactions further supported by other directional weak interactions.

5.4 Conclusion

In conclusion a new organic helical 5,5'-diquinoline derivative is synthesized to establish its self assembling properties in solid state. The helical molecule can encapsulate guest of two different shapes without losing its original helicity. Interaction of this helical molecules with perchloric acid and nitric acid are found to be similar in solution, however, in solid state perchloric acid forms its salt while nitric acid forms co-crystal with it. A rare example where a strong acid does not dissociate in solid state in the presence of a base is established. The structural backbones depicted here are based on quinoline units that are generally component of drugs; therefore it leaves an ample scope to make predictive models from analogous study on drug delivery as well as drug-substrate activity.

5.5 Experimental Section

Compound 5.2:

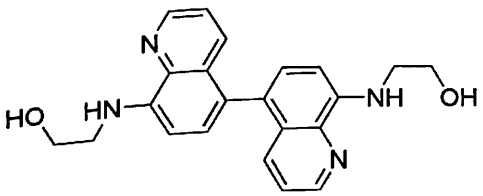

8-aminoquinoline (0.725 g, 5 mmol) was dissolved in dry acetone (20 ml) and potassium carbonate (1.0 g, 7.5 mmol) was added to it. The solution was stirred at room temperature for 15 min and then methyl bromoacetate (0.76 g, 5 mmol) was added and the reaction mixture was then refluxed at 70 ^{0}C for 12 hs (progress of the reaction was monitored at regular intervals using TLC). After completion of the reaction, the reaction mixture was then filtered and the solvent was then removed under reduced pressure to obtain the ester as a yellow colour solid. In the next step, the ester was reduced to the corresponding alcohol (**5.1**) using a reported procedure. Yield: 67%.

IR (KBr, cm^{-1}): 3404 (bs), 2948 (w), 1614 (m), 1582 (s), 1524 (m), 1436 (m), 1384 (m), 1358 (s), 807 (m).

^1H NMR ($CDCl_3$, 400 MHz): 8.7 (1H, d, J = 4.0Hz), 8.0 (1H, d, J = 8.4 Hz), 7.3 (2H, m,), 7.0 (1H, d, J = 8.0Hz), 6.7 (1H, d, J = 8.0Hz), 3.9 (2H, t, J = 5.2Hz), 3.5 (2H, t, J = 6.0Hz).

LC-MS [M+1]: 189.01.

The crude alcohol **5.1** (0.564 g, 3 mmol) was then dissolved in 20 ml methanol and a catalytic amount of $Mn(OAc)_2.4H_2O$ (0.036 g, 0.03 mmol) was added. The reaction mixture was stirred for about 8 hrs at room temperature to obtain compound **5.2** as yellow solid. The product was further purified by recrystallization from a methanolic solution.

Yield: 61%.

IR (KBr, cm^{-1}): 3394 (s), 2929 (w), 2854 (w), 1603 (m), 1578 (s), 1518 (s), 1472 (m), 1440 (m), 1379 (m), 1358 (s), 1071 (m), 817 (m).

^1H-NMR (DMSO-d^6, 400 MHz): 8.9 (1H, s), 7.8 (1H, d, J = 7.6Hz), 7.5 (2H, d, J = 7.6Hz), 7.1 (1H, d, J = 7.6Hz), 4.9 (s, 1H), 3.7 (m, 2H), 3.2 (m, 2H).

^{13}C-NMR (DMSO-d^6, 100 MHz): 59.7, 70.4, 109.6, 119.6, 121.9, 126.9, 129.1, 135.9, 139.7, 148.8, 154.5.

LC-MS [M+1]: 375.34.

UV: (λmax 253 nm), $\varepsilon = 1.79 \times 10^4\ M^{-1}cm^{-1}$.

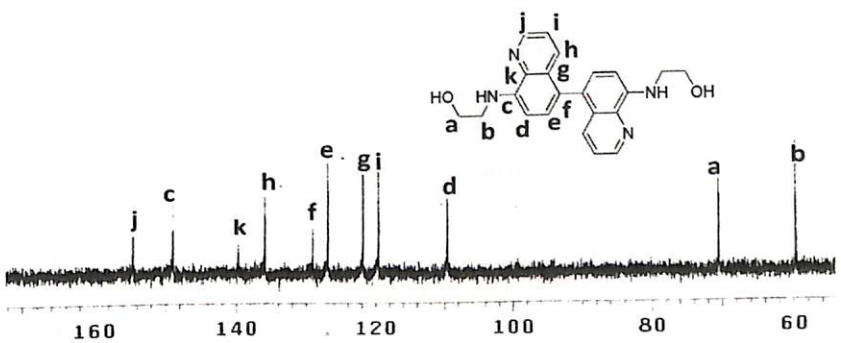

Figure 5.13: ^{13}C-NMR spectra of **5.2**

Compound 5.3:

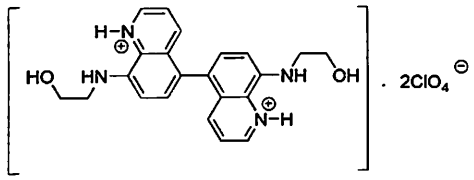

Compound **5.2** was dissolved in a dilute solution of perchloric acid and allowed to stand for three days to obtain the crystals of **5.3**.

Yield: 72%.

IR (KBr, cm^{-1}): 3398 (bs), 2932 (w), 2854 (w), 1627 (s), 1573 (s), 1459 (m), 1407 (m), 1307 (m), 1144 (s), 1111 (s), 1088 (s), 806 (m), 772 (m).

^{1}H-NMR (DMSO-d^6, 400 MHz): 8.8 (1H, s), 7.8 (1H, d, J = 7.6Hz), 7.5 (2H, d, J = 7.6Hz), 7.1 (1H, d, J = 7.6Hz), 5.1 (s, 1H), 3.7 (m, 2H), 3.2 (m, 2H).

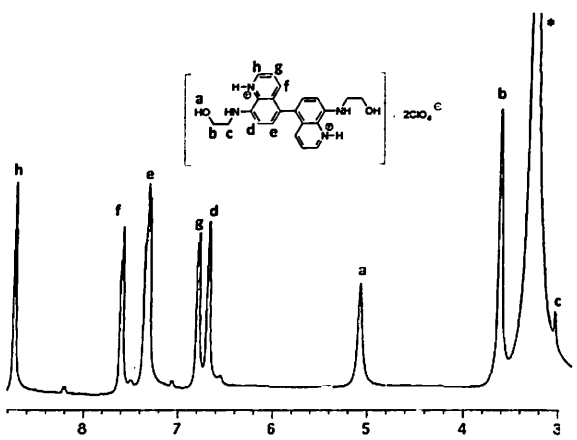

Figure 5.14: ^{1}H-NMR spectra of **5.3** (* indicates the peak for the water associated with solvent, the peak for the –NH proton is merged in the water peak)

Compound 5.4:

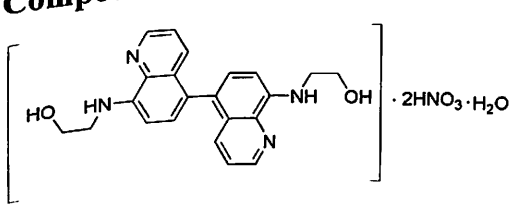

Compound **5.2** was dissolved in a dilute solution of nitric acid and allowed to stand for three days to obtain the crystals of **5.4.**

Yield: 68%.

IR (KBr, cm^{-1}): 3440 (bs), 16287 (s), 1574 (w), 1523 (w), 1458 (w), 1384 (s), 1123 (w), 1059 (m), 815 (m).

^{1}H-NMR (DMSO-d^6, 400 MHz): 8.9 (1H, s), 7.8 (1H, d, J = 7.6Hz), 7.5 (2H, d, J = 7.6Hz), 7.1 (1H, d, J = 7.6Hz), 3.8 (m, 2H), 3.4 (m, 2H).

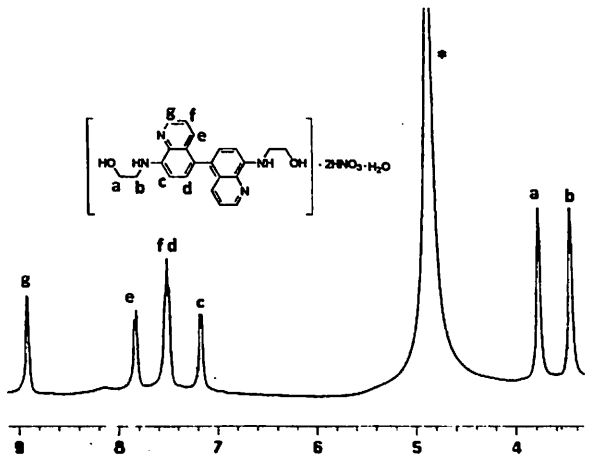

Figure 5.15: ^{1}H-NMR spectra of **5.4** (* indicates the peak for the water associated with solvent, the peak for the –NH and -OH proton is merged in the water peak)

Caution: Perchlorate salts are potentially explosive; however, our systems described here are stable and have not shown such property under ambient condition, it is advisable that care needs to be taken while dealing with perchlorate salts.

References

1. S. F. Alshahateet, A. N. M. M. Rahman, R. Bishop, D. C. Craig and M. L. Scudder, *CrystEngComm.*, 2002, **4** , 585.
2. A. N. M. M. Rahman, R. Bishop, D. C. Craig and M. L Scudder, *J. Supramol. Chem.*, 2002, **2**, 409.
3. S. F. Alshahateet, R. Bishop, D. C. Craig and M. L. Scudder, *Cryst. Growth Des.*, 2004, **4**, 837.
4. A. N. M. M. Rahman, R. Bishop, D. C. Craig and M. L. Scudder, *Eur. J. Org. Chem.*, 2003, 72.
5. J. Ashmore, R. Bishop, D. C. Craig and M. L. Scudder, *Cryst. Growth Des.*, 2007, **7**, 47.
6. S. F. Alshahateet, R. Bishop, D. C. Craig and M. L. Scudder, *Cryst. Growth Des.*, 2010, **10**, 1742.
7. Solhe F. S. F. Alshahateet, R. Bishop, D. C. Craig and M. L. Scudder, *Cryst. Growth Des.*, 2011, **11**, 4474.

8. C. B. Anfinsen, *Science*, 1973, **181**, 223.

9. C. M. Venkatchalam and G. N. Ramachandran, *Annu. Rev. Biochem*, 1969, **38**, 45.

10. J. D. Watson and F. C. H. Crick, *Nature*, 1953, **171**, 737.

11. J. C. Nelson, J. G. Saven, J. S. Moore and P. G. Wolynes, *Science*, 1997, **277**, 1793.

12. C. Piguet, G. Bernardinelli and G. Hopfgartner, *Chem. Rev.*, 1997, **97**, 2005.

13. M. Albrecht, *Chem. Rev.*, 2001, **101**, 3457.

14. B. D. Blasio, E. Benedetti, V. Pavone and C. Pedone, *Biopolymers*, 1989, **28**, 203.

15. D. A. Langs, *Science*, 1988, **241**, 188.

16. H. Kusanagi, *Polymer J.*, 1996, **28**, 708.

17. H. Engelkamp and S. Middelbeek, and R. J. M. Nolte, *Science*, 1999, **284**, 785.

18. M. Koert, M. Harding and J.-M. Lehn, *Nature*, 1990, **346**, 339.

19. B. Hasenknopf, J.-M. Lehn, B. O. Kneisel, G. Baum and D. Fenske, *Angew. Chem. Int. Edn Engl.*, 1996, **35**, 1838.

20. T.W. Bell and H. Jousselin, *Nature*, 1994, **367**, 441.

21. H. Jiang, J.-M. Leger, C. Dolain, P. Guionneau and I. Huc, *Tetrahedron*, 2003, **59**, 8365.

22. Q. Gan, C. Bao, B. Kauffmann, A. G. lard, J. Xiang, S. Liu, I. Huc, and H. Jiang, *Angew. Chem. Int. Ed.*, 2008, **47**, 1715.

23. G. Yuan, K.-Z. Shao, X.-L. Wang, Y.-Q. Lan, Y.-H. Zhao and Z.-M. Su, *Inorganic Chemistry Communications*, 2008, **11**, 1246.

24. D. Prema, A. V. Wiznycia, B. M. T. Scott, J. Hilborn, J. Desper and C. J. Levy, *Dalton Trans.*, 2007, 4788.

25. Y. Liu, Y. Song, H. Wang, H.-Y. Zhang, T. Wada and Y. Inoue, *J. Org. Chem.*, 2003, **68**, 3687.

26. Y. Song, Y. Chen, Y. Liu, *Photochem. Photobiol. A: Chem.*, 2005, **173**, 328.

27. D. Pucci, A. Crispini, M. Ghedini, E. I. Szerb and M. L. Deda, *Dalton Trans.*, 2011, **40**, 4614.

28. D. Laurence, T. Iii and F. Papadimitrakopoulos, *Macromolecular Symposia,* 1998, **125**, 143.

29. G-H. Liu, Y-N. Xue, M. Yao, H-B. Fang, H. Yu and S-P. Yang, *J. Mol. Struct.*, 2008, **875**, 50.

30. A. Karmakar, R. J. Sarma and J. B. Baruah, *CrystEngComm*, 2007, **9**, 379.

31. A. Karmakar, and J. B. Baruah, *Supramol. Chem.*, 2008, **20**, 667.

32. S. L. Childs, G. P. Stahly and A. Park, *Mol. Pharm.,* 2007, **4**, 323.

33. D.-K. Bucar, R. F. Henry, X. Lou, T. B. Borchardt and G. G. Z. Zhang, *Chem.Commun.,* 2007, 525.

34. S. Karki, T. Friscic, W. Jones and W. D. S. Motherwell, *Mol. Pharm.,* 2007, **4**, 347.

35. M. Perakyla, *J. Am. Chem. Soc.,* 1998, **120**, 12895.

Chapter 6

Synthesis, characterization and metal ion recognition by co-ordination polymers of 2-(quinolin-8-yloxy)propionic acid

Coordination polymers have been extensively studied due to their wide variety of applications.[1-9] The coordination polymers derived from quinoline derivatives are also not exception.[10-15] Coordination polymers are known to posses catalytic activity[16] and they are also used as fluorescence probe for detection of different guests.[17]

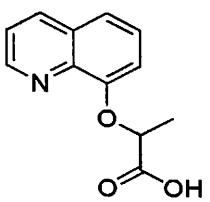

Figure 6.1: 2-(quinolin-8-yloxy)propionic acid (**LH**)

We had difficulty in preparing 2-(quinolin-8-yloxy)propionic acid (**LH**) from reaction of 8-hydroxyquinoline and 2-bromopropionic acid by conventional reagent, potassium carbonate in acetone. But, an ionic coordination polymer of the same ligand (**LH**) is synthesized by the reaction of 8-hydroxyquinoline and 2-bromopropionic acid in presence of sodium hydroxide in methanol. Further, the reaction of this coordination polymer with other metal and anion exchange led to different metal complexes. Hydrolysis of sodium salt by a mineral acid or ligand exchanges by sodium salts are fundamental reactions, but during such processes types of intermediate formed are not clear. The isolation of intermediate complex of reactions is dealt in a limited manner.[18-20] However; it may become a major factor when complicacy occurs in interpretation of unexpected product. This chapter deals with the synthesis, characterization and metal sensing properties of the coordination polymers and metal complexes of 2-(quinolin-8-yloxy)propionic acid (**LH**).

6.1 Synthesis and characterization of coordination polymer 6.1, 6.3 and dinuclear complex 6.2

The reaction of 8-hydroxyquinoline with 2-bromopropionic acid in the presence of sodium hydroxide in methanol led to coordination polymer $[\{Na_2L(H_2O)_3\}Br.H_2O]_n$ (**6.1**) as shown in scheme 6.1. This coordination polymer on treatment with perchloric acid leads to anion exchange to form a dinuclear complex $[Na_2(HL)_2(ClO_4)_2(\mu\text{-}H_2O)]$ (**6.2**). Another coordination polymer $[Cd(L)Br]_n$ (**6.3**) is formed from **6.1** on its treatment with cadmium (II) acetate (scheme 6.1).

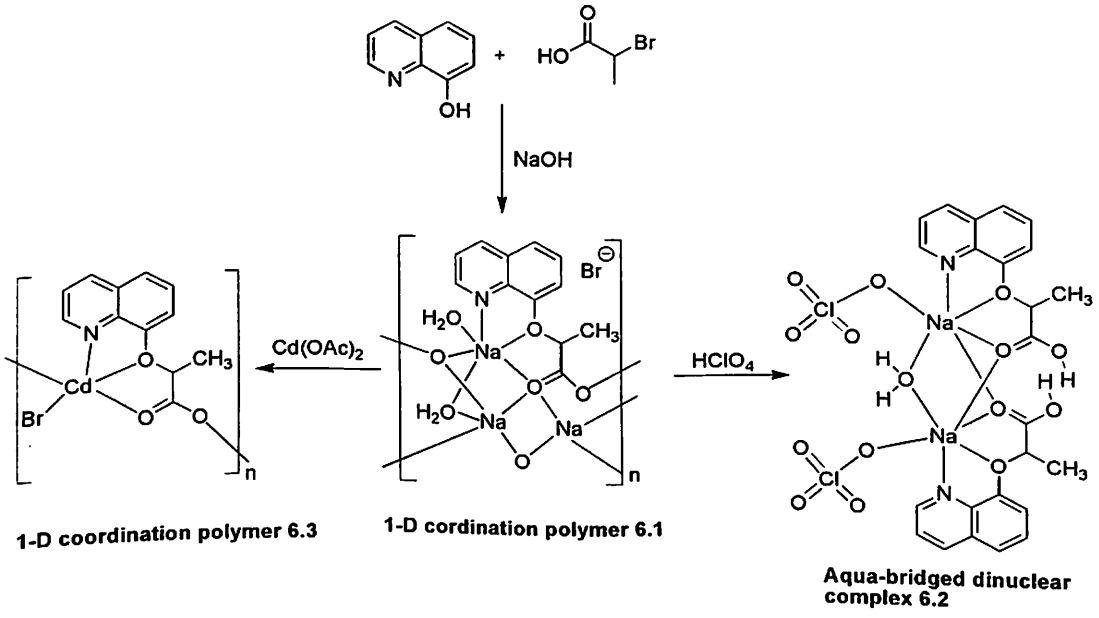

Scheme 6.1: Synthesis of the coordination polymer **6.1**, **6.3** and dinuclear complex **6.2**

The coordination polymers (**6.1**, **6.3**) and the complex (**6.2**) are characterised by determining its crystal structure and also by other spectroscopic techniques. The ^{1}HNMR and ^{13}CNMR of the complex shows the signals of the ligand. The ^{1}HNMR spectrum of the co-ordination polymer **6.1** is shown in figure 6.2.

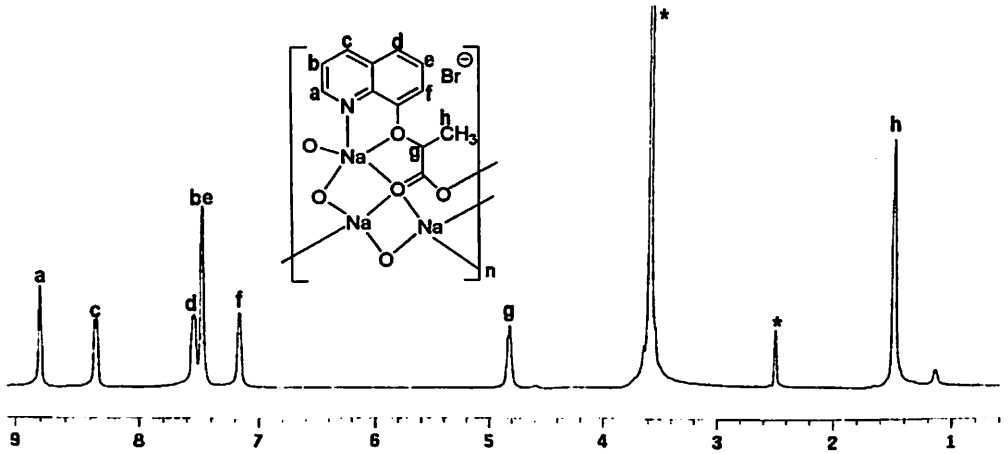

Figure 6.2: ^{1}H-NMR spectra of **6.1** (* indicates the peak for solvent and water associated with solvent)

Among the alkali metal salts, sodium salts are often used as base in chemistry and biology.[21] The sodium being an essential element in biology, its role in biology is immense.[22-26] Sodium ion also plays a major role in neuro-transmission.[27-30] Thus, it is very essential to understand structural features of sodium ions that are interlinked by water molecules and assembled in different ways. Aqua-bridged sodium complexes are very common in chemistry; mono, di-aqua-bridged, polymeric chainlike structures or clusters of different nuclearity are being stabilised by suitable anchoring ligands.[31-40] It is essential to know their structures and reactivity for further utility. Sodium salts of carboxylates are being studied to understand different types of structures in sodium containing complexes.[41-42]

We have also treated the coordination polymer **6.1** with hydrochloric acid and the mass spectra (figure 6.3) of the corresponding solution is recorded which confirms that the complex is completely dissociated to give the ligand (LH).

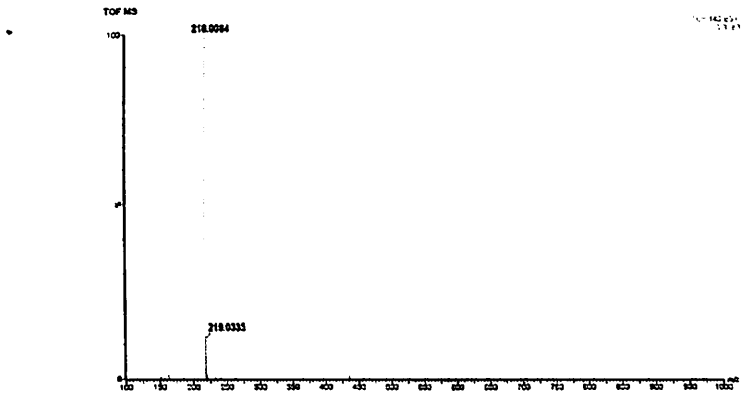

Figure 6.3: Mass spectra of **6.1** after treatment with hydrochloric acid

6.2 Structural study of coordination polymer 6.1, 6.3 and dinuclear complex 6.2

The one dimensional coordination polymer of sodium (**6.1**) has two sodium ions attached to per propionate ligand; and polymer is in a hydrated form. From X-ray crystallography it is evident that there are three sodium ions in different environments; however, all of them are in octahedral environment. The asymmetric unit of the coordination polymer is shown in figure 6.4a and the one-dimensional chain of the cationic part is shown in figure 6.4b. The sodium ions are bound to carboxylate groups in an unusual manner, through bi- and trifurcated coordination mode. The carbonyl group of carboxylate is bifurcated to bridge two sodium ions whereas the other oxygen binds to three sodium ions to form a tetrahedral kind of arrangement as illustrated in figure 6.4c. The ethereal oxygen atom and the nitrogen atom of oxy-quinoline along with an oxygen atom of carboxylate coordinate to form a chelate structure. This chelate is favoured by the sickle shape of the ligand which is also similar to a cavity that provides space for a sodium ion. Actually, this sodium ion is attached to two more coordinating water molecules (one bridging and one terminal). With the terminal water molecule and the chelating ligand a repeating unit of $NaL(H_2O)$ is formed. Two such repeating units are connected by a $Na(\mu\text{-}H_2O)_4$ units through bridging water molecules and carboxylate groups. The charge on the former unit is neutralised by the propionate anion, whereas the later cationic part is neutralised by bromide anion. The bromide ions are held in between the cationic polymer chain and are attached to the chain through O-H···Br interactions with a bridging water molecule (O5) and a coordinated water molecules (O4). The bromide ions are further held by the lattice water molecules via Br···H-O interactions. Water molecules of each layer are held to each other by hydrogen bonds. The hydrogen atoms on the lattice water could not be located, the oxygen atom is disordered. Thus we could not precisely show the hydrogen bond parameters of this water molecule with bromide. The ionic nature of the bromide ion is easily depicted by adding silver nitrate solution, which leads to a dirty white precipitate of silver bromide. There are many examples of water coordinated sodium complexes stabilised by nitrogen donor ligands.[34] As mentioned earlier, the sodium ions can adopt different nuclearities through aqua bridges; such as tetranuclear cluster,[35] linear-chain,[31] mono-aqua bridged[33] and diaqua-bridged structures[32] etc. are reported in literature. However, our

present coordination polymer has novel bi- and tri-furcated carboxylate bridges that connect five sodium atoms simultaneously by one carboxylate ligand, which is unique among the conventionally observed carboxylate binding modes.[43-45]

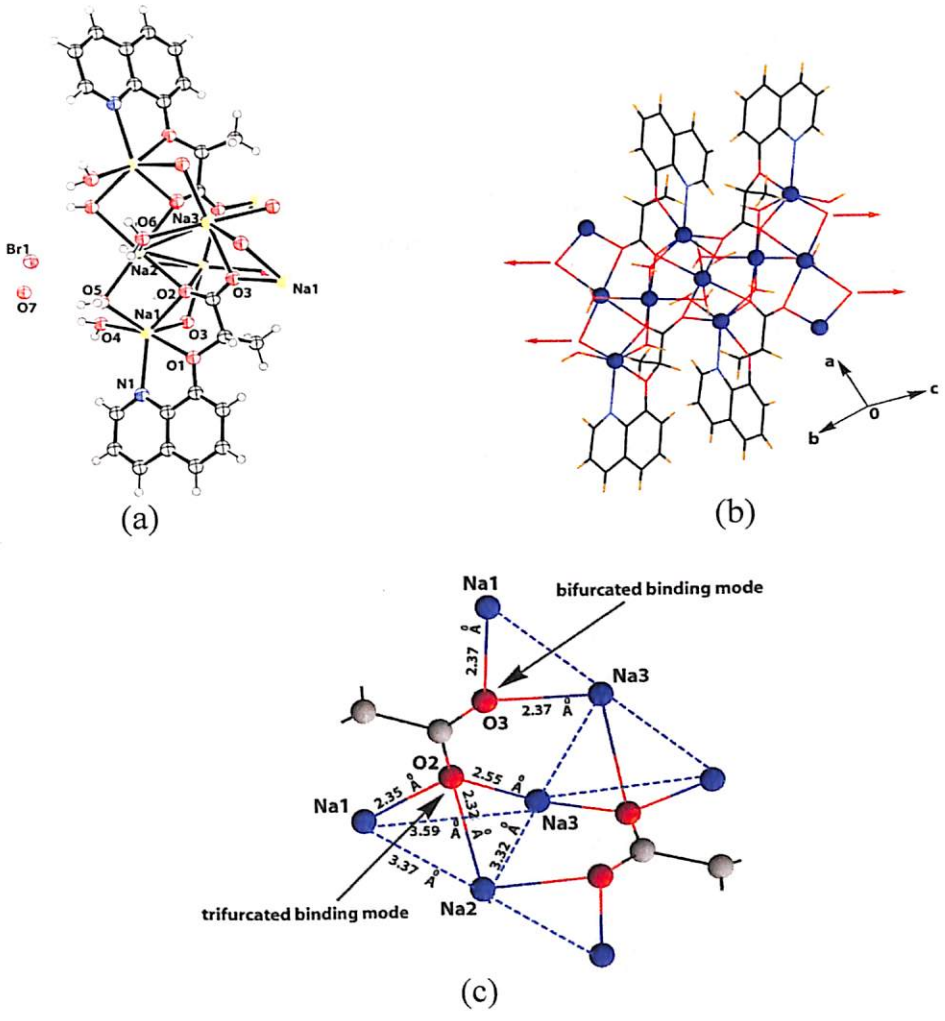

Figure 6.4: (a) Asymmetric unit of **6.1** (ORTEP diagram drawn with 50% elipsoid probability); (b) the coordination polymer; (excluding bromide and lattice water), (c) the binding of carboxylate to sodium cations

The powder X-ray diffraction of the coordination polymer **6.1** shows that the peaks obtained from experiment tallies with the simulated one; however the intensity of the peaks in each case varies (figure 6.5). Some of the prominent bond angles and bond distances contributing to the coordination of sodium ions are listed in table 6.1.

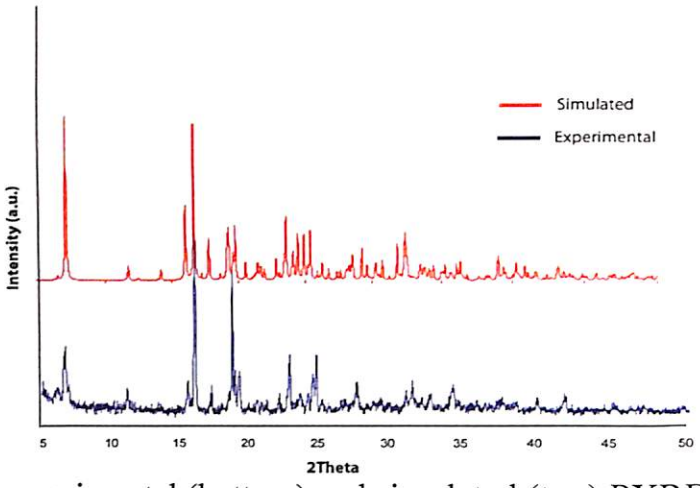

Figure 6.5: The experimental (bottom) and simulated (top) PXRD of coordination polymer **6.1**

Table 6.1: Selected bond distances (Å) and bond angles (◦) of coordination polymer **6.1**

Bond distances (Å)			
Na1-O3	2.373(3)	Na2- O2	2.328(3)
Na1-O1	2.396(3)	Na2 -O5	2.420(4)
Na1-O4	2.412(4)	Na2- O6	2.428(4)
Na1-O5	2.446(4)	Na3 -O2	2.555(3)
Na1- O2	2.357(3)	Na3- O3	2.373(3)
Na1- N1	2.450(4)	Na3 -O6	2.442(3)
Bond angles (◦)			
O2- Na1- O3	79.68(12)	O3 -Na1- N1	107.89(13)
O2- Na1- O1	68.10(11)	O1- Na1- N1	66.31(12)
O3 -Na1- O1	94.93(12)	O4 -Na1- N1	98.50(14)
O2- Na1- O4	127.26(14)	O5- Na1- N1	112.36(14)
O3- Na1- O4	85.39(14)	O2- Na2- O5	175.47(14)
O1 -Na1- O4	164.19(14)	O2- Na2 -O6	84.55(11)
O2- Na1- O5	80.59(13)	O5- Na2 -O6	91.75(13)
O3- Na1- O5	138.14(14)	O4 -Na1 -O5	77.89(15)
O1- Na1- O5	111.18(14)	O2 -Na1- N1	134.23(13)

Since complex **6.1** contains ionic bromide, we tried to exchange this anion by perchlorate anion. Replacement of the bromide by perchlorate on addition of perchloric acid resulted in the formation of a dinuclear complex $[Na_2(HL)_2(ClO_4)_2(\mu\text{-}H_2O)]$ (**6.2**). From the structure of **6.2** it is seen that there is a structural reorganisation of the complex **6.1** to accommodate the perchlorate anion. In the complex **6.2** the perchlorate anions are found to be highly disordered. It acts as a monodentate ligand to sodium ion. Generally an ionic perchlorate maintains a symmetric structure and shows single strong IR-absorption[46-47] around 1100 cm^{-1}. The complex has strong absorptions at 1120 cm^{-1}, which is broad and sharp. Since the perchlorate ligand in

this complex has a relatively symmetric structure, we have not seen splitting of this peak. The complex contains aqua bridges between the sodium ions and IR contains signals for OH stretching 3444 cm^{-1} from such bridging water molecules. The structure of the complex **6.2** is shown in figure 6.6a. The coordination environment around sodium ion as depicted in figure 6.6a shows that each sodium ion is attached to the nitrogen and oxygen atoms of oxy-quinoline and carboxylate oxygen of the ligand. The ligand LH serves as tridentate ligand for sodium ion and also the carboxylate group of the ligand further holds another sodium ion through oxy-bridge. Each sodium ion has one water molecule each, that serves as bridging ligand to anchor another sodium ion. A six coordinate geometry around sodium ion is established in each case. The Cl-O-Na bonds are disordered. This makes uncertain in description of Cl-O bond lengths. The dinuclear complexes self-assemble to form supramolecular polymers as illustrated in figure 6.6b.

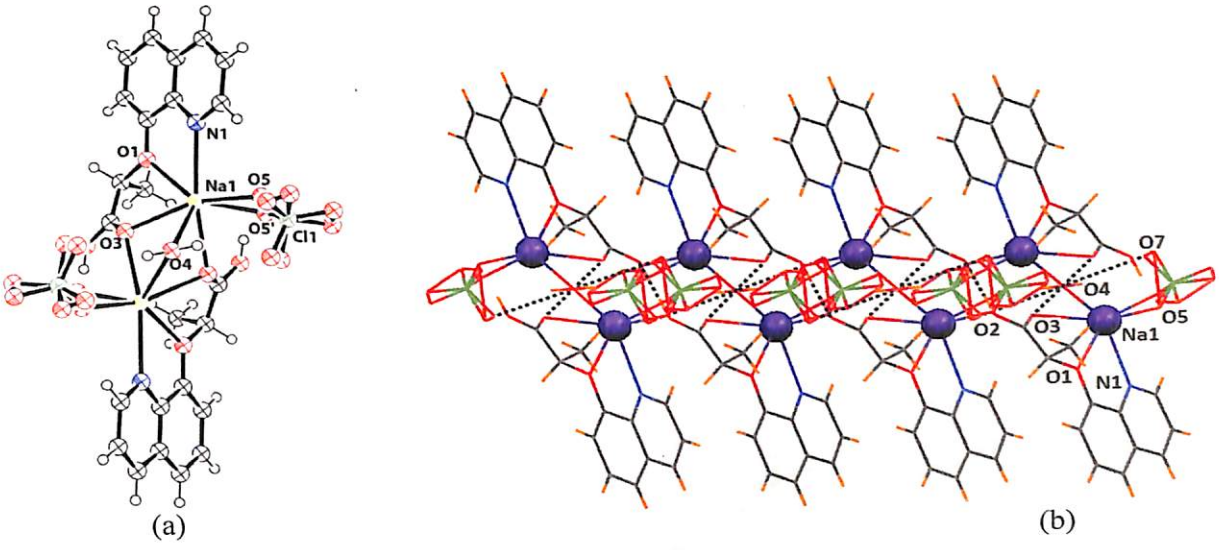

Figure 6.6: (a) Structure of **6.2** (ORTEP diagram drawn with 50% elipsoid probability); (b) hydrogen bonded self-assembly of **6.2**

The powder X-ray diffraction shows that the peaks obtained from experiment tallies with the simulated one; however the intensity of the peaks in each case varies (figure 6.7). Some of the important bond angles and bond distances contributing to the coordination of sodium ions are listed in table 6.2.

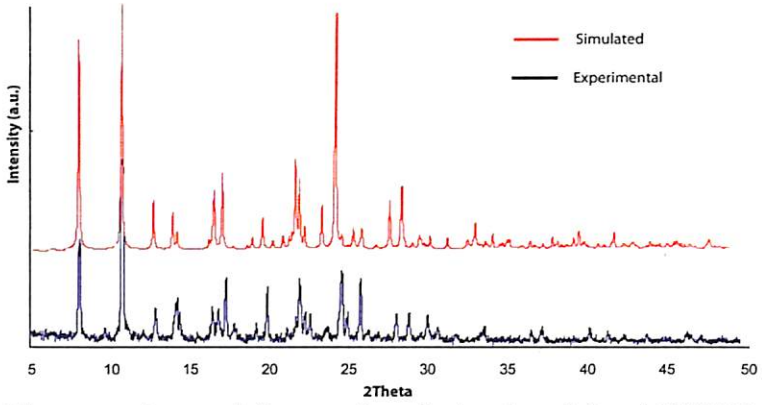

Figure 6.7: The experimental (bottom) and simulated (top) PXRD of dinuclear complex **6.2**

Table 6.2: Selected bond distances (Å) and bond angles (◦) of the dinuclear complex **6.2**

Bond distances (Å)			
Na1- O9	2.472(12)	Na1- O1	2.5411(15)
Na1 -O3	2.4745(18)	Na1- O4	2.567(2)
Na1 -O5	2.478(12)	Na1- N1	2.573(2)
Na1- O2	2.5070(16)		
Bond angles (◦)			
O9- Na1- O3	145.6(3)	O3 -Na1- O5	152.4(3)
O9- Na1- O5	13.2(4)	O9- Na1- O2	82.2(3)
O3- Na1- O2	114.33(6)	O3- Na1- O3	69.34(9)
O5 -Na1- O2	86.4(4)	O5- Na1- O3	100.7(2)
O9- Na1- O3	87.5(3)	O2- Na1- O3	75.67(6)
O9- Na1- O1	152.6(3)	O3- Na1- O1	61.81(5)
O5- Na1- O1	142.5(2)	O2- Na1- O1	84.01(6)
O3- Na1- O1	111.78(6)	O9 -Na1- O4	75.4(3)
O3- Na1- O4	73.61(6)	O3- Na1- O4	72.86(6)
O5- Na1- O4	78.8(3)	O1- Na1- O4	127.76(5)
O2- Na1- O4	141.81(5)	O9- Na1- N1	94.0(2)
O3- Na1- N1	115.55(7)	O5- Na1- N1	81.6(2)
O2- Na1- N1	88.18(6)	O1- Na1- N1	61.97(5)
O3- Na1- N1	163.44(6)	O4 -Na1- N1	123.47(6)
Na1 -O3 -Na1	95.72(7)	Na1-O4 -Na1	92.34(10)

Coordination polymers of 2-(quinolin-8-yloxy)acetate are reported in literature.[48-49] For such studies the alkali metal salts are used as starting material. Earlier results on the lanthanide complexes have shown that chelated complexes of the ligands are assembled by side of coordination of carbonyl groups or by combining them with dicarboxylates.[48] We have selected a relatively large size cation namely cadmium, as it can expand its coordination number from six to nine. We studied the coordination polymer of 2-(quinolin-8-yloxy)propionate with cadmium (**6.3**) by treating coordination polymer **6.1** with cadmium acetate (scheme 6.1). In this case the bromide ion did not get replaced, but it went into the coordination sphere of cadmium ion. Thus, each cadmium ion has five coordination environments; comprise of a ligand occupying three coordination sites, another site is occupied by a bromide ion.

The rest of the position is occupied by an oxygen atom of a carbonyl of the carboxylate from another ligand attached to cadmium. This type of coordination by carbonyl groups from each repeating unit continues and the ligands are disposed at trans-positions to each other. So, such [CdLBr] unit repeats (figure 6.8a) to form chain like structure. The five coordinate cadmium ions are in distorted square pyramidal geometry. The five coordination geometry of cadmium are less in numbers in comparison to other coordination numbers.[50-51] In this case, it may be as a consequence of the presence of a large coordinating bromide ion, further the bromide ions of the two chain are placed parallel, provide interlayer interactions. The coordinated bromides are positioned face to face have contact distance 3.697Å (figure 6.8b). This distance is in agreement with the generally observed bromide-bromide interactions in bromo-organic derivatives. For example the bromine-bromine contact in 4-bromobenzaldehyde[52] is 3.674 Å. The bromide oxygen, and other halogen-halogen[53-54] distances are important in biological molecules and have interest in crystal engineering. These interlayer interactions prevent sixth ligand to come close to cadmium and make it five coordinate coordination polymer.

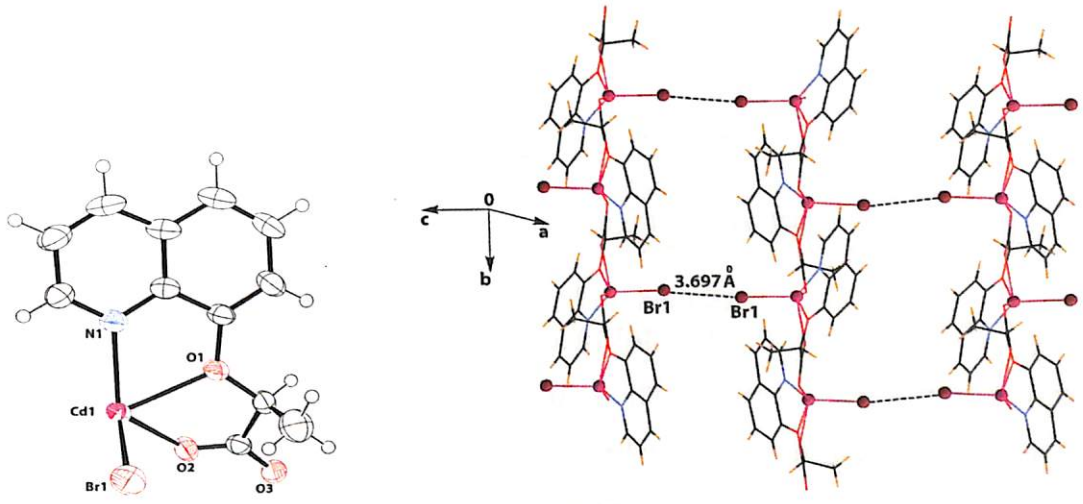

Figure 6.8: (a) Asymmetric unit of **6.3** (ORTEP diagram drawn with 50% elipsoid probability); (b) 1-D coordination polymer **6.3** with Br···Br interactions

Table 2: Selected bond distances (Å) and bond angles (°) of coordination polymer **3**

Bond distances (Å)			
Cd1- O3	2.215(2)	Cd1-O2	2.333(2)
Cd1- N1	2.279(3)	Cd1-O1	2.414(2)
Cd1-Br1	2.5306(7)		
Bond angles (°)			
O3-Cd1-N1	119.66(10)	O2-Cd1-O1	65.66(8)
O3-Cd1-O2	86.79(8)	O3-Cd1-Br1	104.12(8)
N1-Cd1-O2	124.39(9)	N1-Cd1-Br1	116.96(8)
O3-Cd1-O1	146.22(9)	O2-Cd1-Br1	99.31(7)
N1-Cd1-O1	67.80(9)	O1-Cd1-Br1	99.53(7)

Solution study of coordination polymer 6.1, 6.3 and dinuclear complex 6.2

On treatment with hydrochloric acid, the coordination polymer **6.1** shows fluorescence at 474 nm upon excitation at 320 nm (figure 6.9) which shows that the ligand (LH) is fluorescence active in its free state.

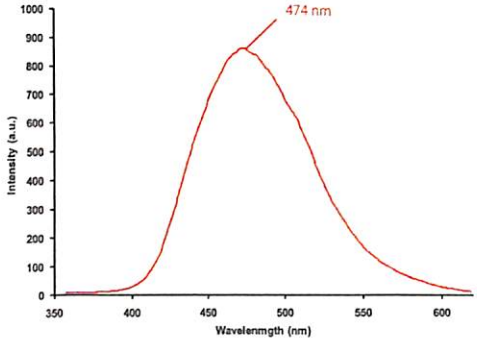

Figure 6.9: Fluorescence spectra of **6.1** after treatment with hydrochloric acid

However, coordination polymer **6.1** and dinuclear complex **6.2** are fluorescence inactive; whereas, the coordination polymer **6.3** is highly fluorescent. The coordination polymers **6.1** and **6.2** have UV-absorption peaks around 310 nm. The coordination polymer **6.1** and complex **6.2**, independently shows a gradual enhancement in the emission intensity at 403 nm upon excitation at 320 nm on addition of cadmium acetate. Generally quinoline derivatives have π to n and π to π^* transitions, the n and π^* energy levels are very close in energy. Upon coordination to metal ion the n level gets stabilised and emission occurs from π^* to π level. Thus, there is enhancement of fluorescence signalling on titration with filled core ions. However when there is incompletely filled d-orbitals are present the electrons can be accommodated from the excited state to the d-orbital, thereby changing the path of

decay and causes quenching of fluorescence.[55] When, we carried out fluorescence titration of **6.1** and **6.2** with different metals at +2 oxidation state, namely that of zinc, mercury, magnesium, calcium, barium, copper, nickel, manganese. The addition of metal ions that have filled core electronic configuration such as zinc, cadmium, mercury, magnesium, calcium, barium showed gradual enhancement of fluorescence intensity, whereas addition of metal (II) acetates with vacant d-orbitals such as copper, nickel, manganese do not cause changes in fluorescence emission of the complex **6.1** and **6.2**. As a representative case, the enhancement of fluorescence intensity of coordination polymer **6.1** and dinuclear complex **6.2** on addition of cadmium (II) acetate is shown in figure 6.10.

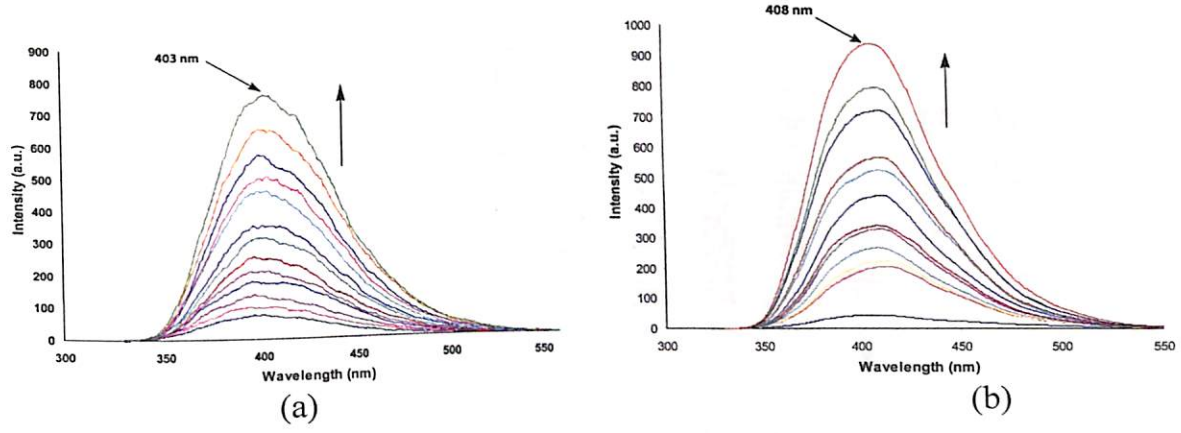

(a) (b)

Figure 6.10: (a) Increase in the fluorescence emission intensity of **6.1** (10^{-4} M in methanol) on gradual addition of 10 μL of cadmium acetate (10^{-3} M in methanol); (b) Changes in the fluorescence emission spectra of **6.2** (10^{-4} M in methanol) on gradual addition of 10 μL of cadmium acetate (10^{-3} M in methanol)

The fluorescence emission by quinoline based receptors are used to detect zinc(II) ions in aqueous medium.[56] The need of zinc receptors in bio-related neuro transmitter is elegantly described.[57] The 1,10-phenanthroline containing cadmium complexes show fluorescence emission.[58-60] It is to be mentioned that the receptors for fluorescence enhancements are generally organic fluorophores, the coordination polymers as receptors are not been studied and our study opens up a new dimension. The use of coordination polymer have interesting process in drug delivery as it would act as probe while delivering another component through dismantling of the polymer upon interaction with a substrate, for example in our case when cadmium binds sodium ions are expelled from the complex to provide a fluorescence emitter, in the

form of cadmium complex **6.3**. We have been able to see a sharp enhancement of fluorescence intensity in protic solvent, namely methanol. A comparative picture on the relative enhancement of emission intensity by different metal ions is illustrated by bar diagrams shown as figure 6.11. In these figures the relative intensity changes of parent coordination polymer with equal amount of each ion are plotted. From these bar graphs it is clear that the presence of bromide ion in and perchlorate ion in the respective complexes **6.1** and **6.2** does not interfere in the emission process. It is also observed that in both the cases zinc and magnesium ions show maximum enhancements in the fluorescence intensity; whereas mercury (+2) ion shows the least enhancement.

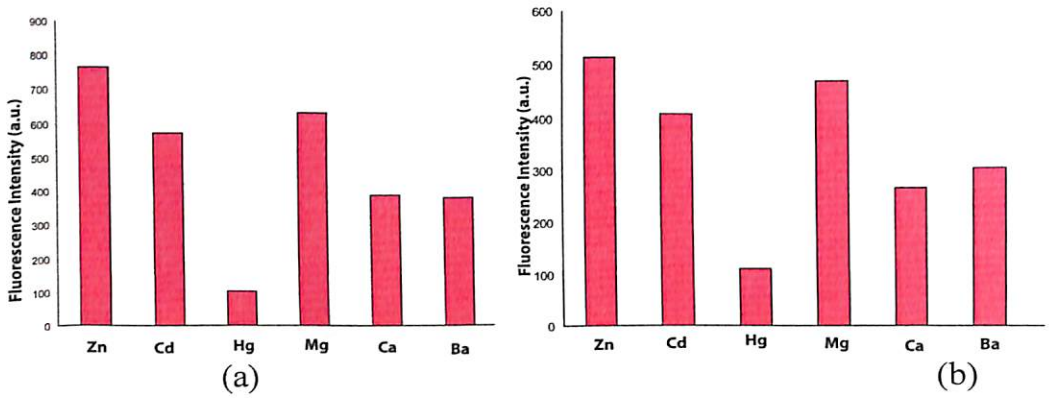

Figure 6.11: Bar graphs showing fluorescence emission intensity of (a) coordination polymer **6.1** (10^{-4} M in methanol) after addition of 100 μL of metal acetate (10^{-3} M in methanol); (b) Dinuclear complex **6.2** (10^{-4} M solution in methanol) after addition of 100 μL of metal acetate (10^{-3} M solution in methanol)

Conclusion

In conclusion, a sodium coordination polymer having unusual di- and trifurcated carboxylate binding modes is shown. Both anion and cation of a coordination polymer can be easily replaced. Bromide is replaced by perchlorate to form a dinuclear complex. The sodium ions are replaced by cadmium (II) ions to give one dimensional coordination polymer. This study also demonstrates the use of coordination polymers as receptors for fluorescence enhancement by selective metal ions.

Experimental

Synthesis of 6.1: $[\{Na_2L(H_2O)_3\}.H_2O.Br]_n$

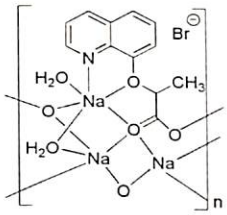

8-Hydroxyquinoline (0.72 g, 5 mmol) was dissolved in methanol (25 ml) and sodium hydroxide (0.28 g, 7 mmol) was added. The reaction mixture was then stirred for 30 minutes at room temperature. 2-Bromopropionic acid (0.75 g, 5 mmol) was added to the reaction mixture and refluxed for 6 hours at 70 °C. The reaction mixture was then allowed to stand at room temperature for 4 days to obtain colourless crystals of **6.1**.

Yield: 72%.

IR (KBr, cm^{-1}): 3430 (bs), 2945 (w), 1602 (s), 1504 (m), 1412 (m), 1316 (m), 1259 (m), 1116 (m), 790 (m).

^{1}HNMR (DMSO-d^6, 400 MHz): 8.7 (s, 1H); 8.3 (d, J = 6.8Hz, 1H); 7.5 (t, J = 4.0Hz, 1H); 7.4 (m, 2H); 4.8 (m, 1H); 1.4 (m, 3H).

^{13}CNMR (DMSO-d^6, 100 MHz): 175.2, 151.9, 149.5, 139.5, 136.8, 129.2, 127.3, 119.4, 109.8, 74.7, 17.7.

λ_{max}(methanol) = 310 nm ($\varepsilon = 7.9 \times 10^3$ $mol^{-1}cm^{-1}$).

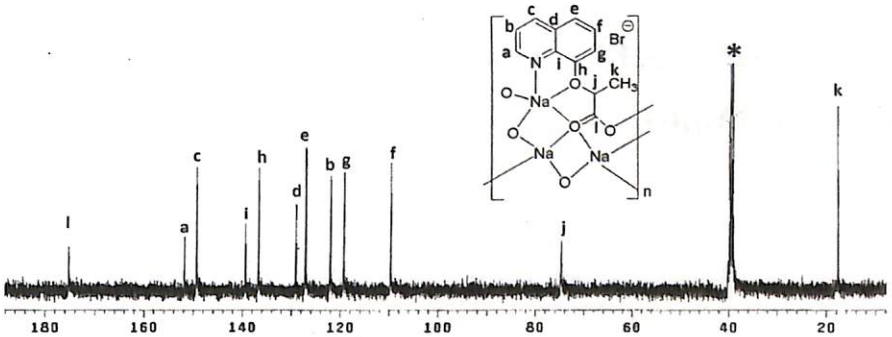

Figure 6.12: ^{13}C-NMR spectra of coordination polymer **6.1** (* indicates the peak for solvent)

Synthesis of 6.2: $[Na_2(HL)_2(ClO_4)_2(\mu\text{-}H_2O)]$

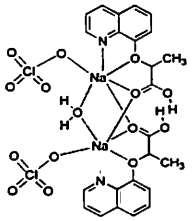

Coordination polymer **6.1** (0.82 g, 2 mmol) was dissolved in methanol and a dilute solution of perchloric acid was added to it. The reaction mixture was stirred at room temperature and allowed to stand for three days to obtain colourless crystals of compound **6.2**.

Yield: 68%.

IR (KBr, cm^{-1}): 3444 (bs), 2977 (w), 1752 (s), 1626 (s), 1504 (m), 1379 (m), 1120 (s), 822 (m), 757(m).

λ_{max}(methanol) = 307 nm ($\varepsilon = 6.6 \times 10^3\ mol^{-1}cm^{-1}$).

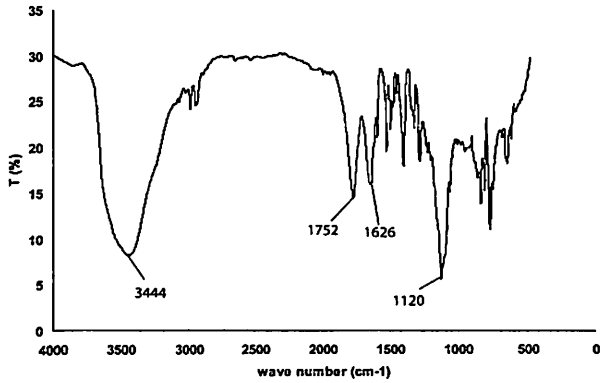

Figure 6.13: IR spectra of the dinuclear complex **6.2**

Synthesis of 6.3: $[Cd(L)Br]_n$

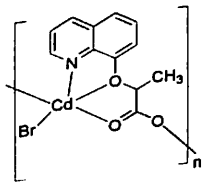

Compound **6.1** (0.82 g, 2 mmol) was dissolved in methanol and $Cd(O_2CCH_3)_2.2H_2O$ (0.53 g, 2 mmol) was added to it. The reaction mixture was stirred at room temperature and allowed to stand for three days to obtain colourless crystals of compound **6.3**.

Yield: 61%.

IR (KBr, cm^{-1}): 3459 (bs), 1624 (s), 1506 (m), 1396 (m), 1320 (m), 1226 (m), 1118 (m), 828 (m).

λ_{max}(methanol) = 311 nm ($\varepsilon = 1.1 \times 10^4$ $mol^{-1}cm^{-1}$).

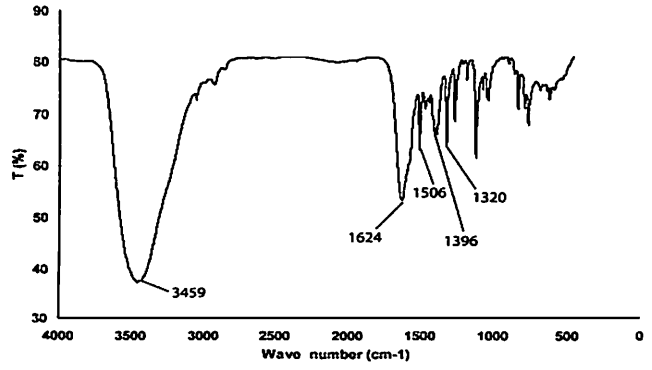

Figure 6.14: IR spectra of the coordination polymer **6.3**

References

1. A. J. Blake, N. R. Champness, P. Hubberstey, W.S. Li, M. A. Withersby and M. SchrTder, *Coord. Chem. Rev.*, 1999, **183**, 117.
2. M. Eddaoudi, D. B. Moler, H. Li, B. Chen, T. M. Reineke, M. O'Keeffe and O. M. Yaghi, *Acc. Chem. Res.*, 2001, **34**, 319.
3. O. R. Evans and W. Lin, *Acc. Chem. Res.*, 2002, **35**, 511.
4. K. Kim, *Chem. Soc. Rev.*, 2002, **31**, 96
5. S. Kitagawa and S. Kawata, *Coord. Chem. Rev.* 2002, **224**, 11.
6. B. Moulton and M. J. Zaworotko, *Chem. Rev.*, 2001, **101**, 1629.
7. O. M. Yaghi, H. Li, C. Davis, D. Richardson and T. L. Groy, *Acc. Chem. Res.*, 1998, **31**, 474.
8. M. J. Zaworotko, *Chem. Soc. Rev.*, 1994, **23**, 283.
9. S. L. James, *Chem. Soc. Rev.*, 2003, **32**, 276.
10. D. Dobrzynska, L. B. Jerzykiewicz, J. Jezierska and M. Duczmal, *Cryst. Growth Des.*, 2005, **5**, 1945.
11. X. H. Bu, M. L. Tong, Y. B. Xie, J. R. Li, H. C. Chang, S. Kitagawa and J. Ribas, *Inorg. Chem.*, 2005, **44**, 9837.
12. X. H. Bu, M. L Tong, J. R. Li, H. C. Chang, L. J. Li and S. Kitagawa, *CrystEngComm.*, 2005, **7**, 411.
13. M. A. M. Abu-Youssef, A. Escuer and V. Langer, *Eur. J. Inorg. Chem.*, 2006, 3177.

14. M. A. M. Abu-Youssef and V. Langer, *Polyhedron*, 2006, **25**, 1187.
15. Z. F. Chen, P. Zhang, R. G. Xiong, D. J. Liu and X. Z. You, *Inorg. Chem. Commun.*, 2002, **5**, 35.
16. Y. Ren, C. Du, S. Feng, C. Wang, Z. Kong, B. Yue and H. He, *CrystEngComm*, 2011, **13**, 7143.
17. N. Yanai, K. Kitayama, Y. Hijikata1, H. Sato, R. Matsuda, Y, Kubota, M, Takata, M, Mizuno, T, Uemura1 and S, Kitagawa, *Nature materials*, **10**, 2011, 787.
18. C. S. B. Gomes, D. Suresh, P. T. Gomes, L. F. Veiros, M. T. Duarte, T. G. Nunes and M. C. Oliveira, *Dalton Trans.*, 2010, **39**, 736.
19. Y.Huang, Y.H. Tsai, W.C. Hung, C.S. Lin, W. Wang, J.H. Huang, S. Dutta and C.C. Lin, *Inorg. Chem.*, 2010, **49**, 9416.
20. J. W. Steed and P. C. Junk , *J. Chem. Soc. Dalton Trans.*, 1999, 2141.
21. *Fieser and Fieser's Reagents for Organic Synthesis* by M. Fieser, Wiley-India, 1990.
22. A. Amtmann and D. Sanders, *Adv. Bot. Res.*, 1999, **29**, 75.
23. E. Blumwald, G. S. Aharon and M. P.Apse, *Biochim. Biophys. Acta*, 2000, **1465**, 140.
24. A. Rus, S. Yokoi, A. Sharkhuu, M. Reddy, B.H. Lee, T.K. Matsumoto, H. Koiwa, J. K. Zhu, R. A. Bressan and P. M. Hasegawa, *Proc. Natl. Acad. Sci. USA*, 2001, **98**, 14150.
25. F. J. M. Maathuis and D. Sanders, *Plant Physiol*, 2001, **127**, 1617.
26. M. P. Apse, G. S. Aharon, W. A. Snedden and E. Blumwald, *Science*, 1999, **285**, 1256.
27. E. Zomot, A. Bendahan, M. Quick, Y. Zhao, J. A. Javitch and B. I. Kanner, *Nature* 2007, **449**, 726.
28. Y. Zhao, M. Quick, L. Shi, E. L Mehler, H. Weinstein and J. A. Javitch, *Nature Chem. Bio.*, 2010, **6**, 109.
29. R. R. Llinas, *Science*, 1988, **242**, 1654.
30. W. E. Crill, *Annu. Rev. Physiol.*, 1996, **58**, 349.
31. X-F. Huang, Y-M. Song, Q. Wu, Q. Ye, X-B. Chen, R-G. Xiong and X-Z. You, *Inorg. Chem. Commun.*, 2005, **8**, 58.

32. H. Chena, T. Zhang, J. Zhang , X. Qiao and K. Yu, *J. Hazardous Mater.* 2006, **A129**, 31.
33. D. K. Gupta, S. Singh, P. Mayer and A. Pandey, *Inorg. Chem. Commun.*, 2011, **14**, 1485.
34. A. Karmakar and J. B. Baruah, *Inorg. Chem. Commun.*, 2009, **12**, 140.
35. D. Dutta, A. D. Jana, M. Debnath, A. Bhaumik, J. Marek and Md. Ali *Dalton Trans.*, 2010, **39**, 11551.
36. P. A.M. Williams, L. G. Naso, G. A. Echeverría and E. G. Ferrer, *J. Mole. Struct.*, 2010, **978**, 124.
37. R.-H. Zeng, Z.-Q. Fang, F. Sun, L.-S. Jiang and Y.-W. Tang, *Acta Cryst.* 2007, **E63**, m1813.
38. G.B. Li, S.H. Yang, M. Xiong and J.H. Lin, *Acta Cryst. C*, 2004, **60**, m612.
39. W. Huang, H. Qian, S. Gou and C. Yao, *J. Mol. Struct.*, 2005, **743**, 183.
40. M. Inosako, C. Shimokawa, H. Sugimoto, N. Kihara, T. Takata and S. Itoh, *Chem.Lett.*, 2007, **36**, 1306.
41. B. Das and J. B. Baruah, *Inorg. Chim. Acta*, 2010, **363**, 1479.
42. A. Karmakar, J. B. Baruah and R. BoomiShankar, *CrystEngComm*, 2009, **11**, 832.
43. C. N. R. Rao, S. Natarajan and R. Vaidhyanathan, *Angew. Chem. Int. Ed.*, 2004, **43**, 1466.
44. T. Dudev and C. Lim, *Acc. Chem. Res.*, 2007, **40**, 85.
45. B. Moulton and M.J. Zaworotko, *Chem. Rev.*, 2001, **101**, 1629.
46. J. D. McCullough, *J. Am. Chem. Soc.*, 1940, **62**, 480.
47. D. N. Sathyanaraya, Vibrational spectroscopy, New Age International Publishers, New Delhi, 2004.
48. J. Fan, Z-H. Wang, M. Yang, X. Yin, W-G. Zhang, Z-F. Huang and R-H. Zeng, *CrystEngComm*, 2010, **12**, 216.
49. Y-H. Wang, R-F. Song and F-Y. Zhang, *J. Mole. Struct.*, 2005, **752**, 104.
50. E. Coaro and S. Baggio, *Inorg. Chem. Acta*, 1969, **3**, 617.
51. J-C. Dai, X-T. Wu, Z-Y. Fu, C-P. Cui, S-M. Hu, W-X. Du, L-M. Wu, H-H. Zhang and R-Q. Sun, *Inorg. Chem.*, 2002, **41**, 1391.
52. D. Britton, *J.Chem. Cryst.*, 1994, **24**, 553.
53. J.A.R.P. Sarma and G.R. Desiraju, *Acc. Chem. Res.*, 1986, **19**, 222.

54. P. Auffinger, F.A. Hays, E. Westhof and P.S. Ho, *Proc. Nat. Acad. Sci USA*, 2004, **101**, 16789.

55. A. P. de Silva, H. Q. N. Gunaratne, T. Gunnlaugsson, A. J. M. Huxley, C. P. McCoy, J. T. Rademacher and T. E. Rice, *Chem. Rev.*, 1997, **97**, 1515.

56. S. Aoki, K. Sakurama, N. Matsuo, Y. Yamada, R. Takasawa, S-I Tanuma, M. Shiro, K. Takeda and E. Kimura, *Chem. Eur. J.*, 2006, **12**, 9066.

57. E. M. Nolan and S. J. Lippard, *Acc. Chem. Res.*, 2009, **42**, 193.

58. A. Meijerink, G. Blasse and M. Glasbeek, *J. Phys. Condens. Matter*, 1990, **2**, 6303.

59. R. Bertoncello, M. Bettinelli, M. Cassrin, A. Gulino, E. Tondello and A. Vittadini, *Inorg. Chem.*, 1992, **31**, 1556.

60. M. D. Allendorf, C. A. Bauer, R. K. Bhaktaa and R. J. T. Houka, *Chem. Soc. Rev.*, 2009, **38**, 1330.

Conclusion

Binding ability of ester and amide derivatives of quinoline towards different acids such as amino acids, hydroxy acids, mineral acids and simple carboxylic acids depends on their structures. The anion binding and stoichiometry changes the orientations of the flexible arm of an amide containing receptors. Such spatial arrangements can also decide the number/s of sites to protonate in case of substrates having multiple sites for protonation. Anion coordination can change a flexible bent molecule to a stretched one and at the same time a stretched molecule can also be converted to a bent structure on interaction with anions. A receptor molecule with closed pack structure can be converted into a structure with uniform cylindrical voids. The amide derivatives of 8-aminoquinoline undergoes multi-component reaction to give novel heterocycles. The same derivatives also shows cyclisation reaction in presence of different metal ions, these reactions are very sensitive towards the metal ions and solvent systems. The anion binding to modified substrates can be used to distinguish between anions. The reactivity pattern of different metal ions with the compounds enables to distinguish the receptors as well as the metal ions. Thus, it can also provide a scope to insitu generate receptors for recognition of metal ions and anions.

Urea derivative of quinoline can be used as a colour sensor to distinguish isomeric dicarboxylic acids. The salts of this urea derivative are of yellow coloured whereas the co-crystals are colourless. By virtue of this property, a pair of stereo isomers (maleic acid and fumaric acid) and a pair of positional isomers (phthalic acid and terephthalic acid) can be distinguished both in solution as well as in solid state. Urea and carbamide derivatives of quinoline show an increase in the number of symmetry non-equivalent molecule in the crystallographic asymmetric unit on coordination with anions.

Quinoline derivative undergoes a $Mn(OAc)_2$ catalysed C-C coupling reaction to give a 5,5'-diquinoline derivative. This 5,5'-diquinoline derivative forms a single helical structure. The helicity of the molecule is maintained on encapsulation of guests having different structure. Further, nitric acid forms a co-crystal, whereas perchloric acid forms a salt with this diquinoline derivative. This is a rare example where a strong acid such as nitric acid is not dissociated in presence of a base like quinoline. However, in solution both the acids behave in a similar way.

Quinoline based carboxylic acid derivatives forms an ionic coordination polymer with sodium. Anion exchange of the coordination polymer leads to a dinuclear complex while the exchange of the metal with cadmium leads to a neutral coordination polymer. This study also demonstrates the use of coordination polymers as receptors for fluorescence enhancement by selective metal ions.

The structural backbones depicted here are based on quinoline units that are generally component of drugs; therefore it leaves ample scopes to make predictive models for analogous study on drug delivery as well as drug-substrate activity.

Appendix

Details of the analytical instruments

X-Ray Crystallography

X-ray diffraction data were collected on Bruker 3-circle diffractometers with CCD area detectors ProteumM APEX or SMART 6000 or Bruker Nonius Apex 2, using graphite-monochromated Mo-$K\alpha$ radiation (λ = 0.71073 Å) from a 60W microfocus Bede Microsource® with glass polycapillary optics or a sealed tube.

X-ray diffraction data for all crystals were collected using Bruker SMART software. This software was also used for indexing and determination of the unit cell parameters. The structures were solved by direct methods and refined by full-matrix least squares against F^2 of all data, using SHELXTL software. The CIF of all the compounds synthesized and characterized are included in the soft copy.

All non-H atom were refined by full-matrix least squares in anisotropic, all H atoms in isotropic approximation, against F^2 of all reflections. All non-H atoms were refined by full-matrix least squares in the anisotropic approximation and the hydrogen atoms attached to these atoms were treated as 'riding' in calculated positions and in some of the cases the hydrogen atoms have been located on the difference Fourier maps. In all cases the hydrogen atoms attached to polar atoms such as O and N were located on the difference Fourier maps and refined in the final structure in isotropic approximation. The crystallographic tables for all the compounds are given at the end of this section, which includes the crystal parameters and the refinement factors.

UV-visible Spectroscopy, emission and IR Spectroscopy

UV-vis absorption spectra were recorded using Perkin-Elmer Lambda 750 spectrophotometer equipped with double cell compartments. All the chemicals and solvents used were as obtained from the satndard suppliers such as E.Merck Germany, Sigma Aldrich USA, Ranbaxy India. The solvents for spectroscopic were of HPLC grade (Aldrich or Merck) and used as obtained. The fluorescence spectra were recorded in Fluoromax-4, spectrofluorometer. The FT-IR spectra were recorded on Perkin-Elmer spectrum one spectrometer in the range 4000-400 cm^{-1}.

NMR Spectroscopy

The NMR spectra were recorded in a Bruker 400 MHz spectrometer. The chemical shifts in the NMR spectra are all given in ppm and tetramethylsilane as the internal standard. The solid state ^{13}C CP-MAS were recorded in a Bruker 500 MHz AV NMR spectrometer.

Crystallographic data and refinement parameters for the compounds

Compound No.	**2.3**	**2.3a**	**2.3b**
Formulae	$C_{20}H_{15}N_3O_2$	$C_{23}H_{25}BF_4N_4O_4$	$C_{20}H_{17}Cl_2N_3O_{10}$
CCDC No.	790481	724792	724793
Mol. wt.	329.35	508.28	530.27
Crystal system	Triclinic	Orthorhombic	Monoclinic
Space group	P-1	$P2_12_12_1$	$P2_1/c$
Temperature /K	296	296	296
Wavelength /Å	0.71073	0.71073	0.71073
a /Å	8.2758(7)	6.7700(3)	9.4742(9)
b /Å	10.0169(8)	11.7365(5)	10.6945(14)
c /Å	10.2197(9)	30.6874(12)	21.747(2)
α/°	85.635(5)	90.00	90.00
β/°	85.319(5)	90.00	90.662(5)
γ/°	77.445(5)	90.00	90.00
V/ Å^3	822.69(12)	2438.30(18)	2203.3(4)
Z	2	4	4
Density/Mgm^{-3}	1.330	1.385	1.599
Abs. Coeff. /mm^{-1}	0.088	0.115	0.360
Abs. correction	None	None	None
F(000)	344	1056	1088
Total no. of reflections	2927	18108	13693
Reflections, $I > 2\sigma(I)$	2336	4444	3377
Max. 2θ/°	50.5	51.0	48.48
Ranges (h, k, l)	$-9 \le h \le 9$ $-11 \le k \le 11$ $-12 \le l \le 12$	$-8 \le h \le 8$ $-14 \le k \le 14$ $-35 \le l \le 35$	$-10 \le h \le 10$ $-12 \le k \le 8$ $-25 \le l \le 25$
Complete to 2θ (%)	98.4	96.9	95.0
Refinement method	Full-matrix least-squares on F^2	Full-matrix least-squares on F^2	Full-matrix least-squares on F^2
Data/ Restraints/Parameters	2927 /0 / 226	4444 / 0 / 343	3377 /0 / 324
Goof (F^2)	1.041	1.043	1.043
R indices [$I > 2\sigma(I)$],	0.0574	0.0628	0.0836
R indices (all data),	0.0653	0.1038	0.1233

Compound No.	**2.3c**	**2.3d**	**2.3e**	**2.4**
Formulae	$C_{20}H_{22}N_4O_8$	$C_{24}H_{20}N_3O_7$	$C_{26}H_{23}N_3O_9$	$C_{20}H_{24}N_2O_5$
CCDC No.	860510	790480	790482	790478
Mol. wt.	446.42	462.43	521.47	372.41
Crystal system	monoclinic'	Monoclinic	Triclinic	Triclinic
Space group	$P2_1/c$	$P2_1/n$	P-1	P-1
Temperature /K	296	296	296	296
Wavelength /Å	0.71073	0.71073	0.71073	0.71073
a /Å	15.3088(9)	6.7151(11)	7.5146(7)	8.7292(14)
b /Å	7.1561(4)	16.530(3)	12.2378(12)	10.675(2)
c /Å	19.0953(11)	19.258(4)	13.6349(13)	11.0402(19)
α/°	90.00	90.00	94.239(7)	87.703(10)
β/°	98.086(4)	91.372 (6)	97.921(7)	72.230(8)
γ/°	90.00	90.00	97.873(6)	80.940(9)
V/ $Å^3$	2071.1(2)	2136.9(6)	1224.7(2)	967.4(3)
Z	4	4	2	2
Density/Mgm^{-3}	1.432	1.437	1.414	1.278
Abs. Coeff. /mm^{-1}	0.112	0.108	0.109	0.092
Abs. correction	None	None	None	None
F(000)	936	964	544	396
Total no. of reflections	5108	3850	4365	3282
Reflections, $I > 2\sigma(I)$	2282	1763	2087	2747
Max. 2θ/°	56.80	50.5	50.5	50.0
Ranges (h, k, l)	$-18 \le h \le 20$ $-9 \le k \le 9$ $-25 \le l \le 25$	$-7 \le h \le 8$ $-19 \le k \le 19$ $-22 \le l \le 23$	$-8 \le h \le 8$ $-14 \le k \le 13$ $-16 \le l \le 16$	$-10 \le h \le 10$ $-12 \le k \le 12$ $-9 \le l \le 13$
Complete to 2θ (%)	98.3	99.6	98.5	96.8
Refinement method	Full-matrix least-squares on F^2	Full-matrix least-squares on F^2	Full-matrix least-squares on F^2	Full-matrix least-squares on F^2
Data/ Restraints/Parameters	5108 / 3 / 313	3850 / 4 / 319	4365 / 0 / 357	3282 / 0/ 265
Goof (F^2)	0.880	1.059	0.871	0.855
R indices [$I > 2\sigma(I)$],	0.0500	0.0998	0.0409	0.0589
R indices (all data),	0.1204	0.1612	0.0958	0.0654

Compound No.	**2.4a**	**2.4b**	**2.5**	**2.5a**
Formulae	$C_{24}H_{24}N_2O_7$	$C_{22}H_{21}N_2O_5$	$C_{20}H_{21}N_3O_2$	$C_{20}H_{22}ClN_3O_6$
CCDC No.	790479	790477	724794	724795
Mol. wt.	452.45	393.41	335.40	435.86
Crystal system	Monoclinic	Monoclinic	Orthorhombic	Trigonal
Space group	$P2_1/n$	$P2_1/c$	$Pna2_1$	R-3
Temperature /K	296	296	296	296
Wavelength /Å	0.71073	0.71073	0.71073	0.71073
a /Å	17.862(3)	17.792(15)	14.6536(8)	33.2881(8)
b /Å	4.8456(8)	4.909(4)	22.5764(12)	33.2881(8)
c /Å	26.550(4)	25.985(16)	5.3987(3)	9.8459(3)
α/°	90.00	90.00	90.00	90.00
β/°	101.540(9)	120.21 (4)	90.00	90.00
γ/°	90.00	90.00	90.00	120.00
V/ Å^3	2251.6(6)	1961 (3)	1786.03(17)	9448.5(4)
Z	4	4	4	18
Density/Mgm^{-3}	1.335	1.332	1.247	1.379
Abs. Coeff. /mm^{-1}	0.099	0.095	0.082	0.224
Abs. correction	None	None	None	None
F(000)	952	828	712	4104
Total no. of reflections	3866	3423	12777	36199
Reflections, $I > 2\sigma(I)$	1418	1967	3166	4017
Max. 2θ/°	50.5	50.5	51.00	51.48
Ranges (h, k, l)	$-21 \le h \le 21$ $-5 \le k \le 4$ $-29 \le l \le 27$	$-21 \le h \le 20$ $-5 \le k \le 5$ $-30 \le l \le 31$	$-17 \le h \le 17$ $-27 \le k \le 26$ $-6 \le l \le 6$	$-40 \le h \le 40$ $-40 \le k \le 40$ $-11 \le l \le 11$
Complete to 2θ (%)	94.8	96.5	99.9	99.9
Refinement method	Full-matrix least-squares on F^2	Full-matrix least-squares on F^2	Full-matrix least-squares on F^2	Full-matrix least-squares on F^2
Data/ Restraints/Parameters	3866 / 0 / 311	3423 / 0 / 273	3166 / 1 / 235	4017 / 0 / 284
Goof (F^2)	0.765	0.679	1.100	1.162
R indices [$I > 2\sigma(I)$],	0.0493	0.0529	0.0600	0.0650
R indices (all data),	0.1454	0.2053	0.0917	0.0873

Compound No.	**3.3**	**3.4**	**3.8a**	**3.8b**
Formulae	$C_{26}H_{29}N_3O_2$	$C_{17}H_{19}ClN_2O_6$	$C_{11}H_8N_3O_4$	$C_{11}H_9ClN_2O_5$
CCDC No.	727520	727521	812208	812210
Mol. wt.	415.52	382.79	246.20	284.65
Crystal system	Monoclinic	Triclinic	Orthorhombic	Monoclinic
Space group	$P2_1/c$	P-1	Pnma	$P2_1/c$
Temperature /K	296	296	296	296
Wavelength /Å	0.71073	0.71073	0.71073	0.71073
a /Å	5.9440(3)	8.5943(4)	15.410(3)	9.2378(7)
b /Å	11.4162(6)	10.4893(4)	9.2617(17)	8.8185(7)
c /Å	33.3131(18)	10.9439(6)	7.3465(13)	14.3709(10)
α/°	90.00	74.363(3)	90.00	90.00
β/°	92.703(3)	67.062(3)	90.00	93.458(5)
γ/°	90.00	87.411(3)	90.00	90.00
V/ Å^3	2258.0(2)	872.94(7)	1048.5(3))	1168.57(15)
Z	4	2	4	4
Density/Mgm^{-3}	1.222	1.456	1.560	1.618
Abs. Coeff. /mm^{-1}	0.078	0.257	0.122	0.346
Abs. correction	None	None	None	None
F(000)	888	400	508	584
Total no. of reflections	2358	2786	959	2038
Reflections, $I > 2\sigma(I)$	1596	2403	426	1388
Max. 2θ/°	42.54	48.98	50.0	50.5
Ranges (h, k, l)	$-5 \le h \le 6$ $-11 \le k \le 11$ $-33 \le l \le 33$	$-9 \le h \le 10$ $-11 \le k \le 12$ $-12 \le l \le 12$	$-16 \le h \le 18$ $-10 \le k \le 10$ $-7 \le l \le 8$	$-10 \le h \le 11$ $-10 \le k \le 10$ $-17 \le l \le 17$
Complete to 2θ (%)	94.4	96.0	97.5	96.1
Refinement method	Full-matrix least-squares on F^2	Full-matrix least-squares on F^2	Full-matrix least-squares on F^2	Full-matrix least-squares on F^2
Data/ Restraints/Parameters	2358 / 0 /284	2786 / 0 / 242	959 / 0 / 109	2038 / 0 / 172
Goof (F^2)	0.838	1.042	0.829	0.983
R indices [$I > 2\sigma(I)$]	0.0443	0.0432	0.0390	0.0566
R indices (all data)	0.0676	0.0508	0.1052	0.0790

Compound No.	**3.11**	**4.1**	**4.2**	**4.3**
Formulae	$C_{12}H_{11}ClN_2O_5$	$C_{16}H_{13}N_3O$	$C_{16}H_{13}N_3O$	$C_{16}H_{12}N_2O_2$
CCDC No.	812209	695409	695412	697831
Mol. wt.	298.68	263.29	263.29	264.28
Crystal system Space group	Monoclinic $P2_1/n$	Monoclinic Pc	Monoclinic $P2_1/c$	Orthorhombic $P2_12_12_1$
Temperature /K	296	296	296	296
Wavelength /Å	0.71073	0.71073	0.71073	0.71073
a /Å	7.2404(8)	12.3447(3)	19.5575(15)	9.8403(8)
b /Å	9.4455(9)	4.59570(10)	8.7354(7)	10.5515(11)
c /Å	18.8974(18)	11.4845(3)	17.3377(18)	13.0173(11)
α/°	90.00	90.00	90.00	90.00
β/°	92.187(5)	95.416(2)	113.379(5)	90.00
γ/°	90.00	90.00	90.00	90.00
V/ Å^3	1291.4(2)	648.64(3)	2718.8(4)	1351.6(2)
Z	4	2	8	4
Density/Mgm^{-3}	1.536	1.348	1.286	1.299
Abs. Coeff. /mm^{-1}	0.317	0.087	0.083	0.088
Abs. correction	None	None	None	None
F(000)	616	276	1104	552
Total no. of reflections	2270	5009	17748	8335
Reflections, $I > 2\sigma(I)$	1569	1779	4940	3326
Max. 2θ/°	50.5	48.20	51.30	56.94
Ranges (h, k, l)	$-8 \le h \le 8$ $-9 \le k \le 10$ $-20 \le l \le 22$	$-14 \le h \le 13$ $-5 \le k \le 5$ $-12 \le l \le 12$	$-23 \le h \le 23$ $-10 \le k \le 10$ $-20 \le l \le 12$	$-12 \le h \le 7$ $-14 \le k \le 13$ $-17 \le l \le 17$
Complete to 2θ (%)	97.0	96.0	96.1	97.5
Refinement method	Full-matrix least-squares on F^2	Full-matrix least-squares on F^2	Full-matrix least-squares on F^2	Full-matrix least-squares on F^2
Data/ Restraints/Parameters	2270 / 0 / 182	1779 / 2 / 189	4940 / 0 / 373	3326 / 0 / 181
Goof (F^2)	1.484	1.093	0.993	1.037
R indices [$I > 2\sigma(I)$]	0.0671	0.0271	0.0632	0.0657
R indices (all data)	0.0862	0.0278	0.1715	0.1121

Compound No.	**4.4**	**4.5**	**4.6**	**4.7**
Formulae	$C_{18}H_{15}N_3O_3$	$C_{20}H_{17}N_3O_5$	$C_{21}H_{18}N_3O_5$	$C_{35}H_{30}N_6O_6$
CCDC No.	733267	740130	733270	733268
Mol. wt.	321.33	379.37	360.38	630.65
Crystal system	Monoclinic	Triclinic	Monoclinic	Monoclinic
Space group	$P2_1/c$	P-1	$P2_1/c$	C2/c
Temperature /K	296	296	296	296
Wavelength /Å	0.71073	0.71073	0.71073	0.71073
a /Å	29.8193(13)	8.983(3)	32.9369(11)	56.260(3)
b /Å	4.5614(2)	9.227(3)	4.58450(10)	4.5849(2)
c /Å	11.7300(5)	12.544(5)	11.9420(4)	11.8816(6)
α/°	90.00	73.06(2)	90.00	90.00
β/°	99.506(3)	69.25(2)	96.803(2)	93.071(5)
γ/°	90.00	70.06(2)	90.00	90.00
V/ Å^3	1573.58(12)	896.6(6)	1790.54(9)	3060.4(3)
Z	4	2	4	4
Density/Mgm^{-3}	1.356	1.405	1.337	1.369
Abs. Coeff. /mm^{-1}	0.095	0.103	0.091	0.096
Abs. correction	None	None	None	None
F(000)	672	396	756	1320
Total no. of reflections	12653	7636	17929	15057
Reflections, $I > 2\sigma(I)$	2738	2740	3503	3018
Max. 2θ/°	49.98	48.50	51.94	51.98
Ranges (h, k, l)	$-35 \le h \le 32$ $-5 \le k \le 5$ $-13 \le l \le 13$	$-10 \le h \le 9$ $-10 \le k \le 10$ $-14 \le l \le 13$	$-40 \le h \le 39$ $-5 \le k \le 5$ $-14 \le l \le 14$	$-67 \le h \le 68$ $-5 \le k \le 5$ $-14 \le l \le 14$
Complete to 2θ (%)	98.8	94.2	99.4	100.00
Refinement method	Full-matrix least-squares on F^2	Full-matrix least-squares on F^2	Full-matrix least-squares on F^2	Full-matrix least-squares on F^2
Data/ Restraints/Parameters	2738 / 0 /226	2740 / 0 / 265	3503 /6 / 262	3018/ 0/ 240
Goof (F^2)	1.061	1.245	1.008	1.062
R indices [$I > 2\sigma(I)$]	0.0409	0.0548	0.0487	0.0486
R indices (all data)	0.0537	0.0824	0.0661	0.0591

Compound No.	**4.8**	**4.9**	**4.10**	**4.11**
Formulae	$C_{24}H_{19}N_3O_5$	$C_{20}H_{16}N_3O_3$	$C_{19}H_{18}N_3O_3$	$C_{23}H_{18}N_4O_5$
CCDC No.	854224	854225	854778	733269
Mol. wt.	429.42	346.36	336.36	430.41
Crystal system	Orthorhombic	Monoclinic	Monoclinic	Triclinic
Space group	Pbcn	$P2_1/c$	$P2_1/c$	P-1
Temperature /K	296	296	296	296
Wavelength /Å	0.71073	0.71073	0.71073	0.71073
a /Å	12.545(2)	32.0957(11)	30.916(4)	7.5517(4)
b /Å	12.547(2)	4.5387(2)	4.5580(5)	8.7121(5)
c /Å	26.022(4)	11.8773(4)	12.1164(15)	16.3472(9)
α/°	90.00	90.00	90.00	90.547(3)
β/°	90.00	99.816(2)	95.876(9)	94.558(3)
γ/°	90.00	90.00	90.00	111.759(3)
V/ Å^3	4096.2(12)	1704.87(11)	1698.4(4)	994.83(10)
Z	8	4	4	2
Density/Mgm^{-3}	1.393	1.349	1.315	1.437
Abs. Coeff. /mm^{-1}	0.099	0.093	0.091	0.104
Abs. correction	None	None	None	None
F(000)	1792	724	708	448
Total no. of reflections	5101	4201	3088	14140
Reflections, $I > 2\sigma(I)$	2671	2510	1106	4830
Max. 2θ/°	56.66	56.80	50.50	56.68
Ranges (h, k, l)	$-16 \le h \le 15$ $-15 \le k \le 16$ $-33 \le l \le 34$	$-42 \le h \le 42$ $-5 \le k \le 5$ $-15 \le l \le 15$	$-34 \le h \le 37$ $-5 \le k \le 5$ $-13 \le l \le 14$	$-10 \le h \le 10$ $-10 \le k \le 11$ $-21 \le l \le 17$
Complete to 2θ (%)	99.6	98.9	99.8	97.3
Refinement method	Full-matrix least-squares on F^2	Full-matrix least-squares on F^2	Full-matrix least-squares on F^2	Full-matrix least-squares on F^2
Data/ Restraints/Parameters	5101 / 0 /297	4201 / 0 / 236	3088 /0 / 234	4830 / 0 / 305
Goof (F^2)	0.897	0.975	0.821	1.052
R indices [$I > 2\sigma(I)$]	0.0567	0.0454	0.0555	0.0430
R indices (all data)	0.1278	0.0790	0.1592	0.0544

Compound No.	**4.12**	**4.13**	**4.14**	**4.15**
Formulae	$C_{48}H_{44}Cl_3N_9O_{17}$	$C_{23}H_{21}N_3O_4S$	$C_{16}H_{14}ClN_3O_5$	$C_{32}H_{28}Cl_2N_4O_{13}$
CCDC No.	695413	854226	695411	697986
Mol. wt.	1125.27	435.49	363.75	747.48
Crystal system	Monoclinic	Monoclinic	Orthorhombic	Triclinic
Space group	$P2_1/c$	C2/c	$Pna2_1$	P-1
Temperature /K	296	296	296	296
Wavelength /Å	0.71073	0.71073	0.71073	0.71073
a /Å	17.719(3)	35.284(2)	19.584(5)	7.428(2)
b /Å	15.831(3)	9.3485(6)	8.0620(19)	13.936(4)
c /Å	18.506(3)	13.8632(8)	20.523(5)	17.274(5)
α/°	90.00	90.00	90.00	108.989(5)
β/°	106.694(9)	111.403(5)	90.00	93.671(5)
γ/°	90.00	90.00	90.00	97.095(5)
V/ $Å^3$	4972.5(16)	4257.5(4)	3240.3(14)	1667.5(8)
Z	4	8	8	2
Density/Mgm^{-3}	1.503	1.359	1.491	1.489
Abs. Coeff. /mm^{-1}	0.269	0.188	0.270	0.269
Abs. correction	None	None	None	None
F(000)	2328	1824	1504	772
Total no. of reflections	43899	3794	22668	11187
Reflections, $I > 2\sigma(I)$	12099	3167	7708	7980
Max. 2θ/°	56.52	50.50	56.54	56.72
Ranges (h, k, l)	$-23 \le h \le 22$ $-20 \le k \le 20$ $-24 \le l \le 24$	$-42 \le h \le 42$ $-8 \le k \le 11$ $-16 \le l \le 15$	$-26 \le h \le 25$ $-9 \le k \le 10$ $-26 \le l \le 27$	$-9 \le h \le 2$ $-17 \le k \le 18$ $-23 \le l \le 23$
Complete to 2θ (%)	98.2	98.3	99.7	95.9
Refinement method	Full-matrix least-squares on F^2	Full-matrix least-squares on F^2	Full-matrix least-squares on F^2	Full-matrix least-squares on F^2
Data/ Restraints/Parameters	12099 / 0 / 722	3794 / 0/ 353	7708/ 1/ 471	7980 / 0 / 468
Goof (F^2)	0.995	1.042	1.233	0.930
R indices [$I > 2\sigma(I)$]	0.0717	0.0450	0.0780	0.0951
R indices (all data)	0.1722	0.0532	0.1793	0.2691

Compound No.	**5.2**	**5.3**	**5.4**
Formulae	$C_{22}H_{22}N_4O_2$	$C_{22}H_{24}Cl_2N_4O_{10}$	$C_{22}H_{24}N_6O_{10}$
CCDC No.	838324	838325	838326
Mol. wt.	374.44	575.35	532.47
Crystal system	Monoclinic	Orthorhombic	Orthorhombic
Space group	C2/c	Fddd	$C222_1$
Temperature /K	296	296	296
Wavelength /Å	0.71073	0.71073	0.71073
a /Å	29.310(14)	51.844(11)	14.640(5)
b /Å	7.026(3)	8.1994(19)	20.521(5)
c /Å	9.173(4)	24.616(6)	8.322(2)
α/°	90.00	90.00	90.00
β/°	106.564(18)	90.00	90.00
γ/°	90.00	90.00	90.00
V/ $Å^3$	1810.5(15)	10464(4)	2500.2(12)
Z	4	16	4
Density/Mgm^{-3}	1.374	1.461	1.415
Abs. Coeff. /mm^{-1}	0.091	0.310	0.114
Abs. correction	None	None	None
F(000)	792	4768	1112
Total no. of reflections	1652	2320	2008
Reflections, $I > 2\sigma(I)$	1011	975	855
Max. 2θ/°	51.0	50.0	49.46
Ranges (h, k, l)	$-35 \le h \le 35$ $-7 \le k \le 8$ $-11 \le l \le 10$	$-61 \le h \le 61$ $-9 \le k \le 9$ $-29 \le l \le 29$	$-16 \le h \le 16$ $-22 \le k \le 22$ $-9 \le l \le 9$
Complete to 2θ (%)	97.6	100.0	94.5
Refinement method	Full-matrix least-squares on F^2	Full-matrix least-squares on F^2	Full-matrix least-squares on F^2
Data/ Restraints/Parameters	1652 / 0/ 132	2320 / 9/ 186	2008 / 0 / 173
Goof (F^2)	0.902	1.972	1.274
R indices [$I > 2\sigma(I)$]	0.0445	0.1216	0.1038
R indices (all data)	0.0763	0.2256	0.2274

Compound No.	**6.1**	**6.2**	**6.3**
Formulae	$C_{12}H_{16}BrNNa_2O_7$	$C_{24}H_{25}ClN_2Na_2O_{12}$	$C_{12}H_{10}BrCdNO_3$
Mol. wt.	412.15	612.87	408.52
Crystal system	Monoclinic	Monoclinic	Monoclinic
Space group	C2/c	C2/c	$P2_1/n$
Temperature /K	296	296	296
a /Å	27.880(4)	22.016(4)	8.5970(4)
b /Å	14.051(2)	12.316(3)	9.5708(4)
c /Å	9.0596(13)	10.604(2)	15.5239(6)
α/°	90.00	90.00	90.00
β/°	98.494(3)	109.15(3)	7.554(3)
γ/°	90.00	90.00	90.00
V/ $Å^3$	3510.0(9)	2716.2(10)	1266.22(9)
Z	8	4	4
Density/Mgm^{-3}	1.567	1.504	2.143
Abs. Coeff. /mm^{-1}	2.422	0.240	4.878
Abs. correction	Empirical	None	Empirical
F(000)	1680	1264	784
Total no. of reflections	3170	2377	2294
Reflections, $I > 2\sigma(I)$	2377	1837	1871
Max. 2θ/°	50.54	50.04	50.50
Ranges (h, k, l)	$-31 \le h \le 33$ $-15 \le k \le 16$ $-10 \le l \le 10$	$-26 \le h \le 25$ $-14 \le k \le 10$ $-12 \le l \le 12$	$-10 \le h \le 10$ $-11 \le k \le 11$ $-18 \le l \le 18$
Complete to 2θ (%)	99.2	98.8	100.0
Data/ Restraints/Parameters	3170 / 31 / 250	2377 / 205 / 248	2294 / 0 / 164
Goof (F^2)	1.045	1.104	1.069
R indices [$I > 2\sigma(I)$]	0.0832	0.0398	0.0304
R indices (all data)	0.0454	0.0525	0.03880

Melting points of the compounds:

Compound	Melting point (^{0}C)
2.1	113
2.3	311
2.4	108
2.5	103
2.6	133
2.7	118
3.3	210
3.7	128
3.10	213
3.12	188
4.1	234
4.2	158
4.3	183
5.2	282

List of Publication

1. **D. Kalita**, J.B.Baruah. Acid inclusion properties of helical self-assembly of 5,5'-biquinoline derivative.
   Crystal Growth and Design, 2011, **11**, 5131–5138.

2. **D. Kalita**, J.B.Baruah. Selectivity in metal ions mediated C-N bond formation reactions of 8-aminoquinoline derivatives.
   Journal of Physical Organic Chemistry, 2011 in press.

3. **D. Kalita**, H. Deka, S. S. Samanta, S. Guchait, J. B.Baruah. Interactions of amino acids, carboxylic acids, and mineral acids with different quinoline derivatives.
   Journal of Molecular Structure, 2011, **990**, 183-196.

4. **D. Kalita**, J. B. Baruah. Visual distinction of dicarboxylic acids and their salts by 1-phenyl-3-(quinolin-5-yl)urea.
   Journal of Molecular Structure , 2010, **969**, 75-82.

5. **D. Kalita**, J. B. Baruah. Different spatial orientations of amide derivatives on anion Coordination.
   CrystEngComm, 2010, **12**, 1562–1567.

6. **D. Kalita**, J. B. Baruah. Rearrangement of 2-bromo-N-quinoline-8-yl-acetamide leading to new heterocycle.
   J. Heterocyclic Chem., 2010, **47**, 459-462.

7. **D. Kalita**, R. Sarma, J.B.Baruah. Catalytic alcoholysis of quinolin-8-yl esters by manganese complexes.
   Inorganic Chemistry Communications, 2009, **12**, 559-571.

8. **D. Kalita**, R. Sarma, J. B. Baruah. Formation of symmetry non equivalent molecules in urea and carbamate derivatives: role of anion.
   CrystEngComm, 2009, **11**, 803-810.